Volume 127, Nos. 1–6

July–August, 1959

PROCEEDINGS OF THE ACADEMY OF SCIENCES

OF THE USSR

(DOKLADY AKADEMII NAUK SSSR)

Physical Chemistry Section

A publication of the Academy of Sciences of the USSR

IN ENGLISH TRANSLATION

Year and issue of first translation:
Vol. 112, Nos. 1-6 Jan.-Feb. 1957

Annual subscription	*$160.00*
Single issue	*35.00*

Copyright 1960

CONSULTANTS BUREAU ENTERPRISES, INC.
227 West 17th Street, New York, N. Y.

A complete copy of any paper in this issue may be purchased from the publisher for $5.00

Note: The sale of photostatic copies of any portion of this copyright translation is expressly prohibited by the copyright owners.

Printed in the United States of America

PROCEEDINGS OF THE ACADEMY OF SCIENCES OF THE USSR

Physical Chemistry Section

Volume 127, Numbers 1-6 July-August, 1959

CONTENTS

	PAGE	RUSS. ISSUE	RUSS. PAGE
Determination of the Ratio Between the Rate Constants in the Stripping of Tritium from n-Heptanes by Methyl Radicals. V. L. Antonovskii and I. V. Berezin	541	1	124
Paramagnetism In Radioactive Solutions. V. M. Vdovenko and V. A. Shcherbakov.	545	1	127
Determination of Flame Temperatures in Condensed Systems. L. N. Gal'perin, V. M. Maltsev, and P. F. Pokhil	549	1	131
The Effects of Composition on the Forbidden Energy Gap in Solid Solutions of InSb + GaSb. V. I. Ivanov-Omskii and B. T. Kolomiets	553	1	135
The Influence of Activated Components of the Reaction Products on the Combustion Processes in Flow. S. M. Kogarko, M. I. Devishev, and B. Ya. Basevich	555	1	137
Fluorometric Investigation of Diffusion Processes in the Adhesion of Polymers. N. A. Krotova and L. P. Morozova	559	1	141
Kinetics of the Reaction Between Hydrogen and Oxygen on Platinum. E. N. Khar'kovskaya, G. K. Boreskov, and M. G. Slin'ko	563	1	145
Electrostatic Repulsion Between Electrical Diffusion Layers on Two-Sided Liquid Films. A. Sheludko and D. Ekserova	567	1	149
The Flow of Elasticoviscous Fluids Under the Action of Two Mutually Perpendicular Shearing Forces. G. V. Vinogradov, A.A. Mamakov, and V. P. Pavlov	571	2	362
Dependence of the Degree of Dispersion of Aluminum Aerosols on the Preparatory Conditions. M. S. Gen, M. S. Ziskin, and Yu. I. Petrov	575	2	366
Sensitization of Radiochemical Reactions by Means of Ionic Charge Transfer. M. T. Dmitriev and S. Ya. Pshezhedskii	579	2	369
The Influence of the Adsorbent Surface on Luminescence Spectrum of Uranyl Ion. G. N. Kobyshev	583	2	373
On the Electron Theory of Chemisorption on a Real Semiconductor Surface. Sh. M. Kogan and V. B. Sandomirskii	587	2	377
Mechanism of the Reaction Between Alcohols and Hydrogen Halide Acids. V. A. Pal'm and A. O. Kyrgesaar	591	2	380
The Effects of Iodine on the Flotation of Sulfide Minerals. I. N. Plaksin, and R. Sh. Shafeev	595	2	384
Mass Spectra and the Structure of Vinylacetylenes. A. A. Polyakova, K. I. Zimina, A. A. Petrov, and R. A. Khmel'nitskii	597	2	386

CONTENTS (continued)

	PAGE	RUSS. ISSUE	RUSS. PAGE
Polymorphism and the Electrolytic Behavior of Carboxylic Acids in Solution. S. S. Urazovskii	601	2	389
Absorption of Ultrahigh Frequency Vibrations In Aqueous and Alcoholic Solutions of the Salts RbCl and CsCl. A. G. Anikin, Ya. I. Gerasimov, and I. V. Gordeev	605	3	589
The Effects of Displacement of the Level of the Chemical Potential of Electrons on the Activity of Semiconductor Catalysts. G. K. Boreskov	609	3	591
Mechanism of the Protective Action of Benzene Rings In the Radiolysis of Polystyrene. Ying Shen-k'ang, A. N. Pravednikov, and S. S. Medvedev	613	3	595
The Electrode Properties, Electrical Conductivity and Chemical Stability of Glasses of the System $Li_2O-La_2O_3-SiO_2$. B. P. Nikol'skii, A. I. Parfenov, and M. M. Shchul'ts	617	3	599
The Theory of the Adsorption Wave. The Relation Between Impoverishment of the Catalyst Bed and the Speed of Movement of the Gas and the Thickness of the Bed. A. S. Predvoditelev	621	3	602
The Conversion of Tetracycline, Adsorbed on a Sulfonated Cation Exchange Resin Into Anhydrotetracycline. E. M. Savistskaya, L. F. Yakhontova, B. P. Bruns, and T. S. Kolygina	625	3	606
The Dynamic Displacements of Atoms and the Coefficients of Linear Expansion of the Arsenides of Aluminum, Gallium and Indium. N. N. Sirota and Yu. I. Pashintsev	627	3	609
The Electrical Conductivities of Different Modifications of Monochloroacetic Acid in Nonaqueous Solutions. S. S. Urazovskii and Z. M. Kanevskaya	631	3	612
A New Method of Determining Thermal Characteristics and Thermal Effects Based on Thermography. M. Sh. Yagfarov	635	3	615
Polarographic Study of the Tautomerism of Some Semi- and Thiosemicarbazones in Solutions. Yu. P. Kitaev, G. K. Budnikov, and A. E. Arbuzov.	639	4	818
Proton Magnetic Resonance in Titanium and Zirconium Hydrides. O. T. Malyuchkov and B. N. Finkel'shtein	643	4	822
The Theory of the Adsorption Wave. Relationship Between the Concentration of Outgoing Gas and the Time of Exhaustion of the Adsorbent. A. S. Predvoditelev	647	4	825
The Nature of the Contact Fusion of Alkali Halide Crystals. P. A. Savintsev, V. E. Avericheva, and V. Ya. Zlenko	651	4	828
Influence of Ionizing Radiations on the Structure of Polyamides. N. A. Slovokhotova	655	4	831
Determination of the Cell Dimensions of Polarizing Disperse Pd—Au and Pd—Cu Alloys Used as Cathodes. I. P. Tverdovskii, Zh. L. Vert, and D. Kondrashev	659	4	835
Mechanism of the Electrolytic Reduction of MnO_4', SeO_4'' and ReO_4' Ions in Their Joint Separation with Chromium. D. N. Usachev, N. L. Klimasenko, and A. T. Vagramyan	663	4	838
Optical Anisotropy of Isotactic Polystyrene Molecules. V. N. Tsvetkov and S. Ya. Magarik	665	4	840

CONTENTS (continued)

	PAGE	RUSS. ISSUE	RUSS. PAGE
The Mechanism of Isotopic Exchange in Molecular Hydrogen on Platinum Films. G. K. Boreskov and A. O. Vasilevich	669	5	1033
Tunnel Transfers Between Systems Described by Morse Potential Curves. V. I. Gol'danskii	673	5	1037
A Polarographic Study of the Stereoisomeric Transformations of Certain Semi-, and Thiosemicarbazones in Solution. Yu. P. Kitaev, G. K. Budnikov, and A. E. Arbuzov	677	5	1041
Paramagnetic Resonance in Solutions of Complex Copper Salts. B. M. Kozyrev, and A. I. Rivkind	681	5	1044
The Transfer of the Energy of Excitation and Sensitization of Chemical Reactions During Radiolysis of Solutions of Aromatic Azo Compounds. V. A. Krongauz and Kh. S. Bagdasar'yan	685	5	1047
The Reduction of Nitrate Ions In the Presence of Low Concentration Lanthanum Ions. Liu Shou-jung and S. I. Zhdanov	689	5	1051
The Heat of Transfer of $[Cd^{++}\ Ag^{\square}]$ Complexes in $AgBr + CdBr_2$ Crystals. A. N. Murin, B. G. Lur'e, and G. N. Shapkin	693	5	1055
The Interrelation of the Physical-Chemical Characteristics of Polar Liquids. E. S. Rudakov	697	5	1058
The Mutual Interaction of Diffusion Currents in Multicomponent Systems. P. Ya. Siver	703	5	1062
The Redox Potential of the Be^+/Be^{++} System In Melts of the Alkali Metal Chlorides. M. V. Smirnov, and N. Ya. Chykreev	707	5	1066
An Investigation of the Effect of Added Liquids In the Fine Dispersing of Quartz. G. S. Khodakov and P. A. Rebinder	711	5	1070
Study of the Structure of Some Ethylene and Styrene Derivatives by Means of Raman Spectra. Ya. S. Bobovich and V. V. Perekalin	715	6	1239
Temperature Dependence of the Rate of Reverse Spontaneous Dissociation Processes. V. I. Gol'danskii	719	6	1242
The Width of the Chemical Reaction Zone in a Trotyl Detonation Wave. A. N. Dremin and P. F. Pokhil	723	6	1245
Study of the Adsorption Properties of Spinels $CoMn_2O_4$ and $MnCO_2O_4$ and Oxides Mn_3O_4 and Co_3O_4. V. R. Linde	727	6	1249
Determination of the Relative Mobility of Alkali Metal Ions in Silicate Melts. V. I. Malkin and V. V. Pokidyshev	731	6	1253
A Contribution to the Study of the Mobility of Copper Ions In Germanium. A. Ya. Potemkin, V. N. Potapov, and D. A. Petrov	735	6	1256
Decomposition of the Carbide Phase of White Cast Iron-Cementite Under the Action of Neutron Rays. I. M. Pronman, V. A. Shalashov, A. Kh. Breger, and Yu. A. Zubov	739	6	1259

DETERMINATION OF THE RATIO BETWEEN THE RATE CONSTANTS IN THE STRIPPING OF TRITIUM FROM n-HEPTANES BY METHYL RADICALS

V. L. Antonovskii and I. V. Berezin

M. V. Lomonosov Moscow State University

(Presented by Academician N. N. Semenov, March 20, 1959)

The relative reactivity of CH bonds in normal paraffins is usually determined from the composition of products of such complex reactions as oxidation, chlorination, sulfochlorination, etc . [1-3], or from comparative reaction rates in a homologous series [4] .

The use of tritium permits a direct comparison between the rates with which free radicals strip hydrogens from different fixed positions in the hydrocarbon molecule. In this work we determined the relative reaction rate constants for the stripping of tritium from all the different positions of CT bonds in n-heptane.

If the CH_3 radicals are generated in an n-heptane medium where the i-th type of CH bonds is labeled by having a small fraction of the hydrogen substituted by tritium, and if the number of CH_3 radicals participating in the reaction is much smaller than the amount of n-heptane, then the composition of methane formed by the reactions

$$CH_3\cdot + C_7H_{16} \rightarrow CH_4 + C_7H_{15}\cdot \qquad \text{(I)}$$

$$CH_3\cdot + C_7H_{15}T \rightarrow CH_3T + C_7H_{15}\cdot \qquad \text{(II)}$$

may be determined from the equation

$$\frac{[CH_3T]}{[CH_4]} = \frac{k_j^T\,[C_jT]}{[C_7H_{16}]\sum\limits_{i=1}^{4} k_i^H n_i}\,. \qquad (1)$$

Since $[C_jT] \ll [C_jH]$ and $[CH_3T] \ll [CH_4]$, the specific activity $I_{RH} = \gamma\ [RT]/\ [RH]$, where γ is a proportionality constant determined by the geometry of the counter, and Equation (1) assumes the form

$$I_m = \frac{k_j^T I_h}{\sum\limits_{i=1}^{4} k_i^H n_i}\,, \qquad (2)$$

where n_i is the number of i -th type of bonds in heptane , k_j^T the rate constant for the Reaction (2) with j-th type of CT bonds, I_m and I_h the specific activities of methane and labeled heptane, measured in the same units.

By alternately labeling all the bonds in n-heptane with tritium and carrying out separate reactions between methyl radicals and each of these labeled heptanes, we will get a ratio between the rate constants which, if we assume that all the labeled forms have a common denominator in Eq. (2), will have the form

$$k_1^T : k_2^T : k_3^T : k_4^T = \left(\frac{I_m}{I_h}\right)_1 : \left(\frac{I_m}{I_h}\right)_2 : \left(\frac{I_m}{I_h}\right)_3 : \left(\frac{I_m}{I_h}\right)_4\,. \qquad (3)$$

TABLE 1

Temp. °C	Position labeled with tritium	Sp. activity for a given counter pressure, counts/min · mm.		$k_i^{T} / {}_{2}^{T}$
		heptane	methane	
85	-1-	85 100±3000	38±2	0,103±0,006
	-2-	48 500±600	211±2 ·	1
	-3-	11 230±260	48,4±0,8	0,99±0,03
75	-3-	11 230±260	43,2±0,8	—
70	-1-	85 100±3000	28,7±0,4	0,098±0,003
	-2-	48 500±600	166±1	1
65	-3-	11 230±260	40,4±0,6	1,05±0,03
	-3-	11 230±260	36,3±0,5	—
55	-1-	85 100±3000	19,0±0,8	0,081±0,006
	-2-	48 500±600	133±3	1
	-3-	11 230±260	32,0±0,6	1,04±0,04
	-4-	21 000±600	60±1,5	1,04±0,05

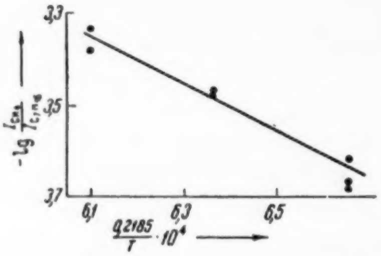

Fig. 1. The logarithm of the ratio between the specific activities of methane and heptane-1-t as a function of absolute temperature T.

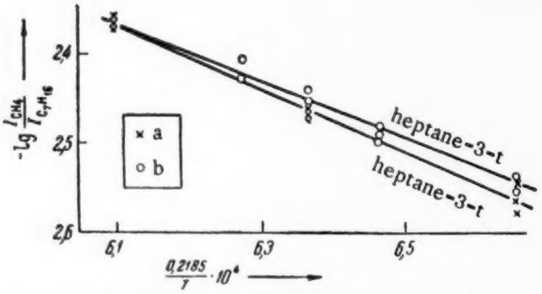

Fig. 2. The logarithm of the ratio between the specific activities of methane and heptane-2-t (a), and heptane-3-t (b) as a function of absolute temperature T.

We used acetyl peroxide as the source of methyl radicals. The peroxide was decomposed by heating a 0.02 M solution in the labeled heptane at 55-85° in sealed ampules. The temperature was maintained constant within ± 0.05°.

Methane was separated from other gaseous (CO_2, C_2H_6) and liquid reaction products by being passed through a series of liquid nitrogen traps in a vacuum apparatus. The specific activities of methane and of the starting heptanes-t was determined in a counter which could be filled with the gas [5]. We prepared the heptane-t by decomposing the corresponding heptylmagnesium bromides with tritium-water.

Equations (1)-(3) are only valid if the composition of the forming methane is solely determined by the reaction between CH_3 and heptane. As our control experiments have shown, the specific activity of methane is independent of the percent decomposition of the peroxide. This indicates that we can neglect the amount of methane formed in the reaction between methyl radicals and the reaction products or acetyl peroxide itself.

In Table 1 we have presented the main experimental* results, and the average specific activities obtained from several parallel experiments. All the errors are given as mean square values. The rate constant K_2^T for the stripping of tritium from heptane-2-t was taken to be one.

A treatment of individual experimental results by the method of least squares and the use of equation

$$\lg\left(\frac{I_m}{I_h}\right)_i = \lg\frac{A_i^T}{A_\sigma^H} - (E_i^T - E_\sigma^H)\lg\frac{e}{RT}, \qquad (4)$$

where $A^H{}_\sigma$ is the frequency factor, and E_σ^H the effective activation energy in the over-all constant of Reaction (I) with n-heptane $k_\sigma^H = \sum_{i=1}^{4} k_i n_i$ gave us (see Table 2) the following ratios:

$$k_1^T/k_2^T = 0{,}96\, e^{-1570/RT}, \quad k_2^T/k_3^T = 0{,}69\, e^{-270/RT}.$$

Despite the fact that k_σ^H is a sum of constants, Equation (4) can be used for our calculations, because in the case of heptanes-1, -2-t, and -3-t $\log(I_m/I_h)$ is a linear function of the reciprocal of absolute temperature, as may be seen in Figure 1 and 2. This indicates that within the investigated temperature range E_σ^H remains practically constant. Since the reactivity of all the secondary C-T bonds and consequently also C-H bonds is practically the same (within the investigated

---

[*] Some of the experiments with heptanes-2-t and -3-t were done by O. B. Mesineva.

TABLE 2

Hydrocarbon	$\lg \frac{A_i^T}{A_\sigma^H}$,	$E_i^T - E_\sigma^H$, cal/mole	$\lg \frac{A_i^T}{A_2^T}$	$E_i^T - E_2^T$, cal/mole
Heptane-1-t	$-0,22 \pm 0,29$	5120 ± 460	$-0,02 \pm 0,30$	1570 ± 480
Heptane-2-t	$-0,20 \pm 0,07$	3550 ± 110	—	—
Heptane-3-t	$-0,36 \pm 0,09$	3280 ± 150	$-0,16 \pm 0,11$	-270 ± 190

temperature interval), one can use any of the I_m/I_h ratios of heptanes-2-t and -3-t to calculate the net kinetic isotope effect for secondary bonds in n-heptane; it is equal to

$$(k^H/k^T)_{\text{sec}} = 0{,}20\, e^{-3400/RT}.$$

This value agrees with the kinetic isotope effect in cycloheptane [6].

On the basis of the K_i^T / K_2^T values obtained in our work the rates of tritium, and obviously also hydrogen stripping from all the secondary C-H (C-T) bonds in n-heptane are equal (with an accuracy of 10%) within the 10-220° C temperature range; this constitutes a direct evidence that all the secondary C-H bonds in n-heptane are equally reactive in free radical reactions, at least within the indicated temperature range.

LITERATURE CITED

[1] F. Asinger, G. Geisler, and H. Eckoldt, Ber. 89, 1037 (1956).

[2] J. L. Benton, M. M. Wirth, Nature 171, 269 (1953).

[3] A. N. Bashkirov, V. V. Kamzolkin, et al., Proc. Acad. Sci. USSR 119, 705 (1958)*.

[4] E. W. R. Steacie, Atomic and Free Radical Reactions, 2 ed. N. Y. 1954.

[5] V. L. Antonovskii, I. V. Berezin, Sci. Rep. of Higher Inst. of Chem. 320 (1958).

[6] V. L. Antonovskii, I. V. Berezin, Sci. Rep. of Higher Inst. of Chem. 731 (1958).

Received March 11, 1959

---

* Original Russian pagination. See C. B. Translation.

PARAMAGNETISM IN RADIOACTIVE SOLUTIONS

Corresponding Member Acad. Sci. USSR
V. M. Vdovenko and V. A. Shcherbakov

V. G. Khlopin Radiation Institute of the Academy of Sciences, USSR

Radiolytic reactions in solution produce a great number of ions, molecules, and radicals. It seems that a great number of the intermediates and of the reaction products are paramagnetic. Hence, it is quite interesting to look into the magnetic properties of such solutions [1]. The purpose of this work was to investigate the nature of magnetic properties of aqueous solutions which had been irradiated by radioactive isotopes in solution or by outside sources of β-and γ-radiation, and to determine the quantitative effects of radiation on the spin-lattice proton relaxation time T_1 in water. The latter is a parameter which under certain conditions determines the signal intensity in nuclear magnetic resonance. Time T_1 is inversely proportional to the signal intensity, i.e., in our case the time required to establish a thermodynamic equilibrium between the proton spin system and the bulk of the solution ("lattice"), and is known to be extremely sensitive [2] to the presence of paramagnetic impurities (particularly if there is a rapid proton exchange in the solution).

No work of this nature is reported in the literature. In this paper we only intend to present some preliminary results.

The relative changes in the proton relaxation time were measured by means of an apparatus designed by us, and which was a modification of the Pound-Knight spectrometer [3]. The proton resonance signals were detected and measured with and oscilloscope, or with a cathode voltmeter. The magnetic field was maintained with a permanent magnet (~ 3080 gauss).

Our method of measuring the relative changes in T_1 was identical with the one described by Rivkind [4,5]. All solutions were made up with twice distilled water. We used chemically pure and radiochemical grades of isotopes (according to the Soyzreaktivsbyt* rating). The internal irradiation was done with a $Eu^{152,154}$ source (~40 mc) sealed in a small ampule and submerged in the solution.

In Table 1 we have presented the results from our observations on solutions containing various isotopes. In order to avoid any possible effects caused by electrical conductance and to improve our accuracy we always used standard blank solutions whose composition was identical with that of the solution containing the radioisotope. The ratio between the signal of such a solution and that of the investigated one, A/A_{st}, was used in Table 1 as the measure of the decrease in T_1. The dose intensities (P) of the β, γ -rays were estimated from the approximation of a "sphere filled with the β, γ -active material"; for the isolated $Eu^{152,154}$ source we used the "point source" approximation (see K. K. Aglintsev [6]). The maximum error in our determinations of the A/A_{st} ratio was about 15%. (The use of a single reference standard, for example 1 N H_2SO_4, increased the error to 25%.) Errors in the determination of P were 10-15%. For a qualitative comparison we have presented in Fig. 1 photorecorded oscillograms of various signals.

As may be seen in Table 1 the presence of radioactivity in solution decreased T_1 (increased the A/A_{st} ratio) far in excess of experimental errors.

The observed decrease in T_1 could neither be attributed to the type of compounds chosen (they were all diamagnetic), nor to the isotope disintegration products (which obviously might have been paramagnetic), since the isotope content in solution did not exceed 10^{-10} g/ml (Table 1). Such low concentrations of paramagnetic materials were below the lower sensitivity limit of our apparatus. Besides, our reasoning was confirmed by the experiments done with the $Eu^{152,154}$ source outside the solution.

---

* Soviet marketing agency for radioactive isotopes.

TABLE 1

Expt. Nos.	Isotope	Solution composition	Activity, in mc/ml.	P_β, in rep/hr	P_γ, in rep/hr	Length of irradiation	$D \cdot 10^{-6}$, r	A/A_{st}
1	Na^{24}	Sat., NaCl in 10% H_2SO_4	75	260 600	269,4	46 hr	4,99	17,0
2	S^{35}	1*N* H_2SO_4	2,2	1080	—	272 days	2,28	4,0
		0,9 *N* H_2SO_4	45,8	22 380	—	20 days	10,16	11,8
3	Sr^{89}	$Sr(NO_3)_2$ in 1 *N* HNO_3	20,0	75 000	—	180 days	119,48	4,0
4	Zr^{95}	$Zr(C_2O_4)_2$ in 1% $H_2C_2O_4$	30,6	11 570	787,6	85 days	16,57	25,5
5	Cd^{115}	$CdCl_2$ in 0,2 *N* HCl	0,4	16 100	0,1	154 days	22,03	4,7
6	$Eu^{152,154}$	0,5 *N* $HClO_4$	~40	51,0	22,5	150 hr	0,01	5,9

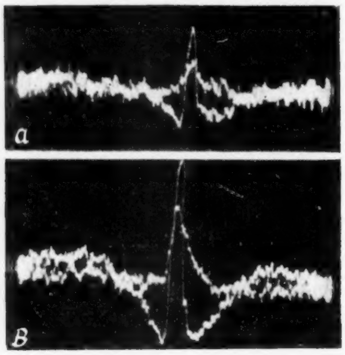

Fig. 1. Photorecorded oscillogram. a) 1% Oxalic acid solution; b) Zr^{95} in 1% $H_2C_2O_4$.

If the observed decrease in T_1 were entirely due to some random impurities in the original solutions and salts or introduced into the solution together with the activity, then it should have become apparent right after the introduction of the activity. In order to clarify this issue we designed some experiments using Na^{24} (see Fig. 2) to show the changes in the A/A_{st} ratio with time and with increasing dosage (D) in solutions of NaCl in 10% H_2SO_4, as well as the increase in dosage with time.

At first we observed a very definite signal increase, followed by a gradual decline (despite the fact that the dosage D kept increasing; in experiments with Na^{24} we were unable to get $A/A_{st} = 1$ even after 360 hr). Similar results were also obtained by a slightly different technique —dilution of Zr^{95}, S^{35} , and other solutions; the signal would initially decrease in keeping with the dilution , then start increasing with a rate proportional to the dose intensity P until it attained a value usually very near to that recorded before dilution. This indicates that T_1 decreases solely as a result of radiation .

The newly acquired properties of the solution were quite stable. This much could already be gathered from the previously mentioned experiments in solutions irradiated with $Eu^{152,154}$. The signal from a 0.5 N $HClO_4$ solution irradiated with $Eu^{152,154}$ remained practically constant for several days. Neither right after the activity was introduced into the solution (Fig. 2) , nor when it was removed after irradiation (for example, after removal of the europium source), did we observe any increase or decrease of the signal. Figure 3 shows how the signal received from irradiated 0.5 N $HClO_4$ solution remained constant for one hour after the europium source had been removed. A slight increase could be blamed on the oxygen from the air, The signal from a twice-distilled water increased slightly (~ 10%) after some air was bubbled through it; Giulotto [7] already had noted that the magnetic moment of oxygen μ affects the value of T_1 in water, and he found out that the effective magnetic moment of oxygen μ_{eff} in water is equal to 1.2 μ_B , where μ_B is the Bohr magneton . The signal decreased on the average by 15% at an angle of about 90° , and heating had no detectable effect on the rate of decrease (this applied to both the internally and externally irradiated solutions). After the solution was heated, at times repeatedly, to 100° the signal would invariably return to its original value .

An attempt to explain the examined results by the changes in the fundamental functions determining the value of T_1 in water free of paramagnetic impurities (the number of nuclei per 1 cm^3, density, distance between neighboring protons r_0, and the rotational motion) [8] failed to account for the phenomena. Actually , on the basis of an approximate calculation, the radiolysis should have produced a tremendous compression of the solution (r_0 should have decreased to less than one fourth of its original value) or else a hard to explain decrease in the rotational motion of water molecules (our experiments detected no viscosity increase, and, in fact, the number of protons did not fluctuate).

Therefore, it seems to us most natural to explain the observed phenomena by the formation of paramagnetic molecules in radiolyzed solutions .

On the basis of certain known relationships, first proposed by Kozyrev and Rivkind [5], we computed the concentrations of paramagnetic materials which would account for the observed shortening in T_1 if we assumed that their μ_{eff} were somewhere between 1 and $3\mu_B$. The concentrations turned out to be between 10^{-4} and 10^{-2} M in solutions containing S^{35} and Zr^{95} (Nos. 2 and 4, Table 1), and in the vicinity of 10^{-6} M and above (depending on the dosage) in solutions irradiated with a europium source (calibration was done with manganese chloride, for which $\mu_{eff} = \mu_{st} = 5.9\ \mu_B$ [4]) .

Since after a while A/A_{st} attains a constant value (Fig. 2, I) larger than unity, one can assume that some of the paramagnetic molecules are stable compounds.

However, the radicals formed by the radiolysis of water and of other solution components may also contribute to the decrease of T_1. The presence and the magnitude of their contribution can probably be inferred from the descending portion of Fig. 2, I . The time change of this curve seems to indicate a certain stabilization of radicals in solution; and the fact that the signal intensity remains constant before and after heating provides some more evidence for the high degree of stabilization.

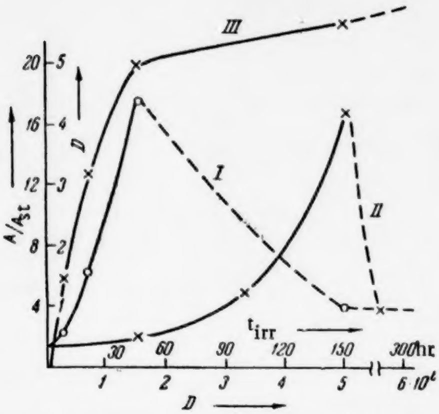

Fig. 2. I) Time change of A/A_{st} during irradiation ; II) A/A_{st} variations with dosage ; III) increase of dosage with time. Saturated solution of NaCl in 10% H_2SO_4.

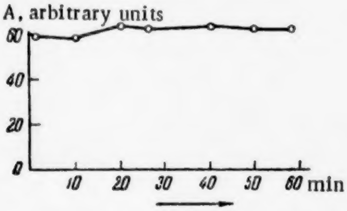

Fig. 3. Variations of A/A_{st} with time after irradiation. A 0.5 N $HClO_4$ solution irradiated "internally" by a $Eu^{152,154}$ source.

The stabilization of radicals has been discussed qualitatively in several papers, for example [1,9] . Recently, on the basis of various models, Golden [10] theoretically analyzed different means of stabilizing free radicals in condensed phases by isolating them from each other.

Using characteristic parameters for stationary irradiation conditions (given in J. L. Magee's paper [11] , we estimated the concentrations of OH and HO_2 radicals which could have formed under our conditions; they turned out to be in the same concentration range as that which we calculated above for the hypothetical paramagnetic particles (for example, for a dose $D = 10^7$ rep the concentration of HO was $6.4 \cdot 10^{-4}$M , and of HO_2 $1.5 \cdot 10^{-3}$ M). It should be noted that when pure water was irradiated with $Eu^{152,154}$ no increase in A/A_{st} was observed until a dose of $2 \cdot 10^4$ rep was attained. At the same time the signal in a 1.91 N NaOH solution has already increased by 2.2 -2.5 times by the time a dose of 5000 rep was attained (no further increase was observed until a dose of $4.3 \cdot 10^{4}$ rep was reached).

LITERATURE CITED

[1] Z. G. Szabo, Acta. Chim. Acad. Sci. Hung. 3, 139 (1953).

[2] N. Bloembergen, R. V. Pound, and E. M. Purcell, Phys. Rev. 73, 679 (1948) .

[3] R. V. Pound and W. D. Knight, Rev. Sci. Instr. 21, 219 (1950) .

[4] A. I. Rivkind, J. Inorg. Chem. 2, 1263 (1957) .

[5] B. M. Kozyrev, A. I. Rivkind, J. Exptl. Theoret. Phys. 27, 69 (1954).

[6] K. K. Aglintsev, Experimental Foundations of Dosimetry and Dosimetric Equipment, Leningrad (1957).*

[7] G. Chiarotti and L. Giulotto, Phys. Rev. 93, 1241 (1954).

[8] E. Andrew, Nuclear Magnetic Resonance (Moscow, 1957) [Russian translation].

[9] N. N. Semenov, Some Problems in Chemical Kinetics and Reactivity, Moscow, p. 154 (1954).*

[10] S. Golden, J. Chem. Phys. 29, 61 (1958).

[11] J. L. Magee, J. Am. Chem. Soc. 73, 3270 (1951).

Received January 21, 1959

---

* In Russian.

DETERMINATION OF FLAME TEMPERATURES IN CONDENSED SYSTEMS

L. N. Gal'perin, V. M. Mal'tsev, and P. F. Pokhil
Institute of Chemical Physics of the Academy of Sciences,USSR

(Presented by Academician V. N. Kondrat'ev, March 10, 1959)

The temperature inside the tongue of a flame is an important parameter which has to be known before we can fully understand the combustion mechanism of powdered systems. Our determination of the flame temperature was done by a modified so-called "blue-red ratio" method, which was applicable to flames emitting a continuous spectrum in the visible region [1-3]. As is well known, to determine the true flame temperature of a powdered sample in degrees, it is necessary to know the relative intensities of any two wavelengths (blue and red) and the absorptivities of flames at these same wavelengths.

Thanks to the large amount of work [4] that had been done in the field of electric discharge in gases, we were able to obtain a strong and steady source of light (xenon lamp) for the determination of the optical density of flames.

The schematic diagram (Fig. 1) shows the set-up by means of which we determined the flame temperatures of powdered samples. B was a bomb designed to burn the powdered sample at pressures up to 150 atm. The bomb has been described in detail in paper [5]. TL was a tungsten band-lamp, used for calibrating the entire optical system, and XeL was a SVDSh-1000 xenon lamp used for measuring the optical density of flames. OS was the optical system, which included a collimator, a biprism, an objective lens, and light filters. BP was a photomultipler bank, which converted the light beam into electric impulses. MPO-2 was an oscilloscope on which the signals received from the photomultiplier bank were recorded. MS was a marker system, designed to record the instant at which the base of the flame approached the projection of the collimator slit on the powdered sample. FU was a feeder unit. A sample of nitroglycerin N,7 mm in diameter and with a jacketed surface, was placed in the bomb and ignited from one end by a Nichrome wire. Facing the bomb window we had a collimator with two slits— principal and auxiliary. The collimator was made of a steel block 200 mm long and contained two slits (with blackened walls) 0.1 mm high and 6 mm wide. The optical system also included a biprism which split the working beam into two . Both light beams, after passing through the corresponding filters (blue and red), impinged on the photomultiplier bank.

The collimator slit would isolate at each instant a narrow surface of the flame which was moving down in a plane perpendicular to the collimator slit. Thus the photomultipliers received a light beam whose amplitude varied in time as the brightness of a fixed line on the flame surface. In order to relate the light intensity from fixed points on the flame surface with the time variations of the light beam, it was essential to know the burning rate of the powdered sample, the recording rate on the cathode ray oscilloscope, and the instant at which a fixed point on the flame surface passed right in front of the slit. With the distance between the slits being known (in our case it was 20 mm), by measuring the time required for a fixed point on the flame (for example the top) to move from one slit to another we could determine the burning velocity of the powder. The optical density of the flame was determined by illuminating the flame with a strong steady (in intensity) xenon lamp XeL (Fig. 1). The light beam from the xenon lamp was passed through a diaphragm and focused on the working collimator slit.

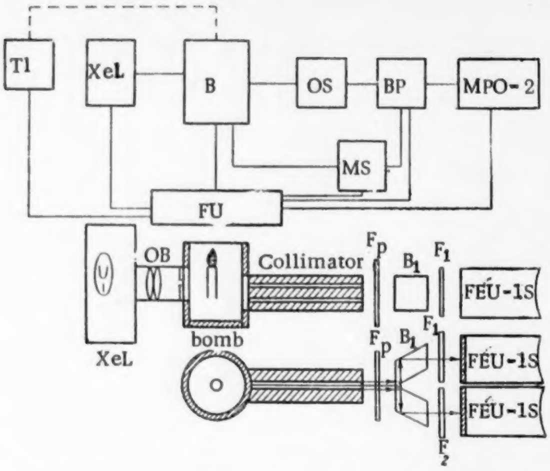

Fig. 1. Diagram of the set-up : F_1 = red filter, F_2 = blue filter, F_p = platinum filter, B = biprism, OB = objective. The remaining symbols are explained in the text.

EXPERIMENTAL

It is known from paper [6] that the combustion of powders is a multistage process. In its initial stage the combustion occurs in the reaction layer of the condensed phase; though the bulk of the condensed material inside this layer becomes dispersed while some is decomposed,the over-all process is exothermic. Thus, the first stage is terminated by the formation of a burning mixture of gaseous smoke in the combustion of powdered nitrocellulose, or a mixture of gas-vapor smoke in the case of nitroglycerin. Under certain conditions the mixture of gaseous smoke will burn up to the final combustion products inside a zone just above the powdered surface. The width of this zone and the completeness of combustion will depend on the pressure of the atmosphere surrounding the mixture of the gaseous smoke. It was experimentally determined that a complete combustion of the nitroglycerin powder N could be achieved at a pressure P = 50-60 kg/cm^2 (in an inert atmosphere). With the help of the designed apparatus we measured the temperature inside a flame tongue of powdered nitroglycerin N and its dependence on pressure ; the experimental results are shown in Fig. 2. Our experimental data showed that with increasing pressure the flame temperature increased, attaining a maximum T = 2200°k at P = 50 kg/cm^2

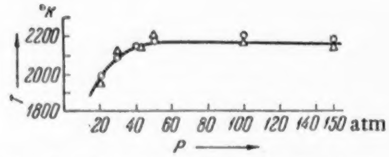

Fig. 2. Temperature within the flame tongue as a function of pressure.

When the pressure was increased some more, to P = 150 kg/cm^2, the maximum flame temperature remained constant; this was in full agreement with the work previously done [6] on the variations of the heat of combustion of powdered nitroglycerin N with pressure.

Figure 3 shows that with increasing pressure the maximum flame temperature occurred closer to the powdered surface; thus for example, at P = 20 kg/cm^2 h_M= 6.2 mm, while at P = 50 kg/cm^2 (when complete combustion is achieved) the distance becomes h_M = 2.7 mm.

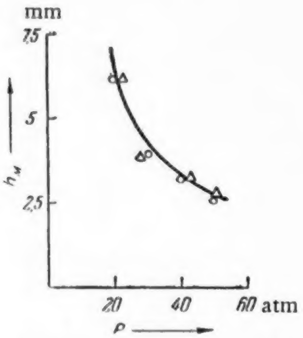

Fig. 3. The distance h_M as a function of pressure.

We have not as yet experimentally established how the width of the combustion zone h_M behaves at pressures above 50-60 kg/cm^2. Our set-up made it also possible to study the absorptivities at different heights of the flame a = f (e) as a function of pressure. The results obtained are shown in Fig. 4.

It can be seen from Fig. 4 that the absorptivity of a mixture of gaseous smoke varied with the height of the flame tongue. Thus, at P = 20 kg/cm^2 the absorptivity had a minimum value a_r = 0.4, a_b = 0.5 at a distance of ~2 mm (at point k_0) from the surface of the powder. Below as well as above point k_0 the absorptivity increased, and inside the zone C, which referred to the maximum flame temperature, it had a constant value a_r = 0.9, a_b = 0.97 . With increasing pressure the combustion zone contracts so that at P = 50 kg / cm^2 the minimum values of a_r = 0.7 and a_b = 0.8 occur at ~ 1.2 mm, but inside the maximum temperature zone the optical density of the flame was the same as at P = 20 kg/cm^2 .

Our interesting results are in full accord with the new hypothesis on the combustion in powders [6] . The

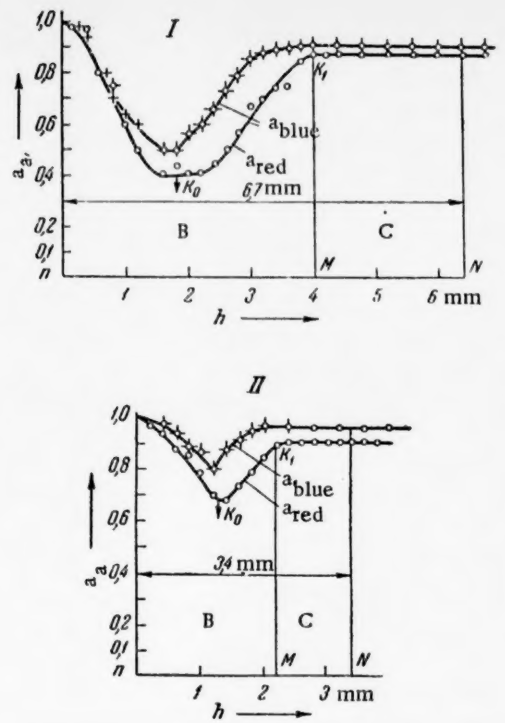

Fig. 4. The absorptivity of the mixture of gaseous smoke a_a at different flame elevations as a function of pressure. I) At P = 20 atm; II) at P = 50 atm.

initial combustion stage, which proceeds in the condensed phase, is terminated by the formation of a burning mixture of gaseous smoke, which then continues to burn above the powdered surface; under certain conditions the combustion may proceed to completion. At the instant that the gaseous mixture is formed the smoke concentration (aerosol particles) will obviously be highest right next to the powdered surface, which explains why the light emitted by an internal source was so extensively absorbed after passing through the mixture of gaseous smoke (flame tongue). Both heterogeneous and homogeneous reactions will occur inside the combustion zone, and consequently as one rises higher (inside the zone) above the powdered surface the smoke concentration (molecular and by weight) will decrease, making the gaseous smoke mixture more translucent. At the same time, as we ascend the zone of mixed gaseous smoke, not only the combustion temperature, but also the number of aerosol particles rich in carbon (soot) will increase. This factor in turn will tend to increase the absorptivity of the flame.

And these two factors are chiefly responsible for the observed maximum flame transparency at a definite distance from the powdered surface; the absolute value of this distance will depend on the pressure.

LITERATURE CITED

[1] N. N. Sobolev, Trans. FIAN 7, (1956)

[2] F. P. Bandy, H. M. Strong, Physical Measurements in Gas Dynamics and Combustion, Chap. 9 (Moscow, 1957) [Russian translation].

[3] A. E. Kadyshevich, Coll. Papers, Flame Temperature Measurements (1954).*

[4] D. A. Goukhberg, Bull. Acad. Sci. USSR, Div. Tech. Sci. No. 9 (1949).

[5] P. F. Pokhil, Coll. Detonation Physics, No. 2, (1953).*

[6] P. F. Pokhil,, Doctoral Dissertation, (Moscow, 1954).*

Received March 10, 1959

---

* In Russian.

THE EFFECTS OF COMPOSITION ON THE FORBIDDEN ENERGY GAP IN SOLID SOLUTIONS OF InSb + GaSb

V. I. Ivanov-Omskii and B. T. Kolomiets

Physicotechnical Institute of the Academy of Sciences, USSR

(Presented by Academician A. F. Ioffe, March 2, 1959)

The forbidden energy gap constitutes one of the most important parameters in any description of the semiconductor properties of materials. In solid substitutional solutions the dependence of the forbidden energy gap on the concentration is now usually explained in terms of the energy band structure in the original solution components. If the components are structurally different, then the forbidden energy gap will be a very complicated function of the solution composition. Such a situation, for example, occurs in the case of silicon-germanium alloys. We are aware of two attempts to determine the forbidden energy gap in solid InSb+GaSb solutions. Blakemore found [1] that the forbidden energy gap, as determined from the temperature dependence of conductivity and the Hall effect, and also from the spectral distribution of photoconductivity, can be represented by the expression $\Delta E = 0.265 + 1.1 \cdot 10^{-3}$ T ev, where ΔE is the forbidden energy gap at 0° K, and T the absolute temperature. Measurements were carried out on materials prepared by zone melting of an alloy whose initial composition was 50% InSb and 50% GaSb. It is a well known fact that zone melting of solid solutions alters their composition, and yet the above mentioned paper gave no analytical data with regard to the composition and degree of homogeneity in the alloy, all of which tends to reduce the validity of the results presented. S. Kolm et al. [2], after measuring the optical absorption of several InSb-GaSb alloys and finding that only one of them constituted a single-phase system, did not bother to offer any quantitative data.

We determined the dependence of the forbidden energy gap on the composition of solid InSb + GaSb solutions through optical transmittance measurements. Alloys were prepared by zone refinement [3] and consisted of single-phase large crystalline bars. The homogeneity was controlled by means of x-ray and microstructural analysis. From Debye plots we calculated the lattice parameter of the alloys used for preparing the samples, then determined the final alloy composition by assuming that Vegard's law was valid for our systems [4,5]. The $20 \cdot 30$ mm^2 samples were ground and polished down to a thickness of 100 μ. Transmittance was measured on a IKS-14 double-beam infrared spectrophotometer. With better samples we could attain an absolute transmittance of 30%. From the transmittance curves we determined the absorption edges (points where absorption bands began). As one may see in Fig. 1, the increase in the GaSb content of solution was accompanied by a monotonic and nonlinear increase in the forbidden energy gap. We can correlate thus obtained energy gap ΔE (at room temperature) with the forbidden energy gaps determined from electrical measurements (ΔE at 0°K) provided we know the temperature dependence of the forbidden energy gap. For an alloy containing 50% InSb and 50% GaSb this dependence was determined in the 77-300° K temperature range from the displacement of the absorption edge with temperature. The temperature coefficient for the forbidden energy gap (dE/dT) was $-4.5 \cdot 10^{-8}$ ev/deg. By measuring the temperature dependence of conductivity and the Hall effect we found that at the above mentioned composition the forbidden energy gap was 0.45 ev; optical measurements gave 0.33 ev. One can easily verify that if the coefficient dE/dT is taken into account both the optically and thermally determined forbidden energy gaps are in good agreement. As is quite obvious from the data presented, our results differed from Blakemore's not only in the absolute value of the forbidden energy gap, but also in the sign and magnitude of the temperature coefficient.

After examining the nature of the relationship between the forbidden energy gap and the composition of solid InSb + GaSb solutions, we decided to plot this function by using different coordinates. The ordinate in Fig. 2

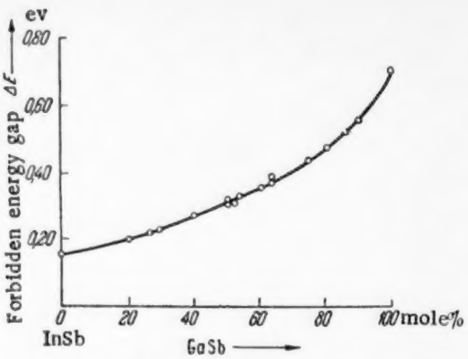

Fig. 1. The forbidden energy gap as a function of the composition in solid solutions of InSb+GaSb.

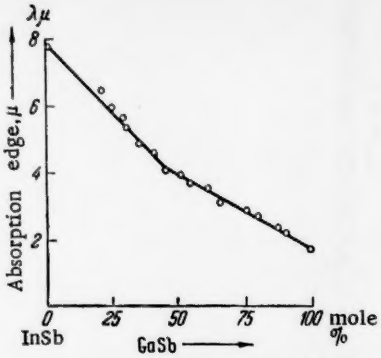

Fig. 2. The absorption edge in InSb + GaSb solid solutions as a function of composition.

gives the wavelengths of the absorption edge, which is equivalent to plotting the forbidden energy gap in hyperbolic coordinates. Such a transformation, as may be seen in Fig. 2, enables us to detect any differences in the type of relationship between the forbidden energy gap and the alloy composition in regions of different compositions. In analogy with silicon-germanium alloys, such changes may show if there are any differences in the band structures of the original binary components, InSb and GaSb. The authors of this paper believe that the interpretation of the results obtained should be postponed until the InSb-GaSb system has been studied more thoroughly and the energy band structure of the initial binary components is better understood.

LITERATURE CITED

[1] J. S. Blakemore, Canad. J. Phys. 35, 91 (1957).

[2] C. Kolm, et al., Phys. Rev. 108, 965 (1957).

[3] V. I. Ivanov-Omskii, B. T. Kolomiets, Solid State Physics 1, 913 (1959).

[4] N. A. Goryunova, N. N. Fedorova, J. Tech. Phys. 25, 1339 (1955).

[5] J. C. Wooley et al., Proc. Phys. Soc. B. 67 , 1339 (1956).

Received March 23, 1959

THE INFLUENCE OF ACTIVATED COMPONENTS OF THE REACTION PRODUCTS ON THE COMBUSTION PROCESSES IN FLOW

S. M. Kogarko, M. I. Devishev, and B. Ya. Basevich
Institute of Chemical Physics of the Academy of Sciences, USSR

(Presented by Academician V. N. Kondrat'ev, January 20, 1959)

Combustion theory tells us that the mechanism of flame propagation is connected with the transfer of heat and of activated particles from the combustion zone into the original mixture. The activated particles by diffusing into the original mixture and reacting with the mixture components help extend the reaction zone. Some of the activated particles remaining among the reaction products will recombine into molecules soon after the reaction is over and thus lose their activity.

The purpose of our work was to study the effects of the activated particles among the reaction products (which exist only until they recombine) on the acceleration of chemical reactions in ignition and combustion processes. The activated particles forming in the hydrogen diffusion flame were fed into the investigated systems at various time intervals after they were formed.

The experiments were conducted in a stream of air, inside a tube (45 mm in diameter) which terminated in a 70·40 mm combustion chamber. The basic outline of our experiment is presented in Fig. 1. In ignition experiments only a single portion of the investigated gas (vapor) would be introduced into a stream of hot air at various distances L beyond the zone of the hydrogen diffusion flame. In experiments where we studied the stability of flames around poorly streamlined materials the fuel gas was being fed continuously through a special mixer. The air was heated by means of an electric heater and by the hydrogen diffusion flame which was being fed through either burner 3 or 4. Such a combination made it possible to keep the O_2 concentration and the temperature constant at various locations of the diffusion burner. In all of our experiments the zone of the diffusion flame was terminated before reaching the point of gas injection; this we verified through a chemical analysis.

The OH (hydroxyl radical) concentrations at various distances from the hydrogen diffusion flame (see Table 1) were determined spectroscopically by the "line" absorption method developed by V. N. Kondrat'ev [1]. The tabulated data indicate that the hydroxyl concentration underwent an approximately 10 fold change when the time period after the initial escape of hydrogen from the diffusion burner was extended from 8 msec to 35 msec.

The study of methane ignition, in a stream of hot air indicated that the ignition temperature differed as the distance between the point of gas injection and the diffusion burner was varied; for the two extreme positions of the burner ignition occurred at 500 and 1000°C respectively. The ignition retardation time varied in the same way; the range of τ could be extended from 2 to 200 msec at identical temperatures and O_2 concentrations (Fig. 2).

Similar results were obtained in experiments with n-butane, isooctane, and n-heptane. It should also be noted that for different initial concentrations of activated particles the apparent activation energy of any one fuel varied extensively, for example, that of methane could change from 71 to 19 kcal/mole.

In Fig. 3 and 4 we have presented the experimental results from our investigation of flame blow-off limits around poorly streamlined bodies; these are given for city (methane) gas and propane at various air-stream temperatures. The ordinate gives flow velocity in m/sec, while the abscissa gives the mixture composition α for lean mixtures and $1/\alpha$ for enriched ones.

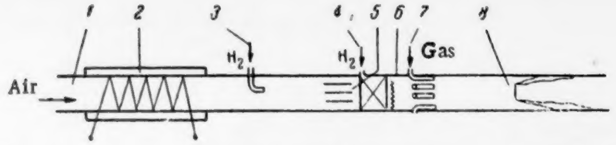

Fig. 1. Basic outline of the experimental set-up. 1) Tube; 2) electric heater; 3,4) hydrogen diffusion burner; 5) regulating device; 6) combustion chamber; 7) mixer; 8) poorly streamlined body.

TABLE 1

Absorption Coefficients and Hydroxyl Partial Pressures

Exptl. Nos.	Temp., °C	Absorption coefficients				Partial press. of OH, in mm (calc.)
		Q_1 (7/2)	Q_1 (9/2)	Q_1 (13/2)	Q_1 (15/2)	
Distance from the hydrogen burner to the measuring point 250 mm						
1	1010	0,11	0,08	0,08	0,1	0,095
2	1050	0,17	0,165	0,135	0,13	0,154
3	1065	0,11	0,14	0,16	0,14	0,14
4	1090	0,19	0,2	0,25	0,18	0,175
Distance from the hydrogen burner to the measuring point 650 mm (average values)						
5–7	1090	0,012	0,0233	0,0166	0,02	0,014

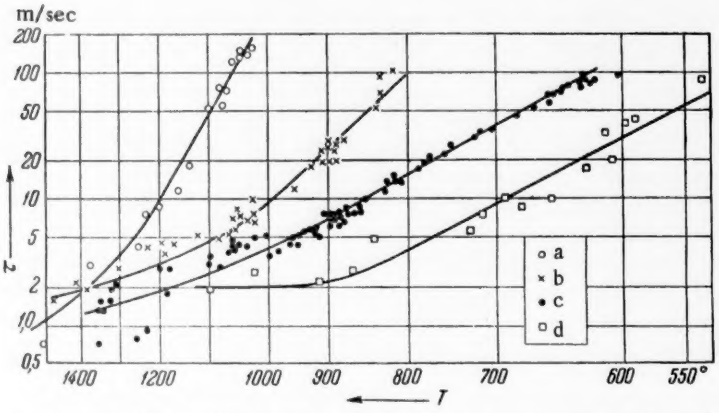

Fig. 2. Retardation of ignition in methane at various distances L from the diffusion burner. a) 650 mm; b) 400 mm; c) 250 mm; d) 150 mm.

After some loss in the hydrogen diffusion flame the oxygen concentration at various flow temperatures was (in percent): 21 at 25°, 20.2 at 120°, 19.5 at 230°, 18.8 at 350°, 18 at 480°, and 17.5 at 550°.

The graphs make it quite obvious that at low concentrations of activated particles in the mixture (at a distance L=3000 mm from the diffusion flame) the flame blow-off limits showed relatively little broadening with increasing temperatures. In the case, however, where the diffusion flame was at a distance L = 200 mm from the point at which the investigated gas was introduced, flame blow-off limits broadened considerably in both the lean as well as enriched mixtures. At higher concentrations of activated particles and when the preheating temperature of the mixture was fixed the observed effect increased with increasing flow velocity.

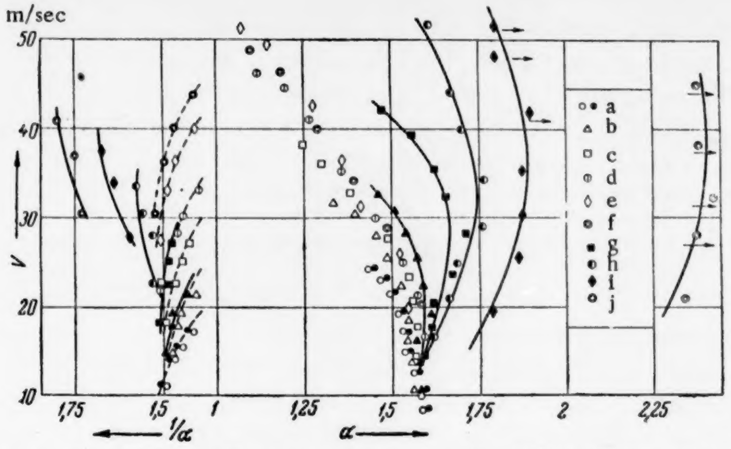

Fig. 3 The limits of collapse for city gas at various initial flow temperatures. L = 3000 mm: a) 25°, two sets of experiments (without preheating); b) 120° c) 230°; d) 350°; e) 480°; L = 200 mm: f) 120°; g) 230°; h) 350°; i) 480°; j) 550°.

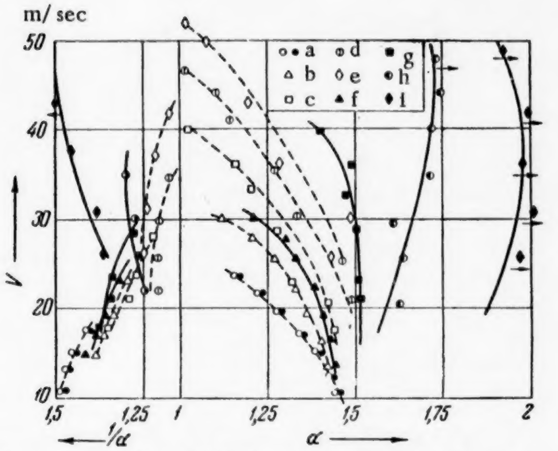

Fig. 4. The blow-off limits at various initial flow temperatures. L = 3000 mm: a) 25°, two sets of experiments (without preheating); b) 120°; c) 230°; d) 350°; e) 480°; L = 200 mm: f) 120°; g) 230°; h) 350°; i) 480°.

It seems to us that our results can best be interpreted in terms of the chain theory developed by N. N. Semenov [2] and his students.

As our measurements demonstrated, beyond the hydrogen diffusion flame there exists a high concentration of hydroxyl radicals (and consequently also other activated particles, for example O and H atoms) which rapidly diminishes in time. Therefore, the suddenly reduced (by almost two orders of magnitude) induction period at a constant temperature can be explained by attributing the increased reaction rate to the high concentration of activated particles present in the mixture. For any fixed induction period this will decrease the ignition temperature from 1000 to 500°. The reduced apparent activation energy, observed at higher concentrations of activated particles, can probably be related to a lesser participation by self induction (which requires a high activation energy) in the over-all chemical reaction.

The substantial improvement in stable combustion limits caused by the presence of activated particles in the mixture seems to come as a consequence of the shortened time required for ignition at the boundary of the recycling zone. One should keep in mind the fact that after the fuel gas enters the air stream, even before the poorly streamlined object is reached, certain chemical reactions have already been induced by the activated particles and are being propagated without any detectable temperature rise.

At more elevated mixture temperatures we observed a great improvement in the stabilizing effect, for as the initial concentration of activated particles increased a smaller portion of them were destroyed by recombination while the majority became involved in chemical reaction with the fuel and any oxidizing agents in the mixture. When the mixture temperature was raised to 480-550°C, both the city gas and propane were spontaneously ignited before the fuel gas introduced into the air stream reached the poorly streamlined object, i.e., the chemical reaction rate in the mixture attained a value high enough to start combustion before an induced ignition could take place on the poorly streamlined object. When the burner was placed much farther we could not get the mixture to ignite in that region.

On analyzing our experimental data we concluded that the addition of reaction products containing activated particles, which were formed by the combustion in the flame reaction zone, to the fuel mixture improved substantially the ignition and combustion of gases in a stream of air.

LITERATURE CITED

[1] V. N. Kondrat'ev, M. S. Ziskin, J. Exptl. Theoret. Phys. 6, 1093 (1936).

[2] N. N. Semenov, Chain Reactions, (1934).*

Received December 29, 1959

---

* In Russian.

FLUOROMETRIC INVESTIGATION OF DIFFUSION PROCESSES IN THE ADHESION OF POLYMERS

N. A. Krotova and L. P. Morozova

Institute of Physical Chemistry of the Academy of Sciences,USSR

(Presented by Academician P. A. Rebinder, December 12, 1958)

In some of our previous papers [1] we pointed out that the force of adhesion between two polymers may be caused by two distinct phenomena :1) the formation of an electrical double layer at the polymeric interface , and 2) diffusion processes in the region of contact.

The latter one should be defined more concisely, since the double layer formed at the interface arises as a result of electronic transitions form one phase into another, which process can also be considered a sort of diffusion [2]. However, such a process has one special feature—it leads to the formation of an electrical double layer. Moreover, as the boundary layers of one phase become electron deficient while those of the other acquire an excess , a potential difference will arise between the two phases. Also the separation boundary and the double layer will last for a long time. Strictly speaking, the existence of a distinct boundary separating the two phases will constitute the specific property characterizing case 1) .

In case 2) the original boundary separating two polymers becomes so diffuse that we can not talk any more about a boundary of separation but about a contact zone. This merging is caused not only by the diffusion of chain fragments and of macromolecular chains , but also by the transfer of entire structural aggregates from one phase into another.

In one of our earlier papers [3] we classified the investigated polymer—polymer systems according to their type of adhesive bond. The electrostatic type of adhesive bond has the following effect on the behavior of polymers after they are separated and the bond is broken.

1) When the two polymers are torn apart the surface of one acquires a negative electric charge,the other a positive (the first surface corresponds to a double layer with an excess of electrons, the second with a deficiency). If the experiment is carried out in vacuo we can observe electron emission from the negatively charged surface.

2) In systems possessing the electrostatic type of adhesive bond the force of adhesion (work function A) usually shows a strong dependence on the rate of separation.

Some workers have proposed [4] that in cases of self-adhesion (when two solids made of the same material are joined together) only macromolecules or their segments are involved in the diffusion which in the end restores a continuous structure of that material where the contact zone was. However, as our recent experimental data have shown, in this case too an electrical double layer is first formed during the early stages of contact, for when the surfaces were separated after being in contact for several minutes they had opposite charges. The same applies to the adhesion between homogeneous surfaces of structurally similar nonpolar molecules.

In this work, same as before, we determined the sign of the charge with a vacuum tube electrometer (Fig. 1). To the anode circuit of a 6K7 vacuum tube we hooked up a neon lamp, the light intensity of which was regulated by means of a potentiometer. The 220 v line current supplying the vacuum tube was passed first through a step-down transformer, then an AVS-7-3P rectifier, and an electrolytic condenser.

TABLE 1

The Effects of Temperature on the Obliteration of the Boundary Separating Paraffin and Guttapercha.

Contact temp., in °C	Thickness of the guttapercha film before contact, in μ	Thickness of the guttapercha film in contact with paraffin, in μ	Depth of guttapercha penetration into paraffin, in μ
60	147	266	119
70	137	296	160
80	150	315	165

A metal reed was soldered to the control grid of the tube. A negatively charged surface brought near the reed would induce a positive charge on it leaving the other end of the grid negative and blocking the current in the tube; consequently, with no current flowing through the circuit the neon lamp would go off. A positive charge induced a negative charge on the electrometer reed. A rapid removal of the positively charged surface away from the metallic reed caused a redistribution of electrons which temporarily extinguished the neon lamp.

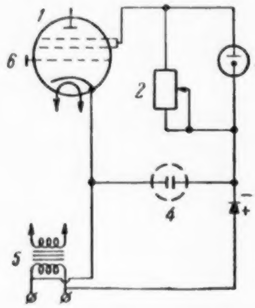

Fig. 1. Vacuum tube electrometer for the determination of charge sign on the surfaces of two polymers torn apart. 1) Vacuum tube; 2) potentiometer; 3) neon lamp; 4) capacitor; 5) step-down transformer; 6) a reed, sealed to the control grid, to which we bring up the investigated charge.

Experiments have demonstrated that the charged surfaces observed after separation constitute a general phenomena common to all types of polymeric contacts. This is in full agreement with the theories of Helmholtz about the appearance of electrical double layers on all interfaces; after separation the two faces of the double layer carry opposite charges. Under conditions where two substances are glued together, the initially formed double layer may in certain systems persist for an indefinite period of time, while in others it may disappear because of diffusion. Increased temperature and pressure will speed up the disappearance of the double layer and help obliterate the contact zone. We investigated the effects of temperature on the degree of obliteration at the contact zone between guttapercha and paraffin by using ordinary microscopic methods.

To study the obliteration of the boundary separating paraffin from guttapercha we prepared several samples at various temperatures. The guttapercha film was poured over glass which had been pretreated with an organosilicon compound (an alkylchlorosilane) to facilitate the subsequent removal of the film. The paraffin film was prepared separately by pouring molten paraffin over a cold glass surface; the cold film was placed over the dried guttapercha film, and the entire systems was placed in an air-controlled thermostat where it was maintained for a fixed length of time (15 min) at various temperatures. After this treatment the guttapercha and paraffin became fused to each other. After the sample had cooled we cut it up into microsections on a freezing microtome. The degree of contact zone obliteration was determined with a MIR-2 comparator (Table 1).

The guttapercha-paraffin sample which was kept at 50° had a sharp boundary of separation. Within the limits of experimental errors (i.e., with an accuracey of ± 1 μ) the width of the guttapercha film before contact was the same as that in the compound.

Separation left a residual chargeon each surface—negative on paraffin and positive on guttapercha. In samples maintained at higher temperatures the contact zone was diffused (to the depth of several tens of microns) due to the diffusion of guttapercha into paraffin and the adhesion in system was stronger. When torn apart, the two surfaces had no charge and the break occurred on the paraffin side. The contact zone was spread over 160 μ in samples processed at 80° and indicated an extensive diffusion of structural elements—polymeric chains and aggregates. Thus even ordinary microscopic methods give us a pretty good idea concerning the nature of processes in the contact zone. The study of such processes can be extended even further by the use of fluorometric techniques for the analysis of microsections.

At present there is quite an extensive literature in this field [5]. As is well known, fluorometric analysis has been extensively applied in biology and medicine, where by observing the secondary, artifically introduced, fluorescence it was possible to follow-up, and in certain cases even visually observe, the migration of substances inside living organisms. Introducing an insignificant amount of a fluorescent material into a liquid we can trace its diffusion in solids by following the emission of light. This method was used to study the penetration of tanning

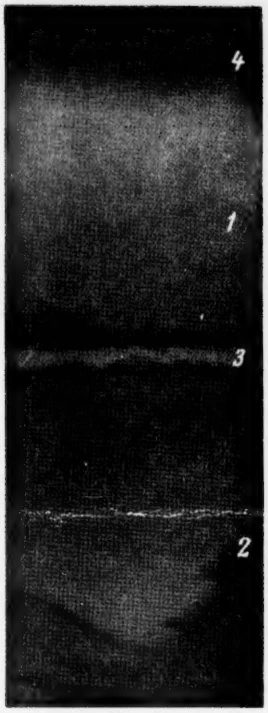

Fig. 2. Gelatin—polyvinyl alcohol. Polymers dyed with a luminophore (tropeolin): gelatin (1) and polyvinyl alcohol (2) show different intensities, and a sharp separating boundary can be seen (3) ; 4) background.*

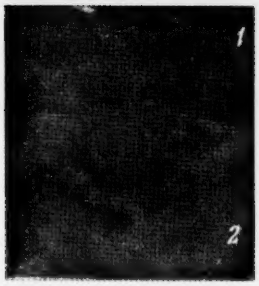

Fig. 3. Guttapercha—paraffin. Sample was worked thermally at 60°. Components are interspersed. Paraffin (1) can be seen deeply disseminated in guttapercha (2).

Fig. 4. Self-adhesion in natural rubber. The separating boundary is obliterated by diffused dispersion: 1) area dyed with the luminophore; 2) undyed ares; 3) background.

agents into the pores of leather, the water permeability of paper, and to detect concealed cracks in rocks and walls of buildings.

Our preliminary experiments were done for the purpose of exploring the applicability of luminescence analysis to the investigation of diffusion processes at the contact zone. This was done by introducing insignificant amounts of some luminophore (tropeolin) into the solvents (1 part per 20,000). Experiments have shown that these amounts of tropeolin would impart a satisfactory coloration to our solvents—water, ethyl acetate, chloroform, and benzene. The color was most intense in water, least in benzene. These solvents were first used to dissolve the investigated polymers; the final working samples were always composed from two polymers, one of which had been dyed with the luminophore. The samples were prepared in the following fashion: a film of the undyed polymer was deposited over glass rendered hydrophobic then covered up with a solution of the dyed polymer. After removing the solvent and waiting for several days we cut the sample up into microsections, which were then examined and photographed under UV light. Our source of light was a SVShA-250 tube, and the observations were done on a model GOI biological microscope, supplied with a photographic attachment for a "Zorkii" camera. An "Agfa Kolor" [6] film and photographic paper were used throughout. We studied both the surface charge and the type of break on control specimens torn apart. The following systems were investigated:

1) Gelatin—polyvinyl alcohol. Both polymers were soluble in water. The luminophore was introduced into the polyvinyl alcohol solution, which was then poured over a dry film of gelatin and the solvent evaporated. On examination the microsections indicated some diffusion of the luminophore into gelatin. The luminescence had the same color in both polymers, but the intensity was different; the separating boundary was distinctly visible (Fig. 2), hence the polymers were immiscible. When the polyvinyl alcohol was torn away from gelatin its surface was negatively charged, whereas that of gelatin positively. The break was of the adhesive type.

---

* These figures were given in color in the original and consequently some of the detail has been lost.

2) Perchlorovinyl—guttapercha. A guttapercha film (β-modification) was covered with an ethyl acetate solution of perchlorovinyl. Microsections resembled those of the preceding system. The luminophore, which was originally introduced into the solution of perchlorovinyl in ethyl acetate, diffused into the guttapercha film. The color intensity in the two polymers was different and boundary of separation could be observed. Tearing the two surfaces apart resulted in charge separation—perchlorovinyl film was positive, guttapercha negative. The break was of the adhesive type.

3) Guttapercha—paraffin. A paraffin film was covered with a chloroform solution of guttapercha which had been dyed with the luminophore. We heated this sample for 15 min at 60° in order to obtain the β-form of guttapercha. Microsections (Fig. 3) showed intermixing between adjoining portions of the two polymers and the boundary separating the two solids had faded away; what rendered these observations particularly easy was the fact that paraffin and guttapercha acquired different coloration after absorbing the luminophore. In Fig. 2 one can distinguish isolated red-colored spots where paraffin had penetrated into guttapercha which was green-colored. Thus by using fluorometric techniques we were able to obtain a better idea as to the nature of the studied processes. When guttapercha was torn apart from paraffin the newly formed surfaces were electrically neutral. The break was of the cohesive type.

4) Natural rubber—natural rubber (a case of self-adhesion). A solvent free rubber film (smoked sheet) was covered with a benzene solution of the same rubber containing the luminophore. Microsections indicated such an extensive diffusion that the original boundary separating the two objects had entirely disappeared (Fig. 3).

Tests performed on control samples torn apart revealed a complete absence of any charges on the new surfaces and indicated a cohesive type of break. From the above presented experimental results one can readily deduce the fact that there are many possibilities open for the application of fluorometric analysis in processes occurring at the contact zones of any two polymers.

At the present time radioactive tracer techniques [7] have found many applications in the study of diffusion in solids, particularly in the investigation of diffusion layers on metals. However, it is unlikely that this method could be successfully applied to the study of two-way diffusion at the contact zone between two polymers. In the first place, the polymer would have to be labeled at the synthetic stage, which besides being inconvenient presents certain hazards inherent in this type of work. Besides, not all polymers could be readily labeled in this way. On the other hand, the marking of polymers with a luminophore could in certain cases successfully replace methods involving labeled atoms, particularly in cases where we would like to study processes occurring at the contact of two polymers.

The authors wish to express their gratitude to T. A. Krotova and M. Ya. Vol'pert for their assistance in this work and to corresponding member Acad. Sci. USSR, B. V. Deryagin for some valuable advice and pointers.

LITERATURE CITED

[1] L. P. Morozova, N.A. Krotova, Proc. Acad. Sci. 115, 747 (1957)*; Colloid. J. 20, 59 (1958).*

[2] S. M. Skinner, S. R. Savage, and I. E. Rutzler, Appl. Phys. 24, 4, 438 (1954).

[3] L. P. Morozova, The Nature of Adhesion Between Polymers, Doctoral Dissertation (1958).**

[4] S. S. Voyutskii, Yu. L. Margolina, Progr. Chem. 18, 449 (1947); S. S. Voyutskii, V. M. Zamazii, Colloid J. 15, 407 (1953);* Proc. Acad. Sci. 81, 64 (1951); S. S. Voyutskii, B. V. Shtarkh, Colloid J. 16, 3 (1954)*; Proc. Acad. Sci. 90, 573 (1953); Colloid J. 18, 404 (1956);* S. S. Voyutskii, A. I. Shapovalova, A. P. Pisarenko, Colloid J. 18, 485 (1956);* Colloid J. 19, 274 (1957).*

[5] M. A. Konstantinova-Shlezinger, Luminescence Analysis, Izd. AN SSSR, (1948).**

[6] D. I. Ivanov, Color Photography, (Leningrad, 1957).**

[7] N. S. Gorbunov, Diffusion Layers on Iron and Steel, Izd. AN SSSR (1958).**

Received December 9, 1959

---

* Original Russian pagination. See C.B. Translation

** In Russian.

KINETICS OF THE REACTION BETWEEN HYDROGEN AND OXYGEN ON PLATINUM

E. N. Khar'kovskaya, Corresponding Member Acad. Sci.
USSR, G. K. Boreskov, and M. G. Slin'ko

L. Ya. Karpov Physicochemical Scientific Research Institute

Many workers had studied the kinetics of the reaction between hydrogen and oxygen, but unfortunately their results were often contradictory. Most of the work was done over a narrow oxygen and hydrogen concentration range and either by the use of static techniques [1-3], which did not allow any determinations of the catalytic activity under equilibrium conditions, or in certain types of flow apparatus [4-5] which made precise reaction rate measurements impossible due to the difficulties involved in maintaining isothermal conditions all the way along the catalytic surface and the additional interferenceof mass-transfer processess.

In the present work we used a stationary flow method [6-7] for measuring the catalytic activity of platinum with regard to the reaction between oxygen and hydrogen over a wide range of concentration; this method made it possible to measure directly the equilibrium reaction rate under isothermal conditions, and in the absence of distorting hydrodynamic effects.

A platinum wire used in our work was 0.1 mm in diameter and had the composition: 99.88% Pt, 0.03% Pd, 0.06% Ir. The true surface area of the wire (determined electrochemically [8]) was 51 cm^3.

The experiments were carried out over a temperature range from 20 to 180°, under pressures from 50 to 750 mm, and with various compositions of the initial reactions mixture: hydrogen, nitrogen—hydrogen mixtures, nitrogen,nitrogen—oxygen mixtures, and oxygen.

Concentration of the oxyhydrogen mixture did not exceed 7%. The gases were circulated at the rate of 400-1100 liters/hr, depending on the composition of the reaction mixture.

The percent oxygen and hydrogen concents in the gaseous phase (P) was computed from the increase in the pressure of the system, relative to the initial pressure before the reacton mixture was introduced; the amount of current used up in the electrolytic cell told us how much oxyhydrogen mixture we had, in cubic centimeters per hour (ω).

EXPERIMENTAL RESULTS

In order to check the effects of mass and heat transfer we determined the temperature difference between the gas and the catalyst, and varied the circulating rate from 250-1100 liters/hr. It turned out that the catalyst was at the same temperature as the gaseous stream, and that the reaction rate did not depend on circulating velocity ; all this indicated that transfer processes could not have in any way affected our experimental reaction rates.

Effects of the nitrogen partial pressure. By varying the initial partial pressure of H_2, O_2 and N_2 we were able to vary the ratio of hydrogen to oxygen over a wide range of values and still preserve all the safety requirements

On the basis of experimental results we established the fact that the reaction rate was independent of the N_2 pressure and was solely determined by the partial pressures of H_2 and O_2.

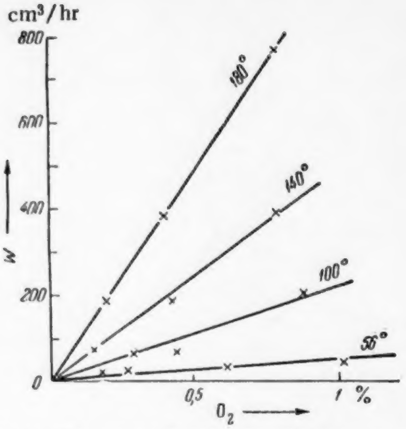

Fig. 1. The rate of hydrogen oxidation as a function of oxygen concentration in gaseous mixtures containing a large excess of hydrogen.

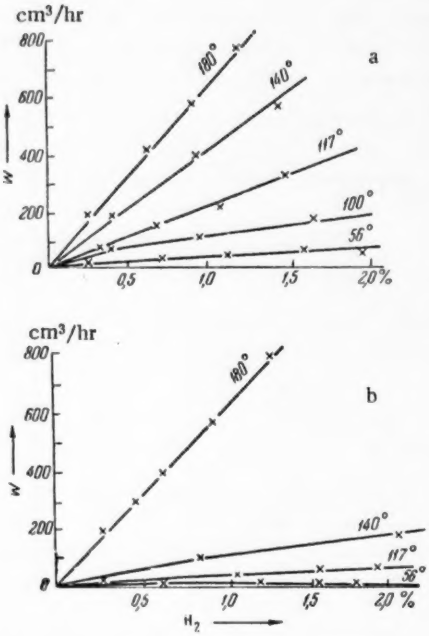

Fig. 2. Rate of hydrogen oxidation as a function of hydrogen concentration in gaseous mixtures containing a large excess of oxygen. a) In the region of high activity ; b) in the region of low activity.

Determination of the reaction order. In Fig. 1 we have presented the results of measurements performed on gaseous mixtures containing excess H_2. The Figure shows quite explicity that within the 50-180° temperature range the reaction rate was directly proportional to the concentration of O_2. The activation energy was 7800 cal/mole.

When using gaseous mixtures with a large excess of H_2 it was extremely important to remove all the O_2 from platinum by exposing it to H_2 gas at 600° before carrying out the experiment [9]. Platinum which had not been pretreated with H_2 was slightly passive and at low temperatures the reaction would be of the zero order with respect to O_2. When the preliminary treatment with H_2 was carried out for 3 and 6 hours at 900° the activity of platinum increased by 2-2.5 times, but after 2.5-3 hours the activity returned to its equilibrium value.

In Fig. 2 we have presented the results of measurements carried out on gaseous mixtures containing a large excess of O_2. After a rapid transition from high (180°) to low temperatures (100-56°) we observed high platinum activity and first order reaction rate with respect to H_2 (Fig. 2a). After a long interval between operations and a quick evacuation at low temperatures the platinum exhibited low activity. The reaction order with respect to hydrogen declined to 0.1-0.2 (Fig. 2b). At the same time the rate of the reaction decreased to 1/10 to 1/15th of its original value. A rapid transition from 180° to lower temperatures yielded a low activation energy, 2400-4600 cal/mole. In the range of low activity and after a transition from low to high temperatures, the activation energy was 8000 cal/mole.

By using a stoichiometric oxygen to hydrogen ratio (Fig. 3) and lowering the temperatures to 100° we succeeded in maintaining a first order reaction with respect to the sum of H_2 and O_2 partial pressures. At lower temperatures the the order of the reaction declined to 0.2. The activation energy in the region where we had a first order reaction was 6700 cal/mole.

Relationship between the reaction rate and the concentration of oxygen and hydrogen. In Fig. 4 we have presented the reaction rates determined at 180° in mixtures containing excess H_2 (P_{H_2} from 760 to 4.1 mm at a constant O_2 partial pressure, $P_{O_2} = 2.05$ mm, and in mixtures containing excess oxygen $P_{O_2} = 2.05$-760 mm at a constant hydrogen partial pressure $P_{H_2} = 4.1$ mm).

When the temperature was lowered from 180° to 120° the over-all effect of H_2 and O_2 partial pressures on the reaction rate remained practically the same, except that the maximum activity was somewhat displaced toward the region of a large excess of O_2 ($P_{O_2} = 160$ mm).

Oxidation of deuterium. The experimentally determined rates of the reaction between deuterium and oxygen showed that in gaseous mixtures containing a large excess of O_2 the ratio between the hydrogen and deuterium oxidation rates was 1.3 in the high activity region and 2.0 in the low activity region. With stoichiometric amounts of H_2 and O_2 the ratio between the oxidation rates of H_2 and deuterium was 1.5 at 100° and 1.98 at 180°.

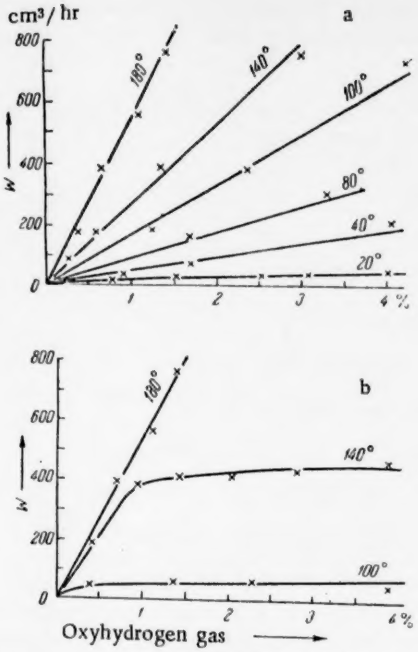

Fig. 3. The rate of hydrogen oxidation as a function of the oxyhydrogen gas concentration at a stoichiometric hydrogen to oxygen ratio. a) High activity region ; b) low activity region .

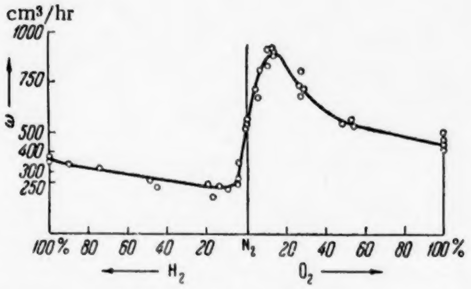

Fig. 4. The oxidation rate of hydrogen as a function of hydrogen and oxygen concentrations at 180°.

Under conditions where H_2 was in a large excess the ratio between the oxidation rates of H_2 and D_2 was 1.6 at 180° and 2 at 100°. This clearly indicates that the activated complex formed in the rate determining step of the reaction between O_2 and H_2 must include hydrogen.

Discussion of results. Our kinetic results cannot be generalized by the use of previously proposed kinetic equations. Thus, though Langmuir's equation

$$\omega = \frac{k_1 k_2 P_{O_2} P_{H_2}}{k_1 P_{H_2} + k_2 P_{O_2}} ,$$

explains the first order with respect to one of the components when the other one is in excess, still it does not represent the true relationship between the reaction rates and partial pressures of O_2 and H_2 over a wide range of gas compositions, and it fails to explain the decreased reaction order at lower temperatures.

If we take into account the effects of nonhomogeneity we will get a similar equation, but containing small exponentials. This equation can't account either for the sum total of experimental data, especially for the existence of extremes when oxygen and hydrogen concentrations are switched or for the decreased reaction order when the temperature is lowered.

The experimental data show that catalytic reactions are very complex; in order to explain the observed phenomena we would have to consider the various forms of chemisorption possible for the reacting gases and the effects of the reaction mixture itself on the properties of the catalyst [10].

For mixtures containing excess H_2 the first order with respect to O_2 and the slight dependence on the pressure of H_2 permit the assumption that the rate determining step is the reaction between the chemisorbed atomic hydrogen (which covers the entire surface) and molecular oxygen. What makes oxygen react even more readily is its ability to interact with the d-electrons of the catalyst (type C absorption according to Dowden's classification [11]). The reduced catalytic activity observed when oxygen had not been completely removed before the reaction was due to tightly bound oxygen atoms which were probably located under the platinum surface (type B) and bound the d-electrons of the metal.

As the excess hydrogen is reduced and we approach stoichiometric mixtures a portion of the platinum surface becomes free of hydrogen and the chemisorption of oxygen (type A) followed by dissociation into atoms becomes possible. Within these concentrations the reaction proceeds as a result of an interaction between hydrogen and the absorbed atomic oxygen, which requires a smaller activation energy and is responsible for the increased reaction rate.

With an excess of oxygen we can have two stationary states which will differ in their reaction rates and in the dependence of rate on the concentration of components. The nature of the transition from rapid to slow reaction state permits the assumption that the fast reaction represents a chain reaction involving some energetic (endothermally formed) species which are being constantly regenerated in the course of reaction. At lower temperatures and pressures these unstable intermediates disappear, leaving behind only the relatively tightly bound oxygen, whose reaction with hydrogen is slow and requires higher energies.

It seems that the decreased rate observed at higher oxygen pressures under usual conditions for a fast reaction is connected with a partial blocking of the platinum surface by tightly bound oxygen.

LITERATURE CITED

[1] L. Langmuir, Trans. Farad. Soc. 17, 621 (1922).

[2] S. Z. Roginskii, V. S. Rozing, Sci. Rep. Leningrad Univ. 5, 38 (1938).

[3] S. Z. Roginskii, O. V. Krylov, Proc. Acad. Sci. 91, 1343, No. 6 (1953).

[4] W. A. Bone and R. V. Wheeler, Proc. Roy. Soc. A. 77, 146 (1906).

[5] S. Ya. Pshezhetskii and M. L. Vladavets, J. Phys. Chem. 14, 353 (1950).

[6] B. K. Boreskov, M. G. Slin'ko, and A. G. Filippova, Proc. Acad. Sci. 92, No. 2, 353 (1953).

[7] M. I. Temkin, S. L. Kiperman, and L. T. Luk'yanova, Proc. Acad. Sci. 74, No. 4, 763 (1950).

[8] T. I. Borisova and M. A. Proskurnin, Acta. Physicochim. URSS, 4, 819 (1936).

[9] G. K. Boreskov, M. G. Slin'ko, and V. S. Chesalova, J. Phys. Chem. 30, 2787 (1956).

[10] G. K. Boreskov, J. Phys. Chem. 32, 2739 (1958).

[11] D. A. Dowden, Bull. Soc. Chim. Belges. 67, 439 (1958).

Received March 30, 1959

ELECTROSTATIC REPULSION BETWEEN ELECTRICAL DIFFUSION LAYERS ON TWO-SIDED LIQUID FILMS

A. Sheludko and D. Ekserova

Physical Chemistry Institute of the Bulgarian Academy of Sciences

(Presented by Academician A. N. Frumkin, March 7, 1959)

Bartsch's work [1] on the stability of foams showed that electrolytes could be used to extend the life of foams stabilized by low-molecular weight foaming agents, which led us to the conclusion that there must be repulsion between the electrical diffusion layers on the two sides of aqueous films. This experimental data indicated that the stability of foams decreased with increasing electrolyte concentration and that the concentrations influencing the stability were of the same order of magnitude as those producing rapid coagulation of hydrophobic colloids; the minimum concentration capable of reducing the stability of foams depends on the valence of the active ions in approximately the way one would expect from the Schultze-Hardy rule .

B. V. Deryagin and Titevskaya [2] were the first to establish by direct measurements the repulsion between diffusion layers on isolated foam films prepared in dilute aqueous solutions of undecylenic acid and calculate the potential under the solution surface responsible for this repulsion; they obtained very reasonable values of the order of 50-80 mv. Unfortunately they failed to control accurately their electrolyte concentration, which gave rather unreliable values for the calculated potential φ_0 of Gouy's layer. We therefore considered it worthwhile to carry out a new investigation under optimum working conditions in order to check the theory of electrostatic repulsion between Gouy's layer. This verification is also interesting for the simple reason that in thin films one may also expect some additional pressures reinforcing the usual wedge effect caused by the electrical diffusion layers.

The most complete theory of the electrostatic wedge effect was developed by B. V. Deryagin and L. D. Landau [3] (presented by Overbeeck and Kruyt's book [4]) ; it gave the following expression for the "wedge pressure" ,

$$\Pi_{el} = 2\pi nkT\left(\mathrm{ch}\,\frac{e}{kT}\,\varphi_\alpha - 1\right) \tag{1}$$

in a mono—monovalent dissociated electrolyte at a concentration of n-molecules per 1 cm^3 . In this case k is the Boltzman constant, T the absolute temperature, e the ionic charge , and φ_α the potential inside the foam film.

The potencial φ_α can be calculated by assuming that it is equal to double the potential at a distance h/2 (where h is the film thickness) from the surface of an infinite liquid. Such an approximation limits the theory to fairly thick films, since it implies that the field on one side of a film surface is not deformed by the field on the opposite side. This limitation also follows (though seemingly to a lesser extent) from the assumption that the surface potential φ_0 and the dielectric constant E are independent of the film thickness. Therefore the theory should be checked on rather thick films.

The above made assumptions concerning φ_α yield the following relationship between h and φ_α :

$$h = 2\sqrt{\frac{\varepsilon kT}{8\pi ne^2}}\ln\frac{\gamma_{\varphi_0}}{\gamma_{\varphi_\alpha}}, \quad \gamma_{\varphi_0} = \frac{\exp\frac{e}{2kT}\varphi_0 - 1}{\exp\frac{e}{2kT}\varphi_0 + 1}, \quad \gamma_{\varphi_\alpha} = \frac{\exp\frac{e}{2kT}\frac{\varphi_\alpha}{2} - 1}{\exp\frac{e}{2kT}\frac{\varphi_\alpha}{2} + 1}. \tag{2}$$

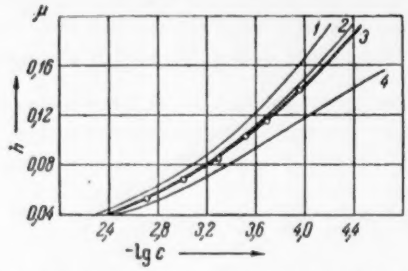

Fig. 1. 1) 200 mv; 2) 100 mv; 3) 90 mv; 4) 50 mv.

TABLE 1

C, in moles/liter	Correction, %	h, μ
$1{,}13 \cdot 10^{-4}$	13,0	0,139
$2{,}05 \cdot 10^{-4}$	2,5	0,114
$3{,}13 \cdot 10^{-4}$	4,3	0,104
$5{,}20 \cdot 10^{-4}$	4,0	0,083
$8{,}10 \cdot 10^{-4}$	1,25	0,067
$2{,}02 \cdot 10^{-3}$	1,0	0,050

In Fig. 1 we have plotted the curves of h against log C (C is the electrolyte concentration in moles per liter) calculated from Equations (1) and (2) for various values of φ_0 and at a constant value of $\Pi_{el} = 730$ at 25°.

Measurements were carried out on microscopic two-sided liquid films in an apparatus described in [5], but with an improved photometric technique described in detail in [6]. The foam film was under the action of a constant sucking tension along the concave ends. This capillary tension $2\sigma/R$ (where σ is the surface tension of the liquid, and R = 0.2 cm the radius of the tube inside which a bi-concave drop was suspended containing a microscopic foam film in the middle) stretched the film until the positive wedge pressure inside the film became equal to it. We would then get a stable equilibrium film whose thickness corresponded to h in Eq. (2) at a pressure $\Pi_{el} = 2\sigma/R$, provided, of course, there were no other components of the wedge pressure. The values of h were determined at various electrolyte concentrations.

In trying to find the optimum conditions for the verification of the theory of the electrostatic wedge effect we found that the proper choice of a foaming agent was very important. Of the stabilizers we tested: sodium oleate, compound OP-10, isoamyl alcohol, and saponin, the last one turned out to be the most suitable. Saponin (Schering Saponin gereinigt) preserved the required tensile strength of foam films at very low concentrations, $5 \cdot 10^{-4}$ %. At the same time the surface tension of the solution was not very different from that of water, so that the capillary suction and consequently also Π_{el} (equal to it at equilibrium) could be considered constant and equal to 730. Our electrical conductance measurements indicated that some undetermined electrolytes introduced into the solution even at low saponin concentration, although present in trace quantities still had to be taken into account. The twice distilled water used by us had an electrical conductance $K_{25} = 1.12 \cdot 10^{-6}$, while saponin solution had $K_{24} = 1.94$%. For a 10^{-4} mole/liter KCl solution (our lowest concentration) such an electrical conductance increase was equivalent to a ~ 10% increase in KCl concentration. Any corrections calculated for the KCl concentration were approximate anyway, since the nature of the electrolyte introduced with saponin was not known. Fortunately, these corrections were small enough to make such calculations quite permissible. The errors resulting from such concentration adjustments quite obviously decreased at higher electrolyte concentrations. In Table 1 we have listed the values of KCl concentrations thus corrected, the corrections in percent, and the corresponding equilibrium values of h. These values are plotted in Fig. 1 (dots), and they fit quite well the curve corresponding to a 90 mv potential.

We have also checked (approximately) the effects of electrolyte valence on the electrostatic repulsion on films. At low values of φ_α Equations (1) and (2) for Z–Z-valent electrolytes can be presented in the form:

$$\Pi_{el} = 64\, nkT \gamma_{\varphi_0}^2 h \exp \sqrt{\frac{8\pi n e^2 Z^2}{\varepsilon kT}}, \quad \gamma_{\varphi_0} = \frac{\exp \frac{eZ}{2kT}\varphi_0 - 1}{\exp \frac{eZ}{2kT}\varphi_0 + 1}, \tag{3}$$

so that for two binary electrolytes with valences Z_1 and Z_2 and equal Π_{el}, φ_0, and n we will get:

$$\frac{h_1}{h_2} = \frac{Z_2}{Z_1}. \tag{4}$$

With $BaCl_2$ and KCl at C = $5 \cdot 10^{-4}$ moles/liter we get 0.045 and 0.088 μ respectively for the equilibrium film thickness; with $La(NO_3)_3$ and KCl at C = 10^{-4} moles/liter we obtained 0.048 and 0.154 μ respectively. Though the width ratios obtained satisfied Eq.(4) the verification of the theory was only approximate, since the electrolytes used were unsymmetrical.

The results obtained indicate that the theory of electrostatic repulsion between electrical diffusion layers on two-sided liquid films accurately describes the observed formation of equilibrium films thicker than 0.05 μ. Hence we are allowed to assume that for the electrolyte concentrations used and with the film thickness obtained no other components of the wedge pressure were present, at least not to any measurable extent. This conclusion is rather surprising, for according to the calculations based on the London forces existing between water molecules we should observe large negative wedge effects in films of the order of 0.1 μ or thinner. We detected this type of pressure (though weaker than the one expected theoretically) in foam films stabilized with OP-10 and saponin [6] at a KCl concentration of 0.1 moles/liter. We finally have to assume that the absence of any measurable van der Waal's effect in the films studied in this paper was due to the low electrolyte concentration and that any concentration increase in the region where the electrostatic repulsion is already suppressed should lead to an increased negative wedge pressure. These assumptions, obviously, need a direct proof; we are working on it at the present time.

LITERATURE CITED

[1] O. Bartsch, Koll. Beih. 20, 1 (1924).

[2] B. V. Deryagin, A. S. Titievskaya, Colloid J. 15, 416 (1953).*

[3] B. V. Deryagin, L. D. Landau J. Exptl. Theor. Phys. 15, 663 (1945).

[4] G. R. Kruyt, Colloid Science (IL, 1955) [Russian translation].

[5] A. Scheludko, Koll. Zs. 155, 39 (1957).

[6] A. Sheludko, D. Ekserova, Bull. Bulgarian Acad. Sci. (1959), in press.

[7] A. Sheludko, Proc. Acad. Sci. USSR 123, No. 6 (1958)*.

Received February 27, 1959

---

* Original Russian pagination. See C.B. Translation.

THE FLOW OF ELASTICOVISCOUS FLUIDS UNDER THE ACTION OF TWO MUTUALLY PERPENDICULAR SHEARING FORCES

G. V. Vinogradov, A. A. Mamakov, and V. P. Pavlov
Institute of Petrochemical Synthesis of the Academy of Sciences,USSR

(Presented by Academician V. A. Kargin, March 2, 1959)

In the gap between two coaxial cylinders one can achieve both axial and circumferential flow, which makes it possible to compare various forms of flow in elasticoviscous fluids in the same apparatus by varying the uniformity of the shearing field and velocity gradients, and also study the influence of one form flow on the other. It seems that so far no one has carried out a systematic study of the mutual interactions of various modes of deformation in elasticoviscous fluids, although the problem is of a considerable theoretical and practical interest. It is important in the general analysis of problems associated with all sorts of states under compound stresses and in the determination of how to detect and correct for the mutual interaction of various deformations. The practical aspects of the problem involve the fact that many elasticoviscous fluids are forced to flow under conditions of compound stress.

In this paper we have analyzed the results obtained with a plastic dispersed liquid exhibiting a very well pronounced anomalous viscosity, and namely an aliphatic grease consisting of 86.2% spindle oil, 12% Ca-soap of cotton seed oil, and 1.8 % water. A control experiment was carried out on a highly viscous Newtonian Fluid, a product obtained by selective solvent extraction of the tars and polycyclic aromatic hydrocarbons found in crude petroleum residues. The experiments were done in a double rotational viscosimeter [1]. The instrument consisted of two coaxial cylinder viscosimeters which differed from each other only in the length of their working cylinder surfaces. Inside the gap between the cylinders we maintained a homogeneous shearing field (τ_{circ}) relative to the circumferential flow; our precision was 97.5 %. The use of two instruments which differed only in the length of their cylinders enables us to disregard any end effects. All the calculations were modeled on those in paper [1]. A double viscosimeter with coaxial cylinders was also used for the study of axial flow. In this case the viscosimeters were attached to an instrument which controlled and ensured steady-state conditions during the experiment [2]. The substance studied was first squeezed through the annular gap of one viscosimeter, then through the gap of the other viscosimeter in another set of experiments. In this manner we eliminated any edge effects associated with the axial flow. The temperature was maintained constant within ± 1° .

The axial flow of Newtonian [3] and elasticoviscous [4,5] fluids through a narrow annular gap was reduced to the case of flow through a flat slit. The shearing stress on the walls of an annular gap $\tau_{\mathrm{ax}} = \Delta p \dfrac{H}{2L}$, where Δp is the pressure drop per unit length in the axial direction of the gap, H the width of the gap, and L the cylindrical surface generatrix on which the pressure drop is measured. The differences between various τ_{ax} values on cylindrical walls did not exceed 1.5 %. From this standpoint the above presented equation for τ_{ax} is valid. For this type of flow we will assume that the mean velocity gradient $\bar{D}_{\mathrm{ax}} = Q(2\pi RH^2)^{-1}$, where Q is the delivery and R the radius of the inner cylinder. The mean velocity gradient $\bar{D}_{\mathrm{ax}}$ for flow in annular gaps was reduced to the velocity gradient on walls D_{ax} by the method given in [6].

When our experimental method and calculations were checked in control experiments on the extract , the agreement between circumferential and axial flow was excellent, just as one would expect. Between 20 and 50°C and over a range of velocity gradients covering more than three orders of magnitude the calculated

TABLE 1

Point nos. in Fig. 1	1	2	3	4	5	6	7
Q, cm³/sec	$1,4\cdot10^{-3}$	$4,77\cdot10^{-3}$	$1,34\cdot10^{-2}$	$6,03\cdot10^{-2}$	$2,03\cdot10^{-1}$	$6,05\cdot10^{-1}$	1,82
$\overline{D}_{ax}$, sec^{-1}	0,201	0,65	1,82	8,22	27,6	82,2	248

Note. The points of net circumferential flow are denoted by squares in all the figures.

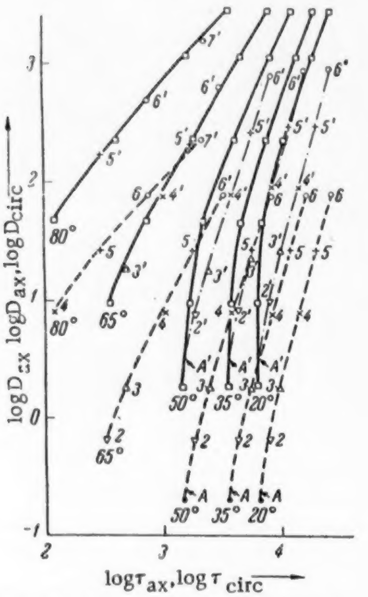

Fig. 1. Characteristic curves for the circumferential and axial flow, and net curves for axial flow.

values did not differ by more than 5% from the experimental. The experimental results obtained on solidol are plotted in Fig. 1 in a log-log scale. Here, as well as in all the subsequent figures the shearing stress is given in dyne/cm^2 and velocity gradient in sec^{-1}. The solid lines for D_{circ} (τ_{circ}) represent the results obtained for circumferential flow. They were obtained by going from low to high D_{circ} after achieving stationary conditions in each experiment. The dotted lines represent $\overline{D}_{ax}(\tau_{ax})$ functions obtained for the axial flow. The experimental points on these curves are numbered 1-7 successively, while points A were determined in the intervals between points 1 and 2. The values of $\overline{D}_{ax}$ and the designations of the corresponding experimental points are given in Table 1.

The transition from $\overline{D}_{ax}$ to D_{ax} values is denoted by points A' and 2'-7' on D_{circ} (τ_{circ}) curves. In each case where the calculated points 2'-7' diverged from the experimental D_{circ} (τ_{circ}) curves, we plotted a calculated $D_{ax}(\tau_{ax})$ flow curve through them; these are given in Fig. 1 by the dot-and-dash lines. The divergence between these lines and the circumferential flow curves is connected with the fact that at higher axial flow velocities one does not attain the ultimate fluid structure deformation usually expected under fixed flow conditions; such deformation takes place only after the circumferential flow had been maintained for a long time under the D_{circ} conditions. It was demonstrated that after the grease had been first subjected to intense deformation during high-velocity circumferential flow, flow curves for the circumferential and axial flows coincided.

Under conditions of simultaneous axial and circumferential flow we applied various constant fluid-input rates, then measured Δp and the stretching moments at various D_{circ}. The results for solidol are given in Fig. 2. Here the No. 1 curves represent only the axial flow ($D_{circ} = 0$); the curves 2-7 give the D_{ax} (τ_{ax}) functions for D_{circ} values equal to: 8.7, 40, 78, $2.6\cdot10^2$, $8.7\cdot10^2$, $3.5\cdot10^2$ sec^{-1} respectively.

The circumferential flow under a homogeneous shearing field deforms the fluid structure inside the entire gap between the coaxial cylinders and actually converts the plastic material into an elasticoviscous liquid. The larger the D_{circ} the more will the effective viscosity of the system be decreased. Therefore, for a given D_{ax} the τ_{ax} will decrease with increasing D_{circ}, and for a given τ_{ax}, D_{ax} will increase sharply with increasing D_{circ}. It turns out that the force required to produce axial flow in plastic systems in the presence of circumferential flow is very insignificant compared to the force needed in the absence of circumferential flow [7]. The outstanding property of systems where circumferential flow acts on the axial is the linear dependence of D_{ax} on τ_{ax} at low values of τ_{ax}. And consequently, known elasticoviscous liquids may under those conditions behave like Newtonian liquids. At large and very large D_{ax} (relative to D_{circ}), as well as at elevated temperatures, the effects of circumferential flow become insignificant. Consequently with increasing τ_{ax}, Curves 2-4 in Fig. 2 will assymptotically approach Curve 1.

The effects of D_{circ} on τ_{ax} at various constant D_{ax} values are represented by the thin solid lines I-VI in Fig. 2. In accordance with that was just said, in systems where the anomalous viscosity was well pronounced at large D_{ax} the circumferential flow became effective at high D_{circ} (Curve 1, at 20°). One can safely assume that at low τ_{ax} values D_{circ} is inversely proportional to τ_{ax}.

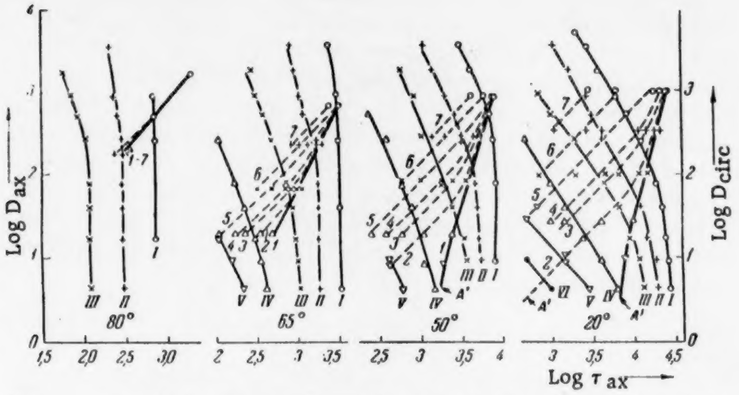

Fig. 2. The effects of circumferential and axial flow on the axial force.

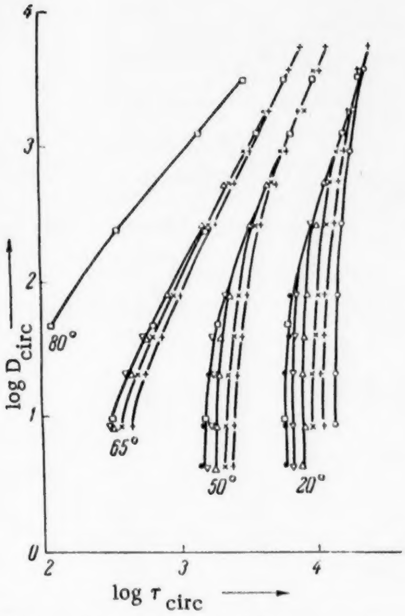

Fig. 3. The effect of axial flow on circumferential.

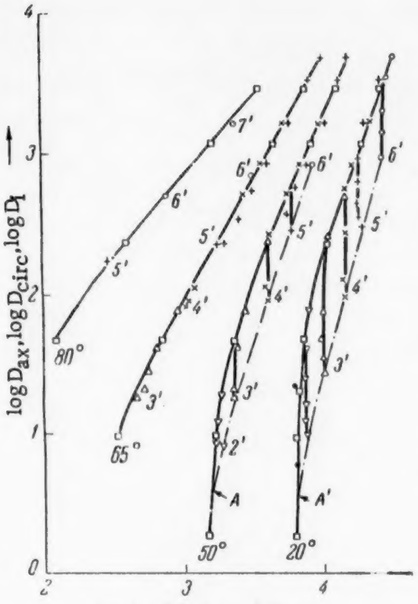

Fig. 4. Characteristic circumferential and axial flow curves and generalized curves for flow under compound forces.

The effect of axial flow on circumferential is represented by the family of curves in Fig. 3. The extreme left curves in each family represent net circumferential flow and cases where a slow axial flow was superimposed on the circumferential. As one moves to the right the curves become steeper and correspond to increasing D_{ax}. The axial flow not only raised slightly the deformation strength against circumferential flow, but also the anomalous viscosity which the system exhibited during circumferential flow. The larger the D_{ax} relative to D_{circ} the more pronounced will this effect be.

The effect is related to the fact that when axial flow is imposed on circumferential, fresh grease is being continuously fed into the annular gap and the time it spends inside the gap is not sufficient to attain the ultimate structural deformation corresponding to the given flow conditions. The examined effect sharply declined at higher temperatures and whenever the grease had been previously subjected to a very high D_{circ} (homogenized).

While analyzing the mutual effects of two net stresses on each other we had to check and see if they were superimposable. The simplest calculation is based on a geometrical addition of τ_{circ} and τ_{ax} and of corresponding velocity gradients. This will be fully valid for Newtonian liquids (the case of the extract). In cooperation with N. V. Tyabin we have shown that a similar approach is also permissible (at least as a first approximation) in elasticoviscous fluids. This is best illustrated in Fig. 4, which was constructed in the same way as Fig. 1. In Fig. 4, besides the $D_{circ}(\tau_{circ})$ and $D_{ax}(\tau_{ax})$ functions, we have used solid lines to show the $D_i(\tau_i)$ functions, where D_i and τ_i were the corresponding resultant velocity gradients and shearing stresses. One can see in Fig. 4 that the generalized flow curves under compound forces fall inside a fork formed by the circumferential and axial flow curves. They correspond to different D_{ax} = const. and continually varying D_{circ}. When the $D_{ax}(\tau_{ax})$ and $D_{circ}(\tau_{circ})$ curves coincide we get a single generalized $Di(\tau_i)$ curve which includes all the possible combinations of axial and circumferential flow conditions at a constant temperature.

The writers wish to express their gratitude to Academician V. A. Kargin for his interest in this work, general comments, and valuable advice.

LITERATURE CITED

[1] V. P. Pavlov, Trans. 3rd All-Union Conference on Colloidal Chem, Izd. AN SSSR, p. 144 (1956).*

[2] G. V. Vinogradov and V. P. Pavlov, Coll. Low-Temperature Properties of Petroleum Products, p. 61 (1949).*

[3] S. M. Targ, Fundamental Problems in the Theory of Laminar Flow, Vol. 2 (Leningrad, 1951).*

[4] M. V. Volarovich and A. M. Gutkin, J. Tech. Phys. 16, 321 (1946).

[5] P. K. Shipanov, Colloid. J. 11, 363 (1949).

[6] J. W. Amner and J. Blott, The Principles of Rheological Measurements, p. 25 (London, 1949).

[7] L. A. Shklyar, Rheological Study of the Behavior of Plastic Greases in Sealed Friction Joints, Doctoral Dissertation, Kazan (1954).*

Received March 21, 1959

---

* In Russian.

DEPENDENCE OF THE DEGREE OF DISPERSION OF ALUMINUM AEROSOLS ON THE PREPARATORY CONDITIONS

M. S. Gen, M. S. Ziskin, and Yu. I. Petrov

Institute of Chemical Physiscs of the Academy of Sciences ,USSR

(Presented by Academician V. N. Kondrat'ev , March 13, 1959)

Finely dispersed metals possess a highly developed surface, which renders them extremely reactive, both chemically as well as absorptionwise. Therefore it seemed very important to carry out a study which would relate the reactivity of metals to their degree of dispersion, particularly when dealing with particles smaller than 10^{-5} cm. It is very difficult to prepare such highly dispersed systems with any degree of particle size uniformity by means of mechanical disintegration.

Gen, Zel'manov, and Shal'nikov[1] showed that it was possible to prepare metallic aerosols by evaporating and condensing the metals in an atmosphere of inert gases or vapors. We used this technique to prepare our aluminum powders.

We placed a weighed Al sample (100 mg) on a tungsten loop located inside a glass container 8 cm in diameter. After evacuating and degassing the flask at $\sim 10^{-5}$ mm of Hg we filled it with argon, helium, or hydrogen to the desired pressure and vaporized the entire weighed sample within 2 min.

The loose and easily removed deposit on the water-cooled vessel walls exhibited different hues depending on the nature and the pressure of the inert gas; the color varied from a deep black to light grey, and the black deposits would occasionally ignite spontaneously in contact with air. The extracted deposits were analyzed chemically for their metal content by measuring the hydrogen evolved upon treatment with weighed samples of alkali. The analytical precision was $\approx 2\%$ (by weight).

In several experiments we allowed a known volume of oxygen into the flask after the Al was vaporized and determined the extent of Al oxidation from the drop in oxygen pressure.

A model ÉMZ electron miscroscope was used to study the degree of dispersion in our aerosols. The object was deposited on a collodion film from a suspension in distilled water. The magnification was calibrated by means of wollastonite wire fastened with Wood's alloy at the end of the lens holder socket in place of the screen.

The dimensions of the wire and of the negative impression were measured with an IZA-2 comparator. On some of the better photographs the resolving power was ≈ 30 A.

The degree of dispersion was determined by measuring and counting the number of particles on each photograph ; sample photographs are shown in Fig. 1.

The differential and integral particle distributions obtained in this manner were consistent and are shown in Fig. 2 for an experiment done at 27 mm of Ar. From the differential distribution we determined the mean suspended particle size.

Figure 3 shows the relationship between the mean suspended particle size and the pressure and nature of the gas.

In all our experiments the majority of particles did not deviate (in size) from the mean by more than a factor of two. With decreasing mean particle size the deposits grew darker. The curves in Fig. 3 show that above

TABLE 1

Gas	Gas pressure, in mm	Deposit oxidation (from O_2 adsorption), %	Analyzed metal content in the deposit,%
H_2	19	—	86
	36	—	86
He	4	17	83
	12	15	80
	31	20	78
Ar	1	24	81
	3	19	82
	5,5	13,5	85
	8	—	86
	15	—	95
	23	—	97
	24	—	96
	26	—	92
	27	—	92

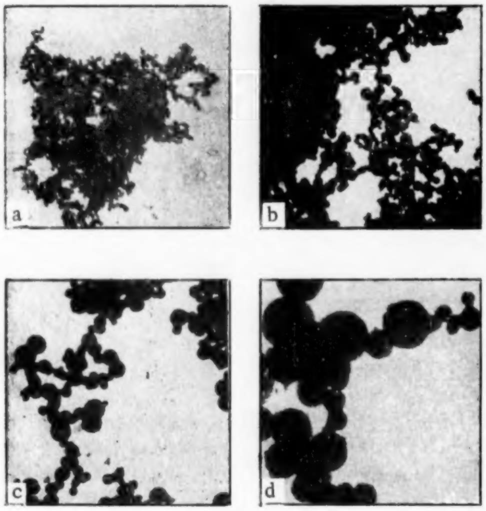

Fig. 1. Al aerosols prepared at various Ar pressures: a) 3 mm; b) 19 mm; c) 27 mm; d) 27 mm. For a, b, and c magnification was 11550 ×, for d 20800 ×.

a certain pressure the mean particle size would not change any more, attaining a value characteristic for each gas. At gas pressures below 1 mm deposits were obtained in which the particle dimensions were of the same order of magnitude or smaller than the resolving power of the electron microscope ($\sim 10^{-7}$ cm).

In Table 1 we have listed the experimentally determined oxidizing powers of these deposits and the chemical analysis data on powders oxidized under atmospheric conditions.

Figure 1 shows the relationship between the metal content in the deposits and the mean particle size. Calculations based on these data showed that the oxidized layer thickness depended only slightly on the particle size consisting generally of about ten molecular layers.

When the powders were subsequently stored under atmospheric conditions for several months their composition and color remained practically unchanged.

The dependence of particle size on the pressure and nature of the gas can be explained qualitatively by assuming that the formation and growth of aggregates can occur only in those gas regions where we have a sufficient concentration of metal atoms with an energy below a certain value. At low pressures, Al atoms may reach the vessel walls without ever colliding with other particles and form a mirror-like deposit. Above certain pressures an aggregation zone will appear near the walls, which will expand toward the center with increasing pressure.

The widening of the aggregation zone will be accompanied by increasing particle size, which is due to the increased number of collisions and the longer path to the walls (initial curve segments in Fig. 3). At pressures corresponding to the flat portions of the curves in Fig. 3 the particles cease growing since the metal atoms are all used up. The relative positions of Ar, H_2, and He curves can be attributed to different exchange energies, following collisions between Al atoms and gas molecules, which depend on the mass and structure of the gases.

A characteristic property of the aerosols obtained is the spherical shape of their particles; an understanding of their structure may shed some light on certain peculiarities observed in the formation of solids. We are currently conducting experiments along these lines.

We feel obligated to express our gratitude to Corresponding Member Acad. Sci. USSR, A. I. Shal'nikov for his valuable advice and several hints.

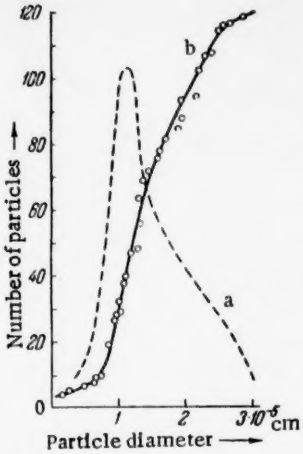

Fig. 2. Differential (a) and integral (b) particle distribution curves at 27 mm Ar pressure.

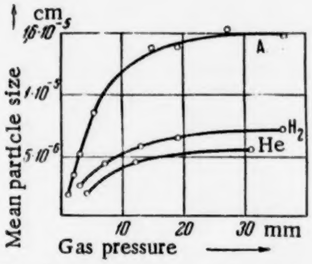

Fig. 3. Dependence of the mean suspended particle size on the pressure of A, H_2, and He.

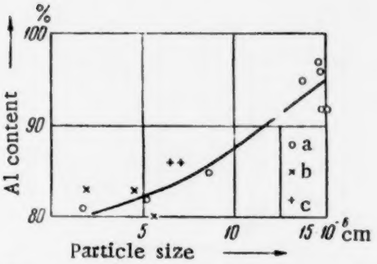

Fig. 4. Dependence of the Al content in the deposit on the mean particle size. a) A ; b) He; c) H_2 .

LITERATURE CITED

[1] M. I. Gen, I. L. Zelmanoff and A. I. Schalnikoff, Koll. Z. 63, H. 3 (1933).

Received March 3, 1959

SENSITIZATION OF RADIOCHEMICAL REACTIONS BY MEANS OF IONIC CHARGE TRANSFER

M. T. Dmitriev and S. Ya. Pshezhetskii
L. Ya. Karpov Physicochemical Institute

(Presented by Academician S. S. Medvedev, March 5, 1959)

Sensitization is one of the means used to accelerate radiochemical reactions. Unlike the case of photosensitization, where excitation energy is transferred, radiochemical reactions can be sensitized through charge transfer during the collisions between ions and molecules.

As is well known, the formation of reactive species through primary ionization is a special feature of radiochemical reactions. Hence a charge transfer may help increase the number of reactive ions. The same principle, of course, may be used to suppress undesirable radiochemical reactions.

In order to find out how effective would a sensitization (of radiochemical reactions) based on the ionic charge transfer principle be, we made use of a reaction previously studied by us—the radiochemical oxidation of nitrogen by oxygen.

We had already established [1] that the reaction proceeded through the formation of nitrogen ion molecules (N_2^+), and that the rate was proportional to the effective nitrogen ionization. Therefore by increasing the N_2^+ ion concentration we should accelerate the reaction, while the increase may be achieved through the transfer of electrons from nitrogen molecules to the inert gas ions; the latter are formed when the gaseous mixture is irradiated. We used for this purpose helium, neon, and argon. The ionization potentials of He, Ne, and Ar atoms are: 24.45, 21.48, and 15.70 ev respectively, and they exceed the ionization potential of nitrogen molecules (15.576 ev). Hence, we should observe some charge transfer processes in any irradiated mixture of nitrogen and an inert gas:

$$N_2 + X^+ \rightarrow N_2^+ + X \,, \qquad (1)$$

where X is an inert gas atom.

Irradiation was carried out in 20-50 cm^3 glass and quartz sealed tubes by means of 2×10^4 curie cobalt source. The purified gases were measured through their pressure. After irradiation we let twice distilled water into the ampules and kept it there for several days to absorb all the oxides of nitrogen.

The nitric and nitrous acids were determined colorimetrically. The amount of γ-ray energy absorbed was determined dosimetrically from the oxidation of ferrous ion. In each experiment we irradiated simultaneously 25 ampules under identical conditions; three of the ampules were dosimetric standards. The exposure times were varied from 70-150 hrs, experimental temperatures 15-30°C, and radiation intensities 10^{13}-5×10^{14} ev/$cm^3 \cdot$sec in different sets of experiments.

Conditions were chosen so as to have only a small percent conversion; in such cases the amount of oxides formed was directly proportional to the absorbed radiation energy, i.e., the decomposition of the reaction products was not yet appreciable.

This linear dependence is illustrated in Fig. 1. The concentrations of nitrogen oxides were 10^{-2} - 10^{-3} mole %.

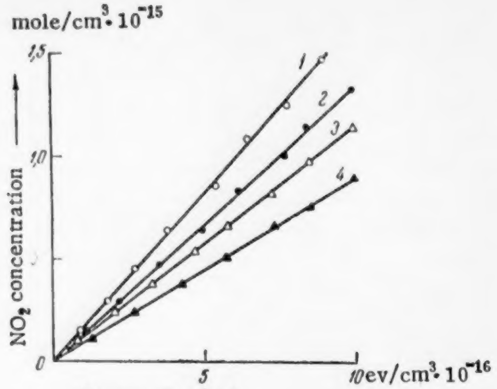

Fig. 1. Concentration of NO_2 as a function of the energy absorbed. Maximum exposure was 120 hr pressure 750 mm, ampule volume 31.5 cm^3, temperature 18° C. 1) Air; 2) 73% A ; 3) 73% Ne; 4) 73% He.

The principal results are shown in Fig. 2. In these experiments portions of the air were respectively replaced with corresponding amounts of inert gases. Although the amounts of oxygen and nitrogen were diminishing,the reaction rate was increasing, and when the amount of air was kept constant (70 and 200 mm) the reaction rate increased with increasing amount of the inert gas. The reaction rate was much greater in reaction mixtures containing an excess of the the inert gas then in those containing none. Thus, the reaction rate in mixtures containing 90% argon was 2.8 times greater than in the absence of argon. Hence, we succeeded in sensitizing appreciably the oxidation of nitrogen by the use of inert gases. Earlier we had established [1] that the ionization of oxygen did not lead to the oxidation of nitrogen. In general no detectable quantities of NO_2 were formed when only oxygen was irradiated [2] . Therefore, basically only the charge transfer process shown in Eq. (1) can be considered responsible for the increased nitrogen oxidation rate in the presence of inert gases.

Let us now compare the relative sensitizing efficiencies of Ar > Ne > He with the relative efficiencies of charge transfer reactions of type (1). For this we will have to make use of an approximate expression for the efficiency of inelastic collisions followed by electron transfer and an energy change ΔE. The probability of such transitions depends on the value of $\frac{a \cdot \Delta E}{hv}$; if the probability of such processes is to be small we will have to satisfy the condition expressed by the following inequality:

$$V = KP_{N_2} \cdot P_{O_2}, \tag{2}$$

where a is a coefficient of the same order of magnitude as the gas-kinetic collision radius, ΔE energy change, h Planck's constant, v relative velocity of colliding particles.

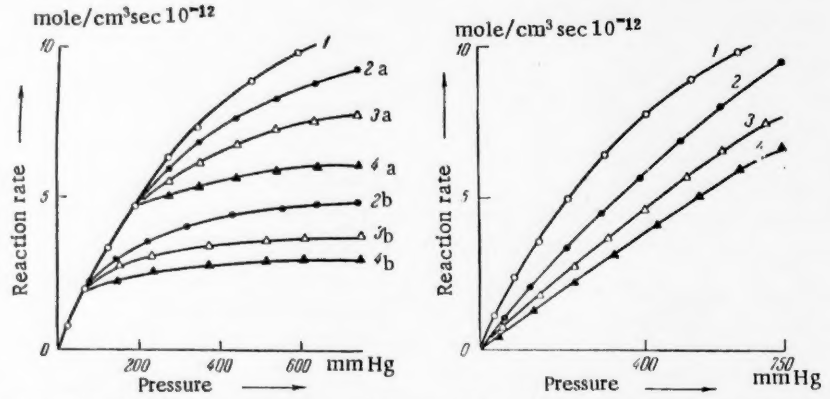

Fig. 2. Relationship between the reaction rate and pressure. On the left: 112 hr exposure, maximum radiation intensity 1.6 × 10^{14} ev/cm^3·sec^3 , temperature 21°, ampule volume 30 cm^3. The initial air pressure was 200 mm: 1) Air; 2) Ar; 3) Ne; 4) He. The initial pressure was 200 mm (a) and 70 mm (b). On the right: 92 hr exposure, maximum radiation intensity 4.9 × 10^{14} ev/cm^3·sec^3, mole fraction of the inert gas 0.5, temperature 25°, ampule volume 28 cm^3. 1) Air; 2) 50% Ar; 3) 50% Ne; 4) 50% He.

TABLE 1

Inert gas	A	Ne	He
Ionization potential, ev	15,70	21,482	24,45
Radius a*, cm • 10^8	3,69	3,17	2,96
ΔE, ev	0,124	5,906	8,874
V, m/sec	391	550	1235
$\frac{a\Delta E}{hv}$	55,3	1650	1025

* For a we took the mean values of the gas-kinetic radii of inert gas atoms and nitrogen molecules.

In Table 1 we have compiled the initial figures for the left side of Inequality (2) for the cases of most interest to us*. Calculations indicate that the interaction with Ar should be more efficient than with Ne and He, just as was found experimentally. However, for the other two the relative calculated efficiencies were in the inverse order to the experimental ones. This may be due to the fact that in our calculations we assumed a Maxwell-Boltzmann distribution for the positive ions formed and mean gas-kinetic velocities. Actually, under our irradiation conditions the ionic velocities may be very different from the mean thermal values. Besides, a change transfer from Ne^+ may produce excited nitrogen atoms (N^{+2} Σ_u^+). In such cases would get $\frac{a\Delta E}{hv} = 693$, since ΔE would be 2.486 ev instead of 5.906 ev. If should be pointed out that the ionizing efficiency also increases in the order He < Ne < A. Hence, the differences in the sensitizing action of these gases may also be connected with this phenomenon.

One can see in the graphs that when a part of the nitrogen-oxygen mixture was replaced by inert gases the reaction rate was smaller than in the pure mixture; this was partly due to the fact that the reaction rate was proportional to the oxygen partial pressure, which was lower in mixtures containing inert gases. Besides, this decrease also depends on the efficiency of the charge transfer reactions (1). Let us try to estimate the efficiency of this reaction from the kinetic data for various gases. According to paper [1] the relationship between the reaction rate and the mixture composition should under our conditions obey the equation:

$$\frac{a\cdot\Delta E}{hv} \gg 1, \tag{3}$$

TABLE 2

Gaseous mixture	Ratio of the oxygen + nitrogen mixture or of nitrogen pressure to that of the inert gas					
	2 : 1	1 : 1	1 : 2	1 . 3	1 : 5	1 : 10
$N_2 + O_2 + He$, 1 atm	0,61	0,34	0,23	0,11	0,07	0,06
$N_2 + O_2 + Ne$, 1 atm	0,71	0,43	0,29	0,15	0,09	0,08
$N_2 + O_2 + A$ 1 atm	0,86	0,48	0,34	0,17	0,12	0,10
$N_2 + H_2O + He$, 40 atm	0,73	0,65	0,63	0,61	0,59	0,58

where P_{N_2} and P_{O_2} are the nitrogen and oxygen partial pressures respectively, and K is the reaction rate constant. Let us assume that the introduction of an inert gas is equivalent to an effective increase in the nitrogen ion concentration, which is proportional to the partial pressure of the inert gas.

The efficiency of charge transfer will be defined by a certain summation coefficient β**.

We will now get an approximate expression:

$$V \simeq K\,(P_{N_2} + \beta P_X)\,P_{O_2}, \tag{4}$$

where P_X is the pressure of the inert gas.

---

* For nitrogen we took the ionization potential of 15.576 ev and the gas-kinetic radius 3.75 A.

** A calculation by the steady state method indicated that the additional concentration of nitrogen ions formed through charge transfer would be independent of nitrogen pressure if only ionization, charge transfer, and recombination processes were to be considered. Equation (4) is obtained irrespective of which elementary reaction limits the process; β, naturally, takes into account the ionizing efficiencies of various gases.

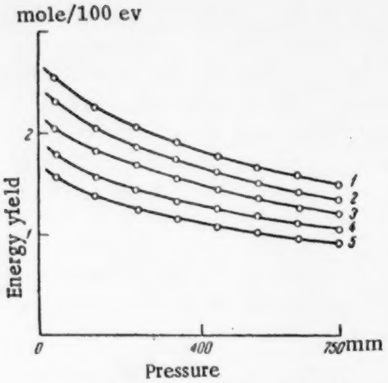

Fig. 3. The relationship between the reaction energy yield and the pressure. A 96 hr exposure, maximum radiation intensity $1.25 \cdot 10^{14}$ ev/cm^3·sec. Mixtures composed of: 1) 80 % N_2 + 20 % O_2; 2) 40% N_2 + 10 % O_2 + 50 % Ar; 3) 40 % N_2 + 10 % O_2 + 50 % Ne; 4) 40 % N_2 + 10 % O_2 + 50 % He; 5) 26 % N_2 + 7% O_2 + 67 % He.

The coefficients β calculated from our experimental data are given in Table 2. In our calculations we assumed that (as was established in [1]) the reaction rate constant varied with the pressure in the following manner:

$$K = b\sqrt{\frac{T}{\alpha P}}, \qquad (5)$$

where α is the ionic recombination coefficient, T the absolute temperature, P the pressure, and b a coefficient determined by the gas properties and radiation conditions. In accordance with experimental data we assumed a first order rate for the reaction between nitrogen and oxygen.

One can see in Table 2 that the effective cross section for the charge transfer from argon may be close to unity. As the nitrogen + oxygen mixture is diluted with the inert gas β decreases in magnitude. This may be connected with an ionic recombination, which competes with the charge transfer process

$$X^+ + O_2^- \rightarrow \vec{X} + \vec{O}_2. \qquad (6)$$

In the absence of oxygen β decreased much slower.

We also can not exclude the possibility that at high inert gas concentrations the charge transfer efficiency is decreased due to the neutralization of ions on the vessel walls.

The reaction energy yield in mixtures containing inert gases is somewhat lower than in the absence of the latter. The relationship between the energy yield in various mixtures and the pressure is illustrated in Fig. 4. The decline in yield with increasing pressure was mainly due to ionic recombinations and was studied in detail in papers [2,3].

LITERATURE CITED

[1] M. T. Dmitriev, S. Ya. Pshezhtskii Coll. The Effects of Ionizing Radiation on Inorganic and Organic Materials, Izd AN SSSR, pp. 145, 171 (1958)*.

[2] M. T. Dmitriev, J. Phys. Chem. 32, 2418 (1958).

[3] M. T. Dmitriev, S. Ya. Pshezhetskii, J. Phys. Chem. 33, 463 (1959).

Received February 28, 1959

---

* In Russian.

THE INFLUENCE OF THE ADSORBENT SURFACE ON LUMINESCENCE SPECTRUM OF URANYL ION

G. N. Kobyshev

A. A. Zhdanov State University of Leningrad

(Presented by Academician A. N. Terenin, March 24, 1959)

Great attention was being paid recently to the spectral investigation of complex compounds of uranyl ion [1-4]. An exceptionaly high sensitivity of the luminescence spectrum to changes in the surrounding medium was pointed out in the literature [5,6]. In order to clarify the nature of that influence an investigation of the changes of luminescence spectra of the uranyl ion in the state of adsorption on the surface of oxidized adsorbents was carried out in this work. In the work of Schwab,only the absorption region of the spectrum of the adsorbed uranyl ion on aluminum oxide was approximately determined [7], the spectrum of the adsorbate however, particularly in vacuum, was not investigated. In this work an attempt was made to use the luminescent spectrum of the coordinated ion with sharply expressed oscillatory structure, characteristic of a given state of the spectrum, as a spectral indicator of the changes in tested molecules (ions) during adsorption. The investigation was also of practical interest, since the uranyl ion is found in a number of sedimentary rocks in just that adsorbed state [8].

The luminescence spectrum was obtained with the usual method in which the exciting light (λ = 3650 A) from the lamp PRK-4 was incident to the viewing direction at 45°. The luminescence spectrum was photographically recorded on "Izopankhrom" film by a spectrograph having relative aperture 1:4 and dispersion of 150 A/mm in the region of 5000 A at the spectral width of the slit 1.5 A. Also used was the photoelectric recording of the spectrum on the spectrograph ISP-51 with an attachment FÉP-1. As a preliminary measure the adsorbent was calcinated in the air for a few hours at the temperature of 650-700° C until the natural bluish luminescence was either greatly reduced or totally disappeared. The adsorption took place in static conditions from aqueous solutions of uranyl salts (nitrate, sulfate potassium-uranyl sulfate) with the solute concentration varying from 10^{-2} to 10^{-4} M/liter. After that, the sample was washed in distilled water in order to remove the anions of the initial solution; the volume of water being ten times greater than the volume of the solvent. Washing with water does not remove the adsorbate from the surface. It is well known that uranyl salts are very soluble in water, the recent cases however show, that the uranyl ion is fixed on the surface of the adsorbent. When the adsorbate is treated with a solution of salt ($Bi(NO_3)_3$) instead of water, a reaction of the ion interchange occurs, which is typical for the state of adsorption and in which the displacement of the uranyl ion, e.g. by the cation Bi^{3+}, from the surface of the adsorbent takes place, whereas the ion Cu^{2+}, which stands after the uranyl ion in the adsorption series [9], that is,it has a weaker sorption than the ion U_2^{++}, does not remove the latter from the surface layer. The presence of the ion interchange reactions may be investigated through the change of color and luminescence of the adsorbent with adsorbate. Thus it follows, that the binding forces between the surface and the adsorbed ion have an ionic character as in the adsorption of other cations [10,11]. In order to observe the luminescence spectra in vacuum at temperatures of 90° K or 77° K the sample was placed in a sectional Dewar vessel connected to a vacuum unit (10^{-4} - 10^{-5} mmHg) and degassed, usually for 5-6 hours at the temperature of 200° C. In Fig. 1 are shown luminescence spectra of a hydrated uranyl ion adsorbed on silica gel , microporous glass prepared according to the method of Grebenshchikov and Molchanov [12]*, alumino gel, aluminosilica gel, Gudra's catalyst, chromatographic paper and magnesium oxide at 90° K. It is evident, that the position of luminescence maxima of the spectral bands of the uranyl ion on different adsorbents does not coincide with their position in any of the spectral series of aqueous solutions of uranyl nitrate. The peculiarities of the adsorbate luminescence spectra and their differences from the spectra of the aqueous solutions do not depend on the concentration of the luminescent matter in the surface layer [13] . Heating in vacuum to 150-250° C may have induced the formation of a crystalline phase on the surface of the adsorbent, the spectra of the adsorbed uranyl ion, however, differ not only from the spectra of solutions, but also from the spectra of crystalline hydrates as much in their magnitude and position of the maxima of the bands, as in the distribution of intensity among them. In the adsorbate spectra no frequencies were observed, which are usually attributed to the vibrations of crystal lattice of uranyl salts.

---

* Taking this opportunity the author would like to express his gratitude to O. S. Molchanov for his kind preparation of the samples of microporous glass.

The appearance of spectrum depends on the type of chosen adsorbent (Fig. 1), which once again points out the influence of the surface, which changes the state of the uranyl ion. In addition to that , the surface of the adsorbent shows strong influence on the intensity of luminescence. The presence of a very strong glow of the uranyl ion was established also at 290° K, in spite of the fact that the latter, as pointed out by Gordon, does not exhibit luminescence either in solutions, or in crystals at temperatures higher than 163° K [13]. No luminescence was observed at room temperatures on adsorption on bentonite (Oglanlinsk vein), and chromatographic paper.

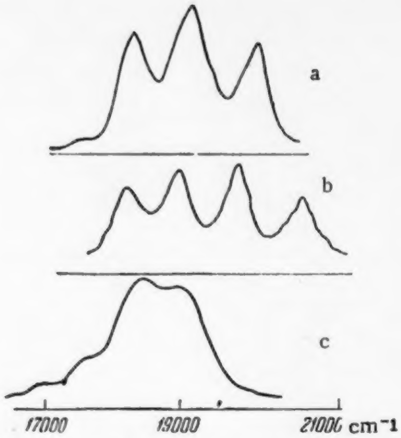

Fig. 1. Luminescence spectra of a hydrated ion at 90° K; a) $(UO_2 \cdot 2H_2O)^{++}$/ silica gel , $(UO_2 \cdot 2H_2O)^{++}$ / microporous glass, $(UO_2 \cdot 2H_2O)^{++}$/ alumino gel, $(UO_2 \cdot 2H_2O)^{++}$/ aluminosilica gel, b) $(UO_2 \cdot nH_2O)^{++}$ / magnesium oxide, c) $(UO_2 \cdot nH_2O)^{++}$/chromatographic paper.

Spectral data, together with the results of experiments after washing out the ions, described above, give the possibility of making a conclusion about the presence of the adsorbed state of the uranyl ion on the surface of adsorbents.

The luminescence spectra of the hydrated uranyl ion in the adsorbed state on microporous glass* at 290° K differs sharply from the spectra of crystalline hydrates [6], aqueous solutions of uranyl nitrate [13], and also from uranyl glasses [14] and hydroxides [15]. In the first , the glow intensity of the adsorbate increases considerably compared to the glow intensity of a solution, and moreover a redistribution of the intensity between individual bands is observed; in the second the number, position,and form of the most intense bands become changed. If in the spectrum of the hexahydrate of the uranyl nitrate, or its aqueous solution, five or six most intense bands are usually observed with their maxima at 20575, 19710, 18840, 17975, 17110 cm^{-1}, then in the luminescence spectrum of the uranyl ion $(UO_2 \cdot nH_2O)^{++}$, in the adsorbed state on porous glass, only three bands are observed with their maxima situated at 20080, 19240, 18420 cm^{-1}. The glow intensity increases when the temperature is lowered to 90° K, in that however, as distinct from crystals, the structure of bands does not appear and the bands become slightly narrower. Hence it follows, that the broadening of luminescence spectra bands depends on the interaction of the ion with the adsorbent surface. The lowering of temperature causes a displacement of the whole spectrum in the direction of shorter wavelengths, and the maxima are observed at 20160,19340,

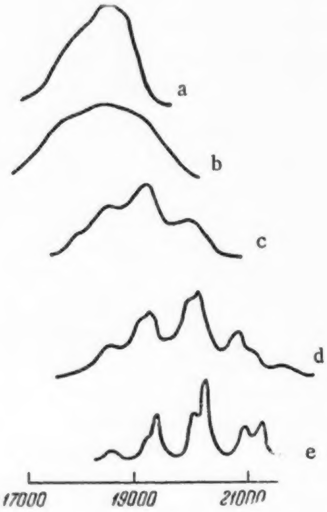

Fig. 2. Luminescence spectra at 77° K: a) dehydrated uranyl ion in the state of adsorption on microporous glass; b) dehydrated uranyl nitrate; c) dehydrated uranyl ion in the adsorbed state after the action of water vapor, d) after the action of NO_2; e) complex compound $UO_2(NO_3)_2 \cdot 2NO_2$.

---

* The description below is also valid for the adsorbed state of the uranyl ion on silica gel, alumino gel and aluminosilica gel.

The bands of luminescence spectra of the adsorbed ion $(UO_2 \cdot nH_2O)^{++}$ are moved by 60-80 cm^{-1} into the shortwave region of the spectrum, with respect to the maxima of the bands of the second series of quick-frozen aqueous solutions of the uranyl nitrate [13]. Since the adsorbate spectrum, which we observed, best of all corresponds to one of the series of spectral bands of $UO_2(NO_3)_2 \cdot 2H_2O$ [6], it is natural to attribute that spectrum to the luminescence of the ion UO_2^{++}, which has two water molecules in the coordination sphere.

The glow intensity of a sample placed in vacuum and subjected to degassing for 2-5 hours at temperatures 150-200° C, diminishes throughout the spectrum with greater change of the intensity in the shortwave band. During that, all spectral bands of the luminescence become even more blurred. Further degassing for 15 hours or more very strongly diminishes the intensity of glow, makes the structure of the spectrum vanish completely, and at the same time, moves the intensity maximum in the direction of the long waves (18300 cm^{-1}). The spectrum exhibits a wide asymmetric band. Prolonged degassing for 6-15 days without heating, leads to analogous changes of the luminescence spectra. Consequently, the transformation of structural luminescence spectrum into a structureless one, depends on the degree of hydration of the uranyl ion. The microporous glass was observed for a few hours after reversing the changes described above by the action of water vapor on the system UO_2^{++}, which brought the reappearance of the spectral structure lost during degassing. In Fig. 2c are shown luminescence spectra of the dehydrated ion after being subjected to the action of water vapor. As seen from the figure the spectrum changes from the wide asymmetrical band into the original spectrum with three distinct maxima. The action of the gas NO_2 is analogous to the action of the vapor H_2O, except for the shift of the entire spectrum and slight change of the distance between the bands. One may thus make a conclusion, that the uranyl ion in the adsorbed state is capable of coordinating several molecules, at which a change in the electron transition is observed, accompanied by a very small change of the frequency of the fully symmetric oscillation of the uranyl ion. For comparison purposes the luminescence spectrum of the complex compound $UO_2(NO_3)_2 \cdot 2NO_2$ and of the anhydrous uranyl nitrate is also shown in the figure.

The results of this work show, that the structural luminescence spectrum appears during the coordination of the uranyl ion, as pointed out earlier [16].

The luminescence spectrum of the uranyl ion adsorbed on an alkali adsorbent (of which MgO was used) has different positions of the bands as compared to acid adsorbents. The maxima of the bands are distributed at 20600, 19800, 19000, 18180 cm^{-1} and moved in the direction of the shorter wavelengths relative to their position in the spectra of crystals and solutions. The lowering of the frequency of the fully symmetric oscillations, as compared to its value in crystals and solutions was observed in the adsorbed state on all types of adsorbents.

This work was conducted under the direct guidance of Academician A. N. Terenin, to whom the author expresses his deep gratitude for the proposed topic, daily help and valuable advice.

LITERATURE CITED

[1] J. Feldman, J. R. Havil, and W. F. Neumann, J. Am. Chem. Soc. 76, 4726 (1954).

[2] O. V. Volod'ko and A. N. Sevchenko, Optika i Spektroskopiya 4, 40 (1958).

[3] M. Freymann and K. Chantrel, C. r. 227, 1029 (1948).

[4] A. Kiss and J. Nyiri, Zs. f. anorg. allgem. Chem. 249, 340 (1942).

[5] V. L. Levshin and G. D. Sheremet'ev, J. Exptl. Theoret. Phys. (USSR) 17, 204 (1947).

[6] A. N. Sevchenko, V. M. Vdovenko, and T. V. Kovaleva, J. Exptl. Theoret. Phys. (USSR) 21, 204 (1951).

[7] M. G. Schwab, Zs. f. Phys. Chem. 53(B), 1 (1942).

[8] A. F. Frederickson, Science 108, 184 (1948).

[9] T. B. Gapon, Doklady Akad. Nauk SSSR 58, 595 (1947).

[10] M. T. Roger and R. V. Vennen, J. Am. Chem. Soc. 75, 1751 (1953).

[11] C. M. French and J. P. Howard, Trans. Farad. Soc. 52, 102 (1956).

[12] O. S. Molchanova and I. V. Grebenshchikov, Zhur. Obsh. Khim. 12, 537 (1942).

[13] B. E. Gordon, Ukr. Khim. Zhurn. 17, 688 (1951); Izv. AN SSSR, Ser. Fiz. 15, 625 (1951).

[14] F. A. Kroger, J. M. Sterels and P. G. Botden, Philips Res. Repts. 3, 46 (1948).

[15] D. T. Vier and M. L. Schultz., J. Opt. Soc. Am. 38, 811 (1948).

[16] G. I. Kobyshev, and D. N. Suglobov, Doklady Akad. Nauk SSSR. 120, 330 (1958).*

Received March 24, 1959

---

* Original Russian pagination. See C.B. Translation.

ON THE ELECTRON THEORY OF CHEMISORPTION ON A REAL SEMICONDUCTOR SURFACE

Sh. M. Kogan and V. B. Sandomirskii

M. V. Lomonosov State University of Moscow

Institute of the Physical Chemistry of the Academy of Sciences,USSR

(Presented by Academician V. I. Spitsyn, March 16, 1959)

Up to the present time a series of experimental data on the influence of adsorption on electronic characteristics of semiconductors was collected, which makes it possible to make our representation of chemisorption in semiconductors more precise. First of all pertinent here are measurements of the changes of the work function during adsorption [1-3] and the measurements of the field effect [1].

The following inherent experimental tendencies may be singled out:

1. The coverage of the surface by the adsorbed molecules, at which perceptible changes of the work function begin to be observed ($\sim$ kT at T = 300° K), is usually greater than $\sim 10^{13}$ cm^{-2}.

2. The dependence of the work function changes on surface coverage is usually linear, sometimes logarithmic [3].

3. The maximum change of the work function during adsorption of different gases on different semiconductors is usually $\sim$0.3 ev (12 kT at T = 300° K).

We shall consider now these experimental tendencies. We shall assume that all changes of the work function are connected with the surface charging during adsorption and deformation of the surface energy zones resulting from that. We shall express the last quantity in units kT and denote it by u. It is easy to show, that the magnitude of the surface charge expressed (in the units of electron charge) at which the change of the work function reaches measurable value ($u \approx 1$), amounts to $\sigma \approx 10^9$-10^{10} cm^{-2}. The calculation of the surface charge, at which the depression of the zone reaches 0.3 ev, gives $\sigma \approx 10^{12}$ cm^{-1}. Thus we can see, that the concentration of the adsorbed particles (N), at which the change in the work function reaches an observable magnitude, exceeds the corresponding surface charge by 2-3 orders of magnitude.

According to the electron theory of adsorption the chemisorbed molecules are in both, neutral states ("weak" bond), and in charged states ("strong" bond) [5]*. It is convenient to introduce the following two definitions. We shall call "idealized" such a surface, on which all surface electron states depend on the adsorption of the considered gas. Precisely that case is usually considered in the electron theory of chemisorption [5,7]. We shall call "real" such a surface, on which a greater number of states exists, which is not connected with the adsorption of the given gas ("nonadsorbed" states).

There are two possible interpretations of the sharp disagreement between the coverage and surface charge.

1. The "idealized" surface. Only a very small part of the adsorbed molecules is charged ($\lesssim 1\%$). The observed changes of the electron conduction and work function depend on the charged molecules.

2. The "real" surface. Nearly all adsorbed molecules may be charged. The corresponding charge is almost

---

* We are not considering here the possibility of the existence of three types of bonds [6].

fully compensated by the change of the charge in the nonadsorbed surface states, so that the resulting change of the surface charge (and zone depression) is relatively small.

We shall consider the first interpretation and, at the same time, for the sake of exactness, we shall have in view the adsorption of an acceptor gas. The share of the adsorbed charged molecules is small except the in the case in which their level is above the Fermi level. Besides that, taking into consideration the first of the above-noted experimental trends, that should take place at the very beginning of the adsorption. Thus, keeping within the frame of the "idealized" model of the surface, one ought to be able to make a conclusion, that the energy levels of the adsorbed particles are above the Fermi level everywhere (and below the Fermi level in the case of donor particles) also at the beginning of the adsorption and do not depend on surface processing. There is little probability of such a coincidence, and its admission is altogether fictitious. Further, the "idealized" surface model leads to an actual failure in a series of electronic representations in catalysis.

In that way, the "idealized" surface model cannot explain all the combinations of experimental data, and that makes it necessary to pass to the analysis of the properties of real surface. Some of these properties were already considered.

The charge density in the nonadsorbed states is equal :

$$\sigma = \sum_i N_{Di}\left(1 + \exp\left[\frac{F - E_{Di}}{kT}\right]\exp\left[-u\right]\right)^{-1} - \\ - \sum_i N_{Ai}\left(1 + \exp\left[\frac{E_{Ai} - F}{kT}\right]\exp u\right)^{-1}, \tag{1}$$

where N_{Di}, N_{Ai} and E_{Di}, E_{Ai} are the concentrations and the energy levels of the donor and acceptor states respectively ; F is the Fermi level within the volume of the semiconductor.

The equation of the crystal electroneutrality has the form

$$\sigma - N^- + R = 0, \tag{2}$$

where N^- is the concentration of the adsorbed charged molecules ; R is the bulk charge contribution to the surface charge per unit area. Hence we obtain

$$du / dN^- = (S + dR / du)^{-1}, \tag{3}$$

where

$$S = \frac{d\sigma}{du} = \sum_i N_i \exp\left[\frac{F - E_i}{kT}\right]\exp\left[-u\right]\left(1 + \exp\left[\frac{F - E_i}{kT}\right]\exp\left[-u\right]\right)^{-2} \tag{4}$$

Here N_i and E_i are the concentrations and energy levels of the surface states irrespective of whether they are acceptor or donor type. According to (3) $\underline{u}$ becomes (1), when the number of charged molecules becomes $\sim [S(u_0)+(dR/du)u_0]$ where u_0 is the initial value of $\underline{u}$.

It can be shown that

$$(dR / du)_{u=0} = \alpha = \varepsilon kT / 4\pi q^2 L. \tag{5}$$

Here ϵ is the dielectric permeability; L is the length of the shield; q is the absolute magnitude of the electronic charge. When $\epsilon = 10$, $L = 10^{-4}$-10^{-5} cm, $T = 300°$ K , $\alpha \approx 10^9 - 10^{10}$ cm^{-2}. Consequently,on an idealized surface (S = 0 , u = 0) the work function should perceptibly change already at $N^- \approx 10^9$-10^{10} cm^2. If the concentration of the nonadsorbed states on a real surface is high, so that $S(u_0) \gg \alpha$, the surface charging will become perceptible only at far greater coverage.

In order to estimate the possible magnitude of S we shall assume a simpler model of the surface energy spectrum. Let the full number of nonadsorbed states N_S be uniformly and smoothly distributed throughout the width of the forbidden zone E_G , and let the Fermi level on the surface be located so that its distance from the edge of the forbidden zone is greater than kT. Writing (4) in the form of an integral and putting $N_S = 10^{15}$ cm^{-2}, $E_G \approx 2$-3 ev, we shall find $S = N_S kT/E_G \approx 10^{13}$ cm. It may be shown, that at reasonable values of $\underline{u}$ the quantity dR/du is not greater than that value of S. Therefore, in the considered model the observable changes of the work function should take place only at $N^- \approx 10^{13}$ cm^{-2}, which agrees with experiments.

We shall integrate the Equation (3) with $S = N_S kT/E_G \gg dR/du$. We obtain

$$S\Delta u = N^-, \tag{6}$$

i.e., a linear dependence of the work function change on the coverage, as observed in experiments. Using the experimental data obtained in [3], we can estimate the magnitude of S with the aid of [6]. We obtain $S \approx 10^{11}-10^{13}\ \text{cm}^{-2}$, corresponding to $N_S \approx 10^{13}-10^{15}$ cm*.

Thus, with the aid of a "real" surface model certain inherent trends, observed in experiments, can be explained.

In our consideration we have not taken into account the possibility of the presence of the dipole moment of neutral molecules and the corresponding contribution to the change in the work function. The following experimental facts point out the usefulness of such an omission: 1) in the case of Ge the changes of u [3] are of the same order as in the field effect ; 2) the observed dependence of Δu on N^- is logarithmic; 3) the magnitudes of Δu are small also at coverages of the monolayer order; 4) departures from Langmuir trends are observed also at small coverages . It must be admitted , however, that these arguments do not solve the problem uniquely.

The authors express their gratitude to the corresponding member of the Academy of Sciences USSR S. Z. Roginski and Doctor of the Physicomathematical Sciences F. F. Vol'kenshtein , and also to all who took part in the seminar in the Catalysis Laboratory of the Institute of Physical Chemistry of the Academy of Sciences USSR for their consideration of the results of this work.

LITERATURE CITED

[1] W. H. Brattain and J. Bardeen, Bell Syst. Techn. J. 32, 1, (1953).

[2] V. I. Lyashenko and I. I. Stepko, Izv. AN SSSR, Ser. Fiz 16, 211 (1952); V. I. Lyashenko, Doctoral Dissertation, Inst. fiziki AN USSR, Kiev, 1958.

[3] É. Kh. Enikeev, L. Ya. Margolis, and S. Z. Roginskii, Doklady Akad. Nauk SSSR 1 4, 606 (1959).

[4] P. Handler, Semiconductor Surface Physics, Univ. Pennsylvania Press. 23, (1957).

[5] F. F. Vol'kenshtein, Uspekhi Fiz. Nauk 50, 253 (1953).

[6] F. F. Vol'kenshtein and S. Z. Roginskii Zhur. Fiz. Khim. 29, 458 (1955).

[7] V. B. Sandomirskii, Izv. AN SSSR, Ser. Fiz. 10, 211 (1957).

Received March 10, 1959

---

* The explanation of the logarithmic dependence of Δu on the coverage is not of great interest. The functions R and σ in Equation (2) in fact depend not on u, but on exp u, logarithmic dependence can, therefore, be determined in different ways.

MECHANISM OF THE REACTION BETWEEN ALCOHOLS AND HYDROGEN HALIDE ACIDS

V. A. Pal'm and A. O. Kyrgesaar

Tartus State University

(Presented by Academician V. N. Kondrat'ev, March 5, 1959)

The kinetics and the mechanism of the reaction between aliphatic alcohols and hydrogen halide acids, which proceeds according to the equation

$$ROH + HHal \rightarrow R - Hal + H_2O \qquad (1)$$

has been studied by several workers. In certain papers, Reaction (1) was treated as a bimolecular nucleophilic substitution [1-3]. Hinshelwood [4] and others [5] believe that the rate determining step in Reaction (1) is the dissociation of the $ROH_2^+ \cdot Hal^-$ ion pairs.

It is not entirely improbable that the rate determining step involves a monomolecular dissociation of alkoxonium ions followed by the simultaneous formation of R—Hal and R—O—R; these arise from the reaction of carbonium ions (which are formed by splitting out water from alkoxonium ions) with halide ions and alcohol molecules respectively.

Consequently, we cannot consider the problem of the reaction mechanism as being completely solved.

We studied the ethanol chlorination kinetics in absolute ethanol and in two water-ethanol mixtures in the 100-140° temperature range. The reaction was carried out in sealed tubes. In cases where the initial HCl concentrations exceeded 0.1 moles/liter the course of the reaction was followed by a Volhard titration of the remaining HCl. At low HCl concentrations the reaction rate was determined by following the changes in electrical conductance with time in a tube to which two electrodes had been sealed. At the same time we introduced certain corrections for the variations of conductance with HCl concentration.

In Table 1 we have listed our experimental monomolecular rate constants h_1^0 for cases where the concentrations were more than 0.1 mole /liter. In experiments performed in absolute ethanol the constants were computed from the initial kinetic curve segments by means of the equation:

$$h_1 = -\frac{1}{[\mathrm{HCl}]}\frac{d[\mathrm{HCl}]}{dt}. \qquad (2)$$

In the case of ethanol—water mixtures the values of h_1 were based on the entire kinetic curve by assuming a monomolecular reaction and averaging the results.

The second column in Table 2 lists the rate constants k^I obtained from the electrical conductance changes for cases with low initial HCl concentrations. Our calculations were performed by means of Equation (2).

As the data presented indicate, we get a first order reaction with HCl concentrations above 0.1 mole /liter. The kinetic curves in ethanol—water mixtures were monomolecular in character. The more complex nature of the kinetic curves in absolute ethanol was connected with the retarding effect of water; however, monomolecular behavior was observed up to 80-90% conversion.

TABLE 1

Temp., °C	Init. HCl conc., moles/liter	k_1^0, 10^4sec^{-1}		
		abs ethanol	96.8 % ethanol	94.0 % ethanol
100	0,5	1,66	—	—
110	0,5	4,70	1,88	1,15
120	0,5	11,2	4,85	3,15
130	0,5	21,9	12,7	8,9
140	0,5	—	—	21
120	0,1070	10,5*	—	—
120	0,4464	10,3*	—	—
120	1,460	9,4*	—	—

* It seems that the ethanol in this set of experiments contained some extra water, making the constants 5-7% too low.

TABLE 2

Temperature 101°C. $k^0_I = 18.5 \cdot 10^{-5}$ sec^{-1}

HCl conc., moles/liter$\cdot 10^4$	$k_I \cdot 10^5$ sec^{-1}, obs.	$\alpha = \frac{\lambda}{\lambda_\sim}$	$k_I \cdot 10^5$ sec^{-1}, calc.
25,50	8,3	0,670	8,37
6,40	4,1	0,820	4,57
3,20	2,7	0,885	2,91
1,60	1,65	0,920*	1,90

* Calculated from Equation (3).

TABLE 3

HCl conc., moles//liter$\cdot 10^3$	$\lambda/\lambda_\sim$	HCl conc moles//liter$\cdot 10^3$	$\lambda/\lambda_\sim$
0,32	0,885	10,10	0,507
0,64	0,820	12,75	0,451
1,28	0,750	25,50	0,387
2,55	0,670	51,0	0,330
5,10	0,570	102	0,280
6,38	0,537	501	0,260

At low HCl concentrations the monomolecular rate constant began to decrease (see Table 2), and the order of the reaction correspondingly increased just as in the case of methanol and HCl [4]. However, in the case of ethanol these changes were observed at much lower HCl concentrations.

We have also determined the equivalent electrical conductance of HCl in absolute ethanol at 101° over a concentration range from $3.2 \cdot 10^{-4}$ to 0.5 mole /liter. The results are presented in Table 3.

Contrary to the usual theories about strong electrolytes we will assume that for HCl solutions in absolute ethanol at 101°C, the degree of dissociation of ion pairs is $\alpha = \lambda / \lambda_\sim$. It is also understood that the system contains no molecular HCl. With all this in mind, at low HCl concentrations the thermodynamic dissociation constant K_i for the ion-pairs will be equal to

$$K_i = \frac{[C_2H_5OH_2^+][Cl^-]}{[C_2H_5OH_2^+ \cdot Cl^-]} 10^{-A\sqrt{\mu}} = \tag{3}$$

$$= \frac{(\lambda / \lambda_\sim)^2 [HCl]}{1 - \lambda / \lambda_\sim} 10^{-A\sqrt{\lambda/\lambda_\sim [HCl]}}, \tag{3a}$$

where μ is the ionic strength; the value of A is calculated on the basis of the Debye-Huckel theory from the equation

$$A = \varepsilon^2 \sqrt{8\pi N \cdot 10^{-3}} (DkT)^{-3/2}. \tag{4}$$

By substituting D = 14.0 (calculated by extrapolating the literature data [7] to 101°) into Eq. (4) we will get A = 9.60.

Plugging our experimental data into Equation (3), we calculated λ_∞ and K_i*. Within the $0.52 \cdot 10^{-3}$ - $2.55 \cdot 10^{-3}$ moles/liter HCl concentration range, K_i remained constant and equal to $(1.45 + 0.06) \cdot 10^{-3}$. At [HCl] > $5 \cdot 10^{-3}$ moles /liter, the values of K_i rapidly decreased with increasing [HCl]. It seems that this HCl concentration is at the applicability limit of Eq. (3).

If we now start from Hinshelwood's theory that the dehydration of ion pairs constitutes the slowest reaction step, then by determining the relationship between ion-pair concentrations and HCl concentrations we should be able to calculate the rate constant k_I at low [HCl] from the formula:

---

* Our experimental λ and λ_∞ values are given in arbitrary units due to inaccurate calibration of our experimental vessel at 101°.

$$k_I = k_I^0 \frac{1 - \lambda / \lambda_\infty}{1 - \lambda_0 / \lambda_\infty}, \tag{5}$$

where $\lambda_0 / \lambda_\infty$ is the average degree of ion-pair dissociation in the range of HCl concentrations within which k_I^0 was measured. At 101°C $\lambda_0 / \lambda_\infty = 0.27$. The results obtained by using Eq. (5) are presented in the fourth column of Table 2. It is evident that the calculated values of k_I are in good agreement with the experimental ones. This we believe constitutes evidence in support of Hinshelwood's original hypothesis [4] about the mechanism of Reaction (1).

The monomolecular kinetics observed at higher HCl concentrations can be explained in two ways. On one hand the value of $\alpha = \lambda / \lambda_\infty$ changes very little in this case with increasing [HCl]. Hence any troubles arising out of this are insignificant and approximate monomolecular kinetics are retained. On the other hand we do not exclude the possibility that at large [HCl] the use of the $\alpha = \lambda / \lambda_\infty$ ratio is invalid and $\alpha = 0$. Then the determined k_I^0 constants would represent true monomolecular rate constants for the dehydration of ion pairs. So far, however, we can not safely assume this to be true. That is why neither the observed activation energies (27,400 cal), nor the frequency factors ($2 \cdot 10^{12}$) can be considered as representing true values.

As the data given in Table 1 indicate the addition of water to ethanol retards appreciably the reaction. The nature of this phenomena can be easily explained by starting from certain general ideas concerning the inhibition of acid-catalyzed reactions [8,9] by basic impurities. Since only protonated particles (ethoxonium ions) participate in the reaction, any reaction with water which would tend to decrease their concentration would correspondingly also decrease the observed reaction rate constant. In water—alcohol solutions of acids the following equilibrium exists:

$$H_3O^+ + C_2H_5OH \rightleftarrows C_2H_5OH_2^+ + H_2O. \tag{6}$$

The concentration equilibrium constant K for this reaction we determined by means of a spectrophotometric indicator method in the 15-45° temperature range; we used as indicator p-nitroaniline [6] in 96.6% ethanol. The values of K obtained will satisfactorily fit the equation

$$\lg K = 7{,}87/4{,}574 - 5100/4{,}574\,T. \tag{7}$$

The observed rate constant k_I in water—ethanol mixtures should fulfill the equation.

$$k_I = \frac{K k_I^0}{K + [H_2O]/[C_2H_5OH]}, \tag{8}$$

where k_I^0 is the rate constant in absolute ethanol.

In Table 4 we have listed the values of K extrapolated from Eq. (7) to the experimental temperatures, and we also compared the values of K_I calculated from Eq. (8) with the experimental ones. The satisfactory agreement between the calculated and experimental values of k provide evidence in support of the proposed scheme for the effects of water on the reaction rate.

TABLE 4

Temp., °C	K	$K_I^0 \cdot 10^4$	$k_I \cdot 10^4$			
			96.8 % ethanol		94.0 % ethanol	
			calc.	obs.	calc.	obs.
110	0,065	4,70	2,03	1,88	1,33	1,15
120	0,078.	11,2	5,32	4,85	3,24	3,15
130	0,096	21,9	11,6	12,7	8,1	8,9

If the rate determining step in the reaction involves the dehydration of ion pairs then the reaction with HBr should be faster than that with HCl due to the fact that Br^- is more nucleophilic. Our preliminary data indicate that the reaction between HBr and ethanol at $[HBr] > 0.1$ mole /liter and 120° obeys first order kinetics. The rate constant is about two times that for HCl.

The authors wish to thank their student Miss L. Ploom for her active participation in the experimental parts of this research.

LITERATURE CITED

[1] S. Kilpi, Soumen Kemistilehti, 26B, No. 2, 9 (1953).

[2] J. F. Norris, Rec. Trav. Chim. 48, 885 (1929).

[3] E. Grunvald, and S. Winstein, J. Am. Chem. Soc. 69, 2051 (1947).

[4] C. N. Hinshelwood, J. Chem. Soc. 1935, 599 .

[5] G. M. Bennett and F. M. Reynolds, J. Chem. Soc. 1935, 131.

[6] E. A. Braude, J. Chem. Soc. 1948, 1971 .

[7] N. Koizumi and T. Hanai, Bull. Inst. Chem. Res. Kyoto Univ. 33, 14 (1955).

[8] N. M. Chirkov, M. I. Vinnik, S. G. Entelis, and V. I. Tsvetkova, Coll. Problems in Chemical Kinetics, Catalysis, and Reactivity, Izd. AN SSSR, p. 496 (Moscow, 1955).*

[9] V. A. Pal'm, J. Phys. Chem. 32, 620 (1958).

Received March 3, 1959

---

* In Russian.

THE EFFECTS OF IODINE ON THE FLOTATION OF SULFIDE MINERALS

Corresponding Member Acad. Sci. USSR, I. N. Plaksin,
and R. Sh. Shafeev

In the course of our work we discovered that elementary iodine tends to aggregate sulfide minerals and activate them during flotation. According to some previously reported data [1] iodine possesses intrinsic floatability. In this respect iodine resembles elementary sulfur due to the fact that the intermolecular forces in both elements are weak in comparison with the interatomic; the interatomic distance in iodine molecules is 2.70 A, while that between its molecules in crystals, 3.54 A. In sulfur these distances are 2.10 and 3.30 A respectively.

We studied the scavenging action of iodine in the flotation of sulfide minerals. To characterize the adsorption of iodine on sulfide minerals we used a saturated solution of elementary iodine in distilled water (0.0266 % at 18.5°C).

We stirred 100 ml of the solution for 10 min with 1g of a sulfide mineral whose grain size was either $-100 + 150\,\mu$ or $-74 + 0\,\mu$. The comparative results obtained for the adsorption of iodine on sulfide minerals are presented in Table 1.

The flotation action of iodine was studied on 40 g samples of mineral in 100 ml flotation chambers. The mixing time with the scavenger was 3 minutes, and the flotation time was also 3 min. The initial sample was a mixture composed of two minerals—the $-74 + 0\,\mu$ grain size sulfide (10 g) and some $-150 + 100\,\mu$ size quartz (30 g). The xanthogenate and iodine were introduced separately in amounts of 10 mg/liter. Pine oil was introduced to induce frothing. The flotation results are shown in Table 2.

Flotation experiments demonstrated explicity the scavenging effect of iodine on sulfide minerals.

The flotational properties of iodine will depend on its scavenging action through its adsorption on the surface of minerals. At the same time the oxidizing action of iodine on the xanthogenate may become very pronounced.

The iodine will oxidize the xanthogenate to give a dixanthogenate. The formation of a dixanthogenate during the treatment of minerals with elementary iodine and xanthogenate was established in experiments on S^{35}-labeled butyl xanthogenate. A 1 g sample of $-74 + 0\,\mu$ size sulfide mineral was stirred with 100 ml of a butyl xanthogenate solution (10 mg/liter) and 0.026% iodine solution. The experimental results are presented in Table 3.

Our results confirmed the formation of a dixanthogenate during the joint treatment of the mineral with iodine and a xanthogenate.

TABLE 1

Iodine Adsorption on Sulfides

Mineral	PbS	$CuFeS_2$		FeS_2		ZnS
Iodine tied-up, in mg/1g of mineral	3,312	4,95	24,6	7,6	20,8	26,6
Mineral grain size, μ	−150 +100	−150 +100	−74 +0	−150 +100	−74 +0	−74 +0

TABLE 2

Experimental Flotation Results

Galenite extracted	Quartz extracted %	Reagents
37,7	0,1	Pine oil 10 mg/liter.
91,7	0,4	Butyl xanthogenate 10 mg/liter, pine oil 10 mg/ / liter.
91,1	0,9	Iodine solution 10 mg/liter, pine oil 10 mg/liter
95,6	3,2	Iodine solution 10 mg/liter, butyl xanthogenate 10 mg/liter, pine oil 10 mg/liter.
Sphalerite extracted		
45,6	—	Pine oil 10 mg/liter.
86,8	0,1	Butyl xanthogenate 10 mg/liter, pine oil 10 mg/ liter.
65,6	—	Iodine solution 10 mg/liter, pine oil 10 mg/liter
87,4	0,2	Iodine solution 10 mg/liter, butyl xanthogenate 10 mg/liter, pine oil 10 mg/liter.

TABLE 3

Changes in the Fixation of Butyl Xanthogenate on Sulfide Minerals Following a Treatment with an Iodine Solution

Xanthogenate fixation, counts/min	Mineral			
	PbS	$CuFeS_2$	FeS_2	ZnS
Treated with the xanthogenate	1315	1370	1770	1009
Treated separately with iodine and the xanthogenate	3080	2326	5890	1800
Treated with xanthogenate and washed with ether	700	530	890	887
Separate treatment with iodine and the xanthogenate followed by ether washing	745	500	687	500

We would like to propose the following mechanism for the activating action of iodine on the xanthogenated flotation of sulfide minerals. After attaching itself to the pulp mineral particle surface the elementary iodine reacts with the xanthogenate to give a dixanthogenate, which then becomes attached to the sulfide mineral.

Thus, elementary iodine acts as a scavenger of sulfide minerals. At the same time it reacts with the xanthogenate at the interface between the mineral and the liquid pulp phase forming a dixanthogenate . Slight amounts of iodine added to the sulfide ores will thus intensify their flotation.

LITERATURE CITED

[1] A. M. Gaudin, H. L. Miaw and H. R. Spedden, Proceedings of the Second International Congress of Surface Activity, 3, London, p. 202 (1957).

Received April 27, 1959

MASS SPECTRA AND THE STRUCTURE OF VINYLACETYLENES

A. A. Polyakova, K. I. Zimina, A. A. Petrov,
and R. A. Khmel'nitskii

All-Union Scientific Research Institute for the Processing
of Petroleum and Natural Gas and for the Preparation
of Synthetic Liquid Fuels

(Presented by Academician B. A. Arbuzov, March 26, 1959)

By studying the reactions of vinylacetylenes with electrophilic, nucleophilic, and free radical reagents we discovered several rules concerning their reactivity, which were related to their chemical structure [1]. In order to clarify these rules we undertook a systematic study of any connections between the structure of vinylacetylenes and the physical properties related to reactivity. The respective data on the infrared spectra [2], Raman spectra [3], and dipole moments [4] of isomeric vinylacetylenes have already been published.

In our present paper we aimed at establishing the connection between the structure and mass spectra of vinylacetylenes. As is well known, by studying these spectra one can make certain general deductions concerning the stabilities and relative reactivities of organic compounds. On the other hand, mass spectra constitute very valuable information for the analysis and identification of various compounds.

We studied the mass spectra of vinylacetylene and of all the possible methyl substituted derivatives (propenylacetylene*, isopropenylacetylene, and vinylmethylacetylene). Only the data for vinylacetylene is found in the literature [5].

The technique used and the physical constants of these hydrocarbons have already been described [1,3,4].

Mass spectra were recorded on a model MS-1 instrument by using a 2500 v accelerating potential, a 1.5 mamp emission current, and 70 ev ionizing electrons. In order to determine the ionization and appearance potentials we modified the method of regulating the ionizing electron energies so as to permit a determination of potentials with an accuracy of ± 0.1 ev.

The mass spectra of vinylacetylene and its closest homologs are described in Table 1. After examining the Table one can deduce the following facts.

In the spectrum of vinylacetylene, as well as in that of divinyl and diacetylene, the ion molecules have the maximum intensity [5]. The most intense ion fragments were formed by the rupture of the C — H bonds. The intensities of mass-51, 50, and 49 ions had only 50, 42, and 13 % of the intensity observed for the maximum peak. The vinylacetylenes had little tendency to form ion fragments through the rupture of carbon—carbon bonds. The only C-C bond rupture observed gave ions with a mass of 26.

The introduction of a methyl radical (in any position) into the vinylacetylene molecule slightly decreased the stability of ion molecules, yet these were still the most intense. Meanwhile in the mass spectra of piperylene and isoprene (and of their more saturated analogs) the maximum intensities are already displaced toward the ion fragments.

Just as in the case of 1,3-dienes and acetylenes the curve of ion distribution versus the number of carbon atoms gave two maxima ($C_3H_X^+$ and $C_5H_X^+$) for each isomer of C_5H_6**.

---

* An approximately equimolar mixture of cis and trans isomers.

** In the case of saturated and ethylenic analogs of these hydrocarbons only one maximum was observed.

The Mass Spectra of Vinylacetylenes

Mass and compn. of fragments	Intensity of ions				Mass and compn. of fragments	Intensity of ions			
	$HC\equiv C-CH=CH_2$(*)	$HC\equiv C-CH=CH-CH_3$	$HC\equiv C-\underset{CH_3}{\underset{\mid}{C}}=CH_2$	$CH_3-C\equiv C-CH=CH_2$		$HC\equiv C-CH=CH_2$(*)	$HC\equiv C-CH=CH-CH_3$	$HC\equiv C-\underset{CH_3}{\underset{\mid}{C}}=CH_2$	$CH_3-C\equiv C-CH=CH_2$
12 C^+	1,5	5,3	2,4	0,9	49 C_4H^+	13,0	47,7	1,6	4,0
13 CH^+	1,3	—	—	—	50 $C_4H_2^+$	41,9	6,5	12,3	10,0
14 CH_2^+	1,2	—	—	—	51 $C_4H_3^+$	50,2	17,5	25,8	17.0
15 CH_3^+	0,4	—	—	2,0	52 $C_4H_4^+$	100,0	9,3	—	—
25 C_2H^+	3,6	—	—	1,6	53 $C_4H_5^+$	4,4	3,7	1,6	—
26 $C_2H_2^+$	11,0	4,8	3,7	3,8	54 $C_4H_6^+$	—	2,2	—	—
27 $C_2H_3^+$	2,9	12,7	9,2	8,3	55 $C_4H_7^+$	—	7,5	5,0	—
28 $C_2H_4^+$	0,5	—	—	—	56 $C_4H_8^+$	—	4,1	1,3	—
36 C_3^+	1,5	—	—	1,7	57 $C_4H_9^+$	—	3,1	1,3	—
37 C_3H^+	5,1	—	—	9,7	60 C_5^+	—	—	—	—
38 $C_3H_2^+$	2,2	—	8,2	17,0	61 C_5H^+	—	6,2	1,6	12,0
39 $C_3H_3^+$	0,8	89,1	71,7	91,5	62 $C_5H_2^+$	—	8,7	2,8	15,0
40 $C_3H_4^+$	0,6	46,8	39,3	—	63 $C_5H_3^+$	—	16,8	5,0	21,9
41 $C_3H_5^+$	—	37,4	29,2	1,8	64 $C_5H_4^+$	—	4,7	0,6	—
42 $C_3H_6^+$	—	7,5	4,4	—	65 $C_5H_5^+$	—	49,5	41,8	38,0
43 $C_3H_7^+$	—	13,1	11,3	1,0	66 $C_5H_6^+$	—	100.0	100,0	100,0
48 C_4^+	2,8	—	—	—	67 —	—	6,9	5,4	—

The rupture of C—H bonds has a relatively high and approximately equal probability (40-50%) in all the isomers, evidently due to the formation of stable conjugated ions with a mass of 65.

The isomers with a normal chain differ from the isopropenyl derivatives by the much greater intensity of peak 63. The ion corresponding to this number is probably formed in the following way:

$$C_5H_6 \rightarrow C_5\overset{+}{H_5} \rightarrow C_5H_3^+ + H_2.$$

In all the isomers except propenylacetylene there is very little (15-25%) cleavage of the bond between the methyl group and the conjugated system. The spectrum of the propenyl derivative differs from the spectra of other isomers chiefly by the presence of an intense 49 peak. The corresponding ion is probably formed by the loss of a hydrogen from the $C_4H_3^+$ ion.

The cleavage of a single bond between two multiple ones and the formation of mass-41 and 40 ions occurred extensively only among vinylacetylenes where the methyl group was next to a double bond. However, all the isomers gave spectra with a very intense mass-39 ion, which evidently resulted from such a cleavage and in two cases was followed by the loss of hydrogen,

$$C_5H_6 \rightarrow C_5H_5^+ \rightarrow C_3H_3^+ + H_2.$$

In the spectrum of vinylmethylacetylene the mass-39 ion could have also arisen on account of the triple bond cleavage; however, the fact that it was detected in the branched-chain isomer, as well as in piperylene and isoprene spectra [5], seems to support the first hypothesis concerning its origin.

One fact becomes apparent right away, that the greatest stability was exhibited by ions for which one could write structural formulas with conjugated bonds, for example $39CH_2^+ \overset{\longleftarrow\mid}{-\,C \equiv} CH$, for the mass-39 ion, $41\ CH_2^+ \overset{\longleftarrow\mid}{-\,CH=} CH_2$, for the mass -41 ion, etc.

The mass spectra together with certain ideas about the reactivities of organic compounds make it possible to compare the ionization potentials of ion-molecules.

Our measurements revealed that isopropenylacetylene was the hardest to ionize (ionization potential 10.1 ev). The ionization potentials of vinylmethylacetylene (9.4 ev) and especially propenylacetylene (8.5 ev) were much smaller than that of vinylacetylene (9.9 ev).

It would be interesting to compare these results with the kinetic data for any ionic reactions of vinylacetylene; however, the literature does not contain any references relating to this problem.

LITERATURE CITED

[1] A. A. Petrov, et al., J. Gen. Chem. 20, 708 (1950)*; 23, 1867 (1953)*; 27, 1805 (1957)*; 28, 1994 (1958)*; Proc. Acad. Sci. 90, 561 (1953); 125, No. 5 (1959)*.

[2] A. A. Petrov, Yu. I. Porfir'eva, and G. I. Semenov, J. Gen. Chem. 27, 1167 (1957).*

[3] A. A. Petrov, V. A. Kolesova, Yu. I. Porfir'eva, J. Gen. Chem. 27, 2081 (1957).*

[4] A. A. Petrov, K. S Mingaleva, B. S. Kupin, Proc. Acad. Sci. 123, 298 (1958).*

[5] Petroleum Institute Research,Project. 44, Mass Spectral data, N. Y. (1952).

[6] K. I. Zimina, A. A. Polyakova, M. V. Tikhomirova, N. S. Sosina, Coll. Composition and Properties of Petroleums, Izd AN SSSR, p. 72 (1957).**

Received March 21, 1959

---

* Original Russian pagination. See C.B. Translation.

** In Russian.

POLYMORPHISM AND THE ELECTROLYTIC BEHAVIOR OF CARBOXYLIC ACIDS IN SOLUTION

S. S. Urazovskii

V. I. Lenin Khar'kov Polytechnical Institute

(Presented by Academician P. A. Rebinder, March 23, 1959)

We have already found out on several occasions that the polymorphic modifications of organic compounds will in many cases preserve different properties even after the crystals had been melted or dissolved [1]. This persistent behavior led us to the conclusion that we should regard polymorphism as a manifestation of the conjugated variables—crystal structures and molecular configurations(or of elementary molecular combinations—associated versus solvated states) which are able to survive for long or short periods of time in the liquid phase. To describe this type of molecular configuration changes, where the chemical nature of the compounds remains unchanged and the energy changes are small (of the order of 1-5 kcal/mole), we coined the name of molecular polymorphism.

Of the numerous cases of molecular polymorphism the most interesting is the case of aliphatic acids, and in particular substituted acetic and propionic acids. Recently we made a detailed study of the electrolytic properties of the polymorphic modifications of monochloroacetic, glycolic, and α,β-dibromopropionic acids in nonaqueous solvents. All the modifications were monotropic and had the following melting points: monochloroacetic acid: $\alpha = 61.3°$, $\beta = 56.2°$, $\gamma = 50.2°$, $\delta = 43.8°$ C; glycolic acid: $\alpha = 78.0°$, $\beta = 63.0°$ C; α,β-dibromopropionic acid: $\alpha = 64.0°$, $\beta = 51.0°$ C.

We only worked with the stable α and the metastable β-modifications. Since the third and fourth modifications of chloroacetic acid were extremely unstable they were not studied. The metastable modifications were prepared by carefully supercooling the stable modifications below their melting points. Properly dried and purified ethyl alcohol, acetone, and dichloroethane were used as solvents. All the measurements were carried out in freshly prepared solutions at 25° C.

The degrees of ionization (electrolyte strength) of individual acid modifications were calculated after determining their dissociation constants. The ionization constants were determined by two independent routes—conductometrically and potentiometrically. Moreover, in the second method we used different variations of concentration cells; in one case we coupled our electrodes against a standard, in another we measured directly the electromotive force (emf) of equimolar cells, i.e., cells composed of two half cells of which the first would contain one acid modification and the second an equal concentration of the other; in this method we used both buffered and unbuffered solutions.

We determined the emf of buffered cells at two acid concentrations—0.002 and 0.005 N. At these concentrations the resultant ΔpK values were independent of concentration. In more concentrated solutions (above 0.01 N) ΔpK increased considerably with increasing concentrations; this can be readily seen in Table 1, which was constructed on the basis of conductometric data and data obtained from measurements of unbuffered equimolar cells of α,β-dibromopropionic acid in acetone.

In Table 2 we have listed the combined ΔpK data calculated from the emf of equimolar unbuffered cells containing 1 N solutions of the α and β acid modifications being compared.

The data presented make it quite evident that the individual polymorphic modifications of any one acid give electrolytic solutions differing considerably in their strength. It is also apparent that the differences increased

TABLE 1

Concen., moles/-/liter	Emf, mv	ΔpK
1	37,8	1,28
0,5	25,5	0,86
0,2	18,5	0,63
0,1	16,0	0,54
0,05	15,0	0,51
0,005	13,0	0,44
0,002	13,0	0,44

with decreasing dielectric constant of the solvent. This is very clearly supported by the data we had previously obtained from measurements performed on monochloroacetic acid in dioxane—water solutions [3]; there we found that with increasing water content the differences in pK levelled off, completely disappearing in pure water.

It should be noted that the observed differences will also level off if the solutions are allowed to stand for 4 to 30 hours; the rate will depend on the solvent and will be greater in buffered than in unbuffered solutions.

Besides the above presented results, obtained potentiometrically, we also got similar data conductometrically.

The electrical conductance was measured in an apparatus described in two earlier papers [4,5]. There we also described the experimental results in more detail [5-7].

The limiting conductances of the different modifications of any one acid in a particular solvent were identical, while in the range of concentrations where λ_φ could be experimentally determined, large differences were observed between the two modifications. By plotting the entire curves of $\lambda(\varphi)$ functions we found that the observed differences between the conductances of α and β- modifications of our acids increased at first with dilution, attaining a maximum at $\varphi \approx 10^6$ liter/mole (where the degree of dissociation was close to one half), then decreased approaching zero in infinitely dilute solutions, where φ_0 became identical for both modifications.

The conductance data obtained were later used to calculate the dissociation constants of the individual polymorphic modifications of our acids. The dissociation constants thus obtained were compared with the corresponding values obtained potentiometrically.

In Table 3 we have listed the differences between the dissociation constants in the form of ΔpK for the two modifications of α, β-dibromopropionic acid; values obtained by various methods are listed.

TABLE 2

Solvent	Diel. const.	α, β-dibromopropionic acid		Monochloroacetic acid		Glycolic acid	
		Emf, mv	ΔpK	Emf, mv	ΔpK	Emf, mv	ΔpK
Ethanol	25,3	22,5	0,76	20,0	0,67	29,2	1,00
Acetone	19,1	37,8	1,28	52,0	1,74	—	—
Dichloroethane	10,3	110,0	3,73	101,0	3,36	—	—

TABLE 3

Nos.	Exptl. method	Δpk of α, β-dibromopropionic acid modifications		
		in ethanol	in acetone	in dichloroethane
1	Electrical conductance	0,15	0,42	—
2	Emf of buffered cell vs. a standard acid (picric)	0,16	0,36	0,49
3	Emf of equimolar buffered cell	0,17	0,37	0,48
4	Emf of an equimolar unbuffered cell	0,18	0,44	—

By comparing the various data we can clearly see that the ΔpK values obtained by different methods are in a satisfactory agreement, which fully convinced us that there exist some real differences in the strength of the α and β-modifications of our acids.

An examination of our results enabled us to conclude that it was the molecules and not the ions which were responsible for the observed differences in the electrolytic properties of individual acid modifications, because in completely dissociated solutions these differences disappeared. The latter fact must be responsible for the conversion of the metastable into the stable modification. As a matter of fact, since the acid molecules are in a dynamic equilibrium with the ions, there will be a constant dissociation $\rightleftharpoons$ association process, with the reservation, however, that the reverse (association) process will lead exclusively to the formation of the stable α-configuration:

$$\left.\begin{array}{l}\beta\text{-configuration} \rightarrow \\ \alpha\text{-configuration} \leftarrow\end{array}\right\} \text{ ionized state,}$$

i.e. to an irreversible $\beta \rightarrow \alpha$ conversion, which was indeed observed.

With regard to the configuration differences between the α and β-modifications of our acids, we assumed different types of association for our molecules—dimeric for α-modifications, and chain or intramolecular forms for the β-modification.

LITERATURE CITED

[1] S. S. Urazovskii, Molecular Polymorphism, Kiev (1956).*

[2] S. S. Urazovskii, Proc. Acad. Sci. 77, 1039 (1951).

[3] S. S. Urazovskii, A. I. Kuris'ko, Trans. Khar'kov Polytech. Inst. 26, No. 6 (1959).

[4] S. S. Urazovskii, Z. M. Kanevskaya, Trans. Khar'kov Polytech. Inst. 4, No. 2, 45 (1954).

[5] S. S. Urazovskii, Z. M. Kanevskaya, Proc. Acad. Sci. (In print).

[6] P. Walden, Elecktrochem. nichtwas. Losungen, Leipzig, p. 98 (1924).

[7] R. Fuoss and C. Kraus, J. Am. Chem. Soc. 55, 176 (1933); 57, 488 (1935).

Received March 20, 1959

---

* In Russian.

ABSORPTION OF ULTRAHIGH FREQUENCY VIBRATIONS IN AQUEOUS AND ALCOHOLIC SOLUTIONS OF THE SALTS RbCl AND CsCl.

A. G. Anikin, Corresponding Member Acad. Sci.
USSR Ya. I. Gerasimov, and I. V. Gordeev

The M. V. Lomonosov Moscow State University

This work is part of a series of investigations on the absorption of ultrahigh and superhigh frequency vibrations by solutions of inorganic and organometallic compounds in various solvents, and on the variation with frequency of the concentration at which maxima occur on the rise in temperature—concentration curve. Only one paper on this subject could be found in the literature: Forman and Crisp [1] investigated absorption at radio frequencies by aqueous solutions of NaCl, $CaCl_2$, $SrCl_2$ and $LaCl_3$. They found, in particular, that the curve relating absorption at uhf and concentration of NaCl solutions had a maximum at a concentration of 0.015 mole/liter at a frequency of 27.3 Mc; the absorption maximum shifted in the direction of lower concentration with decreasing frequency. It therefore seemed probable that further decrease in frequency would shift the maximum of the rise in temperature—concentration curve to still lower concentrations. For comparison, we investigated the adsorption at u.h.f. by aqueous and alcoholic solutions of RbCl and CsCl, over the frequency range 3 to 11 Mc.

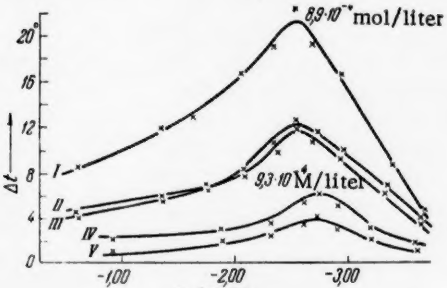

Fig. 1. Absorption at uhf by solutions of RbCl in water and methyl alcohol: I) absorption by solutions of RbCl in CH_3OH at 11 Mc; II) at 3.2 Mc; III) at 6 Mc; IV) absorption by solutions of RbCl in water at 11 Mc; V) at 3.2 Mc.

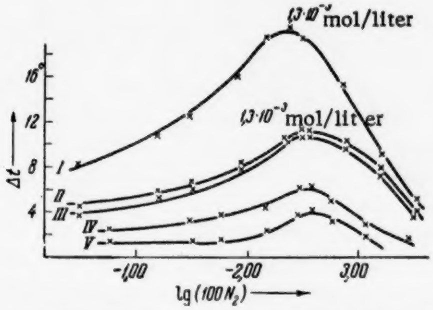

Fig. 2. Absorption at uhf by solutions of CsCl in water and alcohol: I) absorption by solutions of CsCl in CH_3OH at 11 Mc; II) at 3.2 Mc; III) at 6 Mc; IV) absorption by solutions of CsCl in water at 11 Mc; V) at 3.2 Mc.

Method. The solutions were investigated in a quartz vessel placed in the high-frequency electric field of a condenser. The stabilized electric field of a PSK-4 installation was utilized; the nominal power of the generator was 1 kw. The voltage between the plates of the condenser was measured with a C-96 kilovoltmeter. The frequency stability of the generator was within the limits ± 0.001 of the operating frequency. All the experiments

TABLE 1

Absorption at uhf by Methyl Alcohol Solutions of Rubidium Chloride and Cesium Chloride in the Form of Heating up of the Solution

Solutions and their concentrations		Δt, °C		
M/liter	mole %, 100 N_2	at 11 Mc	at 6 Mc	at 3.2 Mc
1. Methyl alcohol		1,7	1	0,7
2. CsCl sol. in CH_3OH				
$1,0 \cdot 10^{-1}$	$3,3 \cdot 10^{-1}$	8	3,8	4,5
$2,0 \cdot 10^{-2}$	$6,5 \cdot 10^{-2}$	11	5	6
$1,0 \cdot 10^{-2}$	$3,3 \cdot 10^{-2}$	12,5	6	6
$4,0 \cdot 10^{-3}$	$1,3 \cdot 10^{-2}$	16	7,2	8,5
$2,0 \cdot 10^{-3}$	$6,5 \cdot 10^{-3}$	19,5	9,1	9,5
$1,3 \cdot 10^{-3}$	$4,3 \cdot 10^{-3}$	21,5	10,5	11,5
$1,0 \cdot 10^{-3}$	$3,3 \cdot 10^{-3}$	19,5	10,5	11,5
$4,0 \cdot 10^{-4}$	$1,3 \cdot 10^{-3}$	13,5	10	11
$2,0 \cdot 10^{-4}$	$6,5 \cdot 10^{-4}$	9	8	7,5
$1,0 \cdot 10^{-4}$	$3,2 \cdot 10^{-4}$	4,5	4	4
$4,0 \cdot 10^{-5}$	$1,3 \cdot 10^{-4}$	2,5	2	2,5
3. RbCl solutions in CH_3OH				
$6,7 \cdot 10^{-2}$	$2,2 \cdot 10^{-1}$	8,5	4	4,5
$1,3 \cdot 10^{-2}$	$4,3 \cdot 10^{-2}$	12	6	6
$6,7 \cdot 10^{-3}$	$2,2 \cdot 10^{-2}$	13	6,5	6,5
$2,7 \cdot 10^{-3}$	$8,5 \cdot 10^{-3}$	16,5	7,8	8
$1,3 \cdot 10^{-3}$	$4,3 \cdot 10^{-3}$	19	10	10,5
$8,9 \cdot 10^{-4}$	$2,0 \cdot 10^{-3}$	23	12	13
$6,7 \cdot 10^{-4}$	$2,2 \cdot 10^{-3}$	21,5	11	11
$3,3 \cdot 10^{-4}$	$1,1 \cdot 10^{-3}$	15	9,5	9,5
$1,3 \cdot 10^{-4}$	$4,3 \cdot 10^{-4}$	8,5	7,5	7
$6,7 \cdot 10^{-5}$	$2,2 \cdot 10^{-4}$	4	4	3.5
$2,7 \cdot 10^{-5}$	$8,6 \cdot 10^{-5}$	2	2	2

TABLE 2

Absorption at uhf by Aqueous Solutions of Rubidium Chloride and Cesium Chloride in the Form of Heating up of the Solution

Solutions and their concentrations		Δt, °C		
M/liter	mole %, 100 N_2	at 11 Mc	at 6 Mc	at 3.2 Mc
1. Water		0,7	0,2	0,2
2. CsCl solutions in water				
$9,8 \cdot 10^{-2}$	$1,8 \cdot 10^{-1}$	2,5	1	1,2
$1,9 \cdot 10^{-2}$	$3,5 \cdot 10^{-2}$	3	—	—
$9,8 \cdot 10^{-3}$	$1,8 \cdot 10^{-2}$	3,5	1,3	1,5
$3,9 \cdot 10^{-3}$	$7,0 \cdot 10^{-3}$	4	2	2
$1,9 \cdot 10^{-3}$	$3,5 \cdot 10^{-3}$	6	3,5	3,5
$1,3 \cdot 10^{-3}$	$2,3 \cdot 10^{-3}$	6	3,5	3,5
$9;8 \cdot 10^{-4}$	$1,8 \cdot 10^{-3}$	5,2	3	3
$4,9 \cdot 10^{-4}$	$8,8 \cdot 10^{-4}$	3,2	1,8	2
$1,9 \cdot 10^{-4}$	$3,5 \cdot 10^{-4}$	1,7	1	1
$9,8 \cdot 10^{-5}$	$1,7 \cdot 10^{-4}$	1,2	0,2	0,2
3. RbCl solutions in water				
$7,0 \cdot 10^{-2}$	$1,3 \cdot 10^{-1}$	2,3	1	1,2
$1,0 \cdot 10^{-2}$	$1,3 \cdot 10^{-2}$	3	2	1,7
$2,8 \cdot 10^{-3}$	$5,1 \cdot 10^{-3}$	3,5	2,5	2
$1,4 \cdot 10^{-3}$	$2,1 \cdot 10^{-3}$	5,5	3,5	3,5
$9,4 \cdot 10^{-4}$	$1,7 \cdot 10^{-3}$	6,6	4,1	4,5
$7,0 \cdot 10^{-4}$	$1,3 \cdot 10^{-3}$	4,5	3	3,5
$3,5 \cdot 10^{-4}$	$6,3 \cdot 10^{-4}$	3,1	2,2	2,3
$1,4 \cdot 10^{-4}$	$2,5 \cdot 10^{-4}$	1,8	1,1	1,0
$7,0 \cdot 10^{-5}$	$1,3 \cdot 10^{-4}$	0,7	0,5	0,3

were carried out under relatively uniform conditions: the anode current in the PSK-4 installation was 0.35 amp, the voltage was 3.6 kv, the sample volume was 5 ml, the exposure time was 30 seconds, measurements were performed at frequencies of 3.2, 6 and 11 Mc. Absorption at uhf was measured by the rise in temperature of solutions of different concentration, for equal irradiation times. Solution temperatures were measured with a mercury thermometer, calibrated in 0.1°. Control experiments showed that, within the limits of precision of measurement, the thermometer was not heated by the uhf field. The experiments were repeated 3 or 4 times. The results obtained are shown in Tables 1 and 2, and in Figs. 1 and 2.

Experimental Results. Absorption at uhf by the pure solvents, water and methyl alcohol, were measured first. It was found that the methyl alcohol absorbed the uhf field more strongly than did water, although water has the higher dipole moment. Correspondingly, alcohol solutions of the salts absorbed the uhf field more strongly than did the corresponding aqueous solutions. We investigated solutions of the salts rubidium chloride and cesium chloride in methyl alcohol and water. These salts were chosen because they were soluble in methyl alcohol [2], so that comparative studies of their aqueous and alcoholic solutions could be carried out at different concentrations. The maximum absorptions at uhf by alcoholic solutions of RbCl were of the order of concentration $C = 8.9 \cdot 10^{\bar{4}}$ mole/liter, i.e. $100\ N_2 = 2.9 \cdot 10^{\bar{3}}$ mole %, and by CsCl solutions were of the order of concentration $C = 1.3 \cdot 10^{\bar{3}}$ mole/liter, i.e., $100\ N_2 = 4.3 \cdot 10^{\bar{3}}$ mole %. For aqueous solutions, the corresponding figures were, for RbCl, $C = 9.3 \cdot 10^{\bar{4}}$ mole/liter, i.e., $100\ N_2 = 1.7 \cdot 10^{\bar{3}}$ mole %, and, for CsCl, $C = 1.3 \cdot 10^{\bar{3}}$ mole/ liter, i.e., $100\ N_2 = 4.3 \cdot 10^{-3}$ mole %. The experimental results were clearly, in fundamental agreement with our presumption that there would be a shift in the absorption maximum of salt solutions at uhf., in the direction of lower concentrations with decreasing frequency compared with that used by Forman and Crisp. It has also been clearly shown, for the first time, that there are maxima in the absorption–concentration curves of alcoholic solutions at uhf

LITERATURE CITED

[1] I. Forman and D. I. Crisp, Trans. Farad. Soc. 42-a, 186 (1946).

[2] V. E. Plyushchev, I. V. Shakhno, L. N. Komissarova, and G. V. Nadezhdina, Sci. Proc. High School, Chem. and Chem. Technol. No. 2, 279 (1958).

Received April 27, 1959

THE EFFECTS OF DISPLACEMENT OF THE LEVEL OF CHEMICAL POTENTIAL OF ELECTRONS ON THE ACTIVITY OF SEMICONDUCTOR CATALYSTS

Corresponding Member Acad. Sci. USSR G. K. Boreskov

The L. Ya. Karpov Physicochemical Scientific Research Institute.

The catalytic activity of a semiconducting catalyst must be connected with the level of chemical potential of the electrons, since the state of the chemical potential is directly related to the energy of the intermediate surface compounds, whose formation is accompanied by electron transfer. Therefore, displacement of the level of chemical potential must affect the probability of formation of active complexes, produced by intermediate surface interaction of the reacting substances with the catalyst, and hence affect the rate of reaction.

Let us consider, as a simple example, the chemisorption of particles of A to form the charged particles A^+ on the surface. The heat of adsorption is

$$Q = \varphi - I_A + W_{A+K}. \qquad (1)$$

Here, φ is the electron work function, directly determined by the state of level of chemical potential. This depends on both the electronic structure of the solid catalysts and the concentration of adsorbed substance. It is related to the space charge, created on the surface by the adsorption of charged particles, which alters φ (edge of boundary zones). I_A is the ionization energy, determined only by the properties of the adsorbed molecule.

W_{A+K} is the energy of interaction of the resulting A^+ ion with the catalyst. It is determined by the properties of both the adsorbed substance and the catalyst, and, generally speaking, must depend on the state of the adsorbed particles on the surface.

Let us consider the effect on the chemisorption rate of a small change in φ, associated, for example, with a stoichiometric change or the introduction of an additive.

Let us assume that any change in W_{A+K} can be neglected. We also suppose that the surface is uniform, and, for the present, will not take into account any change in φ dependent on the degree of coverage of the surface.

Then the heat of adsorption will only alter by the amount of the shift in level of chemical potential.

$$Q = Q_0 + \Delta\varphi.$$

The degree of coverage of the surface is

$$\theta = \frac{bp_A}{1 + bp_A}, \qquad (2)$$

where $b = b_0 e^{Q_0/RT} e^{\Delta Q/RT}$ is the adsorption coefficient and p_A is the pressure of substance A.

With increase in φ the adsorption equilibrium alters continuously, approaching to complete coverage of the surface.

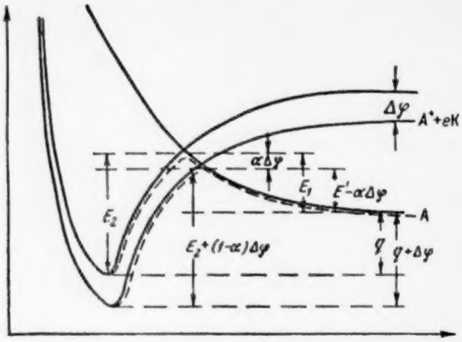

Fig. 1. Change in activation energy of adsorption with displacement of the level of chemical potential.

The rates of adsorption and desorption are determined by the activation energy of the adsorption complex, whose configuration is intermediate between A and A^+K. This energy must also depend on the level of chemical potential of the electrons.

As shown by M. I. Temkin [1], the course of adsorption is in good agreement with an assumption, similar to Bronsted's rule, that the change in activation energy of adsorption forms some part of the change in heat of adsorption.

Then, as shown diagrammatically in Fig. 1, the activation energy of adsorption is

$$E_1 = E_{10} - \alpha\Delta\varphi$$

and the activation energy of desorption is

$$E_2 = E_{20} + (1-\alpha)\,\Delta\varphi,$$

where α is between zero and unity, and is usually close to 0.5 .

The rate of adsorption is

$$w_1 = K_1 p_A (1-\theta) = K_{01}\, e^{\alpha\Delta\varphi/RT}\, p_A (1-\theta).$$

The rate of desorption is $w_2 = K_2\theta = K_{02}\, e^{-(1-\alpha)\Delta\varphi/RT}\,\theta$.

Hence, for the condition of adsorption equilibrium, making use of (2), we find :

$$w_1 = w_2 = K_{02}\frac{p_A b_0 e^{Q_0/RT} e^{\alpha\Delta\varphi/RT}}{1 + p_A b_0 e^{Q_0/RT}\, e^{\Delta\varphi/RT}}\,. \tag{3}$$

It follows from Eq. (3) that, in the equilibrium state, the rates of adsorption and desorption increase with increasing φ at low degrees of coverage, pass through a maximum, and then decrease at high degrees of surface coverage. The adsorption of acceptor electrons is characterized by a reverse rule.

The maximum rate corresponds to the value of φ at which the degree of coverage is $\theta = \alpha$. This agrees with the general result, obtained by Temkin and Kiperman [2], for the relation between adsorption rate and degree of surface coverage.

As has been shown previously, the adsorption of charged particles leads to the creation of a space charge in the layer of catalyst adjacent to the surface, which results in a change in the work function by an amount $\delta\varphi_\theta$, dependent on the degree of surface coverage [3]. With a positive charge on the adsorbed particles $\delta\varphi < 0$, and with a negative charge $\delta\varphi > 0$. The conditions for maximum rate of adsorption, in this case, will also correspond to the degree of coverage $\theta = \alpha$, but this degree of coverage will be attained at a level of chemical potential reduced by the amount $\delta\varphi_\theta = \theta = \alpha$.

In the case of a nonuniform surface, the above conclusions can only be applied correctly to separate groups of parts of the surface, for which differences in properties can be neglected.

These conclusions can be used directly to elucidate the effects of displacement of the level of chemical potential of oxide catalysts, on their activity with respect to the reaction of isotopic exchange with molecular hydrogen. If it is accepted that exchange proceeds by an adsorption—desorption mechanism, and that adsorption takes place in the form of positively charged atoms, then

$$\theta = \frac{\sqrt{bp_{H_2}}}{1+\sqrt{bp_{H_2}}}$$

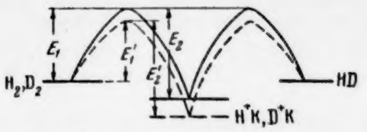

Fig. 2. Change in activation energy of the reaction of isotopic exchange with molecular hydrogen on lowering of the level of chemical potential.

The rate of exchange is

$$w = K_2\theta^2 = K_{02}\frac{b_0e^{\alpha\Delta\varphi/RT}p_{H_2}}{(1+\sqrt{b_0e^{\Delta\varphi/RT}p_{H_2}})^2}. \qquad (4)$$

Lowering the level of chemical potential decreases the activation energy of adsorption and increases the activation energy of desorption (Fig. 2).

Hence, in the region of low degrees of surface coverage ($\theta < \alpha$), lowering the level of chemical potential must increase catalytic activity, but must have the opposite effect in the region of high coverage.

In a similar way we can ascertain the effect of level of chemical potential on the activity of semiconductors in more complicated reactions. If a catalytic reaction passes through a stage associated with electron transfer, then one of the subsequent stages will certainly be associated with electron transfer in the opposite direction.

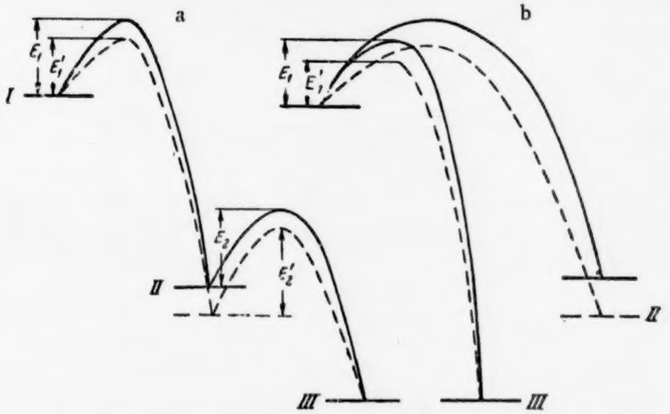

Fig. 3. The effect of displacement of the level of chemical potential on the activation energy for a catalytic reaction of surface interaction with transfer of an electron from the reacting substance to the catalyst: I) initial substance, II) intermediate surface compound and III) reaction products. a) An intermediate product is formed. With a lowering of the level of chemical potential, there is a reduction in activation energy for the stage of formation of the intermediate compound and an increase in activation energy for its subsequent transformation. b) An intermediate compound is not formed. There is a decrease in activation energy for the reaction when the level of chemical potential is lowered.

Thus, if the reaction takes place through the formation of an intermediate surface compound, with transfer of an electron from the catalyst to the reacting substance, then raising the level of chemical potential of the electrons will lower the activation energy for the formation of this intermediate compound and will raise the activation energy of its subsequent transformation (Fig. 3 a).

If the surface interaction does not reach the stage of the intermediate product, then the energy of formation of the intermediate product may determine the energy of the transition state, and reduction in the level of chemical potential will lead to a decrease in the activation energy of the reaction (Fig. 3 b).

Starting from this established relation, we can try to find a connection between catalytic activity and other properties of solid bodies dependent on the level of chemical potential of the electrons. A number of investigations have been made of the connection between the catalytic activity and electrical conductivity of semiconductor catalysts, of different stoichiometric composition or with additives. It is usually accepted that a reduction in the activation energy for electrical conductivity should be associated with a rise in the level of chemical potential of the electrons for n-type semiconductors, and a decrease of the same amount for p-type semiconductors.

But this relation between changes in catalytic activity and electrical conductivity is found, in many cases, to be contradicted by experiment [4]. This is evidently associated with a change in the boundaries of the forbidden band, as the result of introduction of a small amount of additive. In this case, a shift in the level of chemical potential of the electrons may not correspond to a change in the activation energy for electrical conductivity [5].

Thus, unlike its connection with the level of chemical potential, no connection between catalytic activity and electrical conductivity can be simply predicted.

As a second example, we may consider the connection between catalytic activity and the free energy of dissociation of oxides. The transformation of an oxygen ion into molecular oxygen corresponds to a change in the level of chemical potential of an electron, and the dissociation energy of an oxide includes the work function of the electron as one of its components.

It therefore follows that, with a change in composition, unaccompanied by any significant change in other properties, we should expect a linear relation between the activation energy of a catalytic reaction and the dissociation energy of an oxide, or the logarithm of its dissociation pressure :

$$E = \mathrm{A} \pm \mathrm{B}q = \mathrm{A} \pm \mathrm{B}_1 \ln P, \tag{5}$$

where $\underline{q}$ is the dissociation energy of the oxide and P is its dissociation pressure.

The sign of the second term is determined by the direction of electron transfer in the limiting stage of the catalytic reaction.

The relation (5) is usually reckoned to be an indication of the oxidation—reduction mechanism of the reaction taking place. It follows, from the above considerations, that a relation between the dissociation pressure of an oxide and its catalytic activity is also possible with other reaction mechanisms, not directly concerned with interaction of the reacting substance with the oxygen of the catalyst. This may be the result of relations between both oxygen dissociation pressure and catalytic activity of the oxide with the level of chemical potential of the electrons.

LITERATURE CITED

[1] M. I. Temkin, J. Phys. Chem. 15, 296 (1941).

[2] M. I. Temkin and S. L. Kiperman, J. Phys. Chem. 21, 927 (1947).

[3] F. F. Vol'kenshtein, Prog. Chem. 27, 1304 (1958).

[4] N. P. Keier and L. N. Kutseva, Proc. Acad. Sci. USSR 117, 259 (1957).*

[5] G. K. Boreskov, Probl. Phys. Chem. 1, 101 (1958).

Received May 13, 1959

---

* Original Russian pagination. See C.B. Translation.

MECHANISM OF THE PROTECTIVE ACTION OF BENZENE RINGS IN THE RADIOLYSIS OF POLYSTYRENE

Ying Shen-k'ang, A. N. Pravednikov
and Academician S. S. Medvedev

L. Ya. Karpov Scientific-Research Physicochemical Institute

The formation of cross-linkages in the radiolysis of polystyrene requires the expenditure of considerably more energy than is needed for the joining up, under the action of radiation, of polymers which do not contain phenyl groups, such as polyethylene. In the radiolysis of polyethylene 25-35 ev are consumed in forming one cross-linking bond, but this is increased to 3000- 5000 ev in the case of polystyrene [1-3]. At the same time the yield of free radicals produced by irradiating linear paraffins is only 5-7 times the yield from alkylated aromatic compounds (such as toluene and ethylbenzene [4]). Thus the high stability of polystyrene toward radiation cannot be explained by the normal scheme of protective action of benzene rings.

In order to explain the high radiation stability of polystyrene it is necessary to consider the mechanism of the reaction, occurring during the radiolysis of this polymer. A hydrogen atom, formed by rupture of a C-H bond of the polymer molecule under the action of radiation —

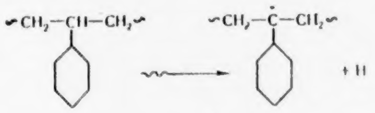

(1)

may react in two ways: 1) by removal of a hydrogen atom from the aliphatic chain

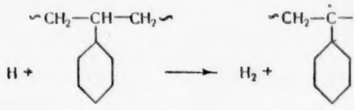

(2)

or 2) by addition to a double bond of a benzene ring to form a free radical of the cyclohexadienyl type

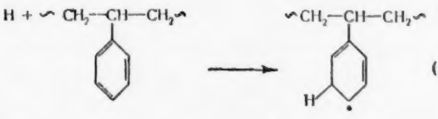

(3)

According to Melville and Robb [5], this reaction is very fast.

Because of the low diffusion rate in glassy polymers, and the high rate of reaction of the atomic hydrogen particle the radical formed in this way must be in the immediate vicinity of the primary radical formed by Reaction(1). Interaction of the primary radical with a radical formed by Reaction (2) will clearly lead to the formation of a cross-linking bond:

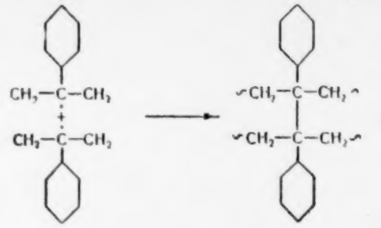

(4)

But interaction of the primary radical with a cyclohexadienyl type radical can occur in two ways. The two radicals can combine with each other to form a cross-linkage.

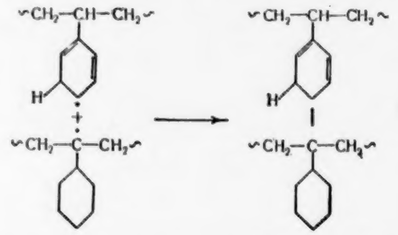

(5)

In favor of the assumption that this reaction occurs is the fact that, in the radiolysis of polystyrene, the yield of cross-linkages is always higher than the yield of hydrogen (it is obvious from the above equation that the formation of a cross-linkage is not accompanied by the liberation of hydrogen in Reaction (5)).

However, the radicals can also take part in a disproportionation reaction:

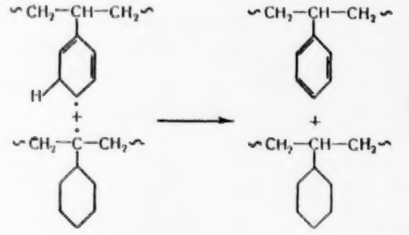

(6)

This disproportionation reaction will lead to a return to the initial state, and consequently, to the dissipation of energy without formation of a cross-linkage. As a result, the effectiveness of the cross-linking process will drop, and the energy, consumed in forming one cross-linkage, will increase.

A necessary condition for the occurrence of Reaction (6) at a high velocity is a low mobility of the polymer chain. An increase in the chain mobility, produced, for example, by addition of solvent to the polymer, will increase the probability of recombination of the primary radicals (this probability is practically zero in the solid polymer), and will consequently reduce the rate of Reaction (6). If this happens, the rate of cross-linking (based on the energy absorbed by the polymer) must increase. Information in the literature [6], on the relation between concentration and rate of cross-linking, shows that, when polystyrene is swollen or dissolved in ethyl acetate, there is a decrease in the energy required to form a cross-linkage to a minimum value of 333 ev at a polymer concentration of 20 %, which value is only an order of magnitude greater than that required to cross-link polyethylene. The value of the energy required for cross-linking increases again with further dilution of the solution, evidently because of the reduced probability of encounters between polymer radicals, so that an increasing part is played by interaction of polymer radicals with radicals formed from the solvent.

In order to obtain an experimental check of the above theory of the mechanism of reaction between primary and cyclohexadienyl type radicals, we synthesized a deuterated toluene, $CD_3C_6H_5$, in which all the hydrogen atoms of the methyl group were replaced by deuterium (by Renand's [7] method from $C_6H_5CCl_3$ and CH_3COOD). The interaction of a deuterium atom, formed by the rupture of a C — D bond under the influence of radiation

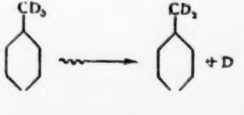

with a benzene ring would produce a methylcyclohexadienyl radical, containing a deuterium atom in the ring.

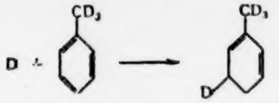

When such a radical reacted with the primary radical, the result of the isotopic effect would be that it was mainly a hydrogen, and not a deuterium atom, which broke away, so that deuterium would be transferred from the aliphatic side chain to the ring

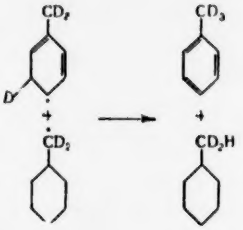

The deuterated toluene was irradiated intensively in the frozen state (at the temperature of liquid air). The irradiated toluene was then oxidized to benzoic acid with aqueous $KMnO_4$ at 95°. The benzoic acid was purified by repeated sublimation in vacuo and burnt in a stream of oxygen. The deuterium content of the water formed was determined by measuring its density. The results obtained are shown in Table 1. In control experiments (without irradiation) it was found that there was no deuterium in the water (and therefore none in the benzene ring).

TABLE 1

Dose in 10^{23} ev/g.	Deuterium content of water, mole %	Energy required to transfer 1 deuterium atom to the ring, ev
3,80	1,25	960
4,75	2,18	750

These results showed that the rate ofReaction (6) was at least 5-6 times greater than the rates of processes leading to cross-linking.

Thus, the high stability of polystyrene is largely associated with the occurrence of disproportionation reactions between primary radicals and radicals of the cyclohexadienyl type.

LITERATURE CITED

[1] A. Charlesby, J. Poly. Sci. 11, 513 (1953).

[2] A. Charlesby, Proc. Roy. Soc. A 215, 187 (1952).

[3] A. Prévot-Bernas, A. Chapiro, et al., Disc. Farad. Soc. No. 12, 98 (1952).

[4] L. A. Wall and D. W. Brown, J. Phys. Chem. 61, 129 (1951).

[5] H. W. Melville and T. C. Robb, Proc. Roy. Soc. A 196, No. 1047, 494 (1949).

[6] A. Henglein, Zs. Phys. Chem. 18, No. 1/2, 56 (1958).

[7] R. Renand, Canad. J. Chem. 34, 98 (1956).

Received March 17, 1959

THE ELECTRODE PROPERTIES, ELECTRICAL CONDUCTIVITY AND CHEMICAL STABILITY OF GLASSES OF THE SYSTEM $Li_2O - La_2O_3 - SiO_2$

Corresponding Member Acad. Sci. USSR
B. P. Nikol'skii, A. I. Parfenov and M. M. Shchul'ts

The A. A. Zhdanov Leningrad State University

In this paper we publish an account of an investigation of the electrode properties, electrical conductivity, and chemical stability of glasses belonging to the simple silicate systems: Li_2O-SiO_2 [1] and Li_2O-La_2O_3-SiO_2 [2]. The properties of more complex silicate systems [3-5] have usually been investigated in the development of practical recipes for electrode glasses.

An investigation of the properties of systems of simple composition was undertaken in this case, so as to elucidate the role of the separate components and their mutual influence with respect to the electrode behavior of the glass. Such an investigation was also necessary to develop a rational means for the subsequent improvement of glass electrodes.

We studied glasses containing 25-33 mole % of lithium oxide and 0-9 mole % of lanthanum oxide, thus covering the permissible range of composition for the preparation of glass electrodes by the normal procedures [1,3,6]. The electrode properties of the glasses were investigated at 25 and 95°C, in solutions containing constant concentrations of alkali metal ions (3 N with respect to the ions Li^+, Na^+, or K^+), at different pH values (from 0 to 14). The method of investigating electrode properties has been described in detail in earlier papers [1,7].

The electrical conductivity of the glasses was measured between 140 and 300° by the method of [8]. In order to calculate the molecular conductivity (λ), the density of the glasses was determined by the method of hydrostatic suspension in benzene and water.

The chemical stability of the glasses was characterized by the amounts of lithium oxide (n_{Li_2O} in millimoles of lithium oxide) and silica which dissoved when the powdered glass (about 1 g) was treated with water at 100° [9].

The data for the electrical conductivity at 150 and 250° (κ is the specific conductivity), the chemical stability (n_{Li_2O}) and density (d), for glasses of the systems Li_2O-SiO_2 and Li_2O-La_2O_3- SiO_2, is shown in Table 1. The density data for glasses of the system Li_2O-SiO_2 is taken from [10], and the electrical conductivity of the glass containing 33 mole % of Li_2O and 67% SiO_2 is taken from [8].

It follows, from the data given in Table 1, that the introduction of lanthanum oxide into lithium glass produced a small increase in conductivity, which was probably associated with a stronger binding of the lithium ions in the glass. The activation energy of the process of electrical conductivity in the glasses had a tendency to increase as lanthanum oxide was added.

All the glasses investigated by us lost a higher proportion of lithium oxide than silica under the action of water (the glass was "leached out"). This led to the formation of a surface layer of glass enriched with silica. The extractability of the glass by water was decreased by the addition of lanthanum oxide. From this viewpoint, lanthanum oxide is a type of component which increases chemical stability.

TABLE 1

Data on the Electrical Conductivity, Density, and Chemical Stability of Glasses of the System $Li_2O - La_2O_3 - SiO_2$

Composition of glass, mole %			d_4^{18}, g/cm³	Electrical conductivity			n_{Li_2O}, mM/ /liter.
Li_2O	La_2O_3	SiO_2		$-\lg \varkappa_{150}$	$-\lg \varkappa_{250}$	λ_{150}	
25	—	75	2,307	5,63	4,15	$2,1 \cdot 10^{-4}$	—
25	3	72	2,579	6,04	4,52	$8,6 \cdot 10^{-5}$	—
25	6	69	2,859	6,40	4,77	$3,8 \cdot 10^{-5}$	—
25	9	66	3,201	6,66	4,98	$2,1 \cdot 10^{-5}$	—
27	—	73	2,319	5,68	4,17	$1,7 \cdot 10^{-4}$	0,42
27	3	70	2,615	6,17	4,55	$5,8 \cdot 10^{-5}$	0,17
27	6	67	2,905	6,17	4,55	$5,8 \cdot 10^{-5}$	0,08
27	9	64	—	6,32	4,74	$8,3 \cdot 10^{-5}$	0,07
33	—	67	2,347	5,24	—	$3,7 \cdot 10^{-4}$	0,49
33	3	64	2,668	5,36	3,93	$3,0 \cdot 10^{-4}$	—
33	6	61	2,990	5,55	4,10	$1,8 \cdot 10^{-4}$	0,23
33	9	58	—	—	—		0,20

Table 2 shows the results of investigation of the electrode properties of glasses at 25°, in solutions of lithium and sodium salts. Our work on glasses of the system Li_2O-La_2O_3-SiO_2 confirmed the conclusions of [1], that a change in the lithium oxide content of the glass (over the range 25-30 mole %) has little effect on the hydrogen functionality limits of the glass electrodes. This circumstance enables us to show, in Table 2, generalized data for a series of glasses with a constant content of lanthanum oxide and a variable content of lithium oxide. Table 2 shows the limits of the hydrogen functionality on the pH scale (on the basis that a deviation of 10 mv constitutes divergence from the hydrogen functionality) and divergences from it at pH 13, expressed in mv (the scatter of these values for glasses with different Li_2O contents was ± 5 mv). The last table of the column shows the values of the constants for exchange of ions between glass and solution

$$\left(K = \frac{a_{H^+}^{sol} \cdot N_{Li}^{gl}}{a_{Li^+}^{sol} \cdot N_{H}^{gl}} \right) ,$$

calculated by the method of [7].

Although a change in lithium content of the glasses we investigated had little effect on their electrode properties, a change in the lanthanum oxide content had a significant effect. It is interesting that this effect was different for lithium salt solutions on the one hand, and for sodium and potassium salt solutions on the other. In lithium salt solutions, an increase in the lanthanum oxide content of the glass impaired the hydrogen functionality in alkaline media (it shifted the upper limit of the hydrogen functionality in the direction of lower pH and increased the divergence from this functionality in alkaline solutions).

A glass, investigated in solutions of lithium ions, acquired a lithium functionality at pH 12 and above, which indicated practically complete replacement of hydrogen ions in the surface layer of the glass by lithium ions from the solution.

The calculated value of the ion exchange constant increased with increasing content of lanthanum oxide in the glass. This may be explained by the relative strengthening of the lithium ion bonds, in the glasses investigated, when lanthanum oxide was introduced. This explanation is in accordance with the relative decrease in mobility of lithium ions in the glass (value of λ) and some decrease in the extractability of lithium oxide.

An opposite effect was produced by increasing the lanthanum oxide content of lithium glasses, when these were replaced in solutions containing sodium or potassium ions. In these solutions, divergences from hydrogen functionality decreased with increasing lanthanum oxide content of the glass, and the limit of this functionality was displaced toward the more alkaline side. This effect may be related to a probable tightening of the glass structure when lanthanum oxide is introduced, which must retard the penetration into the glass of sodium and potassium ions, which are larger than lithium ions, and therefore, the replacement of hydrogen by these ions.

TABLE 2

Data on Electrode Properties of Glasses of the System Li_2O-La_2O_3-SiO_2

Glass, comp. mole %			Na salt solutions		Lithium salt solutions		
Li_2O	La_2O_3	SiO_2	H_2 functionality limits	diverg. from H_2 funct. at pH 13, mv	H_2 functionality limits	diverg. from H_2 funct. at pH 13, mv	K
25—30	—	75—70	0—9,8	106	0—10,8	88	$0,12 \cdot 10^{-11}$
25—33	3	72—64	0—9,4	95	0—9,7	137	$0,53 \cdot 10^{-11}$
25—33	6	69—61	0—(9,5—10)	~70	0—9,2	177	$1,9 \cdot 10^{-11}$
25—33	9	66—58	0—>10,5	~40	0—9,0	182	$4,1 \cdot 10^{-11}$

For all the lanthanum oxide-containing glasses investigated, the alkali metal ions could be placed in the following order with respect to their influence on the hydrogen functionality of the glass: $Li^+ > Na^+ > K^+$. This order is different for other types of glass [1,11].

At 95° the nature of the relations between electrode behavior and compositions of glass and of solution remained the same as at lower temperatures, although the effects were less pronounced at the higher temperature. The limits of hydrogen functionality, for all the glasses of the system Li_2O-La_2O_3-SiO_2 investigated, altered, when changing from 25 to 95°, from 0-9 and 0-11 to 0-7 and 0-8 pH.

The lower limit of hydrogen functionality for electrode glasses of the above system at 95° was at pH < 0, while, for glasses of the system Li_2O-SiO_2 at the same temperature, this limit is at higher pH 2-3, and at pH 0, the divergence from hydrogen functionality amounts to 100 mv [1].

Thus, lithium oxide is a component of lithium silicate electrode glasses, which at high temperatures, markedly decreases divergences from hydrogen functionality in acid solutions.

It should be noted, in conclusion, that the introduction of lanthanum oxide into lithium silicate electrode glasses is beneficial for extending the limits of hydrogen functionality, stabilizing electrode characteristics, and improving chemical stability.

Of the numerous glasses of the system Li_2O-La_2O_3-SiO_2, the following can be recommended for practical measurement of pH in acid solutions: glass KST (TsLA Energochermet*)[12] and glass of composition Li_2O, 24-28% (mole), La_2O_3 4-7 % and SiO_2 65-70%.

Our results confirm previous conclusions [3] that, in order to produce glass electrodes for use over a wide pH range (0-14), it is necessary to add to glasses of the Li_2O-SiO_2 system other components which extend the range of hydrogen functionality toward the alkaline side, in addition to lanthanum oxide which improves hydrogen functionality in acid solutions.

LITERATURE CITED

[1] A. I. Parfenov, Herald of Leningrad Univ. 4, 1, 98 (1959).

[2] Shinzo Okado, Tomoda Nishi, Takeshi Tanaka, and Katsnji Imabuki, Bull. Eng. Res. Inst. Kyoto Univ. 7, 119 (1955).

[3] G. A. Perley, Anal. Chem. 3, 394 (1949).

[4] B. Lengyel, and F. Till, Egypt. J. Chem. 1, 1, 99 (1958).

[5] W. Simon and D. Wegmann, Helv. Chim. Acta. 41, 7, 2099 (1958).

[6] A. N. Fedotov, Ind. Lab. 4, 498 (1958).**

---

* State All-Union Trust for the Design, Planning, Assembly, and Adjustment of Power Installations and Control and Measuring Instruments of the Ministry of Ferrous Metallurgy of the USSR.

** Original Russian pagination. See C.B. Translation.

[7] B. P. Nikol'skii, J. Phys. Chem. 10, 3, 495, 504 (1937).

[8] O. V. Mazurin and E. S. Borisovskii, J. Tech. Phys. 27, 2, 275 (1957).

[9] N. M. Pavlushkin and G. G. Sentyurin, Practical Handbook on Glass Technology, Moscow (1957).**

[10] S. K. Dubrovo and Yu. A. Shmidt, J. Appl. Chem. 32, 4, 742 (1959)*.

[11] B. P. Nikol'skii, M.M. Shchul'ts and N. V. Peshekhonova, Phys. Chem. 32, 1, 19 (1958).

[12] TsLA pH Meters of the Block Type. Instructions for Installation and Use 5056 M. (1958).**

Received May 13, 1959

---

* Original Russian pagination. See C.B. Translation.

** In Russian.

THE THEORY OF THE ADSORPTION WAVE

THE RELATION BETWEEN IMPOVERISHMENT OF THE CATALYST BED AND THE SPEED OF MOVEMENT OF THE GAS AND THE THICKNESS OF THE BED

Corresponding Member Acad. Sci. USSR A. S. Predvoditelev

1. The present theory of the adsorption wave does not cover all the observed phenomena. For instance, the theory does not deal with the described influence of grain size on the time for impoverishment of the bed ; it does not give a correct answer to questions of the actual connection between the critical height of the bed and the logarithm of the initial concentration of gas, etc. The difficulty experienced is associated with the incomplete use made of modern theory of gas flow through porous bodies.

Consider the movement of gas through a porous adsorbent of cylindrical shape. We restrict this motion, from the hydrodynamic point of view, by assuming a constant rate of permeation of gas along the radius of the cylinder. This assumption on the permeation of gas through a porous body is justified by numerous experiments.

The different stages of extraction of the reacting gas from the stream may be characterized by the following processes : 1) diffusion of gas to the surface grains of the adsorbent ; 2) adsorption on the grain surface; 3) chemical reaction on the adsorbent grains; 4) desorption of the reaction products and their removal from the adsorbing layer.

All these processes can be reflected in a definite manner in the distribution of gas pressure gradient along the adsorbent bed, and, consequently, in the distribution of permeation rate. Almost everything indicates that the complicated process of conversion of the substance in the adsorbent bed passes through as a front, i.e. the adsorbent is used up in the same way as a bed of coal burns out, or a bed of gunpowder or a column of combustible gas mixture, ignited from one end. This front is characterized by a very definite speed. For a uniform case, this circumstance enables us to choose, as a special coordinate, the ratio of the flowing coordinate to time, i.e. to reckon that any parameters characterizing the process do not depend simply on time, but on the position of the front at any moment. For instance, the density does not depend on the linear coordinate and time separately, but can be expressed by a relation of the form

$$\rho = \rho\left(\frac{x}{t}\right) = \rho(\xi), \quad \frac{x}{t} = \xi. \tag{1}$$

We designate such processes as frontal. Thus the movement of an adsorption wave will be considered as a frontal process .

2. It is not difficult to demonstrate the validity of the following expressions :

$$\frac{\partial\rho}{\partial t} = -\frac{\xi}{t}\frac{d\rho}{d\xi}, \quad \frac{\partial\rho}{\partial x} = \frac{1}{t}\frac{d\rho}{d\xi}, \quad \frac{\partial W}{\partial x} = \frac{1}{t}\frac{dW}{d\xi};$$

where W is the rate of permeation under pressure p.

The continuity equation for a uniform process has the form

$$m\frac{\partial\rho}{\partial t} + \frac{\partial\rho W}{\partial x} = 0;$$

where m denotes the porosity of the bed.

Changing to the variable ξ, this has the form

$$m\xi\, d\rho = d(\rho W). \tag{2}$$

After integration, this has the form

$$m\xi\rho = \rho W + m\int \rho\, d\xi + B; \tag{2a}$$

where B is an arbitrary constant.

Suppose that experiment shows that the fall in pressure along the permeating stream is in accordance with a linear law. This shows that the rate of permeation through the adsorbing bed is constant.

Let the index (1) apply to the forward surface of the adsorption front at the moment when it has passed through the whole depth of the adsorbent bed. Let the index (2) apply to the position of the front when it is established and first begins to move with constant speed g. Then $\xi = g$.

This enables us to write down the following two identities :

$$mg\rho_1 = \rho_1 W + m\int^{(1)} \rho\, d\xi + B,$$

$$mg\rho_2 = \rho_2 W + m\int^{(2)} \rho\, d\xi + B.$$

Subtracting the second from the first, we have

$$mg(\rho_1 - \rho_2) = (\rho_1 - \rho_2)W + m\int_{(2)}^{(1)} \rho\, d\xi.$$

Whence it follows that

$$g = \frac{W}{m} + \frac{1}{(\rho_1 - \rho_2)}\int_{(2)}^{(1)} \rho\, d\xi. \tag{3}$$

The integral on the right hand side of the above expression is not equal to zero, since uniform motion of the adsorption front cannot begin with a section of the tube. There is always some initial part which, by the above reckoning, approximates to a stepwise change in the variable ξ; we therefore assume the existence of a special point. Denote this integral by g_k; it has the dimensions of a velocity, so that we call it the critical velocity.

Relation (3) may now be rewritten

$$g = \frac{W}{m} + g_k \tag{3a}$$

Let the depth of the initial part of the bed be d_k and the depth of the whole bed d. Let the time taken for the front formed to traverse the whole bed be T. This time will agree precisely with the time for impoverishment of the adsorbing bed. The rate of movement of the adsorption front may therefore be written in the form

$$g = \frac{d - d_k}{T}.$$

Equating this value of the speed of the front with the speed given by Relation (3a), we have

$$T = \frac{m(d - d_k)}{W + mg_k}. \tag{4}$$

It is evident that this formula is a direct consequence of the continuity equation for the flow of gas through porous bodies.

The formula (4) obtained agrees almost exactly with that derived by M. Katz from the conceptions of Amundsen and Denby [1]. It could not be otherwise, since it is impossible to evade the law of the conservation of matter.

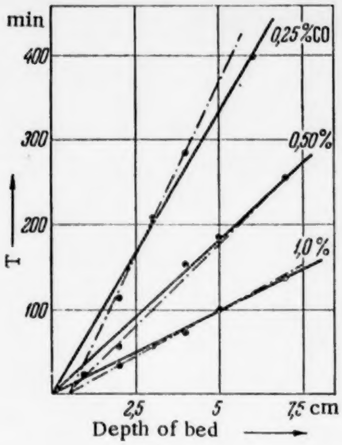

Fig. 1

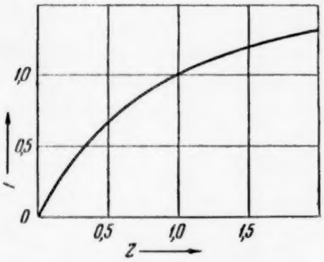

Fig. 2

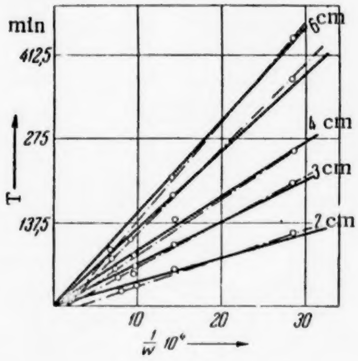

Fig. 3

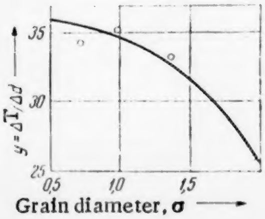

Fig. 4

3. There is experimental data, enabling us to check Formula (4), in the paper by M. Katz on the heterogeneous oxidation of carbon monoxide [1]. The continuous curves in Fig. 1 are drawn for W = 625 cm/minute, on the assumption that the critical thickness, d_k, is equal to zero. The points represent the experimental data. The dotted lines are drawn in conformity with the views of the author. They show that, from the experiments of M. Katz and his colleagues, it is not possible to establish the critical depth with adequate precision; further precise experiments are required for this.

Let z be the reciprocal of the rate of permeation, i.e. z = 1/w. Then Formula (4) may be expressed in the form

$$T = \frac{m(d - d_k)\,z}{1 + mg_k\,z}\,. \tag{4a}$$

The character of the change in the function $T = \frac{2z}{1+z}$ is shown in Fig. 2. The function passes through the origin and approaches asymptotically to a limit. It is obvious from Formula (4a) that the limiting value $T_{\lim}$ is achieved when the rate of permeation is zero. We then have $T_{\lim} = \frac{d - d_k}{g_k}$. It is also evident from Formula (4a) that, with decreasing numerical value for the product $mg_k z$, function T(z) will approximate to a straight line.

Fig. 3 shows the relation between T and 1/W for c_0 = 0.50% for different depths of bed. The continuous lines show with what precision the experimental points fit on straight lines, passing through the origin in accordance with Formula (4a). The dotted lines are drawn in accordance with the views of the author of the paper. Both sets of lines fit the data within the limits of experimental error, though the dotted lines fit much better. But this does not mean that the above ideas are in conflict with experiment.

The function T(z) only passes through the origin on the assumption of infinite rates of permeation for any given porous body. Such a rate of permeation is physically impossible. There must therefore be a limiting rate of permeation for any porous body. Let z_0 be the reciprocal of the limiting rate of permeation. In this case the origin must be transferred to the point (0, z_0) on the system of coordinates used for Formula (4a). Relative to this new system of coordinates, Formula (4a) can be rewritten as

$$T = \frac{m\,(d - d_k)\,(z - z_0)}{1 + mg_k\,(z - z_0)}\,. \tag{4b}$$

For small values of the term $mg_k\,(z - z_0)$, this formula, which fully corresponds to reality, is in agreement with the experimental data of Katz. It should be noted that the rate of permeation, z_0, depends only on the physical nature of the adsorbing bed, and should not depend at all on the chemical nature of the permeating gas.

4. Formula (4) gives the answer to yet another question; it includes a porosity coefficient, which is a function of the grain size. This coefficient readily explains the effects of the grain size of the adsorbent on the time for its impoverishment. In general, the volume occupied by the adsorbent grains can be expressed in the form $V_a = \frac{4}{3}\pi r^3 N$; here r denotes the grain radius, and N the number of

grains in volume v. Thus, introducing the grain diameter, σ, the porosity coefficient may be expressed in the form

$$m = \frac{v - v_a}{v} = 1 - \frac{v_a}{v} = 1 - \frac{1}{6}\pi\sigma^3\frac{N}{v} = 1 - b\sigma^3. \quad (5)$$

The impoverishment time T is proportional to this value. The tangent of the angle of slope of the line, giving the relation between time T, and depth of adsorbent bed, will therefore have the form

$$\frac{\Delta T}{\Delta d} = a\,(1 - b\sigma^3). \quad (5a)$$

Here a denotes a constant, whose meaning is easily explained by Formula (4).

Katz's paper gives some data on measurements of impoverishment time of adsorbent as a function of depth of bed, for different grain sizes. From this data we used the formula $y = 36 - 1.3\sigma^3$ to calculate the tangents of the angles of slope of the lines expressing the above relation. In Fig. 4 the experimental data is shown as points. The continuous curve was calculated by the above formula. It is evident from the figure that there is very good agreement between theoretical calculations and the experimental results. Thus, in this case the porosity coefficient determines the nature of the matter, and no special considerations on the character of the action of the adsorbent grains, as proposed in Denby's theory, are required.

LITERATURE CITED

[1] M. Katz, "Heterogeneous Oxidation of Carbon Monoxide", Coll. Catalysis, Catalysts, in Organic Reactions, Trans. from the English under the editorship of A. A. Balandin and A. M. Rubinshtein, IL, p. 291 (1955).

Received March 30, 1959

THE CONVERSION OF TETRACYCLINE ADSORBED ON A SULFONATED CATION EXCHANGE RESIN, INTO ANHYDROTETRACYCLINE

E. M. Savitskaya, L. F. Yakhontova,
B. P. Bruns and T. S. Kolygina

The All-Union Scientific Research Institute for Antibiotics

(Presented by Academician V. A. Kargin, January 23, 1959)

The antibiotic tetracycline is a naphthacene derivative (I).

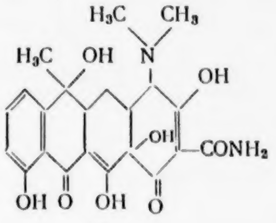

(I)

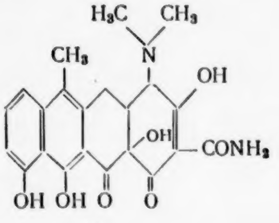

(II)

In an investigation of the ion exchange of tetracycline on acidic resins in their hydrogen form, it was observed that the univalent tetracycline cation, adsorbed on the resin, was capable of splitting off water to give anhydrotetracycline (II). The anhydrotetracycline did not pass into solution, and therefore remained, in the bound state, in the resin phase. This process can be considered as a deactivation of the biologically active tetracycline, since anhydrotetracycline has no microbiological activity.

A specially purified preparation of the base tetracycline was used in this work. Its tetracycline content was 93%. Anhydrotetracycline and mineral impurities were practically absent. The sulfonated ion-exchange resin was pretreated in the normal way (conditioning).

Adsorption was carried out on the hydrogen form of the resin, from a solution of the base tetracycline in 95% methyl alcohol or water. Because of the higher solubility of the base tetracycline in methyl alcohol, it was more convenient to carry out the adsorption from a small volume of methyl alcohol solution than from aqueous solution. The process was effected under static conditions, with continuous stirring of the system. The temperature was maintained at -30° or 0°C (cryostat), so as practically to exclude deactivation of the tetracycline in the resin during the adsorption period. The time for exchange was 3-4 hours. At the end of this time, the sample of resin with adsorbed tetracycline was removed from the solution, washed with cold solvent, drenched with 95% methyl alcohol or water (25°) and kept in a thermostat at 25° for a definite time. Conversion of tetracycline occurred at this temperature. A solution of the base tetracycline, in water or in 95% methyl alcohol, maintained at 25° showed no change during the time in which deactivation of the tetracycline occurred on the resin phase.

Neither the tetracycline, nor its transformation products, passed into the liquid phase while the resin was exposed to the solvent. At the end of the definite time, the resin was transferred to a column, enclosed in a Dewar vessel, and both the tetracycline and its transformation products were eluted, under dynamic conditions,

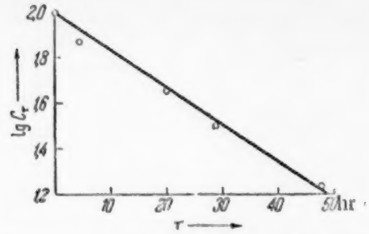

Fig. 1. C_T - concentration of tetracycline in eluate, %.

at 0° or -30°C, with a N solution of hydrochloric acid in methyl alcohol. The elution time was 2-4 hours. Separate experiments showed that, even at 0°, tetracycline was unchanged in these solutions after several days.

The degree of conversion of the tetracycline was determined by analyzing the eluate, obtained under the above conditions of elution, during which there was no change in the tetracycline.

Identical results were obtained by spectrophotometric investigation of the acid eluates and of the eluates neutralized to pH 3-4. After tetracycline had been maintained in the adsorbed state on the resin, the eluate showed the characteristic adsorption spectra in the visible region of both tetracycline and anhydrotetracycline. The quantitative spectrophotometric method gave complete agreement with the similar colorimetric method [1], by which it was also possible to determine both tetracycline and anhydrotetracycline. In view of this, all the subsequent work was carried out by the colorimetric method.

It was found that conversion took place on the hydrogen forms of all the sulfonic acid resins tested (resins obtained from copolymers of vinylnaphthalene and divinylbenzene, and from copolymers of styrene with different amounts of divinylbenzene, and sulfonic acid resin SBS-3). The polymerized cationites were prepared in the Scientific Research Institute for Plastics, and the cationite SBS-3 in the Moscow Mendeleev Chemicotechnological Institute. The resins investigated had different structures and different physical properties.

The rate of conversion of tetracycline, as a function of residence time on the cationite, was investigated on a strongly acid resin, made from a copolymer of vinylnaphthalene and divinylbenzene [2].

The resin was taken in its hydrogen form, with a particle size of 0.25-0.50 mm. The temperature of sorption and desorption was -30°. The static exchange capacity (S.E.C.) of the cationite for Na^+ was 5.12 mg-equiv/g, and the amount of tetracycline adsorbed was 2.90 mg-equiv/g.

Fig. 1 shows the results obtained, which indicate that the conversion of tetracycline was a reaction of the first order. The absence of deactivated tetracycline in the eluate, when elution was carried out immediately after sorption (Fig. 1), confirms the correctness of our choice of those conditions for adsorption and elution, which ensured practically complete stability of the tetracycline, and enabled us to investigate transformation of the antibiotic on the resin in the pure state.

With increasing concentration of tetracycline in the resin, there was a fall in the rate of conversion, i.e., the lower was the concentration of free hydrogen ions, bound by electrovalent forces to the resin, the slower was the conversion of tetracycline.

These results showed that conversion of tetracycline present in the adsorbed state, into the anhydro form, took place as the result of catalytic action by the unsubstituted hydrogen ions of the cationite.

In recent years, the hydrogen forms of strongly acid cationites have found a wide application as catalysts for numerous different chemical processes. But all these reactions take place in a heterogeneous system, with the substance undergoing the catalytic transformation present in the liquid phase. However, the conversion of tetracycline, described in this paper, is an example of a special case of catalytic process, in which the starting material, its conversion products and also the catalysts occur in a single phase — the cationite phase. In the use of ion-exchange resins for the isolation of biosynthetized tetracycline, this process is of undoubted interest from the practical point of view. Since the biologically inactive anhydro form of tetracycline is produced by the conversion reaction, the occurrence of this reaction, in the ion-exchange method for isolating tetracycline is undoubtedly undesirable, and it is necessary to select conditions so as to avoid deactivation of tetracycline on the resin phase.

LITERATURE CITED

[1] I. Levine, E. A. Garlock, and H. Fischback, J. Am. Pharm. Assoc. (Scient. Ed.) 38, 473 (1949).

[2] A. B. Pashkov and S. M. Simanchuk, Author's Certificate 17610 (1952).

Received January 13, 1959

THE DYNAMIC DISPLACEMENTS OF ATOMS AND THE COEFFICIENTS OF LINEAR EXPANSION OF THE ARSENIDES OF ALUMINUM, GALLIUM AND INDIUM

Academician Acad. Sci. BSSR N. N. Sirota
and Yu. I. Pashintsev

The State Scientific Research and Planning Institute for the Rare
Metal Industry

It was shown, in a paper by one of the authors [1], that the temperature change for a mean-square displacement of atoms in the lattice of a solid body is proportional to the change in the square of the coefficient of linear expansion. In investigations, concerned with determination of the characteristic temperatures, and coefficients of linear expansion of germanium [2] and silicon [3], by the method of x-ray structural analysis, the correctness of the above rule, as applied to these elements, was established experimentally, partially in [2] and more or less completely in [3].

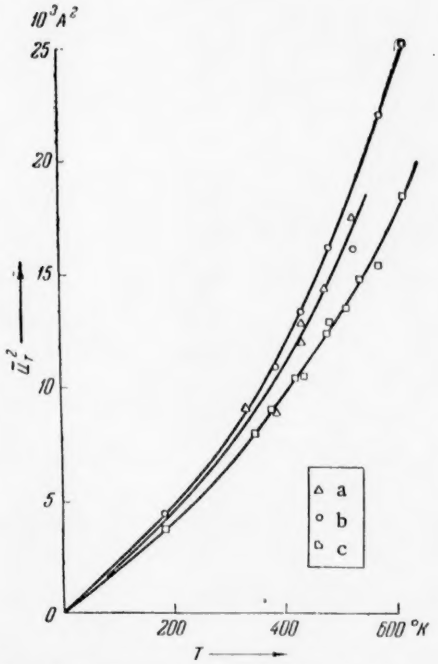

Fig. 1. Changes in the dynamic mean-square displacements of atoms of the arsenides of a) aluminum, b) indium and c) gallium, as functions of temperature.

In this paper we consider the relation between mean-square displacement of atoms and coefficient of linear expansion, as applied to the crystalline lattices of the semiconducting compounds, the arsenides of aluminum, gallium and indium.

Using the data obtained by our x-ray structural analysis method for determining the characteristic temperatures and coefficients of linear expansion of the compounds AlAs, GaAs and InAs [4,5], we calculated the mean values of the mean-square dynamic displacement of atoms in these compounds, and compared them with the squares of the coefficients of linear expansion.

In Table 1, for each of the arsenides investigated, we show the index lines on the x-ray photographs, the temperature ranges, the centers of the temperature ranges, from which were calculated the characteristic temperatures, θ, the logarithms of the ratios of the peak areas of blackening of the lines, measured on the x-ray photographs with a microphotometer ($\log_e(I_{T_1}/I_{T_2})$), the means-square dynamic displacements, $\bar{u}_T^2$, the coefficients of linear expansion, α, and their squares. Calculation of the mean-square dynamic displacements was carried out on the basis of the theory of thermal scattering of x-ray beams of Debye and Waller, according to which the logarithm of the ratio of intensities of the lines (hkl) of X-ray photographs, recorded at different temperatures T_1, T_2, is determined by the twofold difference in temperature factors

TABLE 1

Characteristic Temperatures, Coefficients of Linear Expansion and Mean-Square Dynamic Displacements for the Arsenides of Indium, Gallium and Aluminum

$T_1 - T_2$ (°K)	Center temp range, °K	hkl	$\ln \frac{I_{T_1}}{I_{T_2}}$	Θ (°K)	$\overline{u}_T^2$ (10^3 Å^2)	α (10^6 · °K^{-1})	α^2 (10^6 °K^{-1})
Indium arsenide							
78—290	184	355 246	0,2930 0,2685	249	4,46	3,40	11,6
290—482	386	355 246	0,3351 0,3118	230	10,9	4,84	235
290—573	432	355 246	0,5341 0,4880	220	13,4	5,20	27,0
290—673	482	355 246	0,7835 0,7800	211	16,2	5,67	32,0
482—573	528	355 246	0,2025 0,1672	218	16,2	6,10	37,1
482—673	578	355 246	0,4420 0,4480	198	22,1	6,60	43,5
573—673	623	355 246	0,2438 0,2680	192	25,3	7,04	49,5
Gallium arsenide							
78—290	184	551	0,2263	315	3,75	3,64	13,2
291—398	345	551	0,1572	295	8,00	5,07	25,1
291—468	380	551	0,2593	291	9,05	5,38	29,0
291—560	425	551	0,3868	287	10,4	5,74	33,0
398—468	434	551	0,1063	289	10,5	5,82	33,8
291—680	485	551	0,6330	275	12,9	6,24	39,0
398—560	479	551	0,2535	280	12,4	6,20	38,5
468—560	514	551	0,1495	277	13,5	6,48	42,0
398—680	539	551	0,4770	271	14,8	6,68	44,5
468—680	574	551	0,3520	274	15,4	6,96	48,5
560—680	620	551	0,2195	260	18,5	7,44	55,1
Aluminum arsenide							
291—375	333	551	0,0876	395	9,15	3,66	13,4
291—476	384	551	0,1512	430	8,95	4,00	16,0
291—577	434	551	0,3431	380	12,9	4,28	18,3
375—476	426	551	0,1073	370	13,4	4,28	18,3
375—577	476	551	0,2208	378	14,3	4,68	21,8
476—577	527	551	0,1264	360	17,5	4,92	24,1

$$\ln \frac{I_{T_1}}{I_{T_2}} = 16\pi^2 \left(\overline{u}_{T_2}^2 - \overline{u}_{T_1}^2\right) \frac{\sin^2 \vartheta}{\lambda^2}$$

The mean-square dynamic displacement is related to the Debye-Waller [6] characteristic temperature by the expression

$$\overline{u}_T^2 = \frac{3h^2 T}{4\pi^2 m k \theta^2}\left[\Phi(x) + \frac{x}{4}\right], \qquad (2)$$

where $\Phi(x)$ is the Debye function, m the mean atomic mass, θ the Debye-Waller characteristic temperature, $x = h\nu_g/kT$ and ν_g is the limiting frequency.

The characteristic temperature is known to be determined by the characteristic (limiting) frequency of atomic vibration. It should be noted that, as is obvious from Equation (2), with an increase in the mean-square displacement there is a decrease in the characteristic temperature, and therefore in the limiting frequency of atomic vibration. This fact was noted by A. F. Ioffe [7].

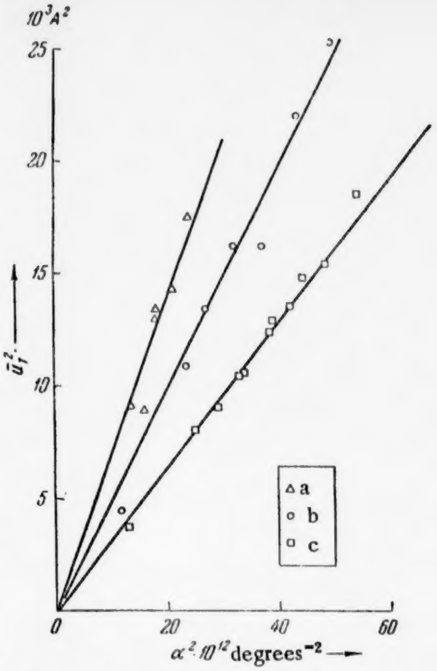

Fig. 2. Changes in the dynamic mean-square displacements ($\bar{u}_T^2$) of atoms of the arsenides of a) aluminum, b) indium and c) gallium, as functions of the squares of their coefficients of linear expansion.

Fig. 1 shows graphs for the change of mean-square displacement ($\bar{u}_T^2$) with temperature for the arsenides AlAs, GaAs and InAs. For all temperatures at which X-ray photographs were obtained, the highest mean-square dynamic displacement was shown by indium arsenide, rather less by gallium arsenide and the least by aluminum arsenide, which is in accordance with their melting point.

Over the temperature range investigated, the value of the mean-square dynamic displacement increased with increasing temperature, evidently according to a general law for all the substances investigated.

Fig. 2 shows graphs relating the changes in mean-square dynamic displacement, for the arsenides investigated, to the squares of their coefficients of linear expansion. For these arsenides, the experimental values of the mean-square displacements, when plotted in terms of the coordinates $\bar{u}_T^2$ α^2, lie close enough to straight lines passing through the origin.

Thus, on the basis of our results for the arsenides of aluminum, indium and gallium over the temperature range 200-650° K, it may be considered as established that the mean-square dynamic displacements are directly proportional to the squares of the coefficients of linear expansion.

LITERATURE CITED

[1] N. N. Sirota, Proc. Acad. Sci. BSSR 2, No. 11 (1958).

[2] E. M. Gololobov and N. N. Sirota, Proc. Acad. Sci. BSSR 3, No. 7 (1959).

[3] N. N. Sirota and A. U. Sheleg, Proc. Acad. Sci. BSSR 3., No. 8 (1959).

[4] N. N. Sirota and Yu. M. Pashintsev, Eng. Phys. J. No. 12, 38 (1958).

[5] Yu. M. Pashintsev and N. N. Sirota, Proc. Acad. Sci. BSSR 3, No. 2, 38 (1959).

[6] I. Waller, Zs. f. Phys. 9, 398 (1923).

[7] A. F. Ioffe, J. Solid State 1, No. 1 (1959).

Received April 5, 1959

THE ELECTRICAL CONDUCTIVITIES OF DIFFERENT MODIFICATIONS OF MONOCHLOROACETIC ACID IN NONAQUEOUS SOLUTIONS

S. S. Urazovskii and Z. M. Kanevskaya

(Presented by Academician P. A. Rebinder March 23, 1959)

The V. I. Lenin Khar'kov Polytechnic Institute

The fact, previously established by us [1], that polymorphic modifications of many organic substances retained their different properties in solution, stimulated us to investigate the electrical conductivity of monochloroacetic acid in nonaqueous solvents.

Monochloroacetic acid has four monotropic modifications with melting points: α -61.2°, β - 56.2°, γ - 50.0° and δ - 43.8°. We only investigated two of these, since the γ - and particularly the δ -modifications are unstable and readily transform into the stable α-modification, so that it would not have been possible to obtained satisfactory results with these. The solvent used was a mixture of acetone and dioxane, made up from batches which had been purified to constant electrical conductivity.

Precise measurement of the electrical conductivity of nonaqueous solutions, in view of their high resistances of the order of tens of thousands of ohms, is a matter of considerable difficulty and requires special methods and apparatus. In this investigation we used our previously developed equipment [2], based in principle on the scheme of V. K. Semenchenko, B. V. Erofeev and V. V. Serpinskii [3], but considerably improved and provided with a device for objective reading — a vibration galvanometer with a type F-50 amplifier. The applicability of this for similar purposes was established in the earlier publication [2], where the apparatus is described in detail.

Electrical conductivity was measured at 25°, over the concentration range 1 to 0.002 N. Measurements were unreliable with more dilute solutions, owing to their high resistances (above 100 000 ohms). The conductivity values for higher dilutions ($\varphi > 500$), like the limiting conductivity (λ_0), were therefore obtained by extrapolation.

Fig. 1 shows curves for the relation between equivalent conductivity (λ) and dilution (φ) for the α- and β -modifications of monochloroacetic acid in acetone.

It is clear from these curves that there was a marked difference in the conductivities for the different modifications of the acid, which increased with dilution over the range investigated. Similar results were obtained with solutions in an 80% dioxane—water mixture. It should be noted that the difference between the conductivities diminished with increasing water content of the dioxane, and disappeared in pure water.

In order to elucidate the nature of the subsequent change in conductivity down to its limiting value (λ_0), we employed one of the more reliable methods of extrapolation.

A rough approximation to the value of the limiting conductivity (λ_0) was obtained by Walden's [4] formula

$$\lambda_0 = \lambda_\varphi + \frac{65.7}{\varepsilon\eta\sqrt{\varphi}}, \qquad (1)$$

where ϵ is the dielectric constant of the solvent and η is its viscosity. A better value was then obtained by the graphical method of successive approximations of Fuoss and Kraus [5].

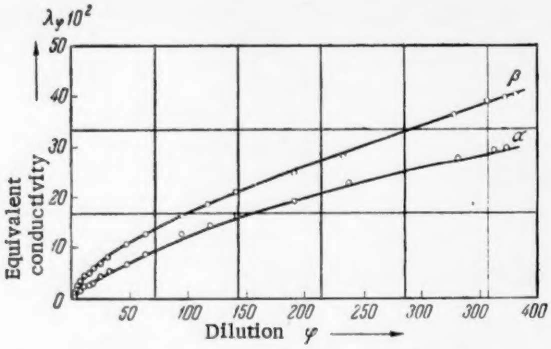

Fig. 1. Variation of equivalent conductivity with dilution for solutions of the α- and β-modifications of $CH_2ClCOOH$ in acetone.

This method of Fuoss and Kraus is based on the Onsager [6] formula for the conductivity of a uni-univalent electrolyte, taking incomplete dissociation into account:

$$\lambda_\varphi = [\lambda_0 - (A + B\lambda_0)\sqrt{\alpha c}]\,\alpha, \qquad (2)$$

where A and B are the electrophoretic and relaxation constants respectively, depending on the viscosity and dielectric constant of the solvent.

From Equation (2) we found the degree of dissociation:

$$\alpha = \frac{\lambda_\varphi}{\lambda_0 \Phi(z)}, \qquad (3)$$

where $\Phi(z)$ could be replaced by the continued fraction:

$$\Phi(z) = 1 - z\{1 - z[1 - z(\,.\;.\;.\,)^{-1/2}]^{-1/2}\}^{-1/2}, \qquad (4)$$

in which $z = \frac{(A + B\lambda_0)\sqrt{\alpha c}}{\lambda_0}$.

$\Phi(z)$ could be found from Fuoss's tables [7] for values of z from 0 to 0.209.

Then, putting the value obtained for α in the known expression for the dissociation constant, we found

$$K = \frac{\lambda_\varphi^2 c \gamma_\pm^2}{\lambda_0 \Phi(z)[\lambda_0 \Phi(z) - \lambda_\varphi]}. \qquad (5)$$

A more convenient form for graphical representation was

$$\frac{\Phi(z)}{\lambda_\varphi} = \frac{1}{\lambda_0} + \frac{1}{K\lambda_0^2}\,\frac{\lambda_\varphi c \gamma_\pm^2}{\Phi(z)}. \qquad (6)$$

On the basis of the data obtained in this way for different dilutions, we constructed graphs with coordinates $\frac{\Phi(z)}{\lambda_\varphi}$; $\frac{\lambda_\varphi c\gamma_\pm^2}{\Phi(z)}$, from which was derived a second approximation λ_0', which could be used for the above calculations and construction of fresh graphs, giving a still more precise value of the limiting conductivity, λ_0'', and so on until there was no difference between λ_0^n and $\lambda_0^{(n-1)}$.

This was achieved in our case after the second cycle of calculations. A constant value was obtained for the limiting electrical conductivity of monochloracetic acid in acetone, which was practically the same for both modifications, namely: $\lambda_{0(\alpha)} = 59.17$ and $\lambda_{0(\beta)} = 59.38$. For subsequent calculations we took a mean value $\lambda_0 = 59.28$, and this was used to calculate the dissociation constants and the contruct the full conductivity curves as a function of dilution.

Dissociation constants were calculated from the known equation $K = \frac{\alpha^2 c}{1-\alpha}\gamma_\pm^2$, which was found to be satisfactory at low concentrations and gave constant values of K at dilutions $\varphi \geq 350$. Mean activity coefficients $\gamma_\pm$ were calculated from the limiting Debye-Huckel law.

The dissociation constants obtained in this way showed considerable differences for the two modifications in acetone: $K_\alpha = 6.75 \cdot 10^{-8}$, $K_\beta = 12.28 \cdot 10^{-8}$.

Fig. 2 shows the full curves for the relation between equivalent conductivity and dilution, constructed from λ_φ data calculated as above.

It is evident from the curves that the observed difference, in conductivity of the α- and β-modifications of monochloroacetic acid in acetone, at first increased with dilution, reached a maximum at $\varphi \sim 10^6$–10^7 liter/mole,

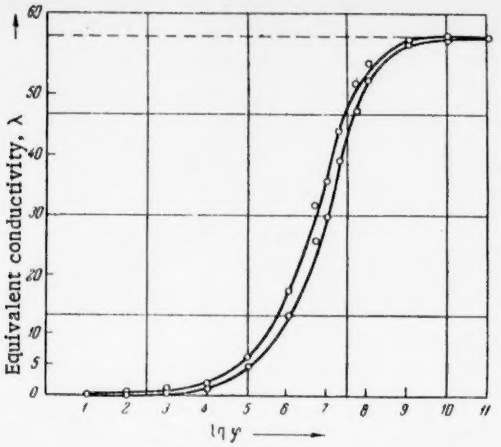

Fig. 2. Full curves for λ as a function of φ for acetone solutions of the α- and β-modifications of $CH_2ClCOOH$. Limiting conductivity $\lambda_0 = 59.27$.

when the degree of dissociation was close to a half, and then decreased, approaching zero at infinite dilution when λ_0 became the same for both modifications.

The nature of the change in equivalent conductivity with dilution enabled us to conclude that the observed difference in the electrolytic properties of the two modifications of monochloroacetic acid was due to a difference in capabilities to dissociate, and was therefore determined by a difference in configuration of the molecules, and not of the ions, since the mobilities of the latter were obviously the same.

The immediate cause of the different dissociation capabilities of the α- and β-modifications of monochloroacetic acid is their different types of association in the crystal lattice, which are preserved in nonaqueous solutions: monomer with intramolecular hydrogen bonding or chains for the β-modification, and the normal dimer for the α-modification.

LITERATURE CITED

[1] S. S. Urazovskii, Molecular Polymorphism, Kiev (1956).*

[2] S. S. Urazovskii and Z. M. Kanevskaya, Trans. Khar'kov Polytech. Inst. 4, No. 2, 45 (1954).

[3] V. K. Semenchenko, B. V. Erofeev and V. V. Serpinskii, J. Gen. Chem. 2, 893 (1932).

[4] P. Walden, Elektrochem. nichtwäs. Lösungen, Leipzig (1924) S. 28.

[5] R. Fuoss and C. Kraus, J. Am. Chem. Soc. 55, 476 (1933).

[6] R. Fuoss and C. Kraus, J. Am. Chem. Soc. 57, 488 (1935).

[7] L. Onsager, Trans. Farad. Soc. 23, 341 (1927).

Received March 20, 1959

---

* In Russian.

A NEW METHOD OF DETERMINING THERMAL CHARACTERISTICS AND THERMAL EFFECTS BASED ON THERMOGRAPHY

M. Sh. Yagfarov

Chemical Institute of Kazan affiliated to the Academy of Sciences of the USSR

(Presented by Academician B. A. Arbuzov April 4, 1959)

A new method has been developed which makes possible simultaneous measurements of thermal characteristics (thermal capacity, thermal conductivity, temperature conductivity) and thermal effects.

Measurements can be carried out over a wide temperature range. The temperature used is only restricted by the thermal stability of the materials and of the thermocouple. We used chromel-alumel thermocouples, so that measurements could be made up to 1000°.

The method is rapid, so that measurements up to 1000° could be performed in 1 hour 20 minutes to 2 hours. The results are obtained in the form of objective traces, with coordinates temperature and time (thermograms).

The conduct of the experiments and construction of the equipment are quite simple, and could be carried out in any laboratory. To obtain records of the results, it is necessary to use a recording pyrometer or potentiometer.

The method is based on the laws of the temperature field with linear heating, i. e. of a quasi-stationary heating state. The principle used will be discussed first. It consists essentially of an analysis of the thermal flux passing through the substance under investigation. The thermal flux is first set to a given value (using a known thermal capacity), and the change in it, when passing through the substance under investigation, is determined by the factors provoking the change , i.e. the thermal characteristics of the substance. A differential method of measurement is used, consisting in the synchronized comparison of two thermal fluxes, passing simultaneously in two different places through the substance under investigation, in one case to a body of known thermal capacity and in the other case to one of "zero" thermal capacity, i.e. air.

The principle is clear from Fig. 1, which shows a diagram of the apparatus. The substance under investigation is placed between two coaxial cylinders. The outer cylinder is a block heater, which maintains a uniform quasi-stationary heating field. The internal cylinder, which contains a material of known reproducible thermal capacity (such as a metal) and a standard air space, serves to create two separate previously known thermal fluxes through the substance under investigation.

At the ends of the block, the cylinders are separated from each other by heat-insulating rings (of fire clay, porcelain, etc). The inner cylinder is usually composed of two heat-resisting steel cylinders, separated from each other by heat-insulating material (fire clay, porcelain, quartz, etc). A cylinder of heat-resisting steel has the advantage that it permits inequality of heat flow in the different positions.

The temperature field in the block is measured by two differential thermocouples, whose junctions are inserted at the points 1-1, 1-2 and 2-1, 2-2 respectively (Fig. 1) . The second thermocouple is combined with a simple thermocouple, which provides a simultaneous measurement of the temperature rise of the substance.

Under quasi-stationary state conditions. the temperature drop across the substance under investigation, opposite the standard air gap , will only depend on the thermal capacity and thermal conductivity of the substance itself; but , opposite the internal metal cylinder, it will also depend on the thermal capacity of this metal cylinder.

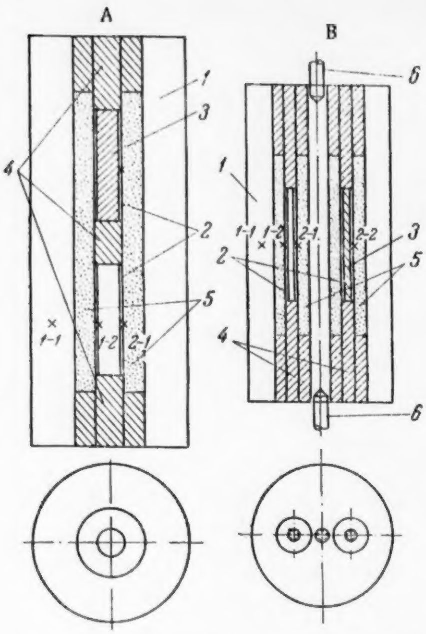

Fig. 1. Diagram of block. A) First variant B) second (simplified) variant. 1) Cylinder of heat-resisting steel (or aluminum or nickel); 2) internal cylinder of heat-resisting steel (or nickel); 3) material of known reproducible thermal capacity; 4) heat insulating partitions in variant A, and plugs and rings of heat-insulating material in variant B (these were hermetically sealed at the top, the thermocouple leads passed through them, the lower rings were removable for insertion of the substance under test); 5) the substance under test in A and B ; 6) pins for centering the block in the furnace (B).

Knowing the value of the latter, it is possible to derive the thermal conductivity of the substance under investigation from a comparison of the two temperature gradients.

Under quasi-stationary state conditions, when one of the thermal characteristics can be determined independently, it is possible to make simultaneous determinations of thermal capacity and thermal conductivity, as is obvious from the temperature conductivity equation [1]

$$a = \frac{\lambda}{C},$$

where a is the temperature conductivity coefficient, λ is the thermal conductivity coefficient, and C is the thermal capacity per unit volume.

Mathematical analysis of the temperature field in the block leads to very simple formulas for calculation, where the only measurements required are distances on the thermogram corresponding to angles of rotation of the galvanometer mirror.

The formula for measurement of thermal capacity, has the following form

$$m \cdot c_{p_1} = k \cdot m_1 \cdot c_{p_1} \frac{L_1}{L_2} - k \cdot m_2 \cdot c_{p_2},$$

where $m \cdot c_p$ is the thermal capacity of the substance under investigation; $m_1 \cdot c_{p_1}$ is the thermal capacity of the material of known thermal capacity, placed in the inner cylinder; $m_2 \cdot c_{p_2}$ is the thermal capacity of the shell containing the standard (air); L_1 and L_2 are the distances from zero of the two differential lines on the thermogram, corresponding to the thermal emfs developed by the differential thermocouples (Fig. 1); k is a constant dependent on the dimensions of the block.

The formula for determination of the thermal conductivity coefficient has the form:

$$\lambda = m_1 \cdot c_p \frac{v}{\Delta t} \cdot K_1,$$

where v is the heating rate; Δt is the temperature difference between the substance of known thermal capacity and the standard (air); k_1 is a constant dependent on the dimensions of the block.

It is clear that the formulas do not include any factors which are variable and difficult to determine, and which might lead to systematic error. Thus the method has the possibility of obtaining very accurate results. The precision attained in measurement of thermal capacity was not worse than 1% (see Table 1 for some results of measurements of the thermal capacity of KNO_3).

A knowledge of the thermal constants makes it possible to determine the values of thermal effects from the areas under the peaks of the differential traces. There was a maximum error of up to 2% in measurement of the heat effects, which was obviously due to secondary factors (for instance, errors in measurement of peak areas, particularly lack of precision in selecting the boundary of the peak area).

Satisfactory results were also obtained for measurements of thermal conductivity. It was therefore possible, by this method, to determine all the thermal characteristics and the value of the thermal effects. The conduct

TABLE 1

Specific Heat of KNO_3

Temperature, °C	Literature data	Found		Difference from literature value, %	Difference between experiments, %	Temperature, °C	Literature data	Found		Difference from literature value, %	Difference between experiments, %
		1st expt.	2nd expt.					1st expt.	2nd expt.		
50	0,2328	0,2356		1,2		105	0,2617	0,2609		0,3	
55	0,2355	0,2353		0,8		110	0,2643	0,2622		0,7	
60	0,2381	0,2374		0,3		160	0,2905	0,2879	0,2876	0,9	0,1
65	0,2407	0,2400		0,3		170	0,2957	0,2934	0,2924	0,8	0,3
70	0,2433	0,2421		0,5		180	0,3010	0,2973	0,2976	1,2	0,1
75	0,2460	0,2463		0,1		190	0,3062	0,3029	0,3044	1,1	0,5
80	0,2486	0,2491		0,2		200	0,3115	0,3087	0,3096	0,9	0,4
85	0,2512	0,2515		0,1		210	0,3141	0,3119	0,3113	0,7	0,2
90	0,2538	0,2548		0,4		220	0,3272	0,3250	0,3254	0,7	0,1
95	0,2565	0,2562		0,1		230	0,3324	0,3298	0,3308	0,8	0,3
100	0,2590	0,2577		0,5		240	0,3403	0,3358	0,3352	1,3	0,2

of an experiment was very simple: since the positions of the thermocouples were fixed, it was only necessary to insert and remove the substance under investigation. There was no need to calibrate the apparatus or the thermocouples (if the same galvanometer sensitivity was used).

A simplified variant of the apparatus was developed (see Fig. 1). In this, the standard (air) and substance of constant thermal capacity were placed in two different channels, drilled in the block. A normal electric furnace, with an adequate length at uniform temperature, could be used for heating the block. This apparatus was specially suitable for small amounts of substance, and was simpler to prepare and use.

The method can also be used for thermal measurements under laboratory conditions, as in various physicochemical investigations.

LITERATURE CITED

[1] A. V. Dykov, Theory of Thermal Conductivity, p. 331 (Moscow, 1952) [In Russian].

Received April 1, 1959

POLAROGRAPHIC STUDY OF THE TAUTOMERISM OF SOME SEMI- AND THIOSEMICARBAZONES IN SOLUTIONS

Yu. P. Kitaev, G. K. Budnikov and Academician A. E. Arbuzov

A. E. Arbuzov Chemical Institute Kazan Branch of the Academy of Sciences of the USSR

Among the many classes of compounds showing antitubercular activity, the thiosemicarbazones hold a prominent position at the present time. In addition, thiosemicarbazones are used in the preparation of motion picture materials and in analytical chemistry, while the semicarbazones are used for rodent control and as insecticides.

It is known that the thiosemicarbazones of aliphatic aldehydes and ketones are much weaker antitubercular agents than the thiosemicarbazones of aromatic aldehydes. An unequivocal relationship exists between the structure of these compounds and their bacteriostatic activity, and for this reason a study of the structure of thiosemicarbazones is of great theoretical interest.

A study of the IR-spectra of some thiosemicarbazones revealed that in the crystalline state these compounds do not contain SH groups [1]. It was postulated that it is possible for thiosemicarbazones to migrate to the thiol form either by dissolving in alkalies [1] or by irradiation of the thiosemicarbazone solutions with ultraviolet light [2].

As a result, the important and interesting question as to the structure and tautomerism of semi- and thiosemicarbazones has failed to receive a conclusive answer at the present time. This circumstance caused us to begin a systematic study of the structure and behavior in solutions of representative members of the indicated classes of compounds.

The polarographic method was used to make the study. We studied the semi- and thiosemicarbazones of acetone, methyl ethyl ketone, acetaldehyde, propionaldehyde, cyclopentanone, cyclohexanone, benzaldehyde and acetophenone, and also the thiosemicarbazone of p-isopropylbenzaldehyde (cutisone).

The work was done using a Heyrovsky LP-55 polarograph, with a photographic recording of the polarographic curves. A dipping saturated calomel electrode was used as the reference electrode. The polarograms were taken at t = 20°, keeping the solutions of the studied compounds in 20% methanol—water buffered at pH 5.7, 7.3, and 9.3. The molar concentrations of the semi- and thiosemicarbazones in the solutions were roughly 5×10^{-4} to 5×10^{-3}.

A family of curves was obtained for each solution with a definite pH. The polarographic data obtained by us testify to the large similarity in the behavior, and consequently, in the structure of the semi- and thiosemicarbazones.

The following rules were revealed in the changes of the polarograms of water—alcohol solutions of the semi- and thiosemicarbazones of aliphatic aldehydes and ketones and alicyclic ketones: with time the initial waves, the $E_{\frac{1}{2}}$ of which lies between -1.4 v and -1.55v, decrease somewhat, appear, increase, then decrease, or the waves with $E_{\frac{1}{2}}$ about 1.10 v disappear completely. The polarogram of a solution of acetone thiosemicarbazone at pH 7.3 is shown in Fig. 1. Consequently, it is possible to trace two curves in the sets of polarograms for the solutions of the studied derivatives of aliphatic and alicyclic oxo compounds, corresponding to the two forms of these compounds. The form, corresponding to $E_{\frac{1}{2}}$ about -1.5v, dominates in acid and neutral media; the form, corresponding to $E_{\frac{1}{2}}$ about -1.1 v, dominates in weakly alkaline medium. The latter form shows a tendency to saponify, which is evidenced by our above mentioned disappearance of its wave.

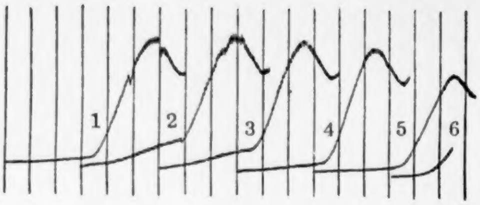

Fig. 1. One division along the abscissa = 200 mv; origin of the curves = -0.7v; sensitivity 1/70; (mean galvanometer sensitivity = 3.1 × 10^{-9} 1/mm); storage time: 1) fresh, 2) 2 hr, 3) 4 hr, 4) 6 hr, 5) 18 hr.

To decipher the obtained polarograms, we also took the polarogram of an aqueous-alcohol solution of cyclohexanone S-methylthiosemicarbazone (Fig. 2,3). The two waves on the polarogram of this compound corresponds to the two possible tautomers:

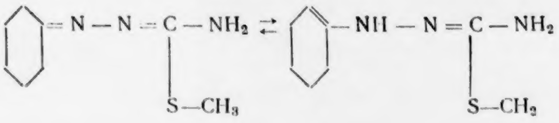

(I) (II)

The first form, being the more reactive, has $E_{\frac{1}{2}}$ ~-0.8 v; the second is reduced at a dropping electrode at $E_{\frac{1}{2}}$ ~-1.15 v. It now becomes clear that the appearing, and then decreasing wave with $E_{\frac{1}{2}}$ ~-1.10v corresponds to the tautomer with structure (II), while the wave with $E_{\frac{1}{2}}$ ~-1.5v belongs to the other possible tautomer, in whose molecule the double bonds are conjugated through two pairs of 2π-electrons of the nitrogen atoms.

We observed that the alcohol solutions of the thiosemicarbazones of acetone and cyclohexanone change color on standing: being colorless at the start, they later turn yellow. The change in the color of the solutions of these compounds is evidence that the dissolved substances suffer some sort of change with time. The polarograms of these solutions, taken 3.5 months after their preparation, each contain two waves: 1) a wave with $E_{\frac{1}{2}}$ ~-0.8 v, belonging to the tautomer with structure (I), and 2) a wave with $E_{\frac{1}{2}}$ ~-1.28 v, corresponding to the other possible tautomer with a carbonyl structure. The polarogram of a solution of acetone thiosemicarbazone is shown in Fig. 2, 1, while that of a solution of cyclohexanone thiosemicarbazone is shown in Fig. 2, 2.

Deciphering the obtained polarograms led us to the unexpected conclusion that all of the studied semi- and thiosemicarbazones of the aliphatic aldehydes and ketones and alicyclic ketones have an enesemi- and enethiosemicarbazide structure in water and water—alcohol solutions. Obviously, the indicated compounds also have the same structure in the crystalline state, since it seems hardly probable that at the moment of solution the double bond of the azomethine group migrates almost completely into the carbonyl radical at a rate incapable of being measured.

Such a migration of the double bond into the carbonyl radical is impossible for benzaldehyde derivatives. Only one wave was observed on the polarograms of water—alcohol solutions of benzalsemi-and thiosemicarbazone. Solutions of the semi- and thiosemicarbazone of acetophenone, and also of cutisone, when polarographed, likewise gave only one wave with $E_{\frac{1}{2}}$ ~-1.15 v. In Fig. 3 we show the polarograms for solutions of the compounds at pH 5.7: 1) acetophenone thiosemicarbazone, 2) benzalsemicarbazone, and 3) benzalthiosemicarbazone. An exception is the weakly alkaline solution of acetophenone thiosemicarbazone, for which two waves were observed on polarographing: a wave with $E_{\frac{1}{2}}$ ~-1.15v, corresponding to the tautomer with the carbonyl structure, and a wave with $E_{\frac{1}{2}}$ ~-1.60 v, belonging to the tautomer with structure (III):

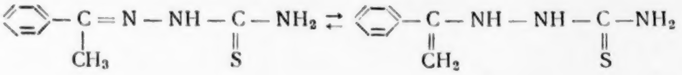

(III)

Consequently, the polarographic study of a number of semi- and thiosemicarbazones revealed that in the general case they can exist in four tautomeric forms:

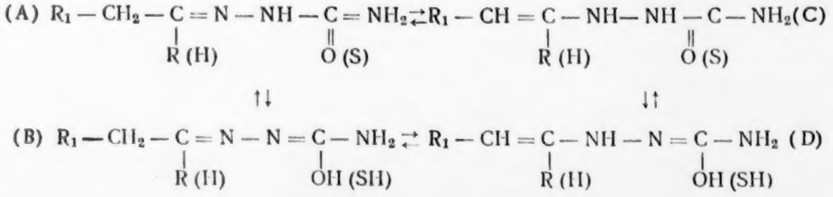

$$\text{(A)}\ R_1-CH_2-\underset{R\,(H)}{\underset{|}{C}}=N-NH-\underset{O\,(S)}{\underset{\|}{C}}=NH_2 \rightleftarrows R_1-CH=\underset{R\,(H)}{\underset{|}{C}}-NH-NH-\underset{O\,(S)}{\underset{\|}{C}}-NH_2\ \text{(C)}$$

$$\uparrow\downarrow \qquad\qquad \downarrow\uparrow$$

$$\text{(B)}\ R_1-CH_2-\underset{R\,(H)}{\underset{|}{C}}=N-N=\underset{OH\,(SH)}{\underset{|}{C}}-NH_2 \rightleftarrows R_1-CH=\underset{R\,(H)}{\underset{|}{C}}-NH-N=\underset{OH\,(SH)}{\underset{|}{C}}-NH_2\ \text{(D)}$$

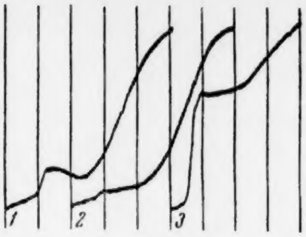

Fig. 2. One division along the abscissa = 200 mv; origin of the curves = -0.6 v; sensitivity 1/30; 80% ethanol; support: 0.1 M $LiNO_3$ + borate buffer with pH 9.3.

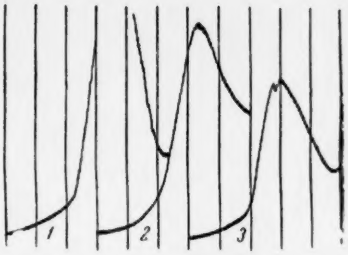

Fig. 3. One division along the abscissa = 200 mv; origin of the curves = -0.7 v; sensitivity 1/70.

It should be mentioned that the semicarbazones show a somewhat greater tendency than the thiosemicarbazones to form structure (D). At pH 9.3, the solutions of the aliphatic aldehyde derivatives contain form (D) almost exclusively; for the derivatives of the aliphatic and alicyclic ketones, under these conditions, form (D) is also accompanied by form (C). A transition of tautomer (A) to the tautomer with structure (B) was not observed under our conditions for the semi- and thiosemicarbazones of the aromatic aldehydes and aliphatic aromatic ketones. This is in harmony with the ultraviolet spectroscopic data obtained for benzalsemicarbazone [3]. Benzaldehyde S-methylthiosemicarbazone, in which structure (B) is fixed, was reduced at $E_{\frac{1}{2}} \sim -0.74$ v.

It is interesting to mention that a structure, similar to (C), was established by us earlier for the arylhydrazones of aliphatic and alicyclic ketones [4-6].

Consequently, the results obtained by us indicate that the abnormal reduction in the physiological activity of thiosemicarbazones of the aliphatic and alicyclic series, when compared with the derivatives of the aromatic series, is explained by the different structure of these compounds—only the latter type contains the active grouping

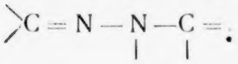

$$>C=N-\underset{|}{N}-\underset{|}{C}=.$$

In our opinion, fixing the double bonds of this grouping in the thiosemicarbazone molecule by introducing substituents, should result in increased tuberculostatic activity.

LITERATURE CITED

[1] S. G. Bogomolov, I. Ya. Postovskii, and Yu. N. Sheinker, Proc. Acad. Sci. USSR 91, No. 5,1111 (1953).

[2] G. Gummerus and T. Enkvist, Acta. Chem. Scand. 10, 3, 461 (1956).

[3] G. Cilento, J. Am. Chem. Soc. 71, 1112 (1949).

[4] A. E. Arbuzov and Yu. P. Kitaev, Proc. Acad. Sci. USSR 113, No. 3 577 (1957).*

[5] Yu. P. Kitaev and A. E. Arbuzov, Bull. Acad. Sci. USSR, Div. Chem. Sci. 1037 (1957).*

[6] A. E. Arbuzov and Yu. P. Kitaev, Bull. Kazan Branch of the Academy of Sciences of the USSR, Chemical Series, No. 3, 3 (1957).

Received May 21, 1959

---

* In Russian.

PROTON MAGNETIC RESONANCE IN TITANIUM AND ZIRCONIUM HYDRIDES

O. T. Malyuchkov and B. N. Finkel'shtein

I. V. Stalin Moscow Steel Institute

(Presented by Academician G. V. Kurdyumov, March 27, 1959)

A study was made of the magnetic resonance of the protons in titanium and zirconium hydrides at a frequency of 21499 kc in a magnetic field with an intensity of 5035 oersteds. A radiofrequency spectrometer with a permanent magnet* was used to make the measurements [1]. Transmission of the resonance line was accomplished by slowly changing the frequency of a generator of the Pound and Watkins type [2], using a synchronous motor and a reducer with a large impedance. The signal of proton magnetic renonance (p.m.r.) as a function of the frequency was recorded on the tape of an electronic potentiometer with a constant time of 1.5 sec. The inhomogeneity of the field in a specimen length of 2 cm did not exceed 0.1 oersted.

The investigated titanium and zirconium hydrides were taken as powder specimens, and had the following hydrogen content: $TiH_{1.98}$, $TiH_{1.75}$, $TiH_{1.06}$, $TiH_{0.95}$, $TiH_{0.65}$, $TiH_{0.50}$, $TiH_{0.20}$, ZrH_2; hydrides with the maximum amount of hydrogen were heated in vacuo at different temperatures to obtain the indicated compositions.

Determination of the phase composition of the hydrides by the x-ray structure analysis method gave results that coincided with the literature data [3]. Titanium hydrides containing less than 20 atom% hydrogen are one-phase, and possess a hexagonal lattice with a/c = 1.62; hydrides in which the hydrogen concentration ranges from 20 to 55 atom % are two-phase, and consist of a hexagonal α-phase and a face-centered cubic β-phase.

Hydrides with a hydrogen content greater than 55 atom % are one-phase, with a face-centered cubic lattice and a period, increasing from 4.40 kX to 4.45 kX.

A tetragonal distortion of the lattice when the hydrogen content exceeds 60 atom %, mentioned in [4], was not observed by us. Zirconium hydride has a tetragonally distorted face-centered lattice with a = 4.97 kX and c = 4.44 kX, which is in good agreement with the literature data [3,4].

In one-phase titanium α-hydrides, having a hexagonal lattice, the width of the p.m.r. line is independent of the hydrogen content and is equal to 0.6 oersted. When the hydrogen concentration exceeded 20 atom % the line widened due to the appearance of a β-phase rich in hydrogen; when the hydrogen content exceeded 35 atom % the width did not change and was equal to 14 oersteds. This result is in agreement with the data given in [5]. A slight asymmetry of the p.m.r. line is observed at small hydrogen concentration, which disappears when the hydrogen content is increased.

Change in the width of the p.m.r. line permits assuming that in the α-hydrides the hydrogen atoms are found in rapid, probably, rotational motion, the same as in the hydrides of palladium and tantalum. In harmony with the theoretical concepts of Bloembergen [6], the asymmetry of the p.m.r line discovered by us supports the theory expressed by Ubbelohde [7] that is possible for a metallic bond to exist in certain hydrides.

In the hydrogen-rich β-hydrides the p.m.r. line widens considerably, indicating a decreased mobility of the protons, and also an important change in the type of hydrogen bonding with the metal. Transition of the shape

---

* V. S. Pavlovskaya took part in the design and building of the radiofrequency spectrometer.

TABLE 1

Specimen	Theoretical value of the second moment, oersted²	Experimental value of the second moment, oersted²
$TiH_{1,98}$	23,8	35,6±0,5
ZrH_2	15,7	14,8±0,5

of the p.m.r. line from Lorentzian in α-hydrides to Gaussian in β-hydrides can serve as additional proof of this fact.

The problem as to the positions occupied by hydrogen in the compounds TiH_2 and ZrH_2, remaining unsolved for a long time, was recently solved by the neutron diffraction method [8] for the case of ZrH_2, which, it proved, has the structure of tetragonally deformed CaF_2; the hydrogen atoms are located in tetrahedral pores. Similar data are lacking for TiH_2. We measured the second and fourth moments of the p.m.r. lines for $TiH_{1.98}$ and ZrH_2, and compared them with the calculated values of the second moments for the cases of introducing molecular hydrogen into either octahedral or tetrahedral pores; and also as individual protons into tetrahedral pores; here, for the cubic hydride $TiH_{1.98}$, we used the data given in [9] for powders. The theoretical value of the second moment of the p.m.r. for positions in the tetragonal pores of the ZrH_2 lattice was calculated using the equation:

$$\Delta H^2 = \frac{3}{5} \cdot I \cdot (I+1) \cdot g^2 \cdot \beta^2 \cdot \sum_j r_{0j}^{-6} + \frac{4}{15} \sum_f I_f (I_f + 1) \cdot g_f^2 \cdot \beta_f^2 \cdot r_{0f}^{-6}.$$

For both hydrides the best agreement of the calculated and experimental values of the second moments is obtained if it is assumed that protons enter into the tetrahedral pores, which is in harmony with the data given in [8] for the structure of ZrH_2. The assumption that hydrogen enters either the octahedral or tetrahedral pores in molecular form leads to a very large difference between the calculated and experimental values of the second moment, and consequently, is obviously not in accord with the truth.

A difference in the deviations of the calculated and experimental values of the second moments for $TiH_{1.98}$ and ZrH_2 (Table 1) indicates that the bonding between the protons and the atoms of the metal is different in these compounds.

The better agreement of the calculated and experimental data for ZrH_2 permits assuming that the bonding between the proton and zirconium is accomplished by electron pairs with compensated spins, and for this reason there is compensation of the local magnetic fields in the vicinity of the nucleus. In contrast, a difference of 33% between the calculated and experimental values for the second moments of $TiH_{1.98}$ indicates that here it is possible for the magnetic moments of the protons to interact with the conductance electrons.

A difference between the hydrides of titanium and zirconium permits assuming that the bond present in zirconium hydride approximates a covalent bond, whereas in titanium hydride the bond strengths have a metallic character. The paper [10] in which the paramagnetic susceptibility of the indicated compounds is measured can serve in support of such an assumption. A covalent directed bond in ZrH_2 leads to the appearance of a tetragonal distortion of the lattice, while a metallic bond in $TiH_{1.98}$ gives the more symmetric cubic lattice.

Measuring the shifts, made by us in order to determine more accurately the influence exerted by the conductance electrons on the p.m.r., failed to lead to a quantitative result, since the magnitude of the shifts does not exceed 0.003%.

We wish to thank Prof. Ya. S. Umanskii for his valuable counsel.

LITERATURE CITED

[1] O. T. Malyuchkov, and V. S. Pavlovskaya, Sci. Reports of the Higher Schools, Metallurgy Section, No. 3, 231 (1958).

[2] R. V. Pound, Progr. Nucl. Phys. 2, 21 (1952).

[3] G. V. Samsonov and Ya. S. Umanskii, Solid Compounds of High-Melting Metals, (Moscow, 1957).*

[4] V. V. Sof'ina, Z. M. Azarkh and N. N. Orlova, Crystallography 3, No.5, 539 (1958).

[5] M. A. Garstens, Phys. Rev. 81, No. 2, 288 (1951).

---

* In Russian.

[6] N. Bloembergen, Report of the Conference on Defects in Crystalline Solids. (London, 1955) p. 1.

[7] A. R. Ubbelohde, Advances in Chemistry (USSR) 7, 1692 (1938).

[8] R. Rundle, C. Shull, and E. Wollan, Acta Cryst. 5, 22 (1952).

[9] H. S. Gutowsky, J. Chem. Phys. 16, 1164 (1948).

[10] W. Trzebiatowski and B. Stalinski, Bull. Acad. Polon. Sci. Classe III, 1 (3-4), 131 (1953).

Received March 27, 1959

---

* In Russian.

THE THEORY OF THE ADSORPTION WAVE*

RELATIONSHIP BETWEEN THE CONCENTRATION OF OUTGOING GAS AND THE TIME OF EXHAUSTION OF THE ADSORBENT

Acad. Sci. USSR Corresponding Member A. S. Predvoditelev

1. In the theory of the movement of gases through porous materials, besides the equation of continuity, there is also another very important rule, relating the filtration rate with the head-pressure gradient. This rule is known as the Darcy rule. We will designate the filtration rate by W. Then for the one-dimensional case the Darcy rule can be written in the form

$$W = -\beta \frac{\partial p}{\partial x}. \tag{1}$$

The factor β is called the coefficient of resistance of the porous layer. It depends on the structure of the layer. Many investigators have occupied themselves with interpreting the physical significance of this coefficient and here the most important results were obtained by Slichter. This rule cannot be neglected in constructing the theory of the adsorption wave. Together with the kinetics of adsorption in porous materials, the Darcy rule should play a prominent role in the theory of the adsorption wave.

2. We will desingnate by $\underline{c}$ the concentration of the reacting substance in the gas stream moving through a porous adsorbent. Because of physical and chemical processes this concentration will change in accordance with some rule. We will write this rule in the highly general form:

$$\frac{\partial c}{\partial t} = \alpha f(c); \tag{2}$$

here α designates the reaction rate constant. The phenomenon controlled by rule (1), and the phenomenon controlled by rule (2). should go harmoniously. It is easy to show that such joint processes can proceed as a front, i.e., the integrals describing the behavior of the main parameters will depend on the character of the movement of some surface of the front, We will examine the one-dimensional case. Here the surface of the front will be a plane. We will designate the position of the front by the coordinate $\underline{x}$. We will introduce into the treatment the variable $\xi = x/t$. If the front moves uniformly, then this ratio will coincide with its rate.

Having transposed Equations (1) and (2) with respect to the variable ξ, we obtain

$$W = -\frac{\beta}{t}\frac{dp}{d\xi}, \quad -\frac{\xi}{t}\frac{dc}{d\xi} = \alpha f(c).$$

Having eliminated the time from these two equations, we obtain

$$W\xi\, dc = \beta\alpha f(c)\, dp. \tag{3}$$

The found equation shows that a frontal progress of the joint processes, obeying rules (1) and (2), is possible.

---

* See [2]

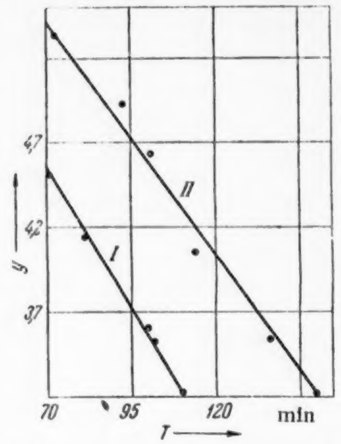

Fig. 1. I) c_0 = 0.515%; II) c_0 = 0.426%.

3. We will analyze a particular case. In his studies, M. Katz postulates that the change in the concentration c goes according to the first order, i.e., according to the kinetic equation

$$\frac{\partial c}{\partial t} = -\alpha c. \tag{4}$$

With this in mind, Equation (3) can be rewritten in the form

$$W\xi\, dc = -\beta\alpha c\, dp. \tag{5}$$

Equation (5) should be valid at any period of time, and consequently, at any movement of the front, in particular, when the movement is uniform. It is specifically the latter case that we will consider, and such a condition permits integrating Equation (5) between the start of the process and its end. Thus, we will have:

$$W\xi \lg \frac{c_d}{c} = \beta\alpha (p - p_d). \tag{6}$$

Here the subscript d indicates that the proper values should be taken at the end of the tube.

For the initial point of the process it is possible to obtain from Equation (6) a ratio with the form

$$W\xi \lg \frac{c_d}{c_0} = \beta\alpha (p_0 - p_d). \tag{7}$$

But with a constant filtration rate, the following equation holds

$$W = \beta \frac{p_0 - p_d}{d},$$

(d is the thickness of the adsorption layer), with the aid of which Equation (7) can be rewritten in the form

$$\lg \frac{c_d}{c_0} = \frac{\alpha d}{\xi}. \tag{7a}$$

As is easily seen, the ratio d/ξ is the time of exhaustion of the adsorption layer, which we will designate by T, and in place of Equation (7a) we can write

$$\lg \frac{c_d}{c_0} = \alpha T.$$

From this it follows that

$$c_d = c_0 e^{\alpha T}. \tag{8}$$

For small values of the product α T, where its second orders can be neglected, by decomposing the exponential function in order we obtain

$$c_d = c_0 (1 + \alpha T).$$

The concentration c_d corresponds to the outgoing gas. We will designate the reciprocal of this value by y, and from the last equation we obtain

$$y = (1 - \alpha T) \frac{1}{c_0}. \tag{9}$$

4. If we plot the values of y along the ordinate, and the time of exhaustion of the adsorption layer along the abscissa, we then obtain straight lines with a negative tangent slope. As an illustration, we have plotted in Fig. 1 the experimental results obtained by M. Katz and co-workers.

The work done by M. Katz also contains some experimental results that do not satisfy the linear rule. The author himself mentions this. He states that the indicated (linear) relationship held for most of the cases investigated, but that deviations were observed at very low concentrations of the outgoing gas. M. Katz attempts to explain most of these deviations as being due to errors in chemical analysis, which could rise at low concentrations of the outgoing gas. However, from the graphs given in the work of M. Katz it can be seen that in some cases a nonlinear distribution of the points is quite distinct, and for this reason an attempt to approximate these points by a straight line must be considered to be somewhat forced.

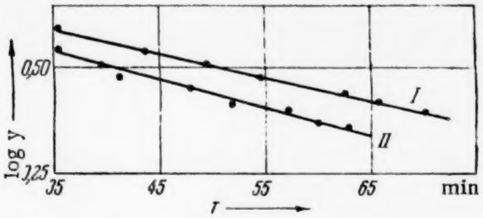

Fig. 2. I) $c_0 = 0.772\%$; II) $c_0 = 1.01\%$.

If the indicated experimental results are plotted on a semilogarithmic scale, we obtain the plot shown in Fig. 2. From Fig. 2 it can be seen that the experimental points fall well on straight lines. For this reason, we believe the discussed concept is less faulty than the conclusions deriving from the Danby theory.

5. In some cases the oxidation of carbon monoxide proceeds by a kinetic equation of zero order. This, for example, occurs on the surface of hopcalite.

Equation (3) for a zero order reaction assumes the form

$$W\xi\, dc = -\beta\gamma\alpha\, dp.$$

From this, after integrating, we obtain

$$W\xi\,(c_d - c) = \beta\gamma\alpha\,(p - p_d).$$

For the initial state we will have

$$W\xi\,(c_d - c_0) = \beta\gamma\alpha\,(p_0 - p_d).$$

If the filtration rate is constant, then from the given equation it follows that

$$c_d = c_0 + \gamma\alpha T.$$

At small values of the product, by decomposition in the c_d reciprocal series, we will have .

$$y = \frac{1}{c_d} = \frac{1}{c_0}\left(1 - \frac{\alpha}{c_0}\,T\right). \tag{10}$$

The obtained equation is also capable of describing some of the above mentioned experimental results obtained by M. Katz, and this means that the conditions under which M. Katz ran his experiments are far from sufficient to answer the question as to the order of the reactions progressing in a porous adsorption layer.

As a result, the discussed considerations clearly demonstrated the narrowness and limited scope of the Danby theory. Without improving on it, and without a further expansion of experiments pertaining to catalytic reactions studied by the dynamic method, it is hardly fair to arrive at any conclusion as to the mechanism of chemical transformations.

LITERATURE CITED

[1] M. Katz, Heterogeneous Oxidation of Carbon Monoxide [Russian Translation], Monographs on Catalysts for Organic reaction . Editors-in-Chief A. A. Balandin and A. M. Rubinshtein (IL, 1955) p. 191 .

[2] A. S. Predvoditelev, Proc. Acad. Sci. USSR 127, No. 3, 602 (1959).*

Received March 30, 1959

---

* Original Russian pagination. See C.B. Translation.

THE NATURE OF THE CONTACT FUSION OF ALKALI HALIDE CRYSTALS

P. A. Savintsev, V. E. Avericheva and V. Ya. Zlenko

(Presented by Academician V. D. Kuznetsov, April 8, 1959)

Contact fusion is used in practice as a method of physicochemical analysis [1-2], and also as a method for obtaining low-melting alloys [3]. The basic rules for the contact fusion of crystals, forming eutectic alloys and solid solutions, have been discussed in a series of papers [4-6], but the mechanism and kinetics of this process have not been studied. The theory has been expressed that the contact fusion of crystals, possessing unlimited mutual solubility, bears a diffusion character [7].

We made an x-ray study of mixtures of alkali halide salts at elevated temperatures. We used both the method and the high-temperature x-ray chamber that had been developed in the x-ray Laboratory of the Institute of General and Inorganic Chemistry of the Academy of Sciences of the USSR [8]. The mixture of powders in a thin-walled quartz capillary was heated to the given temperature, which was maintained constant during x-raying.

For the mixture of KCl-NaCl powders the lines of the component are observed on the debyograms up to 600°, disappearing at 635°, and then the lines of the solid solution appear in place of them.

For the eutectic mixture of KCl— KI salts the formation of a homogeneous solid solution could not be detected on the x-ray patterns at any of the temperatures used. At $t \leq 300°$ the x-ray pattern lines of the mixture coincide with the x-ray pattern lines of the components , and at $t \geq 500°$ their shift is observed, which is evidence that solid solutions of KCl in KI and of KI in KCl are formed. It was found that the x-ray patterns of the eutectic mixture and of the eutectic KCl—KI alloy are identical in the temperature range from 20 to 580°, i.e., clear up to the melting point; consequently, similar processes take place in both the mixture and the eutectic alloy when heated.

The change in the lattice periods of the free components, and of the same components in the eutectic mixture, as a function of the temperature is shown in Figs. 1 and 2 .

At temperatures up to 300° the KCl and KI periods in the alloy increase mainly due to heat expansion, which occurs at the same rate for both the free components and the components in the alloy (and also in the mixture). At $t > 300°$, together with heat expansion, the effect of the diffusion factor becomes noticeable, as a result of which the KCl period in the alloy increases at a more rapid rate than in the free KCl, while the KI period in the alloy decreases. Such a change in the periods is in qualitative agreement with the Vegard rule, and indicates the formation of solid solutions in the eutectic mixture of the powders.

The process of diffusion at temperatures close to the contact fusion temperature was studied on the monocrystals KCl—KBr, NaCl—NaBr, and KCl—KI , heated separately to the given temperature, and then brought into contact with each other. Having kept the crystals at the given temperature for a variable length of time, we took the reverse x-ray pattern of the compositions forming at the contacting surfaces. On the surface of the KCl crystal, at a temperature 50° below the contact fusion temperature, a solid solution with the composition 60 mole% KBr + 40 mole % KCl is formed in 200 min, corresponding to the composition of the solid solution at the minimum on the fusion diagram for the system KCl—KBr. Here a solid solution, analyzing 30 mole% KCl + 70 mole% KBr , is formed on the surface of the KBr.

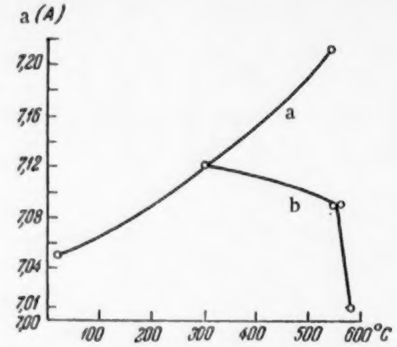

Fig. 1. Change in the KI lattice period with temperature: a) pure KI; b) KI in the alloy.

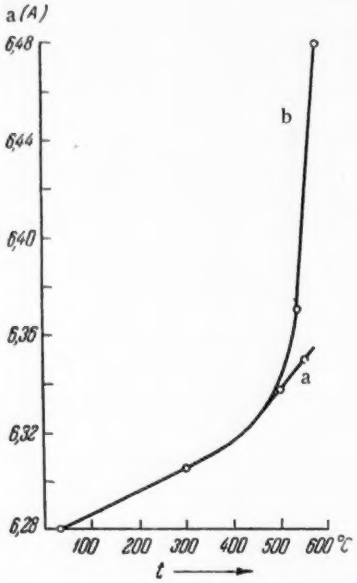

Fig. 2. Change in the KCl lattice period with temperature: a) pure KCl; b) KCl in the alloy.

TABLE 1

Heat of Formation of Solid Eutectics

Expt. No.	Eutectic alloy	Time of storage (hr)	Heat of formation (cal/mole)
1	KCl — KI	to 200	180
2	KCl — K_2CrO_4	to 24 to 72 to 220	250 150 80

The time, required to form solid solutions with such compositions, decreases as the experiment temperature approaches the contact fusion temperature, where the formation of the indicated compositions occurs in a matter of several minutes.

Similar results were obtained for the NaCl—NaBr crystals.

For the case of contacting the KCl—KI crystals we observed that limited solid solutions are formed on each of their surfaces. At 550°, the maximum amount of KI in the KCl surface layer, $3 \cdot 10^{-3}$ cm thick, was 32 mole %, whereas the KI surface layer was found to contain only 12% KCl.

The mechanism for the contact fusion of crystals, forming eutectic alloys and solid solutions, is similar. The presence of contact fusion can be regarded as proof that a mutual solubility of the components exists. This is supported by the experiments on measuring the heats of formation of the solid eutectic alloys KCl—KI and KCl—K_2CrO_4. The fusion diagrams of these crystals are described in [9, 10].

We used the method developed and described by M. S. Ivankina [11] to measure the heats of formation. The experiments were run at 25°, both on the first day of preparing the alloys, and also subsequently. The results are given in Table 1.

The heat of formation of the eutectic alloy KCl—K_2CrO_4 decreases sharply with increase in the time of storage, and consequently the alloy passes from an unstable state to a more stable one with a lower mutual solubility of the components. At room temperature the eutectic alloys KCl—K_2CrO_4 and KCl—KI are not additive mechanical mixtures of the components. The fact that the heat of formation differs from 0 indicates the presence of molecular interactions in the solid eutectic alloy, and also the presence of a mutual solubility of the components.

Both the high-temperature x-ray study of mixtures of alkali halide salts and a study of diffusion on monocrystals, brought into contact with each other at temperatures close to the contact fusion temperature, revealed that diffusion processes precede the contact fusion of crystals, forming solid solutions (KCl — NaCl, KCl— KBr, NaCl — NaBr) and eutectic alloys (KCl—KI).

Solution of the solid components goes rapidly at temperatures close to the contact fusion temperature and is the first preparatory stage in the contact fusion of alkali halide compounds.

LITERATURE CITED

[1] M. Kh. Gluzman and V. P. Rubtsova, J. Gen. Chem. 27, No. 3, 704 (1957).*

[2] M. Kh. Gluzman and A. L. Gershuns, J. Phys. Chem. (USSR) 27, No. 3 (1953).

[3] P. A. Savintsev and A. V. Vyatkina, Bull. of the Institutions of Higher Education, Physics, No. 4 (1958).

---

* Original Russian pagination. See C.B. Translation.

[4] D. D. Saratovkin and P. A. Savintsev, Proc. Acad. Sci. USSR 33, 4 (1941); Proc. Acad. Sci. USSR 58, No. 9 (1947); Proc. Acad. Sci. USSR 80, No. 4 (1951).

[5] S. V. Avakyan and N. F. Lashko, Proc. Acad. Sci. USSR 65, No. 1 (1949).

[6] P. A. Savintsev and V. E. Avericheva, Proc. Acad. Sci. USSR 119, No. 5 (1958)*; Bull. Tomsk Polytech. Inst. 95 (1958).

[7] D. D. Saratovkin, Bull. of the Institutions of Higher Education, Physics, No. 2 (1958).

[8] V. G. Kuznetsov, J. Inorg. Chem. (USSR) 1, No. 7 (1956).

[9] I. S. Rassonskaya and A. G. Bergman, J. Gen. Chem. 22, 1089 (1952).*

[10] V. P. Radishchev, J. Gen. Chem. 5, No. 4 (1935).

[11] M. S. Ivankina, Bull. Tomsk Polytech. Inst. 95 (1958).

Received April 8, 1959

---

* Original Russian pagination. See C.B. Translation.

INFLUENCE OF IONIZING RADIATIONS ON THE STRUCTURE OF POLYAMIDES

N. A. Slovokhotova

L. Ya. Karpov Research Institute of Physical Chemistry

(Presented by Academician V. A. Kargin, April 8, 1959)

In this paper the action of ionizing radiations on the structure of polyamides was studied using the infrared spectroscopy method. The irradiation was done in a vacuum, using accelerated electrons (intensity of the accelerating field was 200 kv, and the current density was 2.2 μa / sq cm) and Co^{60} γ-radiation. Films of capron and of a capron—nylon copolymer (1 : 1) were irradiated. The experimental procedure was described in detail in a previous paper [1].

From a comparison of the infrared spectra of polyamides, taken before and after irradiation in a vacuum, it follows:

1. Irradiation of polyamides with ionizing radiations leads to a change in the amount of methylene groups in the methylene chains of the polyamides. This is indicated by a decrease in the intensity of the adsorption bands in the infrared spectra of the irradiated polyamides (Fig. 1) in the 1250 cm^{-1} region, belonging to the deformation vibrations of the CH_2 group [2]. Here, simultaneously with a reduction in the intensity, the maximum of the band is shifted toward longer wavelengths, and the shape of the band widens strongly. This can be due to the number of units in the methylene chains of the polymer changing during irradiation, for the adsorption bands corresponding to the vibrations of the CH_2 group in the methylene chains of various polyamides lie in the 1290-1210 cm^{-1} region, and the position of these bands in the indicated region depends on the length of these methylene chains [3].

2. The intermolecular hydrogen bonds in the polyamides suffer scission during irradiation, which is evidenced (Fig. 2) in the spectra by a reduction in the intensity of the 3080 and 3306 cm^{-1} bands, corresponding to the valence vibrations of the NH bonds, included in the intermolecular hydrogen bonds [4], and also by an over-all reduction in the intensity of the doublet band in the 1550-1540 cm^{-1} region and a shift of the maximum of this band in the 1540 cm^{-1} region (Fig. 3). The 1550 cm^{-1} component of this doublet is characteristic for peptide groups, involved in intermolecular hydrogen bonds, where the NH and C=O of one unit of the polymer chain are found trans with respect to each other [5].

3. Together with a scission of the intermolecular hydrogen bonds, in polyamides when irradiated, intramolecular hydrogen bonds are formed, i.e., the stretched β-form of the polyamides, for which intermolecular hydrogen bonds are characteristic, is converted under the influence of radiation into the coiled α-form, to which intramolecular hydrogen bonds are inherent. This is supported by the fact that in the frequency region of the valence vibrations of the carbonyl group a shift is observed in the maximum of the adsorption band at 1638 cm^{-1} in the spectrum of the unirradiated polyamide to the 1650 cm^{-1} region in the spectrum of the irradiated polyamide (Fig. 3). The position of the maximum of this band at 1638 cm^{-1} is characteristic for the β-form, and at 1650 cm^{-1} for the α-form of the polymer [6].

4. The same as when melted, polyamides migrate to the amorphous state when irradiated. The picture for the change in the spectrum of the polyamide when irradiated is very similar to the picture for the change in the spectrum of the polyamide when melted (Fig. 3) in both the 3300-3000 cm^{-1} and 1650-1540 cm^{-1} regions. Further evidence of this is the disappearance of the crystallinity band [2] at 936 cm^{-1}, which band is at the same time characteristic for intermolecular hydrogen bonds.

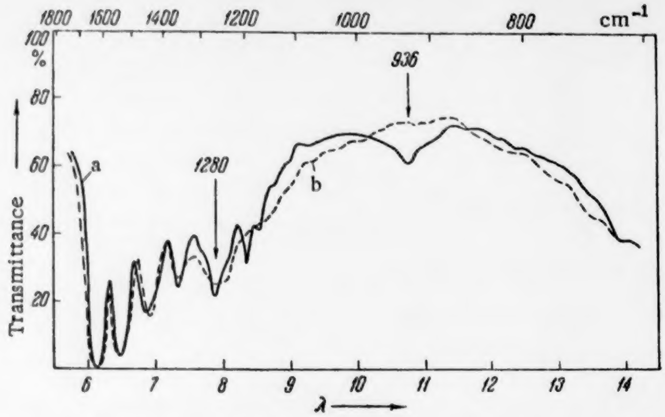

Fig. 1. Infrared spectra of films of capron–nylon copolymer (d = 10 μ): a) unirradiated film; b) film irradiated with accelerated electrons in a vacuum for 2 hr.

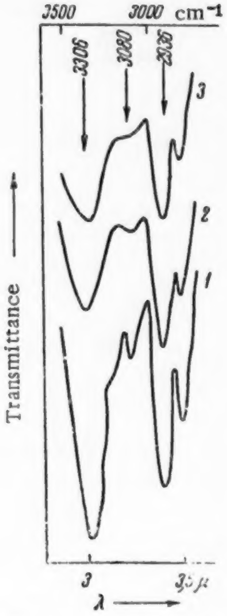

Fig. 2. Infrared spectra of films of capron–nylon copolymer (d=5μ): 1) unirradiated film at 20°; 2) unirradiated film at 250° (molten); 3) film irradiated with accelerated electrons in a vacuun for 4hr at 20°.

It is possible to assume that the loss of crystallinity for the polymers when irradiated is due not only to the formation of cross links between the chains, but also to a twisting of the polymer chains when irradiated, with the formation of rings. Polyamides are a good example of this: when irradiated their molecular chains suffer coiling with the formation of rings closed by hydrogen bonds. Formation of rings during irradiation, together with the polymer becoming amorphous, was also observed by us for the case of Teflon [1].

The same as polyethylene, polyamides become cross linked when irradiated [7], and here the main portion of the gaseous products evolved from a polyamide such as Perlon is hydrogen (56%) [8]. This makes it possible to assume that the mechanism, used by many authors [9] to explain the cross linking of polyethylene when irradiated, can also be used to explain the processes that take place in polyamides, i.e., scission of the CH bonds can take place in the irradiation of polyamides:

$$\begin{gathered}\mathrm{RNHCH_2 - CH_2 - CH_2 - CH_2 - CHC_2COR'} \longrightarrow \\ \longrightarrow \mathrm{RNHCH_2 - \dot{C}H - CH_2 - CH_2 - CH_2 - COR + H.}\end{gathered} \tag{1}$$

The hydrogen atom formed here can remove still another hydrogen atom from either a neighboring methylene group or from another methylene chain. Molecular hydrogen is evolved as a result of this, and either a double bond is formed, or a cross link is formed as the result of two of the free radicals obtained from different methylene chains recombining with each other. This process, in turn, should lead to a change in the length of the methylene chains, and according to the infrared spectra of the irradiated polyamides, this is exactly what was observed by us.

It should be mentioned that trans-vinylene double bonds are formed when polyethylene is irradiated [10], and the band in the 964 cm⁻¹ region corresponds to their presence in the spectrum of the irradiated polyethylene. An absorption band in this same region also appears in the spectra of irradiated polyamides; however, relating it to the presence of double bonds cannot be made with the same assurance as for the case of polyethylene, since the spectra of polyamides have bands in this region that characterize the presence of other structural groups in the polyamide molecules [2].

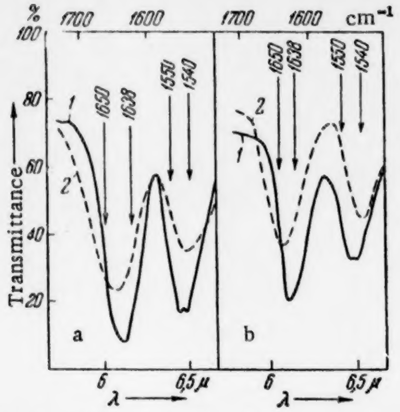

Fig. 3. Infrared spectra of films of capron–nylon copolymer: a) films (d = 5μ): 1) unirradiated; 2) irradiated with accelerated electrons in a vacuum for 4 hr ; b) unirradiated film (d = 3μ): 1) at 20° ; 2) at 250° (molten).

As was shown by Petrov and Karpov [8], who studied the gas evolution of polymers when irradiated, polyamides are approximately 3 times as stable to the action of ionizing radiations as polyethylene, and are less stable than polystyrene. The stability of polystyrene is explained by the presence of phenyl rings in its molecule. It is entirely probable that the greater stability of polyamides to ionizing radiations when compared to polyethylene is linked with the presence of hydrogen bonds in them, and, in particular, with the formation of stable rings, closed by hydrogen bonds, in the polyamides when irradiated. Migration of the energy and its subsequent scattering can occur via the hydrogen bonds.

Transition of the β-form into the α-form during irradiation is interesting in view of the fact that many of the properties of synthetic and natural polyamides, polypeptides and proteins are determined by whether the α- or the β-form is present in the given substance. Thus, the crimp of the wool fiber and some of its other properties are linked with the α-form of keratin [11]. The biological activity of a natural polypeptide like gramicidin is obviously linked with its spiral α-configuration [12]. At the same time, very important functions of the living organism are determined by the presence of intermolecular hydrogen bonds in proteins [13]. It is possible that our observed transition of polyamides from the β-form to the α-form is one of the reasons for upsetting the normal activity of the organism when exposed to ionizing radiations.

I wish to sincerely thank Academician V. A. Kargin for discussing the obtained results and for his invaluable counsel.

LITERATURE CITED

[1] N. A. Slovokhotova, Action of Ionizing Radiations on Inorganic and Organic Systems, Collection of Articles [In Russian] (Izd. AN SSSR, 1958), p. 295.

[2] I. Sandeman and A. Keller, J. Polymer, Sci. 19, 401 (1956).

[3] P. Bouriot, Bull. Inst. Text. France 61, 1 (1957).

[4] D. N. Shigorin, N. V. Mikhailov and S. P. Makar'eva, Proc. Acad. Sci. USSR 97, 717 (1954).

[5] M. Asai, M. Tsuboi, T. Shimanouchi, and S. Mizushima, J. Phys. Chem. 59, 322 (1955).

[6] S. Krimm, J. Chem. Phys. 23, 1371 (1955).

[7] V. L. Karpov, Session of the Academy of Sciences of the USSR on the World Utilization of Atomic Energy, Meeting of the Division of Chemical Sciences [In Russian] (Izd. AN SSSR ,1955), 3 .

[8] I. Ya. Petrov and V. L. Karpov, Transactions of the First All-Union Conference on Radiation Chemistry [In Russian] (Izd. AN SSSR, 1958), p. 279 .

[9] R. W. Pearson, J. Polymer Sci. 25, 189 (1957).

[10] N. A. Slovokhotova and V. L. Karpov, Collection of Articles on Radiation Chemistry [In Russian] , p. 206 (Moscow, 1955).

[11] W. T. Astbury, Scientific Principles of the Structure of Textile Fibers [Russian Translation] (1936).

[12] N. B. Abbot and E. J. Ambrose, Proc. Roy. Soc. 219, 17 (1953).

[13] G. Gamov, A. Rich and M. Ycas, Advances in Biol. and Med. Phys. 4, 23 (1956).

Received April 8, 1959

DETERMINATION OF THE CELL DIMENSIONS OF POLARIZING DISPERSE Pd-Au and Pd-Cu ALLOYS USED AS CATHODES

I. P. Tverdovskii, Zh. L. Vert and Yu. D. Kondrashev

State Institute of Applied Chemistry

(Presented by Academician A. N. Frumkin , April 13, 1959)

In most cases the x-ray study of metal—hydrogen systems is run on compact samples at the end of the physichochemical process involved, leading to a dissolving of the gas in the studied object. Direct photographing is done either in a H_2 atmosphere or under ordinary conditions, on the assumption that the rate of degasification is small. Together with this, a study of disperse alloys of palladium with nickel , silver and copper [1,2], obtained by common electrolytic deposition, has shown that, judging by the lattice period, the specimens, as the result of unavoidable drying, lose their absorbed hydrogen completely.

Measuring the parameters of polarizing electrodes has not been done earlier, although using the metal as the cathode in an electrolytic cell permits dissolving much more hydrogen in it than when saturation is from the gas phase [3]. Such experiments, besides having independent interest, permit checking some of the theories relative to the relationship between the overvoltage of hydrogen evolution and the interatomic distance [4,5].

As the object of study we chose the binary disperse alloys of palladium with gold and with copper, dissolving hydrogen in a quite broad range of compositions [6,7]. To remove the hydrogen, dissolved in the alloy during its electrolytic deposition, the specimens were anodically polarized until the first bubbles of oxygen appeared.

A special cell made of plexiglas was built for the investigation. A diagram of the cell is shown in Fig. 1.

A partially lacquer-coated platinum cathode, occupying approximately 1/3 of the cell in width, was fastened firmly by means of a rubber stopper and a support on the bottom of the vessel. The filled cell contained a thin layer of the electrolyte between the front wall of the cell, a polyethylene film 30μ thick, and the electrode.

A URS-50-I diffractometer was used for the photographing, making it possible, with suitable balancing, to obtain the lattice-period values with an accuracy of ~ ± 0.001 kX without any difficulty. We used $\mathrm{Cu}_{K\alpha}$ as the radiation ; the travel rate of the indicator w as 0.5°/min, the travel rate of the paper was 600 and 2400 mm/hr, and the time was constant at 4 and 8 sec. The recording was done within the interval of the measured line, with a marking of the angles. The directed toward the diffractometer lacquer-free operating surface of the cathode, on which the studied alloy had been electrolytically deposited in advance, was lined up as accurately as possible with the focal plane of the goniometer, since any deviation fron this position, possible both in the assembling and in the operation of the cathode, was a reason for measurement error, not connected with the state of the investigated specimen. The experiments were run in 1 N H_2SO_4 at room temperature. The hydrogen bubles evolving at the cathode, especially at high current densities, distorted the peaks on the x-ray patterns, and for this reason the current density was reduced to 10-20 ma/sq cm when recording the maxima.

The measurement technique was checked on 2 specimens of smooth platinum. The lattice period values, collected in Table 1, were calculated from the 420 line.

Considerating that diffractometer measurements give a systematic error of approximately $3 \cdot 10^{-2}\%$ on the low side [8], the obtained values show good agreement with the value of 3.9158_0 given in the table [9] .

Naturally, such an accuracy could not be attained on electrolytically deposited disperse alloys. Due to a

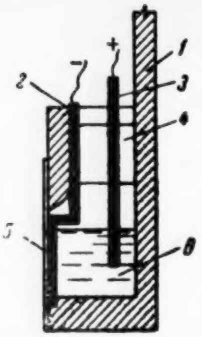

Fig. 1. Diagram of the cell. 1) Cell jacket; 2) cathode; 3) anode; 4) stopper; 5) polyethylene film; 6) electrolyte.

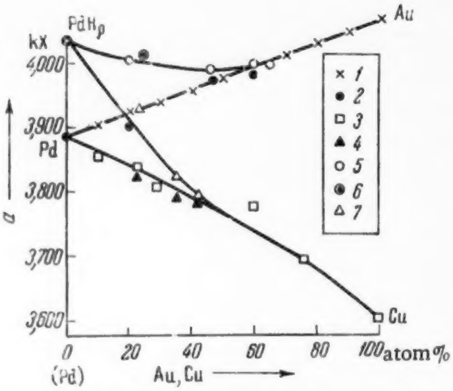

Fig. 2. Lattice periods of studied systems: Pd-Au: 1) [10], 2) our data; Pd-Cu: 3) [2], 4) our data; Pd-Au-H: 5) our data, 6) [11]; Pd-Cu-H: 7) our data.

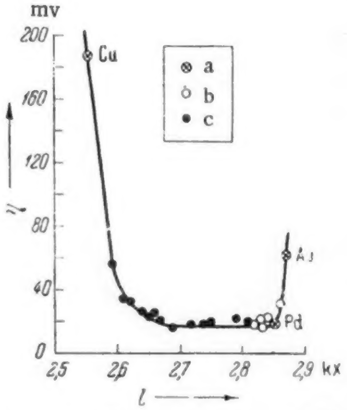

Fig. 3. Relation between η_{H_2} and the interatomic distance at D_k = 9 ma/sq. cm: a) pure metals; b) Pd-Au; c) Pd - Cu.

large degree of dispersion, the peaks on the x-ray patterns, especially for the Pd-Cu alloys, proved to be diffuse. In addition, the lines of the support were observed at the same time, which, with a close arrangement of the maxima of the 111 and 200 lines for the alloys and Pt, led to their mutual displacement. The calculations were made from several lines (111, 200; 311 and 222), in which connection the deviations from the mean values were 0.001-0.003 kX.

The results of determining the lattice periods of the disperse Pd-Au and Pd-Cu alloys after anodic polarization, and also during hydrogen evolution at a current density of 9 ma/sq cm, are given in Fig. 2. In the first case, the values of a show good agreement with the measurements of Kuznetsov [10], obtained on compact Pd-Au alloys, and with the data, obtained on disperse Pd-Cu alloys by the usual method of powder patterns [2]. The sharpest increase in the parameter, caused by the introduction of hydrogen atoms into the metal lattice, was observed for the case of palladium. With increasing concentration of either the gold or copper, this change decreased and became unnoticeable for the alloys containing 65% Au or 50% Cu. The hydrogen solubility in the indicated binary systems drops to zero at a somewhat lower palladium content [6,7]; however, the change in the lattice period in this region of concentrations probably does not exceed the possible accuracy of the experiment.

With increase in the gold content, the cell dimensions of the hydrogen-containing Pd-Au alloys change along a curve with a shallow minimum, reminiscent in this respect of the results obtained by Kruger and Sacklowski [12] and by Rosenhall [13] when they studied the system Pd—Ag—H. For both metallic systems the introduction of either gold or silver into the alloy is accompanied by an increase in the cell dimensions. The introduction of copper into an alloy with palladium is accompanied by a decrease in the interatomic distance, while the value of the lattice period for the hydrogen-containing alloys diminishes monotonically.

Changing the current density under the conditions of our experiments was practically without effect on the value of the lattice period: in the case of palladium, for example, increasing D_k from 9 to 90 ma/sq cm increased the parameter a from 4.034 to 4.037 kX.

The overvoltage values for hydrogen evolution on disperse Pd-Au and Pd-Cu alloys at D_k= 9 ma/sq cm [14, 15] as a function of the distance between neighboring metal atoms are shown in Fig. 3. The value of $l = \frac{a\sqrt{2}}{2}$ for polarizing of intermediate composition was calculated from the data shown in Fig. 2. In contrast to the curves with a sharp minimum, obtained when the values of η_{H_2} and l for pure metals are compared [4,5], in the case of the alloys studied by us a constancy of the overvoltage values is observed when l is changed from 2.65 to 2.85 kX.

TABLE 1

Lattice Periods of Smooth Platinum in kX

Location	Pure platinum spectrum	Pure platinum
Outside the cell	$3,913_9$	$3,914_1$
In the cell		
without electrolyte	$3,914_0$	$3,913_5$
with electrolyte	$3,914_0$	$3,913_9$
with a current	$3,914_5$	$3,913_8$

LITERATURE CITED

[1] Yu. K. Kondrashev, I. P. Tverdovskii, and Zh. L. Vert, Proc. Acad. Sci. USSR 78, 729 (1951).

[2] Yu. D. Kondrashev and I. P. Tverdovskii, Proc. Acad. Sci. USSR 99, 109 (1954).

[3] A. Michel and M. Gallisot, C.r. 208, 434 (1939).

[4] H. Leidheiser, Jr., J. Am. Chem. Soc. 71, 3634 (1949).

[5] N. E. Khomutov, J. Phys. Chem. (USSR) 24, 1201 (1950).

[6] R. A. Karpova and I. P. Tverdovskii, J. Phys. Chem. (USSR), No. 6 (1959).

[7] I. A. Mosevich, I. P. Tverdovskii and Zh. L. Vert, Collection of Transactions of State Institute of Applied Chemistry on Physical Chemistry, No. 42 (1959).*

[8] H. Neff, Zs. angew. Chem. 8, 505 (1956).

[9] E. Owen and J. Iball, Phil. Mag. 16, 606 (1933).

[10] V. G. Kuznetsov, Bull. Platinum Section 20, 5 (1947).

[11] J. Benard and J. Talbot, C. r. 222, 493 (1946).

[12] F. Kruger and A. Sacklowski, Ann. Phys. 78, 72 (1925).

[13] G. Rosenhall, Ann. Phys. (5), 24, 297 (1935).

[14] I. A. Mosevich, I. P. Tverdovskii and Zh. L. Vert, Collection of Transactions of State Institute of Applied Chemistry on Physical Chemistry, No. 42 (1959).*

[15] R. A. Karpova and I. P. Tverdovskii, Collection of Transactions of State Institute of Applied Chemistry on Physical Chemistry, No. 42 (1959).*

Received April 13, 1959

---

* In Russian.

MECHANISM OF THE ELECTROLYTIC REDUCTION OF MnO_4' ; SeO_4'' and ReO_4' IONS IN THEIR JOINT SEPARATION WITH CHROMIUM

D. N. Usachev, N. L. Klimasenko and A. T. Vagramyan
Institute of Physical Chemistry Academy of Sciences of the USSR

(Presented by Academician P. A. Rebinder, April 13, 1959)

In previous studies it had been shown [1] that a necessary condition for the cathodic reduction of hexavalent chromium to the metal in chromic acid solution is the presence of a film on the electrode surface: this film retards progress of the associated reactions of reduction of hexavalent chromium to the trivalent stage and the discharge of hydrogen ions, and this makes the deposition of metallic chromium possible.

The presence of a film on the cathode in the electrodeposition of chromium makes the electrode process specific. Thus, the introduction into the electrolyte of cations more electropositive than chromium makes their joint precipitation with chromium impossible, despite the high value of the cathodic polarization [2].

It can be assumed that the reduction of hexavalent chromium ions to the metal in the presence of a film on the cathode takes place directly from the products forming the film. As was shown earlier [3], to form the film it is necessary to have foreign anions present in the solution.

Since the film is impermeable for cations and the presence of anions is necessary for its formation, it can be assumed that the discharging chromium ions also enter into the film as anions; other substances, that may be found in the solution as negatively charged ions, will facilitate the formation of the film and will be reduced at the cathode together with chromium.

To verify this theory we studied the reduction of a number of anions in chromic acid solution containing sulfuric acid.

Selecting the metal for coprecipitation with chromium proved to be restricted, for of the metals, which, according to the thermodynamic data may be isolated from aqueous solutions, only a few can exist as the anion in chromic acid medium. One of these elements is manganese, which gives the MnO_4^- ion. This ion is reduced at highly positive values of the potential, so if the above expressed theory is valid, then manganese should precipitate together with chromium.

Before describing the experiment, it should be mentioned that since it was necessary to establish only the fact that such coprecipitation is possible, the quality of the precipitate in the given case played a secondary role, and the electrolysis conditions were selected more or less arbitrarily.

Manganese was added to chromic acid solutions as potassium permanganate. The electrolysis was run at 20° and a current density of 0.1 amp/sq cm. It was found that from a solution, containing 2 moles of CrO_3, 0.02 mole of H_2SO_4 and 0.25 mole of $KMnO_4$ per liter, an alloy of chromium with manganese is deposited, containing, according to the analysis data 15% manganese and 85% chromium. Here the yield based on the current hardly changed when compared with the solution not containing manganese. For comparison, a solution containing the manganese not as an anion but as the bivalent cation, was subjected to electrolysis. As was to be expected, in this case hardly any manganese was contained in the electrolytically deposited chromium.

As a result, our experiments show that if the metal is found in the chrome-plating electrolyte as the anion, it is deposited together with chromium on the cathode; if it is present as the cation, its coprecipitation with the chromium fails to be observed. This indicates that the discharging ion enters into the film as the anion.

As another object of study we used the SeO_4^{--} ion, which has a sufficiently high positive potential to be isolated from aqueous solution. The potential of the system $SeO_3^{--} + 4e \rightleftharpoons Se$ is equal to +0.74 v, so that it could be expected that selenium, like manganese, will also precipitate together with chromium at the cathode.

A standard chrome-plating electrolyte was used for the experiments, containing 2.5 mole/liter of CrO_3 and 0.025 mole/liter of H_2SO_4. The selenium was added as selenic acid H_2SeO_4. It proved that in this case also the selenium coprecipitates with chromium. For example, at a selenic acid concentration in the solution of 0.25 mole/liter, the electrolytic deposit, obtained at 20° and a current density of 0.50 amp/sq cm, contained 63% Cr and 37% Se. The total yield based on the current did not differ from the yield of chromium obtained when selenic acid was absent from the solution. Similar results were obtained when potassium perrhenate was added to the electrolyte. Qualitative analysis revealed that rhenium was present in the precipitate in this case also, thus indicating that it is possible to reduce the ReO_4^- ion jointly with the chromium.

Besides the described experiment, the viewpoint that joint precipitation with chromium is possible only when the coprecipitating element is present in the chrome-plating electrolyte as the anion is confirmed by the studies of Shome [4] and of Rogers and Burr [5] (although the latter was done under conditions that differed from those usually used in chrome plating). Shome was the first to precipitate an alloy of chromium with molybdenum from an electrolyte, containing chromic, molybdic and sulfuric acids. Rogers and Burr obtained an alloy of chromium with tungsten from a solution, containing chromic anhydride, tungstic anhydride, sulfuric acid and ammonium citrate, at a pH of 8. The next attempt was to obtain an alloy of chromium with gold. It is known that gold forms stable complexes of the anionic type with a whole series of ions, and for this reasont it could be assumed that it also will permeate through the film and discharge at the cathode together with chromium. Experiment revealed that from a solution, containing 2.5 mole/liter of CrO_3, 0.25 mole/liter of $H[AuCl_4]$ and 0.025 mole/liter of H_2SO_4, only chromium separates at the cathode. Gold could not be found in the electrolytic deposit.

The experiments with aurichloric acid reveal that not all anions are capable of being reduced jointly with chromium. In our opinion, the absence of gold in the chromium deposit is evidence that not all anions, but only a certain type, are capable of forming the film.

As a result, from the above described experiments it is abvious that only those substances coprecipitate with chromium at the cathode that are present in the chrome-plating electrolyte as anions, and are capable of entering into the composition of the film. The same metals, if present in the solution as cations, do not deposit with chromium in the electrolytic precipitate, even though they may have a higher positive potential for separation than some of the mentioned anions. This supports the theory that the process for the electrolytic deposition of chromium takes place directly from the products forming the film, and that the discharging ions enter into the cathodic film as anions.

LITERATURE CITED

[1] A. T. Vagramyan, D. N. Usachev and G. I. Chervova, Theory and Practice of Electrolytic Chrome Plating [In Russian] (Izd. AN SSSR, 1957).

[2] C. Kasper, J. Res. Nat. Bur. Standards 14, 693 (1935).

[3] A. T. Vagramyan and D. N. Usachev, J. Phys. Chem. (USSR) 32, No. 8, 1900 (1958).

[4] S. C. Shome, J. Indian Chem. Soc. 34, No. 5, 399 (1957).

[5] D. G. Rogers and A. A. Burr, J. Electrochem. Soc. 97, No. 2, 67 (1950).

Received April 13, 1959

OPTICAL ANISOTROPY OF ISOTACTIC POLYSTYRENE MOLECULES

V. N. Tsvetkov and S. Ya. Magarik

Institute of High-Molecular Compounds, Academy of Sciences of the USSR

(Presented by Academician A. A. Lebedev, March 27, 1959)

Up to now the difference in the structure of isotactic and atactic polymers was observed only in the solid state. Judging the structure regularity of the molecular chain of a polymer is usually done on the basis of the data relating to its ability to crystallize. However, only in dilute solution, independent of whether the dissolved high-molecular substance was found in the amorphous or the crystalline state, is it possible to directly study the degree of structure regularity of its macromolecules. The statistical theory of polymeric chains shows that in principle it is possible for the stereospecificity of the chain structure to affect its configuration, changing its degree of coiling (thermodynamic flexibility) [1-3].

However, experimental studies failed to show any differences in the dimensions and hydrodynamic properties of the macromolecules of isotactic and atactic polystyrene [4-8], and of polypropylene [9-12], in solutions.

In this paper an attempt is made to study the stereospecificity of a polymer utilizing the optical anisotropy of its molecules, a property that is more sensitive than the size in respect to the structure of the molecular chain.

A good example of this sensitivity is, for example, the results obtained in a parallel study of poly(methyl methacrylate) (PMMA) and poly(p-tert-butylphenyl methacrylate) (PBPMA), polymers having the same structure of the principal valence chains, but differing in the structure of the side molecular groups. Study revealed that with the same degree of polymerization, the linear size of the molecules of the second polymer exceeds that of the molecules of the first polymer by not more than 20% [13], whereas their optical anisotropy differs by a factor of more than 20, and has an opposite sign [14,15].

In this paper we made a comparative study of the optical anisotropy of isotactic and atactic polystyrene. The x-ray pattern* of isotactic polystyrene, processed in known manner [5, 16], showed a crystalline structure. The molecular weight of the isotactic polystyrene, determined by light scattering** in toluene, proved to be equal to 800,000. The atactic polystyrene specimen was one of the fractions of the block polymer obtained by polymerization at room temperature without initiator.

The optical anisotropy of the polymers was determined by the method of flow birefringence in a solvent (bromoform), the refractive index of which coincides with the refractive index of polystyrene ($n = 1.6$) i.e., with the effect of the form described in [17] absent. In this case the difference in the two principal polarizations of a statistical segment of the molecule $(\alpha_1 - \alpha_2)$ can be determined directly from the intrinsic values of the birefringence $[n]$ and viscosity $[\eta]$ of the solution [18].

To eliminate possible errors in determining the concentrations, we also made use of the calculation method proposed by Peterlin [19], according to which the ratio $[n]/[\eta]$ can be replaced by the ratio $\Delta n/g(\eta - \eta_0)$. With these conditions, the difference $(\alpha_1 - \alpha_2)$ can be calculated from the values of the birefringence $\Delta n/g$ and viscosity η of the solution, without determining its concentration c (η_0 is the viscosity of the solvent). The applicability of Peterlin's method to polystyrene in bromoform over a broad concentration range has been demonstrated in a number of papers [20,21].

---

* The x-ray patterns were obtained by L. A. Volkova in Prof. M. V. Vol'kenshtein's laboratory.

** The light-scattering measurements were made in our laboratory by V. E. Éskin.

TABLE 1

Viscosity and Birefringence of Two Types of Polystyrenes

Isotactic polystyrene				Atactic polystyrene			
C, g/100 ml	$\frac{\Delta n}{g}\cdot 10^{10}$	η, centi-poises	$\frac{\Delta n}{g(\eta-\eta_0)}\cdot 10^{10}$	C, g/100 ml	$\frac{\Delta n}{g}\cdot 10^{10}$	η, centi-poises	$\frac{\Delta n}{g(\eta-\eta_0)}\cdot 10^{10}$
0,69	1,22	7,9	21,0	0,80	0,97	9,0	13,5
0,58	0,93	6,8	19,6	0,62	0,67	6,9	13,5
0,45	0,67	5,3	20,8	0,42	0,41	5,1	13,6
0,33	0,48	4,4	21,1	0,32	0,30	4,2	14,0
0,22	0,28	3,5	20,4	0,23	0,20	3,5	13,2
0,12	0,15	2,8	20,4	0,13	0,10	2,9	12,3

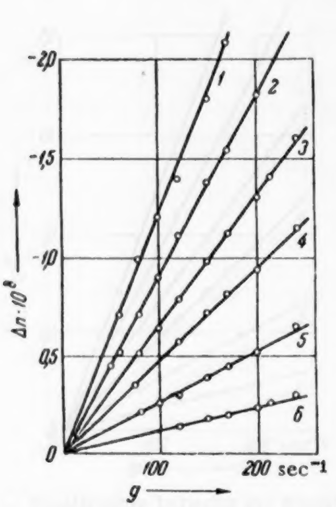

Fig. 1. Relationship between the birefringence Δn and the velocity gradient g. Isotactic polystyrene in bromoform. Concentration (g/100 ml): 1) 0.69, 2) 0.58, 3) 0.45, 4) 0.33, 5) 0.22, 6) 0.12.

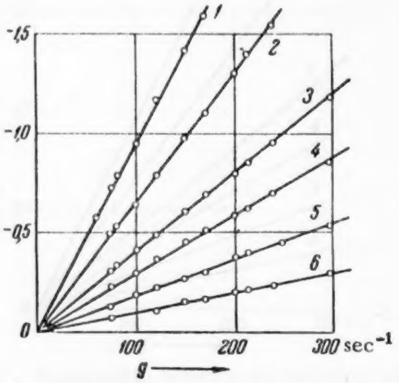

Fig. 2. Relationship between the birefringence Δn and the velocity gradient g. Atactic polystyrene in bromoform. Concentration (g/mole): 1) 0.80, 2) 0.62, 3) 0.42, 4) 0.32, 5) 0.23, 6) 0.13.

Special attention was given to checking the optical purity and molecular nature of the solution. The absence of any noticeable amount of colloidal impurities (insoluble crystallites, micelles) was shown by measuring the birefringence in a magnetic field (Cotton-Mouton effect), and by determining the degree of depolarization and asymmetry of light-scattering of the solution.

The conventional Ostwald viscosimeter was used to measure the viscosities. The universal dynamooptimeter and optical layout were described earlier [22]. The rotor length in our apparatus was 96 mm, and the gap width was 0.86 mm. The difference in the travel of the elliptic compensator was $\delta = 0.041\,\lambda$, where $\lambda = 5.5\cdot 10^{-5}$ cm.

The results of measuring the birefringence as a function of the velocity gradient are shown in Figs. 1 and 2. The corresponding values of $\Delta n/g$, in the second column in Table 1, were obtained taking the inherent birefringence of bromoform to be $\Delta n/g = 1\cdot 10^{-12}$. As can be seen from Fig. 3, the intrinsic value of the birefringence for the case of isotactic polystyrene is $[n] = -52\cdot 10^{-10}$, and for atactic polystyrene it is $[n] = -34\cdot 10^{-10}$. For both specimens, the intrinsic viscosity in bromoform proved to be $[\eta] = 2.6\cdot 100$ ml/g. As a result, for isotactic polystyrene the ratio $[n]/[\eta] = -20.0\cdot 10^{-10}$, and for atactic polystyrene the same ratio $= -13.1\cdot 10^{-10}$. The values $\Delta n/g(\eta - \eta_0)$, given in the last column in Table 1, show good agreement with the value $[n]/[\eta]$.

Using the equation given in [18], the calculated value of the optical anisotropy for isotactic polystyrene is $(\alpha_1 - \alpha_2) = -224\cdot 10^{-25}$ cm^3 and for atactic polystyrene it is $(\alpha_1 - \alpha_2) = -146\cdot 10^{-25}$ cm^3. The last value is in satisfactory agreement with the results obtained in a number of papers [20-24].

The results of measuring the angles of orientation α are shown in Fig. 4, where the function $\alpha = f(g)$ is plotted for solutions of isotactic (Curve 1) and atactic (Curve 2) polystyrene, corresponding to the conditions of infinite dilution. The given graphs show that the intrinsic value of the orientation $\left[\frac{\varphi}{g}\right] = \lim\limits_{\substack{c\to 0\\ g\to 0}}\left(\frac{\pi/4-\alpha}{g}\right)$

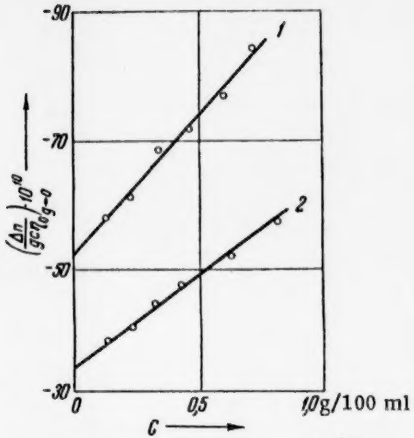

Fig. 3. Relationship between $\left(\frac{\Delta n}{gc\eta_0}\right)_{g\to 0}$ and the concentration. 1) Isotactic polystyrene, and 2) atactic polystyrene.

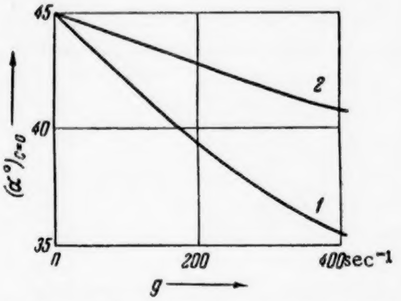

Fig. 4. Relationship between angles of orientation at infinite dilution $(\alpha^\circ)_{C=0}$ and the velocity gradient g. 1) Isotactic polystyrene, and 2) atactic polystyrene.

for the isotactic specimen is considerably greater than for the atactic polystyrene. Taking into consideration the fact that the medium viscosity dimensions of the macromolecules in the two specimens are equal (their intrinsic viscosities in bromoform coincide), the fact that the values of $[\varphi/g]$ are different must obviously be explained as being due to a greater polydispersity of the isotactic (unfractionated specimen [25-27].

In discussing the principal result of the study, i.e., the fact that the value of $(\alpha_1-\alpha_2)$ for the isotactic specimen is more than 1.5 times that for the atactic specimen, it must be remembered that in principle it is possible for two factors to exist here, affecting the optical anisotropy of the molecular chain when its degree of stereoregularity is changed. The first reason, already mentioned above, may be a change in the configuration of the principal molecular chain with increase in its stereoregularity. This change can lead to either an increase in the statistical dimensions of the polymeric chains [1-3], and together with this, also change their optical anisotropy [28].

The second factor that must be considered is a possible change in the extent to which rotation is hindered in the side groups of the molecule when going to the stereoregular polymer. Hindrance of rotation in the side groups, due to interaction of the latter [14], can rise sharply in going from the syndiotactic to the isotactic form, since in the latter the distance between the side radicals of the chain is greatly reduced.

It is obviously possible for this circumstance to have important bearing for polystyrene chains, the anisotropy of which is determined mainly by the difference in the polarity and position of the benzene ring. Here a negative anisotropy $(\alpha_1-\alpha_2)$ of the polystyrene chain is due to the fact that the planes of the side phenyl groups, oscillating around the $C_{\text{aliphatic}}-C_{\text{aromatic}}$ bonds, bear a direction that is predominantly normal to the primary valence chain. Disturbing these oscillations in going from the atactic to the isotactic structure should obviously increase the negative anisotropy of the chain, as was discovered in our experiments.

To what extent the rules observed by us are general for polymers of a different structure (for example, not containing benzene rings in the side groups) can be answered at the present time only by doing further experimental work.

The present study shows that at least for the type of polymers investigated by us it is possible to use the flow birefringence as a method of quantitatively characterizing their degree of stereo regularity.

The authors take this opportunity to thank L. A. Volkova and V. E. Éskin for assisting in the work, O. M. Shibanova for valuable help in preparing the solutions, and O. B. Ptitsyn for an interesting discussion.

LITERATURE CITED

[1] T. M. Birshtein and O. B. Ptitsyn, J. Phys. Chem. (USSR) 28, 213 (1954).

[2] T. M. Birshtein and O. B. Ptitsyn, J. Tech. Phys. (USSR) 24, 1998 (1954).

[3] O. B. Ptitsyn and Yu. A. Sharonov, J. Tech. Phys. (USSR) 27, 2744 (1957).

[4] F. W. Peaker, J. Polymer Sci. 22, 25 (1956).

[5] F. Danusso and G. Moraglio, J. Polymer Sci. 24, 161 (1957).

[6] G. Natta, F. Danusso, and G. Moraglio, Makromolek. Chem. 20, 37 (1956).

[7] F. Ang, J. Polymer Sci. 25, 126 (1957).

[8] W. R. Krigbaum, D. K. Carpenter, and N. S. Newman, J. Phys. Chem. 68, 1586 (1958).

[9] G. Ciampa, Chim. et Industrie 38, 298 (1956).

[10] F. Ang and H. Mark, Monatsh. Chem. 88, 427 (1957).

[11] R. Chiang, J. Polymer. Sci. 28, 235 (1958).

[12] F. Danusso and G. Moraglio, Makromolek. Chem. 28, 250 (1958).

[13] V. N. Tsvetkov and S. I. Klenin, J. Tech. Phys. (USSR) 28, 1019 (1958).

[14] V. N. Tsvetkov and L. N. Verkhotina, J. Tech. Phys. (USSR) 28, 97 (1958).

[15] S. Ya. Magarik and V. N. Tsvetkov, J. Tech. Phys. (USSR) 33, No.4, 835 (1959).

[16] J. Williams, J. Van Den Berghe, K. Dunham, and W. Dulmage, J. Am. Chem. Soc. 79, 1717 (1957).

[17] V. N. Tsvetkov, and É. V. Frisman, Proc. Acad. Sci. USSR 97, 647 (1954).

[18] W. Kuhn and H. Kuhn, Helv. Chim. Acta. 29, 71 (1946).

[19] A. Peterlin, Bull. Sci. Conseil Acad. RPF. Yougoslavie 1, 39 (1953).

[20] É. V. Frisman, and V. N. Tsvetkov, J. Polymer Sci. 30, 297 (1958).

[21] É. V. Frisman, M. A. Sibileva and A. V. Krasnoperova, High Molecular Compounds (USSR), No. 3 (1959).

[22] É. V. Frisman and V. N. Tsvetkov, J. Exptl. and Theoret. Phys. (USSR) 23, 690 (1952).

[23] V. N. Tsvetkov, J. Polymer Sci. 23, 151 (1957).

[24] V. N. Tsvetkov and S. Ya. Magarik, Proc. Acad. Sci. USSR 115, 911 (1957).*

[25] C. Sadron, J. Phys. Radium 9, 381 (1938).

[26] H. Scheraga, J. Chem. Phys. 19, 983 (1951).

[27] V. N. Tsvetkov and É. V. Frisman, J. Phys. Chem. (USSR) 21, 261 (1947).

[28] Yu. Ya. Gotlib, J. Tech. Phys. (USSR) 28, 80 (1958).

Received March 27, 1959

---

* Original Russian pagination. See C.B. Translation.

THE MECHANISM OF ISOTOPIC EXCHANGE IN MOLECULAR HYDROGEN ON PLATINUM FILMS

Corresponding Member Acad. Sci. USSR
G. K. Boreskov, and A. O. Vasilevich

The L. Ya. Karpov Scientific-Research Institute of Physical Chemistry

Two possible mechanisms for the isotopic exchange of molecular hydrogen on solid catalysts, the adsorption-desorption (Bonhoffer-Farkas) and the chain (Rideol-Eley), have been discussed in a number of papers.

The first of these mechanism postulates that the exchange reaction

$$H_2 + D_2 \rightleftarrows 2HD$$

takes place through adsorption of the hydrogen molecules, followed by dissociation of the molecules into atoms which then undergo a rearrangement on desorption. The chain mechanism represents the exchange as resulting from the interaction of hydrogen molecules with atoms which are already adsorbed on the catalyst surface.

The present work is an attempt to elucidate the possibility of the second of these mechanisms through direct measurements on the rate of isotopic exchange between molecular hydrogen and hydrogen adsorbed on a platinum surface, comparison being made with the rate of isotopic exchange in molecular hydrogen. Similar studies with deuterium have been carried out by Eley [1] (on tungsten), by G. Schuit and his co-workers [2] (on nickel), and by A. and L. Farkas [3] (on nickel, palladium and platinum). The exchange rate of hydrogen chemisorbed on W and Ni proves to be of the same order as the rates of para-ortho transformation and isotopic exchange in molecular hydrogen. These latter rates are lower in the case of Pd and Pt.

We used radioactive hydrogen to increase the accuracy of the determination of the exchange rate. This permitted observation of differences in the rates of exchange in the hydrogen adsorbed on various portions of the surface, permitting an appraisal of the nonuniformity of the platinum surface with respect to the value of the activation energy of this process by the method developed in the papers of N. P. Keir [4], S. Z. Roginskii [5], and R. P. Eischens [6].

These measurements were carried out in the apparatus which is sketched in Figure 1. The platinum film was formed through vacuum evaporation of a platinum wire. The surface of this film was measured from the adsorption of krypton and hydrogen at the temperature of liquid air. The number of adsorbed hydrogen atoms was found to be approximately the same as the number of platinum atoms in the surface. In studying the exchange, tritium was first deposited on the platinum film until the surface was almost completely covered; protonium at a pressure of 0.1 mm of Hg was then introduced into the reaction vessel and the increase in the radioactivity of the gas was measured with an internally filled counter from which small portions of the gas were periodically removed. Measurements of the rate of isotopic exchange between molecular hydrogen and deuterium were carried out on this same film and under these same conditions. The exchange rate was calculated from the variation in the thermal conductivity determined with platinum filament lamps.

Figure 2 shows the results of measurements on the rate of exchange of chemisorbed tritium with molecular protonium at 90° K. The exchange rate diminishes rapidly with an increase in the percentage exchange. The exchange proceeds so rapidly at 162°K that its rate can not be determined.

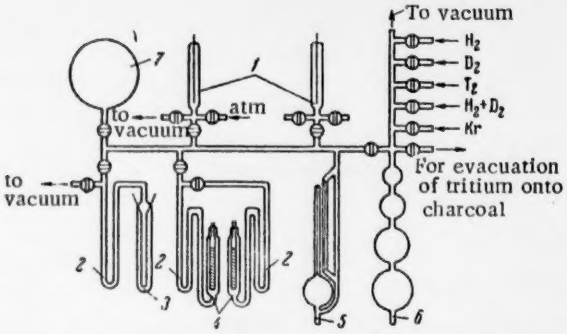

Fig. 1. Diagram of apparatus: 1) chamber for the analysis of tritium; 2) traps, cooled with liquid nitrogen; 3) reaction vessel; 4) lamps for the analysis of deuterium; 5) McLeod gauge; 6) burette; 7) ballast volume.

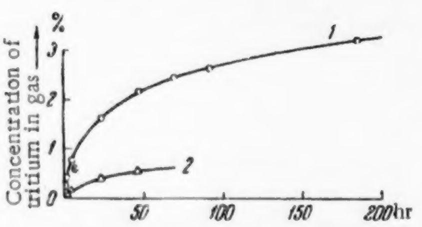

Fig. 2. The rate of exchange of chemisorbed tritium with molecular hydrogen at a temperature of 90° K: 1) rate of exchange after introduction of tritium; 2) rate of exchange on the same film after replacement of the gas by pure protonium.

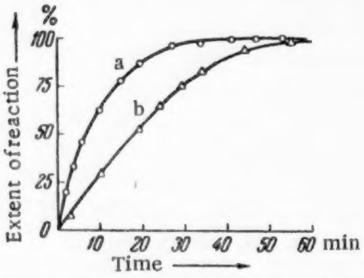

Fig. 3. The rate of isotopic exchange between molecular H_2 and D_2: a) at 78° K, b) at 90° K.

The results obtained from measurements on the rate of exchange of molecular H_2 and D_2 on this same film at 78, and 90° K, are shown in Figure 3. The reaction is of 0.5 order with respect to the hydrogen pressure. The energy of activation is approximately 1200 cal/mole. The specific catalytic activity of this film was approximately the same as that of other platinum catalysts which had been studied earlier [7].

Comparison shows the rate of exchange between H_2 and D_2 at 78° K to be 1200 times greater than the rate of exchange between molecular hydrogen and adsorbed hydrogen under the same conditions, even in the initial stage of the reaction. From this it follows that the bulk of the hydrogen which is adsorbed on the platinum at the temperature of liquid air does not participate in the exchange between the hydrogen molecules.

It is necessary to determine the separation coefficient for the isotopes in adsorption,

$$\alpha = \frac{C'(1-C)}{C(1-C')},$$

if the kinetics of the isotopic exchange between adsorbed hydrogen and molecular hydrogen is to be elucidated. Here, C is the fraction of tritium in the hydrogen of the gaseous phase and C' is the same fraction as measured on that portion of the surface which comes into equilibrium with the molecular hydrogen.

The value of α was determined by replacing the hydrogen in the reaction vessel with pure protonium once a definite percentage exchange, S, had been reached and then once more measuring the increase in the radioactivity.

A comparison of the rates of increase of the activity over various time intervals in the first, and the second, fillings showed that the coefficient of separation, α, had the values, ~ 8 at 78° K, and ~ 6 at 90° K.

These values were used to determine the rate of exchange of the adsorbed hydrogen, and the energy of activation of the exchange, as functions of the percentage exchange, S (Fig. 4).

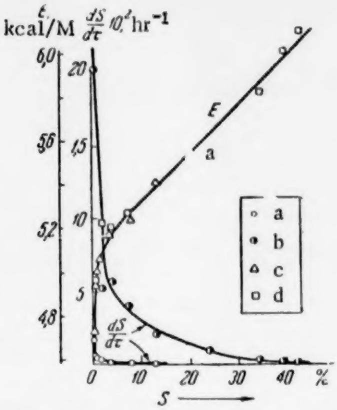

Fig. 4. The relation between the rate of isotopic exchange of chemisorbed tritium with molecular hydrogen, the energy of activation, and the percentage exchange, S: a) dS/ dτ , at 78°K; b) dS/ dτ , at 90°K; c) E, at 78°K; d) E, at 90° K .

Over the major portion of the surface, the energy of activation of exchange increases linearly with the percentage exchange, just as would be expected with the so-called uniform inhomogeneity. Extrapolation of this linear segment to the entire surface gives an energy of activation of approximately 2100 cal / mole. The energy of activation at the beginning of this segment is 5200 cal/mole. The energy of activation falls off sharply when the percentage exchange is very low (less than 1.0%).

The rate of exchange proves to be independent of the hydrogen pressure. From this it can be concluded that the exchange proceeds through a desorption mechanism and that it does not result from an interaction between the molecular hydrogen and the adsorbed hydrogen.

This fact lends weight to the supposition that the exchange between hydrogen molecules also proceeds through an adsorption—desorption mechanism. At low temperatures (78-90°K), this reaction takes place rather rapidly over the very small portion of the surface on which the energy of binding of the adsorbed hydrogen atoms is approximately one-half of the binding energy of the molecular hydrogen and the heat of adsorption of the hydrogen is quite low. The energies of activation for adsorption and desorption are not large on such sectors and Figure 4 shows their contribution to diminish markedly as the activation energy falls. As a result of the low value of the heat of adsorption, that portion of the surface on which isotopic exchange in molecular hydrogen proceeds through an adsorption–desorption mechanism is only partially covered. The rate of exchange on this portion of the surface is dependent on the hydrogen pressure and the order of the exchange reaction is approximately 0.5.

These results agree with the data on the temperature dependence of the rate of isotopic exchange in molecular hydrogen on platinum catalysts which were obtained earlier in this laboratory. The energy of activation is approximately 7.5 cal/mole at temperatures above 273°K and falls to 0.5-1 cal/ mole at lower temperatures. At the same time, the value for the frequency factor is five orders less than it would be if the reaction were to take place over the entire surface of the catalyst.

This is explained by the fact that differences in the energy of activation for desorption of hydrogen at high temperatures do not lead to significant differences in the rate of isotopic exchange on the various portions of the catalyst surface. Thus, there is only a 2-3 fold change in the rate of reaction at 500°K over the range of linear variation of the activation energy. The rate of reaction is two orders higher over the sectors of minimum activation energy, but these sectors represent such a minute fraction of the whole surface that they make practically no contribution to the observed reaction rate. On the other hand, the reaction on the principal part of the surface becomes infinitesimally slow at temperatures as low as 78°K, the rate being only 10^{-9} of that on the sectors of minimum activation energy. The observed rate is then fixed by the reaction occurring on these latter sectors. From this it follows that the change in activation energy which is observed when the temperature is diminished is itself the result of a transfer of the reaction to the principal portion of the surface. The nature of this portion of the surface is determined by the presence of added substances, by the adsorption of other gases, by the non-uniform distribution of the adsorbed atoms on the surface, etc. It is most reasonable to assume that the exchange on these sectors is analogous to the high-temperature exchange on the remaining portion of the surface and that it therefore follows an adsorption—desorption mechanism; this does not preclude the possibility that the reaction also proceeds through the formation of more involved active complexes . At the higher temperatures, the surface of a platinum film is practically homogeneous with respect to the reaction of isotopic exchange in molecular hydrogen.

LITERATURE CITED

[1] D. D. Eley, Proc. Roy. Soc. A178, 452 (1941).

[2] G. G. Schuit, N. H. de Boer, et al., Chemisorption, p. 39 (London, 1957).

[3] A. Farkas and L. Farkas, J. Am. Chem. Soc. 64, 1594 (1942).

[4] N. P. Keir, Problems of Kinetics and Catalysis 8, 224 (1955); 9, 283 (1957) [In Russian].

[5] S. Z. Roginskii, The Theoretical Principles of Isotopic Methods for the Study of Chemical Reactions (In Russian), Acad. Sci. USSR Press. p. 525 (1956); Problems of Kinetics and Catalysis 9, 5 (1957).

[6] R. P. Eischens, J. Am. Chem. Soc. 74, 61 (1952).

[7] M. A. Avdeenko, G. K. Boreskov, and M. G. Slin'ko, Problems of Kinetics and Catalysis 9, 61 (1957).

Received May 23, 1959

TUNNEL TRANSFERS BETWEEN SYSTEMS DESCRIBED BY MORSE POTENTIAL CURVES

V. I. Gol'danskii

The P. N. Lebedev Institute of Physics of the Academy of Sciences, USSR

(Presented by Academician V. N. Kondrat'ev, April 11, 1959)

In treating the role of the tunnel effect in the kinetics of chemical reactions (see, for example, [1,2]) it is customary to assume a Maxwellian distribution of relative translational velocities over the reacting molecules. At the same time, the contribution arising from the tunnel effect can prove to be essentially dependent on the initial distribution of energy, especially at low temperatures where this contribution is quite marked. Thus a solution of the problem of the tunnel effect in a system having a quantized distribution of energy is of considerable interest. The tunnel transfer of a system from a state described by one Morse potential curve into a state described by a second such curve could serve as the most simple instance of case of this kind. In evaluating the role of such transfers, we will here consider the simplest case of the superposition of two identical and intersecting Morse potential curves (Fig. 1).

$$\begin{aligned} U_1 &= D\left\{\left(1-\exp\left[-\alpha\frac{r-r_0}{r_0}\right]\right)^2-1\right\}, \\ U_2 &= D\left\{\left[1-\exp\left[-\alpha\frac{(R-r)-r_0}{r_0}\right]\right]^2-1\right\}, \end{aligned} \tag{1}$$

where D is the energy of dissociation; $\underline{r}$ is the variable coordinate; r_0 is the equilibrium distance corresponding to the minimum potential energy on each of the curves; $R-2r_0$ is the distance between the minima on the two curves; $\alpha = 2\pi\nu_0\sqrt{I_0/2D} = 2\pi\nu_0 r_0\sqrt{\mu/2D}$; ν_0 is the characteristic frequency of vibration; I_0 is the moment of inertia; and μ is the reduced mass of the system.

The total potential curve, $U_{tot} = U_1 + U_2$, has the form

$$U_{tot} = D\left\{\left(1-\exp\left[-\alpha\frac{r-r_0}{r_0}\right]\right)^2+\left(1-\exp\left[-\alpha\frac{(R-r)-r_0}{r_0}\right]\right)^2-2\right\}. \tag{2}$$

A potential barrier arises only when the point of intersection of the two Morse curves lies beyond the point of inflection, r_1, for which $\frac{d^2(U/D+1)}{dr^2} = 0$. From this it follows that the conditions for the appearance of the barrier is

$$\frac{R}{2} \geqslant r_0\left(1+\frac{\ln 2}{\alpha}\right) \quad \text{or} \quad \alpha\left(\frac{R/2-r_0}{r_0}\right) = \alpha b = K \geqslant \ln 2.$$

In the general case, the expressions for the coordinates of the minima on the total potential curve, and for the height of the barrier, $U = U_{tot} - (U_{tot \cdot min})$, with respect to these minima, prove to be quite complex.

When, however, $K \geqslant 2$, it can be assumed, to a sufficiently good degree of approximation, that these minima on the total potential curve are located at $r = r_0$ or $R-r = r_0$, so that

$$\begin{aligned} U \approx D\Big\{&\left(1-\exp\left[-K\frac{r--r_0}{d}\right]\right)^2+ \\ &+\left(1-\exp\left[-K\frac{(R-r)-r_0}{d}\right]\right)^2-(1-\exp[-2K])^2\Big\}, \end{aligned} \tag{3}$$

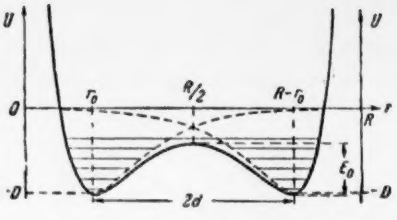

Fig. 1. $\alpha = 1.5; b = \frac{R/2-r_0}{r_0} = 1.5$; $K = \alpha b = 2.25$.

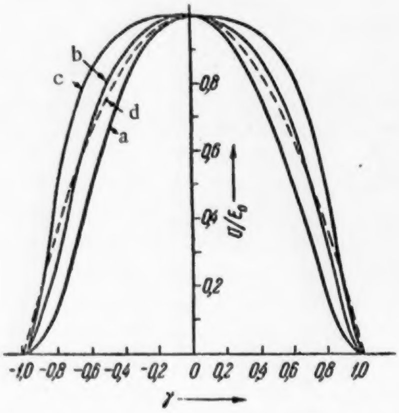

Fig. 2. a) K = 2; b) K = 4 ; c) K = 6; d) parabola.

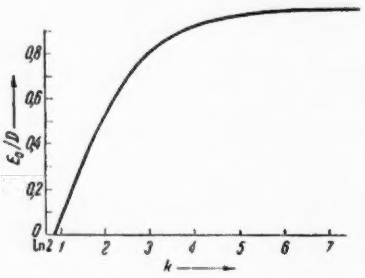

Fig. 3.

where d= R/ 2-r_0 is the half-width of the barrier at its base. In this case, the height of the barrier in the center (r = R/2) is approximately equal to

$$E_0 \approx D\{2(1-e^{-K})^2-(1-e^{-2K})^2\}, \qquad (4)$$

and the barrier form is described by the relation

$$\frac{U}{E} \approx \frac{(1-2e^{-K}\operatorname{ch}K\gamma)^2-e^{-4K}}{2(1-e^{-K})^2-(1-e^{-2K})^2}, \qquad (5)$$

where $\gamma = \frac{1}{K}\frac{R/2-r}{R/2-r_0}$ (on the base of the barrier, γ varies from -1 to +1; at the peak, $\gamma = 0$).

In Figure 2, barriers are plotted for which K = 2, 4, or 6 and, also, a parabolic barrier. In Fig. 3, the $E_0/D = f(K)$ relation which follows from (4) is shown.

The superposition of the second potential curve leads to a splitting of the level for the quantized distribution of the initial system with respect to energy, such that (see [3]) in the n-th vibrational level with the energy $E_n = \epsilon_n D$, this splitting amounts to

$$\Delta E = \varepsilon_n \frac{D}{\pi}\exp\left\{-2K\frac{D}{h\nu_0}\int_{-\gamma_n}^{+\gamma_n}\sqrt{\frac{U}{D}-\varepsilon_n}\,d\gamma\right\}, \qquad (6)$$

where

$$\gamma_n = \frac{1}{K}\operatorname{Arch}\left\{\frac{1}{2}e^{K}[1-\sqrt{\varepsilon_n+e^{-4K}}]\right\}. \qquad (7)$$

Thus, the probability of a tunnel transfer is determined by an exponential whose exponent,

$$C = -2K\frac{D}{h\nu_0}\int_{-\gamma_n}^{+\gamma_n}\sqrt{(1-2e^{-K}\operatorname{ch}K\gamma)^2-e^{-4K}-\varepsilon_n}\,d\gamma = -K\frac{1}{2x_e}I, \qquad (8)$$

is to be evaluated through numerical integration.

For Morse curves, the relation

$$D/h\nu_0 = {}^1\!/_4\, x_e = {}^1\!/_2\,(1+n_{\max})$$

in which x_e is the anharmonicity constant of the vibrations and $n_{\max}$ is the number of the highest vibrational level, is valid. It is to be noted that the problem of tunnel transfer under a Maxwellian distribution [2] is completely determined by three energy quantities; the barrier height, E_0; the characteristic energy of the system, $\epsilon = \hbar^2/\mu d^2$, a function of the width of the barrier; and the thermal energy, kT. From these three quantities there can be formed the two dimensionless parameters E_0/kT and E_0/ϵ. In a consideration of the temperature dependence of tunnel transfers in a system with a quantized distribution of energy, it is necessary to introduce a new quantity, the energy of the characteristic vibrations, $h\nu_0$. For each given level, the tunnel transfer is now fixed by the ratios D/ν_0 and D/ν_0, since $K = \frac{h\nu_0}{D}\frac{1}{\sqrt{2}}\sqrt{\frac{D}{\varepsilon}}$. The averaging of these data, taking into account the statistical weights of the various levels, leads to the ratio $h\nu_0/kT$, a third dimensionless parameter which is indispensable to the consideration of the problem at hand.

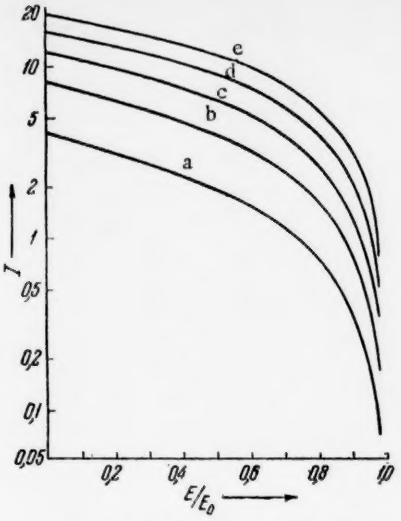

Fig. 4. a) K= 2; b) K = 3; c) K = 4 ; d) K = 5 ; e) K = 6 .

For use in calculations based on (8), Figure 4 presents values of the integral I for K equal to 2, 3, 4, 5 and 6, and for E/E_0 values ranging from 0 to 1 .

Without stopping here on numerical examples, we will note just one more detail in conclusion. As has been shown in [2], for any potential barrier which at the peak can be described by a parabola, there exists a definite characteristic temperature, $T_q = \hbar\sqrt{E_0}/k\pi d\sqrt{2\mu}$, below which the velocity constant for tunnel interaction begins to predominate exponentially over the "Arrhenius" constant for reaction above the barrier. A Maxwellian distribution of velocities over the interacting particles is supposed here.

In the case under consideration, where the reacting system is characterized by a quantized distribution of energies, the solution in its general form is reasonably complex. On the other hand, it can be shown that the characteristic temperature introduced above will retain its sense even for a quantized distribution of energy in the simplified case of a parabolic barrier (which is a reasonably good approximation to the barrier formed by the superposition of two Morse curves) if the anharmonicity constant is neglected.

In actuality, when the barrier is of height E_0 and $(n+{}^1/_2)\,h\nu_0 < E_0 < (n+{}^3/_2)\,h\nu_0$, the velocity constant for the reaction is proportional to

$$Z \sim \left(1-\exp\left[-\frac{h\nu_0}{kT}\right]\right)\sum_{l=0}^{n}\exp\left[-l\frac{h\nu_0}{kT}\right]\exp\left[-a\left(1-(l+{}^1/_2)\frac{h\nu_0}{E_0}\right)\right]+ \\ +\exp\left[-(n+1)\frac{h\nu_0}{kT}\right], \qquad (9)$$

where $a = \pi\sqrt{2}\sqrt{E_0/\varepsilon}$, the first term being the tunnel member and the second, that due to reaction above the barrier.

As has been shown in [1,2], the dominance of tunnel interaction with a parabolic relation corresponds to essential invariance of the velocity constant under further reduction of the temperature. From Equation (9) it is not difficult to see that such an invariance of Z with temperature corresponds to an exponential predominance of the contribution from the null level, i. e. , to the condition

$$a\left[1-\frac{1}{2}\frac{h\nu_0}{E_0}\right] < \frac{h\nu_0}{kT} + a\left[1-\frac{3}{2}\frac{h\nu_0}{E_0}\right] \quad \text{or} \quad kT < \frac{E_0}{a},$$

which is equivalent to the above-introduced expression for T_q. It can thus be considered that the criterion proposed earlier [2] to characterize (within the framework of the one-dimensional problem) the limits of the temperature interval within which the tunnel effect plays a predominant role is a sufficiently general one and that it retains its force even for a quantized distribution of energies.

The author wishes to express his thanks to D. G. Knorre and to N. D. Sokolov for discussion of this work.

LITERATURE CITED

[1] R. P. Bell, Proc. Roy. Soc. (A) 139, 466 (1933); 148, 241 (1935); 158, 128 (1937).

[2] V. I. Gol'danskii, Proc. Acad. Sci. USSR 124, 1261 (1959).*

[3] L. D. Landau and E. M. Lifshits, Quantum Mechanics (in Russian), Moscow (1948).

---

* Original Russian pagination. See C.B. Translation.

Received April 1, 1959

A POLAROGRAPHIC STUDY OF THE STEREOISOMERIC TRANSFORMATIONS OF CERTAIN SEMI-, AND THIOSEMICARBAZONES IN SOLUTION

Yu. P. Kitaev, G. K. Budnikov and Academician A. E. Arbuzov

The A. E. Arbuzov Institute of Chemistry of the Kazan Branch of the Academy
of Sciences of the USSR

There is rather extensive literature on the problems of stereoisomerism in the nitrogen-containing derivatives of the carbonyl compounds. Many instances of the formation of stereoisomeric pairs of oximes, hydrazones, and arylhydrazones have been noted. The literature contains, however, little information on the stereoisomerism in the semi-, and thiosemicarbazones. Attempted separations of the isomers of the semicarbazones of certain aromatic-aliphatic ketones through irradiation of their chloroform solutions with ultraviolet light have met with failure because of molecular breakdown [1]. It is interesting to note that, in certain cases, differences exist in the values of the melting points of the individual semicarbazones and thiosemicarbazones as these appear in various sources [2-4]. In such cases, it is clear that the melting point is not that of an individual compound, but rather, of a mixture of isomers, the composition of which obviously depends on the method of separation of the semi- and thiosemicarbazones.

Brockman and Pearson [5] have studied the polarographic reduction of isomeric pairs of the semicarbazones of the benzophenones. These authors have found that there is only a very insignificant difference in the half-wave potentials of the stereoisomers in this case.

Thus it is that the study of the stereoisomerism of the semi- and thiosemicarbazones has been far from adequate, and we, for this reason, have decided to investigate systematically the stereoisomeric transformations in these classes of compounds. The results which have been obtained through a polarographic study of the transformations of certain semi-, and thiosemicarbazones are presented in the present work.

The semi-, and thiosemi-,carbazones of methylethyl ketone, diethyl ketone, cyclopentanone, cyclohexanone, benzaldehyde, and acetophenone, and the thiosemicarbazone of para-isopropylbenzaldehyde (kutizone) were studied in 20% methyl alcohol—water solutions at pH 5.7 under irradiation from the ultraviolet light from a PRK-2 quartz lamp. A phosphate buffer served as background; the concentration of each investigated compound was $\sim 10^{-3}$ mole/liter. This study was carried out on a Geirovskii system LR-55 photorecording polarograph.

Since we have shown [6] that the semi- and thiosemicarbazones of the aliphatic ketones and aldehydes and the alicyclic ketones in water—alcohol solution gave the enesemi-, and the enethiosemi-,carbazone structures, stereoisomerism, of the derivatives of methylethyl and diethyl ketone could be anticipated on the basis of difference in the positions of the substituents with reference to the $>C=C<$ bond. This type of transformation was not, however, observed in these derivatives.

On the other hand, stereoisomeric transformation proceeds with relative ease in an alicyclic series. On irradiation of solutions of these compounds, a new wave with a more positive value of $E_{1/2}$ appears on the polarogram; the height of this wave increases with an increase in the period of irradiation.

The thiosemicarbazone of cyclopentanone is an exception to this statement, since this compound decomposes under irradiation. The polarogram of a solution of the semicarbazone of cyclohexanone is given in Figure 1.

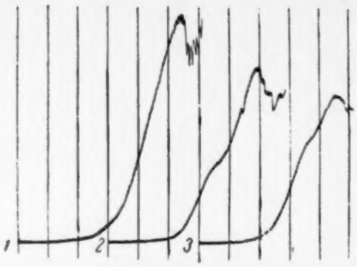

Fig. 1. One division on the axis of abcissas = 200 mv; curves originate at 0.7 v; sensitivity 1/300 (mean current sensitivity of galvanometer, $3.1 \cdot 10^{-9}$ amp/mm); time of irradiation; 1) 0 hours, 2) 5 hours, 3) 8 hours.

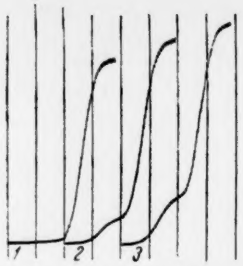

Fig. 2. One division on the axis of abscissas = 200 mv; curves originate at 0.7 v; sensitivity 1/100; solution contains 0.3 M/liter thiosemicarbazone; time of irradiation; 1) 0 hours, 2) 5 hours, 3) 9 hours.

TABLE 1

Compound	$E_{\frac{1}{2}}$, v		Energy of sterioisom. transform. kcal/m.
	of labile form	of stable form	
Semicarbazone of cyclopentanone	1,27	1,52	11,5
Semicarbazone of cyclohexanone	1,28	1,54	12,0
Thiosemicarbazone of cyclohexanone	1,23	1,46	10,6
Thiosemicarbazone of benzaldehyde	0,93	1,17	11,0
Semicarbazone of acetophenone	1,03	1,26	10,6
Thiosemicarbazone of acetophenone	0,95	1,24	13,4
Kutizone	1,05	1,22	8,3

The appearance of the second wave on the polarogram, and the increase in the height of this wave with an increase in the period of irradiation are the results of the production of lal forms. With the cyclic derivatives, isomerizaton clearly resul from the situation of the substituents, either on the same side c on opposite sides of the ring:

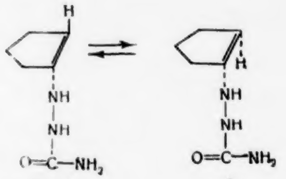

trans cis

A similar situation is observed in regard to the polarograms which are obtained on irradiating solutions of the derivatives of the aromatic series, where the formation of stereoisomeric pairs is explained by the presence of the

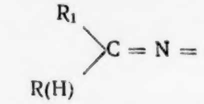

$$\begin{matrix} R_1 \\ \quad \rangle C = N = \\ R(H) \end{matrix}$$

group in the molecule. A polarogram of a solution of the thiosemicarbazone of acetophenone is presented in Figure 2.

The appearance of a new wave is not observed on irradiating a solution of the semicarbazone of benzaldehyde; here it is clear that the difference in the half-wave potentials is not great and, as a result of the superposition of two waves, a single wave, corresponding to a mixture of isomers is observed on the polarogram, this being indicated by the alteration of the $E_{1/2}$ value in the course of the irradiation of the solution.

Table 1 presents the values which we have found for the half-wave potentials of the stereoisomers (with respect to the saturated calomel electrode) and the values of the energy change accompanying transfer between isomers, as calculated from these potentials.

It should be noted that the values of the energy of the cis-trans transformations are more or less approximate in the case of the alicyclic series, since the reduction of these derivatives on the dropping mercury electrode is irreversible. On the other hand, the reduction of the semicarbazones and the thiosemicarbazones of the aromatic series is very nearly reversible.

It is understood that polarographic data alone are inadequate for distinguishing the structures of the stereoisomers, although, in conjunction with chemical and physical methods, polarography can solve even this problem. In the present work, we have used polarography to detect the formation of labile isomers during the irradiation of the stable forms of semi-, and thiosemicarbazones in weakly acidified water—alcohol solution. As a rule, these labile forms are cis (or trans), but exceptions are known so that a further investigation of the structures of the stereoisomers of these classes of compounds is called for.

It is striking that the stereoisomeric transformations of the semi-, and the thiosemicarbazones, in water-alcohol solutions are less characteristic than is the case with the arylhydrazones which we have studied earlier [7-9], also by the polarographic method. It is exactly in this point that the derivatives of the aliphatic series differ.

LITERATURE CITED

[1] F. Wilson and R. Macaulay, J. Chem. Soc. 125, 841 (1924).

[2] Chemistry and Medicine, Thiosemicarbazones (a collection of articles under the editorship of G. N. Pershin), (Moscow, 1954)*.

[3] Dictionary of Organic Compounds, Foreign Lit. Press. (1949).*

[4] Handbook of Chemistry 2, p. 293 (Moscow, 1951).

[5] R. Brockman and D. Pearson, J. Am. Chem. Soc. 74, 4128 (1952).

[6] Yu. P. Kitaev, G. K. Budnikov and A. E. Arbuzov, Proc. Acad. Sci. USSR 127, No. 4 (1959).**

[7] A. E. Arbuzov and Yu. P. Kitaev, Proc. Acad. Sci. USSR 113, No. 3, 577 (1957).***

[8] Yu. P. Kitaev and A. E. Arbuzov, Bull. Acad. Sci. USSR, Div. Chem. Sci. No. 9, 1037 (1957).***

[9] A. E. Arbuzov and Yu. P. Kitaev, Bull. Kazan Branch, Acad. Sci. USSR, Chem. Ser. No. 3, 3 (1957).

Received May 22, 1959

---

* In Russian.

** See C.B. Translation.

*** Original Russian pagination. See C.B. Translation.

PARAMAGNETIC RESONANCE IN SOLUTIONS OF COMPLEX COPPER SALTS

B. M. Kozyrev and A. I. Rivkind

The Kazan Branch of the Academy of Sciences of the USSR

(Presented by Academician A. E. Arbuzov June 8, 1959)

Paramagnetic resonance spectra of solutions containing the acetylacetonate, nitrate, ethanolamine, and diethanolamine complexes of Cu (II) have been studied at the frequencies ν_1 = 9392 Mc and ν_2 = 1569 Mc. The nitrate, $Cu(NO_3)_2 \cdot 3H_2O$, served as the starting point in the preparation of these solutions. At the frequency ν_1, these spectra were similar to those observed by McGarvey [1] in the case of the complexes of copper with acetylacetone and its derivatives. Figure 1, a and b, gives spectra obtained at the frequency ν_1 with 0.15 molar solutions of the acetylacetonate (1a) and the nitrate (1b), complexes in dioxane. On passing to the frequency ν_2, these spectra alter radically (Figure 1, c and d); the outer hyperfine lines become less intense than the two center lines, and the spectra prove to be better resolved and more symmetrical. Qualitatively, these effects can be readily explained on the basis of the relaxation theory of McConnell[2], according to which the terms $\Delta g \beta H_0$ and bI_Z make contributions to the width of the hyperfine components, $\Delta \nu$; here $\Delta g = g_{\|} - g_{\perp}$, β is the Bohr magneton, H_0 is the resonance value of the external magnetic field, b = A - B is the coefficient of nuclear anisotropy, and I_Z is the nuclear spin magnetic quantum number. The McConnelltheory describes the observed asymmetric spectra at the frequency ν_1 (Fig. 1, a and b) when it is assumed that $\Delta g \beta H_0$ and b are of approximately the same order of magnitude. The contribution to the line width arising from anisotropy in the g-factor becomes small when H_0 diminishes by a factor of 1/6 ($\nu_1/\nu_2 \sim 6$), and the relaxation must then be determined principally by the hyperfine interactions of the ion.

In this case, it is obvious that the theory of [2] would predict a more symmetrical spectrum with outer components ($I_Z = \pm 3/2$) widened with respect to the middle ones ($I_Z = \pm 1/2$), just as is actually observed experimentally. Values of the g-factors for thehyperfine components of the spectra which have been investigated, as obtained at the frequency ν_1 with an accuracy ~ 1 % are compiled in Table 1.

Our values of the g-factors of the acetylacetonate complex in dioxane are essentially larger than those reported by McGarvey [1]. In addition, all four components of the spectrum were resolved on the 3 centimeter spectrometer of [1], whereas in our own case it proved possible to fully resolve only the first two lines corresponding to $I_Z = -3/2$ and 1/2 at $\lambda \sim 3$ cm (frequency ν_1) (Figure 1 a), a fact which points to a greater width of the hyperfine components.

This situation could arise only from the existence of structural differences between the acetylacetonate complexes which were studied in [1] and those which we have investigated. It is clear that there entered into the coordination sphere of our complexes not only acetylacetone, but also molecules of the water of crystallization of the $Cu(NO_3)_2 \cdot 3H_2O$ from which the solutions were prepared. The solutions of [1] were obtained directly from solid copper acetylacetonate, and the inclusion of water was thus avoided. The presence of the electric dipoles of the water molecules in the inner sphere of the complexes would result in an increase in the anisotropy of the g-tensor and this, in turn, would lead to: 1) an increase in the effective g-factors of the spectral lines, and 2) an increase, according to the McConnell theory, in the width of the hyperfine components. Both of these effects actually appeared in our measurements.

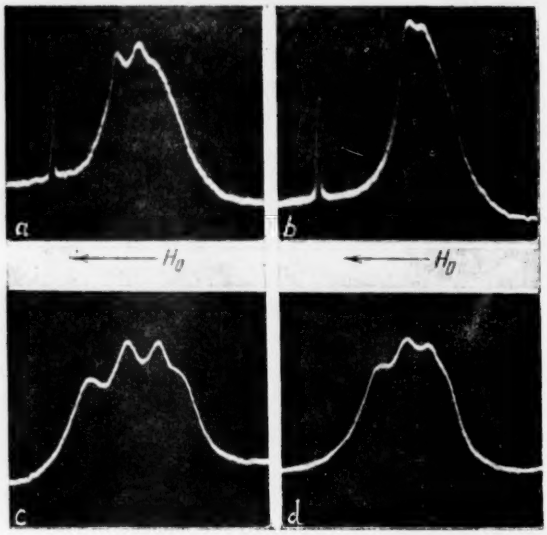

Fig. 1. Paramagnetic resonance spectra in solutions of complex copper (II) salts: a) copper acetylacetonate complex in dioxane, solution concentration, 0.15 M/liter, $\nu = \nu_1 = 9392$ Mc; b) 0.15 molar solution of $Cu(NO_3)_2 \cdot 3H_2O$ in dioxane, $\nu = \nu_1 = 9392$ Mc; c) the same, with the frequency of the oscillating field, $\nu = \nu_2 = 1569$ Mc; d) the same, at the frequency $\nu_2 = 1569$ Mc. Curves a and b have been plotted with the same units of scale for the field H_0. The same is true of the curves c and d, although the field scales are different for the frequencies ν_1 and ν_2. The fine lines on the left of the spectra of the curves a and b are signals from the $\alpha\alpha$-diphenyl-β-picrylhydrazyl free radicals.

TABLE 1

Values of the g-Factors for the Component of the Hyperfine Structure at the Frequency $\nu_1 = 9392$ Mc in Solutions of Complex Copper (II) Salts, T ~ 300° K

Complex	g_1	g_2	g_3	g_4
Acetylacetonate complex in dioxane	2,11	2,15	—	—
Nitrate complex in dioxane	2,16	2,19	—	—
Ethanolamine complex in water	2,04	2,09	2,14	2,19
Diethanolamine complex in water	2,05	2,10	2,15	2,19

Figure 1, b and c, shows that a nitrate complex is formed on dissolving the salt $Cu(NO_3)_2 \cdot 3H_2O$ in dioxane. This complex is broken down by further addition of 5-7% of water (to the body of the solution), and the line becomes homogeneous, being then approximately the same as that which is observed in aqueous, and in alcoholic, copper nitrate solutions where there are no anion complexes. The hyperfine-structure constant for the nitrate complex (~ 36 oersted) is smaller than that for the acetylacetonate complex by a factor of almost one-half. This points to instability in the nitrate complex, just as does the effect of the addition of water; with the weak bonding of the addenda to the central ion, the dynamic character of the Jahn-Teller effect becomes still more pronounced and this leads to a greater mean value for the constant for the hyperfine interaction. The influence of the time of correlation, τ_c, [2], on the form of the spectra was also studied. Additional electrical "friction" was produced in solution by the addition of diamagnetic ions. A marked increase in the asymmetry of the spectrum resulted from the addition of 4 M/liter of LiCl to a 0.15 molar aqueous solution of the ethanolamine copper complex. Similar additions of KCl and NaCl acted in the same direction, but much more weakly. This last is clearly connected with the fact that the magnitudes of the electrical ionic fields of Na^+ and K^+ are smaller than that of Li^+. There is an almost complete disappearance of the hyperfine structure in an alcoholic solution of the ethanolamine copper complex after adsorption on silica gel; this clearly results from the increase in the internal friction of the liquid which arises from the forces of adsorption. A second factor, however, is not to be excluded here; a marked alteration in the concentration of the complex which arises from differences in the degrees of adsorption of the complex, and of the solvent molecules, on the silica gel.

At a concentration of 1.2 mole/liter, an aqueous solution of the ethanolamine complex gives a single line at the frequency ν_1, the width of this line being 30-40% less than the full width of the hyperfine structure spectrum which is observed in more dilute solutions, a fact which would seem to point to the presence of exchange interactions. However, the interpretation of this effect is still not clear.

In conclusion, it can be said that the McConnell mechanism of relaxation in solution [2] proves to be more effective in the cases which we have investigated than does the mechanism which has been proposed by Al'tshuler and Valiev [3]. This probably results from the following fact. The second of these mechanisms supposes the existence of orbital levels which lie reasonably close to one another. This is actually the case in aqueous solutions of the $Cu(H_2O)_6^{2+}$ ions where the Al'tshuler- Valiev theory is fully confirmed. The principal part of the "crystal" field in such compounds as the nitrate complexes is undoubtedly noncubic the energy intervals between the orbital levels are large, and, as a consequence, the effectiveness of relaxation through normal vibrations of the complex is low. According to McGarvey [4], these intervals are also large in the complexes with acetylacetone. It is probable that the same is true in the other copper complexes which we have treated.

In conclusion, the authors express their thanks to K. A. Valiev for a discussion of this work.

LITERATURE CITED

[1] B. R. McGarvey, J. Phys. Chem. 60, 71 (1956).

[2] H. M. McConnell, J. Chem. Phys. 25, 709 (1956).

[3] S. A. Al'tshuler and K. A. Valiev, J. Exptl. Theoret. Phys. 35, vol. 4 (10), 947 (1958).

[4] B. R. McGarvey, J. Phys. Chem. 61, 1232 (1957).

Received April 4, 1959

THE TRANSFER OF THE ENERGY OF EXCITATION AND SENSITIZATION OF CHEMICAL REACTIONS DURING RADIOLYSIS OF SOLUTIONS OF AROMATIC AZO COMPOUNDS

V. A. Krongauz and Kh. S. Bagdasar'yan
The L. Ya. Karpov Scientific - Research Institute of Physical Chemistry

(Presented by Academician S. S. Medvedev, April 15, 1959)

Our earlier studies on the radiolysis of benzoyl peroxide in benzene solution [1,2] have disclosed a strong sensitization of the radiolytic breakdown of this compound . For example, the rate of decomposition of the peroxide at a concentration of 0.01 mole/ liter is twenty times greater than would correspond to the direct action of irradiation. In view of this pronounced departure of the rate of decomposition of benzoyl peroxide from the law of additivity, the transfer of energy from the solvent to the dissolved solute could be presumed to be an effective one.

Sensitized breakdown of benzoyl peroxide occurs when the solvent is of the aromatic type (benzene, styrene) and cannot be detected in solvents which are not aromatic (cyclohexane, ethylacetate) [1,3]. Radiolytic decomposition of the dissolved substances is not observed in the radiolysis of solutions of tertiary butyl peroxide, or dinitryl azobutyric acid [3, 4]. Since these compounds break down into radicals with about the same ease as does benzoyl peroxide, it can be concluded that the energy transfer is effective only if both components of the solution are aromatic substances. The mere presence of an aromatic ring in the molecule of one component is clearly not a sufficient condition to assure an effective energy transfer. For example, there is no energy transfer in a solution of benzoyl peroxide in chlorobenzene [5].

The rate of radiolysis of benzoyl peroxide in benzene solution is markedly decreased by the addition of small amounts of phenanthrene or anthracene [6]. Work on the sensitized fluorescence of solutions [7] has shown that such luminophores as phenanthrene and anthracene are effective acceptors of energy. It is clear that some of the excited benzene molecules transfer their energy to the luminophore molecules, so that these enter into competition with the peroxide molecules. It thus becomes possible to establish the relative ability (in comparison with the peroxide) of a compounds to absorb the energy of activation from a solvent by noting the relative diminution in the rate of radiolysis of benzoyl peroxide in the presence of this substance.

The radiolysis of solutions containing various aromatic compounds which involve the azo group has been investigated in the present work, the aim being to study the influence of the molecular structures of dissolved solutes on the effectiveness of the energy transfer, and the degree of utilization of the absorbed energy, in radiolytic decomposition reactions. Benzene solutions of phenylazotriphenylmethane (PATM), diazoaminobenzene (DAB), benzylphenyltriazine (BPT), and methylphenyltriazine (MPT) were studied. Since the energies of activation for the decomposition of PATM, BPT, and MPT do not exceed 30 kcal/mole, and that of DAB is clearly less than 40 kcal/mole [8-10], it would appear that a study of the kinetics of the breakdown of these compounds would be a very sensitive means for detecting a transfer of energy from the solvent to the dissolved solute.

Radiolysis was carried out under the action of the γ-radiation from Co^{60} in solutions which had been carefully freed of air. The dose strength was $2.5 \cdot 10^{18}$ ev/liter· sec. The initial decompositional yield per 100 ev of energy absorbed by the solvent, G_{tot}, was determined when the amount of the decomposed material did not exceed 10-20 % of that corresponding to the starting concentration. The concentrations of the azo compounds were measured on a SF-4 spectrophotometer before and after radiolysis. The rate of decomposition of the benzoyl peroxide was determined iodometrically.

Figure 1 shows the relation which exists between the radiational yield in the breakdown of PATM and the concentration of the latter in benzene. This figure indicates that the yield from the decomposition of the PATM at first increases quite rapidly; this continues up to a concentration of ~0.1 mole / liter, after which the yield increases more gradually and the concentration — yield relation becomes linear.

When calculated from the slope of the initial segment of the curve (OA) showing the radiational yield in the decomposition of PATM per 100 ev of energy absorbed by the PATM itself, G_{PATM} proves to be ~190 molecules. This figure is twice as large as the number of molecules (82) which would decompose if the energy taken up by the PATM were completely utilized in the breakdown. The thermal decomposition of PATM is not a chain reaction [8], so that this high value of G_{PATM} is clearly not due to secondary chain processes. It is obvious that there is a transfer of the excitation energy from the benzene to the PATM during radiolysis.

Comparison shows the curve of Figure 1 to be similar to the corresponding curve for benzoyl peroxide [1]. The transition to the more inclined linear portion of the curve occurs at the same concentration (~ 0.01 mole /liter) in each case.

On the basis of our earlier calculations [1], it can be concluded that each of those molecules which are excited at concentrations of ~ 0.01 mole / liter and are responsible for the energy transfer at low acceptor concentrations, will succeed in giving up its energy to the molecules of the dissolved solute. The further increase in the yield in decomposition with increasing acceptor concentration is in a large measure due to the direct action of the radiation.

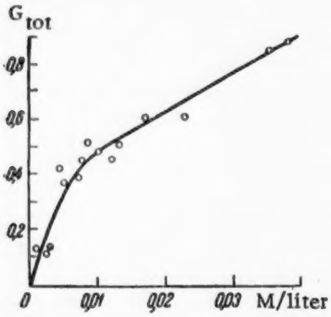

Fig. 1. The relation between the radiational yield in the breakdown of PATM and the concentration of the latter in benzene .

TABLE 1

The Effect of Added Substances on the Yield In the Decomposition of Benzoyl Peroxide in Benzene (Concentration of Peroxide and Azo Compounds, 0.01 mole/ liter)

Added substance	G_{tot}, benzoyl peroxide
Without addition	3±0,1
PATM	1,9±0,2
DAB	1,7±0,2
Dinitrylazoisobutyric acid	2,8±0,2
Azobenzene	3,2±0,2

A comparison of the G_{tot} value for the decomposition of PATM (section OA) with the G_{tot} value for benzoyl peroxide (at the same concentrations) shows the mean rate of radiolysis of PATM to be only one-seventh as large as that for the peroxide. This could be due to either a lowered effectiveness in the transfer of energy from the benzene to the PATM, or to a less effective utilization of the energy absorbed by the PATM in undergoing decomposition.

In order to clear up this point , the radiational yield in the decomposition of a 0.01 M solution of benzoyl peroxide in benzene was determined in the absence of PATM. Table 1 shows that equimolar addition of PATM up to ~ 40 % lowers the rate of radiolysis of the peroxide. Thus, PATM is almost as effective an acceptor of energy as benzoyl peroxide. It follows that the low yield in the decomposition of the PATM as compared with benzoyl peroxide is due to a smaller probability for the decomposition of the excited PATM molecule compared with the benzoyl peroxide molecule.

DAB does not decompose with a measureable rate during radiolysis of benzene solutions of this compound. On the other hand, the rate of radiolysis of benzoyl peroxide in 0.01 molar solution can be reduced by almost one-half by the addition of an equimolar amount of DAB (Table 1) . DAB is therefore just as effective an acceptor of energy as the peroxide, although the energy which it absorbs is dissipated without leading to the breakdown of the molecule.

It is not very likely that the PATM and DAB could quench the excited peroxide molecules since this process could not compete with the dissociation of the excited peroxide molecules into radicals, a reaction which is completed in a period of the order of 10^{-13} seconds.

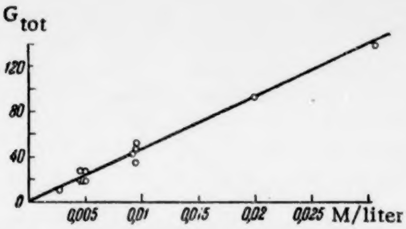

Fig. 2. The relation between the radiational yield in the cis-transisomerization of azobenzene and the concentration of the latter in benzene. The circles designate the yield in the isomerization of azobenzene in the presence of 0.01 mole per liter of benzoyl peroxide.

TABLE 2

The Rate of Cis-Trans Isomerization of Azobenzene in Various Solvents (initial concentration of cis-azobenzene, 0.01 mole/liter)

Solvent	G_{tot}	Radiational yield of primary free radicals from solvent
Benzene	44,2	0,75 (1)
Styrene	7,4	0,52 (3)
Cyclohexane	292	6,4 (1)
Carbon tetrachloride	697	9

Solutions of BPT and MPT in benzene undergo practically no decomposition during γ-irradiation (G_{tot} for 0.01 M solution, < 0.1). The effect of additions of these compounds on the rate of radiolysis of solutions of benzoyl peroxide could not be studied since these substances interact with the peroxide to give brightly colored products.

It is characteristic that the earlier-studied [3,4] dinitrylazobutyric acid and tertiary butyl peroxide do not protect the peroxide in radiolysis.

Table 1 shows azobenzene to be the simplest of the aromatic azo compounds which fail to protect the peroxide from breakdown. There is practically no decomposition of azobenzene during irradiation of a benzene solution of this compound (G_{tot} for a 0.01 M solution, < 0.1). It should also be noted, however, that there is no thermal breakdown of azobenzene in solution, since this substance differs from the other azo compounds which we have studied by being very stable. It was of interest to investigate the possibility of a radiational cis-trans isomerization in azobenzene. This reaction is known to occur in solutions which are acted on by radiation from the region of natural absorption of the compound azobenzene. Experiment shows that radiational cis-trans isomerization of azobenzene does not take place in benzene solution.

The cis-trans isomerization of azobenzene is known to require no more than 23 kcal / mole [11] and this reaction can therefore be used for detecting a transfer of energy from the excited benzene molecules to the molecules of azobenzene. Experiments which we have carried out show that this radiational cis-trans isomerization proceeds very rapidly at a rate which is proportional to the concentration of the cis-azobenzene (Fig. 2). All of the compound goes over into the trans-form when irradiation is continued long enough.

The cis- trans isomerization is clearly not related to a transfer of the energy of excitation from the solvent to the dissolved solute, even through it proceeds much more rapidly than would correspond to the direct action of the radiation on the azobenzene. The addition of azobenzene is actually without influence on the rate of radiolysis of the benzoyl peroxide and, in turn, the addition of benzoyl peroxide does not affect the rate of the isomerization of azobenzene (Fig. 2). The fact that the isomerization proceeds only in the direction of the formation of the more stable trans-form also indicates that the reaction does not involve a transfer of the energy of electronic excitation to the azobenzene. A definite photostationary state between the cis- and the trans- isomers is always established in photochemical isomerization [12].

It is clear that the isomerization of azobenzene is a chain process which is initiated by the radicals formed in the radiolytic breakdown of the solvent. In actuality, the rate of isomerization is greater in cyclohexane, which is a poor energy donor [1,13], but one in which the radiational yield of radicals is approximately 8 times greater than in benzene (Table 2). The rate of izomerization is still higher in CCl_4, and this is also true of the yield of primary radicals. Azobenzene isomerizes much more slowly in styrene than in benzene , and it is possible that this is related to an interaction between the primary radicals and the monomer with the formation of less active polymeric radicals .

It is known that those chain reactions of spatial isomerization of organic compounds in solution which are initiated by free radicals always lead to the formation of the more stable isomer.

The results which have been obtained show that there is no simple relationship between the structure of a molecule and the ability of this molecule to absorb the energy of electronic excitation, or to utilize this energy in chemical transformations. For example, azobenzene is not, in general, an acceptor of energy, even through the molecule contains two phenyl rings conjugated with a double bond. At the same time, certain other substances which are good acceptors of energy (PATM, DAB) either do not utilize the energy which they obtain from the solvent for dissociating into radicals, or utilize this energy only incompletely, and that despite the fact that thermal breakdown proceeeds readily.

LITERATURE CITED

[1] V. A. Krongauz and Kh. S. Bagdasar'yan, The Action of Ionizing Radiations on Organic and Inorganic Systems[in Russian], Acad. Sci. USSR, Press, p. 205 (1958).

[2] V. A. Krongauz and Kh. S. Bagdasar'yan, Proc. Acad. Sci. USSR 114, No. 4, 829 (1957).*

[3] V. A. Krongauz and Kh. S. Bagdasar'yan, J. Phys. Chem. 32, No. 8, 1863 (1958).

[4] V. A. Krongauz and Kh. S. Bagdasar'yan, J. Phys. Chem. 32, No. 3, 717 (1958).

[5] V. A. Krongauz, Candidate's Dissertation, L. Ya. Karpov Institute of Physical Chemistry (Moscow, 1957).

[6] V. A. Krongauz and Kh. S. Bagdasar'yan, Proc. Acad. Sci. USSR 116, No. 5, 817 (1957).*

[7] H. Kallmann and M. Furst, Phys. Rev. 85, 816 (1952).

[8] G. L. Davies, D. H. Hey, and G. H. Williams, J. Chem. Soc. 4397 (1956).

[9] L. M. Romanov, B. A. Dolgoplosk, and B. L. Erusalimskii, Proc. Acad. Sci. USSR 112, No. 4, 703 (1957).*

[10] B. A. Dolgoplosk, D. S. Korotkina, G. A. Parfenov, B. L. Erusalimskii, and E. B. Milovskaya, Problems of Chemical Kinetics, Catalysis and Reactivity [in Russian] p. 303 (Moscow, 1955).

[11] J. Halpern, G. Brady and C. Winkler, Canad. J. Res. 28, 140 (1950).

[12] G. Zimmerman, Lue-Yung Chow, Un-jin Paik, J. Am. Chem. Soc. 20, No. 14, 3528 (1958).

[13] M. Furst and H. Kallmann, J. Chem. Phys. 23, 607 (1955).

Received April 11, 1959

---

* Original Russian pagination. See C.B. Translation.

THE REDUCTION OF NITRATE IONS IN THE PRESENCE OF LOW CONCENTRATION LANTHANUM IONS

Liu Shou-jung and S. I. Zhdanov

The Institute of Electrochemistry of the Academy of Sciences
of the USSR

(Presented by Academician A. N. Frumkin,May 9, 1959)

The influence of the solution composition on the reduction of NO_3^- ions at low concentration on the dropping mercury electrode has been studied in earlier papers [1,2]. Attempted investigations of the effect of small additions of salts of the polyvalent cations on the kinetics of the reduction of NO_3^- ions under these same conditions [3,4] have met with failure, the formation of OH^- ions in the nitrate reduction leading to large and irregular variations in the current strength. Trustworthy data in the presence of low concentrations of La^{3+}can be obtained through the study of highly concentrated nitrate solutions, i.e., systems in which the concentration ratio is the inverse of that which is usually employed in polarography.

Reduction of NO_3^- ions in 0.1 M KNO_3 begins at -1.55 v relative to the saturated calomel electrode (Fig. 1, 2). The addition of $LaCl_3$ markedly accelerates this reaction, and the reduction then begins at potentials which are much less negative (Fig. 1, 3).

A NO_3^- wave with a minimum appears when the $LaCl_3$ concentration is approximately $4 \cdot 10^{-4}$ M (Fig. 1,4). This wave rises with an increase in the $LaCl_3$ concentration (Fig. 1, 5); the minimum becomes less pronounced (Fig. 1, 6) , and finally disappears (Fig. 1, 7). But the wave form is anomalous, even under these latter conditions. The wave covers a narrow potential interval (approximately 150 mv) and shows a point of inflection instead of a horizontal segment corresponding to the limiting current, this last being an indication of a diminution in the rate of acceleration of the reaction with increasing cathode potential. There is a direct proportionality between the square root of the height of the mercury column and the current strength at the beginning of current fall-off, or the current strength in the region of the inflection point, when there is no such fall-off (Fig. 2), and this indicates that it is a diffusional factor which limits the reaction velocity at these potentials. This reaction cannot be limited by the diffusion of NO_3^- ions at these high concentrations and the kinetics of the reaction must therefore be determined by the diffusion of the lanthanum ions. This is in agreement with the fact that there is a direct proportionality between the current strength at a fixed potential value in the neighborhood of the inflection point (for example, -1.2v) and the $LaCl_3$ concentration when the latter is $\sim 10^{-3}$ M or larger, the factor of proportionality being 0.83, i.e., nearly unity. Thus the current strength in the region of the inflection point is determined by the rate of diffusion of the lanthanum ions, on the one hand, and by the rate of reduction of the NO_3^- ions, on the other. The absence of a curve segment which would correspond to a limiting current is the result of an increase in the rate of reduction with increasing negative potential and this, in turn, is due to a diminution in the energy of activation of the reaction.

The wave for NO_3^- in the presence of $LaCl_3$ at low concentration is quite similar to the earlier-studied [1] wave for NO_3^- in the presence of $LaCl_3$ at high concentrations. For example, these waves are observed at approximately the same potentials. It is also true that the wave for NO_3^- in the presence of small amounts of $LaCl_3$ originates with an abrupt rise in the current strength , which shows the reaction to be autocatalytic. The origin of the wave is displaced toward more negative potentials when the solution is acidified, i.e., the reaction

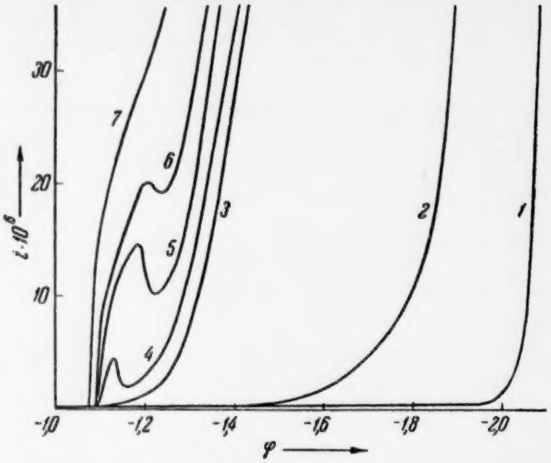

Fig. 1. The effect of the $LaCl_3$ concentration on the reduction of NO_3^- ions. Solution concentrations: 1) 0.1 M KCl; 2-7) 0.1 M KNO_3 + $xLaCl_3$: 2-x = 0 ; 3) $x=1 \cdot 10^{-4}$; 4) $x = 4 \cdot 10^{-4}$; 5) $x = 8 \cdot 10^{-4}$; 6) $x = 10^{-3}$; 7) $x = 2 \cdot 10^{-3}$ M ; t = 25°. Capillary characteristics: m = 2.3 mg / sec and τ = 4.2 sec (in 0.1 M KNO_3 at h = 30 cm and $\varphi = 0$).

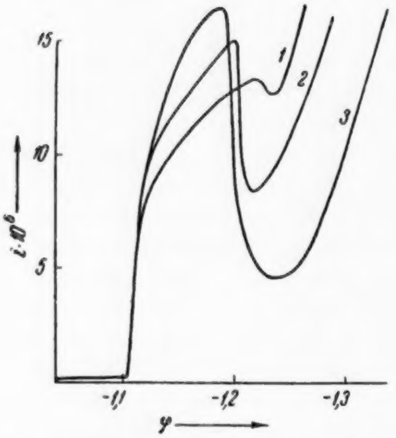

Fig. 2. The effect of the height of the mercury column on the NO_3^- wave at t = 25° in a solution of 0.1 M KNO_3 + $7 \cdot 10^{-4}$ M $LaCl_3$. 1) h = 20; 2) h = 30; 3) h=60 mm of Hg.

is then retarded, and toward more positive potentials when the solution is made alkaline, the reaction being then favored*.

There are, however, a number of peculiarities associated with the NO_3^- wave in the presence of $LaCl_3$ at low concentrations, above all, the previously mentioned fall-off of the current. Further more, the current strength diminished at the minimum, or at still more negative potentials, as h increases, as is to be seen from Figure 2. The current strength at constant h also diminishes when the drop period is artificially reduced by the use of a "hoe" of the type of E. M. Skobets and N. S. Kavetskii [5] and the wave almost completely disappears over the potential intervals from -1.1 to -1.25 v (Fig. 3).

This type of relation between the current strength and the capillary characteristics is an uncommon one, and has only rarely been observed [6]. Such a relation is associated with autocatalytic reactions in which the catalyst is generated slowly. It is impossible to explain this phenomenon by supposing the simple hydrated La^{3+} ion is the catalyst for the reaction. It is clear that the catalytic action arises here from the interaction of the La^{3+} ion with the OH^- ions resulting from the reduction of the NO_3^- ions.

The partially hydrolyzed lanthanum ions can be assumed to promote the reduction of the NO_3^- ions more strongly than the simple hydrated La^{3+} ions [7]. From this point of view , the effect of acidification of the solution is explained as resulting from the repression of the hydrolysis of the La^{3+} ions by the OH^- ions. Measurements of the differential capacity of the dropping mercury electrode in alkaline solutions of lanthanum salts also show that equilibrium is slowly established between the La^{3+} and the OH^- ions [8]. The structure of the hydrolysis

---

* At the same time, there is a reduction in the current strength for the nitrate ion reduction when the solution is acidified or made alkaline .

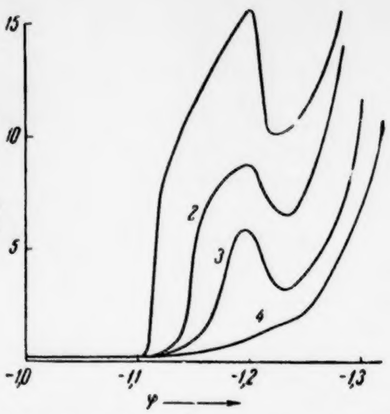

Fig. 3. The effect of the drop period on the NO_3^- wave in a solution of 0.1 M KNO_3 + $7\cdot10^{-4}$ M $LaCl_3$: 1) τ = 4.2 sec; 2) τ = 2.2 sec; 3) τ = 1.1 sec; 4) τ=0.8 sec; 1) natural dropping; 2-4) cut off by "hoe"; t = 25° ; h = 30 cm .

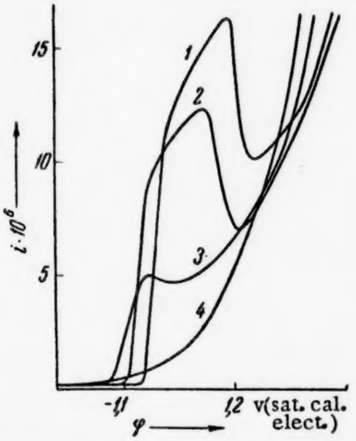

Fig. 4 . The effect of K_2SO_4 on the NO_3^- wave in a solution of 0.1 M KNO_3 + $7\cdot10^{-4}$ M $LaCl_3$[K_2SO_4]: 1) 0 ; 2) $2\cdot10^{-5}$; 3) $5\cdot10^{-5}$; 4) $1.5\cdot10^{-4}$ M; t = 25° ; h = 30 cm .

products which are absorbed on the electrode surface has not as yet been cleared up. It has been pointed out in [8] that these are possibly polar complexes of the composition $La_x(OH)_y^{(3x-y)+}$; such complexes would carry a high average positive charge and would be able to alter the structure of the double layer more profoundly than do the La^{3+} ions. Lack of complete information on the structure of the absorbed complexes makes it impossible to draw definitive conclusions concerning the origins of the current drop which is observed in the interval of potentials from -1.1 to -1.15 v. It could be supposed that this is the result of a displacement of the ψ_1-potential toward negative values with increasing cathodic polarization. This movement of the ψ_1-potential toward negative values must occur at potentials which are much more negative than that of the null-charge point when polycharged cations are present. In the light of this interpretation, the polarization curves which have been obtained in the present work must be considered similar to the curves for the electroreduction of $S_2O_8^{2-}$ ions in the presence of low concentrations of La^{3+} [9], the only difference being that the reduction of $S_2O_8^{2-}$ is not accompanied by the appearance of OH^- ions, and the reaction is catalyzed by the simple La^{3+} ions rather than by the products arising from the hydrolysis of these ions.

It is also possible that there is a second factor which is responsible for the fall-off in the current , namely, the alteration in the conditions for absorption of the partially hydrolyzed lanthanum ions which arises from the increase in the negative potential. This could also result in a diminution in the positive ψ_1-potential, or in the movement of this potential toward negative values. This interpretation would assign different origins to the fall-off of the current in the superficially similar reductions of anions of the types of NO_3^- and $S_2O_8^{2-}$, this effect supposedly arising as the result of a lowering of the catalyst concentration in the surface layer during reduction of the NO_3^- ions at the higher negative potentials,and to be due to a drop in the depolarizer concentration at the electrode surface when $S_2O_8^{2-}$ is reduced under the same conditions.

A sharp fall-off in the current is once more noted on the NO_3^- wave when the $LaCl_3$ concentration is raised to 0.02 M, but at more negative potentials (~ -1.5 v). This is due to the fact that a visible film of the hydrolysis products of $LaCl_3$ is formed around the drop, so that the reduction of the NO_3^- ions is retarded. This film is carried to the bottom of the cell by the falling droplets and prevents the coalescence of these droplets with the mercury which is already there. The film dissolves when an acid is added and the droplets then coalesce. This effect is observed only at the higher $LaCl_3$ concentrations, and it can therefore be concluded that the precipitation of lanthanum hydroxide is retarded at the lower La^{3+} concentrations.

The addition of sulfate ions leads to a marked retardation of the reduction of the NO_3^- ions in the presence of La^{3+} at low concentrations (Fig. 4). A SO_4^{2-} ion concentration one and a half orders less than the $LaCl_3$ concentration is enough to bring about a measureable effect. The wave completely disappears when the SO_4^{-2} concentration is one-fourth that of the $LaCl_3$ (Fig. 4, 4). This action is due to the high negative charge of the SO_4^{-2} ions. Actually, KI will suppress the NO_3^- wave, but only when its concentration is 0.2 M. From this concentration ratio for the La^{3+} and SO_4^{2-} ions, it follows that it is impossible to explain the SO_4^{2-} ion effect in terms of a displacement of NO_3^- anions from the ionic pairs which the latter form with the La^{3+} ions in the bulk of the solution. An interpretation of this data should take into account that discreet structure of the double layer on the electrode which was first described by A. N. Frumkin [10]. Reduction of the anions occurs in the neighborhood of the absorbed cations at points where the ψ_1-potential has its highest positive value (essentially the same conclusion would follow from the theory of the formation of ionic pairs, or cation bridges, in the double layer). Any doubly charged SO_4^{2-} anions which are introduced into the solution will take up some of these positions in the double layer and the ψ_1-potential will be displaced toward more negative values into the region which should be occupied by the centers of the reduced anions, thus impeding the entrance of the NO_3^- ions into the surface layer. If the absorbed layer of condensed polynuclear La^{3+} cations is catalytically active, it is quite likely that it contains only a limited number of positions for those anions which are subject to reduction. The SO_4^{2-} ions displace the NO_3^- ions from these positions because of their higher negative charge. It is clear that a concentration of SO_4^{2-} anions which is too low to have noticeable effect on the state of ionic pairs in the bulk of the solution would still be adequate for effects which are bound up with surface interactions.

We count it our pleasant duty to express our thanks to Academician A. N. Frumkin for the valuable advice which he offered in the course of a discussion of these results.

LITERATURE CITED

[1] A. N. Frumkin and S. I. Zhdanov, Proc. Acad. Sci. USSR 92, 629 (1952); 96, 793 (1954); 97, 867 (1954).

[2] S. I. Zhdanov, V. I. Zykov and T. V. Kalish, Proc. Fourth Conference on Electrochemistry, Acad. Sci. USSR Press, p. 164 (1959).

[3] S. I. Zhdanov, Dissertation, (Moscow, 1954) [In Russian].

[4] Z. R. Grabowski and W. Turnowska, Roczn. Chem. 29, 746 (1955).

[5] E. M. Skobets and N. S. Kavetskii, Ind. Lab. 15, 1299 (1949).

[6] S. G. Mairanovskii, Proc. Acad. Sci. USSR 114, 1272 (1957).*

[7] Z. R. Grabovskii, Proc. Fourth Conference on Electrochemistry, Acad. Sci. USSR Press, p. 233 (1959).

[8] B. B. Damaskin and N. V. Nikolaeva- Fedorovich, Scientific Reports, Higher Schools, Chem. Ser. 43 (1959).

[9] A. N. Frumkin and G. M. Florianovich, Proc. Acad. Sci. USSR 80, 907 (1951).

[10] A. N. Frumkin, Actualités Scientifiqnes et Industrielles, p. 373 (Paris, 1936).

Received May 8, 1959

---

* Original Russian pagination. See C.B. Translation.

THE HEAT OF TRANSFER OF [Cd^{++} $Ag^{\square}$] COMPLEXES IN AgBr + $CdBr_2$ CRYSTALS

A. N. Murin, B. G. Lur'e and G. N. Shapkin

The A. A. Zhdanov State University, Leningrad

(Presented by Academician A. F. Ioffe, May 16, 1959)

Solid solutions of cadmium and silver bromides have served as the subjects for numerous experimental and theoretical investigations. Cd^{++} ions are capable of replacing the Ag^{+} ion in the AgBr lattice to form equimolar "solution" of $Ag^{\square}$ cation vacancies. Interaction leads to the association of the Cd^{++} ions (with an unbalanced charge of + e) and the $Ag^{\square}$ vacancies (with an unbalanced charge of − e) into a "neutral" complex of the type [Cd^{++} $Ag^{\square}$]. The degree of association, p, is determined here by the concentration of the cadmium bromide, C, and the temperature, T. The law of mass action shows that, at sufficiently high Cd concentrations [1]

$$\frac{Cp}{[C(1-p)]^2} = K_2(T). \qquad (1)$$

A thermal diffusion current of cadmium must be observed when a temperature gradient exists in the AgBr + + $CdBr_2$ system. The cadmium ions which then move through the crystal are exclusively in the form of the [Cd^{++} $Ag^{\square}$] complexes since the nonassociated Cd^{++} ions are practically immobile. When a stationary state is reached, the relative concentration difference in the solution $\Delta C/C$, is fixed by the equation [2]

$$\frac{\Delta C}{C} = \frac{-(1+p)\,Q_K^{*} + (1-p)\,\chi}{2kT^2}\,\Delta T, \qquad (2)$$

in which ΔT is the difference between the temperatures of the hot and the cold ends of the specimen, Q_K^{*} is the so-called heat of transfer of the [Cd^{++} $Ag^{\square}$] complex, and χ is the heat of association of this complex as determined from measurements on the electrical conductivity of mixed AgBr + $CdBr_2$ crystals. According to Teltow [3], χ = 0.16 ev.

The heat of transfer of the free $Ag^{\square}$ vacancy, and the quantity Q_K^{*}, as defined by the equation

$$\Phi = \frac{E}{dT/dx} = \frac{1}{eT}\left(Q_1^{*} - \frac{1}{2}Q_K^{*} + \frac{1}{2}\chi\right). \qquad (3)$$

can be evaluated through measurements of the emf of thermal diffusion in pure AgBr crystals and in mixed AgBr + + $CdBr_2$ crystals.

The measurements of Patrick and Lawson [4] give Q_1^{*} = −0.385 ev and ΦT = 0.076 v. From this it follows that Q_K^{*} = 0.46 ev.

It is to be noted that Hovard and Lidiard [5] have shown that the value of ΦT remains constant while thermal-diffusional equilibrium is being established. The determination of $\Delta C/C$ in the stationary state gives and independent method for fixing the value of Q_K^{*} and use has been made of this fact in the present investigation. This method has the advantage of eliminating the necessity of taking contact phenomena (AgBr/Ag) into account. Such phenomena introduce an element of arbitrariness in the data which have been obtained by Patrick and Lawson, although these data are in good agreement with our own results.

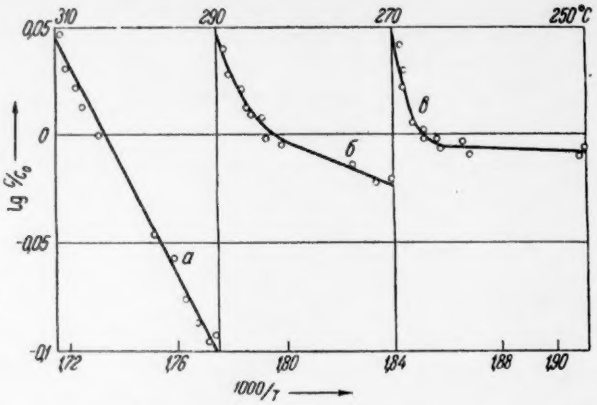

Fig. 1. The distribution of Cd^{++} in three specimens of AgBr + + $CdBr_2$: a) ΔT = 310-290° ; b) 290-270° ; c) 270-250°

The degree of association, p, of the Cd^{++} ions in the complexes, or, differently expressed, the value of the mass action law constant of Equation (1), must be known at the working temperature before Q^*_K can be evaluated from Equation (2). Acceptable values of K_2 for temperatures ranging from 150 to 275° are found in [3]. We have obtained a corresponding value for 300° (K_2 = 143) by extrapolation.

We have observed the Soret effect in silver bromide containing 1 mole % of $CdBr_2$. Specimens were prepared by pressing (P = 4000 atmos) finely dispersed AgBr, $CdBr_2$ mixtures which had been tagged with radioactive Cd^{115m} (T = 43 days). The resulting tablets were homogenized by being subjected to an extended annealing. The tablets were placed in a furnace which had been especially constructed so as to have a uniform linear temperature gradient along the tablet axis. A thermal regulator was used to insure constancy of the temperature over time and this constancy was checked with six thermocouples. Five tablets were annealed simultaneously, separated from one another by insulating layers of mica. Each tablet was 3 mm thick and was under a temperature gradient of 20°, so that the total temperature difference amounted to 100° (210-310°). The tablets were held in the furnace for approximately 315 hours and the activity distribution in them was then determined by the method of sections (divisioning into thin layers). Figure 1 shows the activity distribution in three of these tablets which were taken from the hot end of the furnace.

In the case of the hottest of these specimens, the linear log C/C_0 (C_0 is the cadmium concentration in an unheated specimen), reciprocal absolute temperature, $1/T$, relation is that which would correspond to Equation (2), i.e., this relation is consistent with the assumption that a stationary state was attained. The establishment of equilibrium was not observed in those tablets which were taken from the regions of lower temperatures, despite the fact that they had been subjected to an extended annealing (Fig. 1, b and c).

The approach to equilibrium in experiments similar to our own has been roughly described [6] by a law which is exponential in the relaxation time, $\theta = a^2/\pi^2 D$ (D is the diffusion coefficient for the Cd^{++} ions and a, the tablet thickness).

Rough values of D for our entire range of working temperatures have been obtained by Schöne, Stasiw and Teltow [7]. The θ value calculated from these data is such as to indicate that equilibrium would be established within time intervals ranging from one day (at 300°) to 10 days (at 220°), i.e., the annealing times which we selected would appear to have been long enough.

We have attempted to clear up this contradiction by measuring the diffusion coefficient of Cd^{++} ion in mixed AgBr + 1 mole % $CdBr_2$ crystals through the same method of radioactive indicators used in our earlier works [8]; the results obtained $(1.24 \pm 0.01) \cdot 10^{-8}$ cm²/sec at 300° and $(0.425 \pm 0.025) \cdot 10^{-8}$ cm²/sec at 260°, are approximately one order lower than the values of the above-cited authors. It follows from our determinations of the diffusion coefficients that our thermal diffusion experiments were continued long enough only in the case of the 310-290° temperature interval, the time of relaxation at 300° being θ = 204 hours. The annealing period for the other tablets was considerably less than θ and, for this reason, a stationary state was not established in them.

We have evaluated the quantity Q^*_K, using our experimental data (Fig. 1a) and Equations (1) and (2) (the latter in its integrated form), and have found the value -0.54 ev (T = 300°); this is very close to the $Q^*_K = -0.46$ ev obtained by Patrick and Lawson from an experimental determination of the thermoelectromotive force.

On the basis of the kinetic theory of Wirz [9], Hovard [2] has shown that the heat of transfer, Q^*_K, should be of the same order of magnitude as the heat of transfer of the free vacancy, $Q^*_1 = -0.385$ ev. Our results are in agreement with this theoretical estimation of Q^*_K.

LITERATURE CITED

[1] A. B. Lidiard, Handb. d. Phys. 20, Ionic Conductivity (1956).

[2] R. E. Hovard, J. Chem. Phys. 27, No. 6 (1957).

[3] J. Teltow, Ann. d. Phys. 6, 5, 63, (1949).

[4] L. Patrick and A. W. Lawson, J. Chem. Phys. 22, 1492 (1954).

[5] R. E. Hovard and A. B. Lidiard, Disc. Farad. Soc. 23, 113 (1957).

[6] S. R. de Groot, L'effet Soret (North Holland), Amsterdam, (1945)

[7] E. Schöne, O. Stasiw, and J. Teltow, Zs. Phys. Chem. 197, 145 (1951).

[8] A. N. Murin and B. G. Lur'e, J. Phys. Chem. 32, No. 11, 2575 (1958).

[9] K. Wirz, Phys. Zs. 44, 221 (1943).

Received May 13, 1959

THE INTERRELATION OF THE PHYSICAL CHEMICAL CHARACTERISTICS OF POLAR LIQUIDS

E. S. Rudakov

The All-Union Scientific-Research Institute for the Reactions
of Petroleum Chemistry

(Presented by Academician M. I. Kabachnik February 25, 1959)

An explanation of the thermodynamic properties of polar liquids, and of the effect of polar liquid solvents on chemical reactions, solubilities, and ionic conductivities in particular, is not found within the framework of the theory of dielectric polarization. The intermolecular field of the liquid arises from the interactions of the charges of neighboring molecules and is fixed by the magnitude of these charges and their distribution rather than by the total dipole moment. We will arbitrarily characterize the field of microcharges by the microdielectric permeability, D_0, thereby underscoring the fundamental difference between it and the usual dielectric field.

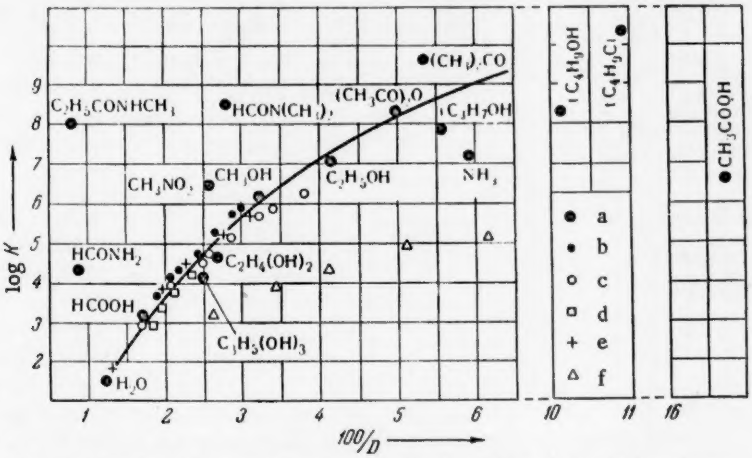

Fig. 1. The specific rate of solvation of $(CH_3)_3CCl$ and the dielectric permeability of solvents at 25°; a) pure solvents; b) methanol—water system; ethanol— water system; d) ethylene glycol—water system; e) acetone— water system; f) dioxane— water system.

Although it is impossible to establish a direct functional relation between D, D_0, and μ, it is still natural to suppose that D and D_0 would vary in the same manner in going from one liquid to another in a homologous series. The case of water and the normal alcohols will be accepted as the normalized condition; here $\mu_0 = 1.6-1.8$ debye and $D_0 \simeq D$. In view of the dependence of D on μ, it could then be expected that $D > D_0$ when $\mu > \mu_0$ and that $D < D_0$ when $\mu < \mu_0$.

TABLE 1

An Ordering of Liquids in Terms of Decreasing D_0 Value; 25°

Liquid	D	D_0 *	$-\lg K$ (sec^{-1})
Hydrogen peroxide	87	(87)	—
Water	78,5	(78)	1,5±0,1**
Hydrogen fluoride	65	(65)	—
Hydroxylamine	—	59	—
Iodine chloride	—	58	—
Formic acid	56,1	(56)	3,0±0,1
C_3F_7COOH	—	55	3,3
Hydrazine	51,7	(52)	—
Selenium oxychloride	46	(46)	—
Glycerin	40,1	43	4,1±0,2
Formamide	109,5	42	4,33
Ethylene glycol	37,7	39	4,6±0,05
Hydrogen cyanide	116	33	—
Acetonitrile	35	33	—
Methyl alcohol	31,5	(32)	6,10
Ethanolamine	—	30	—
Nitromethane	39	28	6,5±0,1**
Acetic acid	6	27	6,67±0,05
Furfural	41,7	26	—
Ethyl alcohol	24,3	(24)	7,05±0,05
Ammonia	17	24	7,28
Ethylenediamine	12,9	22	—
Sulfur dioxide	12	22	—
Propyl alcohol	20,1	(20)	—
Isopropyl alcohol	18,3	20	7,8
Methylamide of propionic acid	166	20	8,6±0,3
Nitrobenzene	36,4	20	—
Butyl alcohol	19	(19)	—
Tertiary butyl alcohol	[illegible],9	19	8,3
Acetic anhydride	20	19	8,32
Dimethylformamide	36,7	19	8,45
Acetone	19,1	15	9,9±0,3**
Tertiary butyl chloride	9	14	10,4±0,5
Dioxane	2,1	13	10,8±0,5**
Gaseous phase	1,0	(1)	19,5±2**

---

* D_0 values for the substances which were used in constructing the water—alcohol line are enclosed in parentheses.

** Values obtained from the data of the literature through the use of temperature and concentration relations .

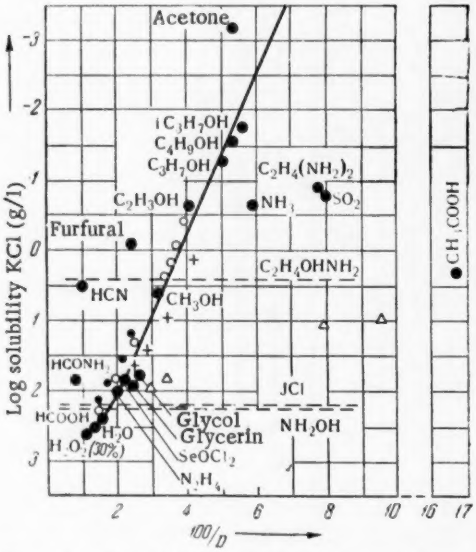

Fig. 2 . The solubility of KCl [13] and the dielectric permeability at 25°. Same symbols as in Figure 1.

We will now review the regularities which follow from a study of the kinetics of the unimolecular solvation of tertiary butyl chloride (Figure 1, Table 1).

The data of the literature [1-12] were compared and supplemented by our measurements on liquid $(CH_3)_3CCl$ and its solutions in glycerin, ethylene glycol, and binary mixtures of water and ethylene glycol.

A curve passing through the points for water and the alcohols (for these liquids, $D = D_0$, by definition) divides Figure 1 into two parts, media for which $\mu > \mu_0$ is located to the left of this line and those for which $\mu < \mu_0$ lies to the right of it, with the dioxane—water system sharply displaced to the right. The D_0 value for any liquid which does not fall on the water—alcohol curve can be found by simply extending the horizontal line log K = const to intersection with this curve and reading off the abscissa of the cut-point as $100/D_0$.

An analysis of: 1) the rates of solvation of certain alkyl halides such as $(CH_3)_3$ CBr, and the reaction between bromoacetate and thiosulfate ions; 2) the solubilities of electrolytes such as KCl, NaF and CH_3COOAg; 3) the solubilities of nonelectrolytes such as glycine, benzene and naphthalene; 4) the behavior of the Pisarzhevskii-Walden constants of such ions as Cl^-; and 6) the electromotive force of such half-cells as $(Pt)H_2$ | HCl and medium | AgCl-Ag, brings out the similarity in the effect of the medium on processes occurring in solution.

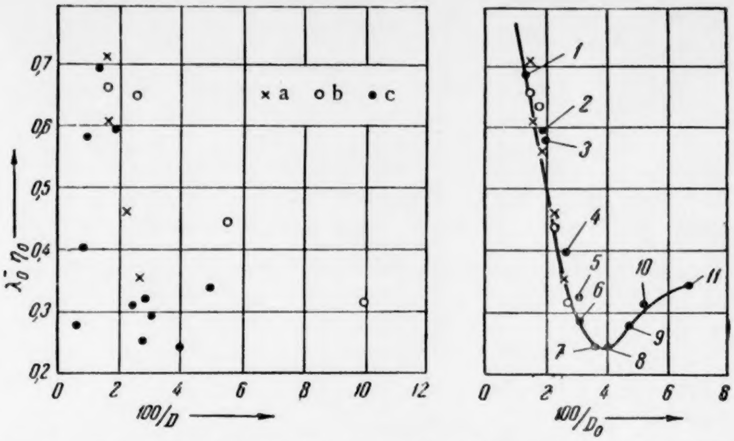

Fig. 3 . The relation between $\lambda_0^- \eta_0$ for the Cl^- ion and D and D_0 at 25° according to the data of [18–25]: a) methanol—water system; b) water—dioxane system; c) individual media (according to the curve); 1) water; 2) hydrazine; 3) formamide; 4) hydrogen cyanide; 5) acetonitrile; 6) methanol; 7) nitromethane; 8) ethanol; 9) methylamide of propionic acid; 10) nitrobenzene; 11) acetone .

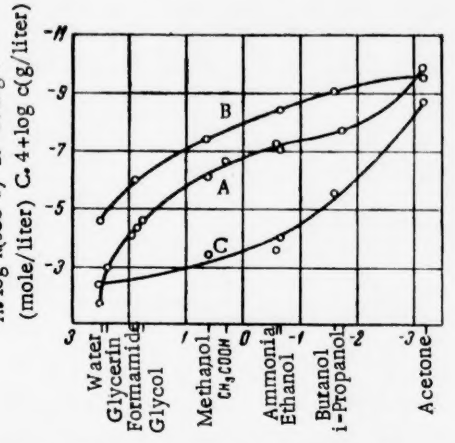

Fig. 4. The relation between certain effects of the medium at 25°. On the axis of abscissas, the solubility of KCl, log C (g/l): A) specific rate of solvation of $(CH_3)_3CCl$, log K (sec^{-1}); B) solubility of glycine [13], -5 + log C (mole/l); C) solubility of NaF [13], -4 + + log c (g/l).

Figure 3 gives values of the product of the ionic conductivity and the solvent viscosity, $\lambda_0^- \eta_0$, and shows the variation of this product with D and D_0 (D_0 values were obtained from Figures 1 and 2) for the case of the Cl^- ion, the particle which has been most thoroughly studied. It is clear that the point-scatter is sharply contracted when D is replaced by D_0 and that the relation then acquires a well defined form with $\lambda_0^- \eta_0$ falling rapidly as D_0 diminished to reach a minimum at D_0 = 25.

The similarity between certain of these effect-of-medium vs 1/D graphs is so marked , that it is possible to plot one effect as a function of another and thereby obtain an all-embracing relation which will cover a wide range of individual substances and binary mixtures of radically different chemical properties (Fig. 4).

There have been many unsuccessful attempts to relate the dielectric permeability and the physical properties of pure liquids. The problem of setting up such relations in the quantity D_0 is one which is easily solved. The simplest of these relations is

$$D_0 = 4{,}3\,\frac{T_{\text{b.p.}}\rho^{1/2}}{M} \pm 10\% \quad \text{for} \quad D_0 > 17 \qquad (1)$$

this involves the absolute boiling point of the pure liquid, its density, ρ , and molecular weight, M.

Each of the phenomena which have been considered above opens up the possibility for another independent determination of the value of D_0. Thus at 25° one obtains :

Acetic acid	D_0 = 29 , 26, 28	D = 6,
Formamide	D_0 = 53, 42, 45, 42,	D = 109.5
Hydrogen cyanide	D_0 = 27, 31, 35,	D = 116,
Acetone	D_0 = 16, 15, 15, 15, 15,	D = 19.1
Dioxane—water system(30 wt %)	D_0 = 36, 36, 38, 37,	D = 17.7

The first value in each of these rows was found from Equation (1) and the remaining entries were then read off from graphs of effect-of-medium vs 100/D. The extent of the deviations which arise from the crudeness of the above-considered relations can be judged from these figures. Mean values of D_0 are given in Table 1.

The question of the existence of a parallelism between the dielectric permeability and the various physical chemical characteristics of liquids has been repeatedly treated in the literature. Theoretical calculations have been carried out in this field, "rules" have been advanced and linear relations have been established. Thus, Kirkwood's Equation for the activity coefficient of the elastic dipole has been applied to the kinetics of solvation of the alkyl halides [17], the Born Equation, to reactions between ions [14] and to the solubility of salts [15], and the Semenchenko Equation, to the solubility of KCl and other substances [16]. There is, however, no general parallelism between the dielectric permeability and the medium-effect in any one of these phenomena. It is easy to be convinced of this by studying the data for such solvents as formamide, dioxane—water solutions, etc. The lack of concordance here has been noted by many investigators [12], but it has usually been ascribed to such secondary effects as the formation of chemical compounds, specific solvation, association, or polymolecular reactions. It seems to us that these "discrepancies" come out of the mistaken assumption that there is a parallelism between the thermodynamic properties of a medium and its dielectric permeability.

The relations which have been developed here can be used for determining the effectiveness of various solvents in various processes and in many cases numerical values have been predicted from them for effects which had not yet been studied. It seems to us even more significant that there is the possibility of a unified treatment of the effect of the medium on various physical chemical processes in solution once a deep inner relationship has been established between phenomena in solution.

I wish to express my thanks to V. V. Voevodskii, Corresponding Member of the Academy of Sciences of the USSR, and to Academician M. I. Kabachnik for their interest in this work and for discussions of it .

LITERATURE CITED

[1] E. D. Hughes, J. Chem. Soc. 255 (1935).

[2] B. D. Brearley, G. B. Kistiakovsky, and C. H. Stauffer, J. Am. Chem. Soc. 58, 43 (1936).

[3] L. C. Bateman and E. D. Hughes, J. Chem. Soc. 1187 (1937); 935 (1940).

[4] A. R. Olson and R. S. Halford, J. Am. Chem. Soc. 59, 2644 (1937).

[5] W. Kokoski, H. Thomas, and R. D. Fowler, J. Am. Chem. Soc. 63, 2451 (1941) .

[6] G. S. Markova and A. I. Shatenshtein, Proc. Acad. Sci. USSR 35, 73 (1942).

[7] C. G. Swain and S. D. Ross, J. Am. Chem. Soc. 68, 658 (1946).

[8] E. Grunwald and S. Winstein, J. Am. Chem. Soc. 70, 846 (1948).

[9] W. H. Cropper, F. Spieth and A. R. Olson, J. Am. Chem. Soc. 76, 6248 (1954).

[10] C. E. Boozer , J. D. Robinson, et al., J. Am. Chem. Soc. 78, 3428 (1956).

[11] A. H. Fainberg and S. Winstein, J. Am. Chem. Soc. 78, 2770 (1956).

[12] S. D. Ross and M. M. Labes, J. Am. Chem. Soc. 79, 4155 (1957).

[13] A. Seidell, Solubilities, 1, 2, N. Y. , (1940); A. Seidell and W. F. Linke, Solubilities, N. Y. (1951).

[14] V. K. La-Mer and M. E. Kamner, J. Am. Chem. Soc. 57, 2663 (1935).

[15] T. W. Davis, J. E. Ricci , and C. G. Sauter, J. Am. Chem. Soc. 61, 3274 (1939).

[16] M. I. Shakhaparonov, Introduction to the Molecular Theory of Solutions [in Russian] (Moscow, 1956) .

[17] S. Glasstone, K. Laidler, and G. Eyring, The Theory of Absolute Reaction Rates[Russian Translation], Foreign Lit. Press (1948).

[18] G. Harned and B. Owen, The Physical Chemistry of Solutions of Electrolytes [Russian Translation] (Moscow, 1056).

[19] P. Walden, Elektrochemie Nichtwassriger Lösungen (Leipzig, 1924) .

[20] L. Odrit and Ya. Kleinberg, Nonaqueous Solutions [in Russian] (Moscow, 1955).

[21] L. R. Dawson and C. Berger, J. Am. Chem. Soc. 79, 4269 (1957).

[22] B. B. Owen and G. W. Waters, J. Am. Chem. Soc. 60, 2371 (1938).

[23] L. G. Longsworth and D. A. MacInnes, J. Phys. Chem. 43, 239 (1939).

[24] P. Walden and E. I. Birr, Zs. Phys. Chem. 163A, 321 (1933).

[25] L. R. Dawson, R. H. Graves, and P. G. Seavs, J. Am. Chem. Soc. 79, 298 (1957).

Received February 16, 1959

THE MUTUAL INTERACTION OF DIFFUSION CURRENTS IN MULTICOMPONENT SYSTEMS

P. Ya. Siver

The Chernovitskii State Institute of Medicine

(Presented by Academician S. I. Vol'fkovich March 21, 1959)

Investigators have recently turned their attention to the study of diffusion in multicomponent systems[1-5].

The modern theory of diffusion [6,7] indicates that there is a mutual interaction between the diffusion currents in a multicomponent system; the diffusion current of each component of the system must affect the diffusion currents of all of the other components and, conversely, all of these other currents must exert an influence on the diffusion current of any one component.

Although there can be no doubt of the actual existence of a mutual interaction between such diffusion currents, there is very little quantitative information concerning it [8-10]. On the other hand, a quantitative interpretation of the interaction of diffusion currents would be of theoretical and practical interest for a number of disciplines, and especially for physical chemistry and biology.

The present work was undertaken with the aim of obtaining a quantitative interprepation of the mutual interaction of diffusion currents. In distinction to the work of other authors [9] in which the attempt has been made to interpret the interaction of currents in systems involving two electrolytes (water—electrolyte 1—electrolyte 2), radioactive isotopes have been used here to study the mutual interaction of the currents in the simultaneous diffusion of tagged and untagged diphosphate ions ($HP^{32}O^{2-}$ and $HP^{31}O^{2-}$) in the system water—doubly substituted sodium phosphate—nonelectrolyte.

The coefficients of self-diffusion of the diphosphate ion in various water—sodium diphosphate—nonelectryte systems has been measured earlier by the author. The nonelectrolytes selected in this work were urea, glucose and lactose. Solutions of a fixed concentration in diphosphate (0.05 M) and a variable concentration in nonelectrolyte were first prepared for this study and then other solutions were built up in which the concentration of the nonelectrolyte was held constant (0.1 M) and the diphosphate concentration varied. The coefficient of self-diffusion of the tagged diphoshate ion in solution was determined by the open capillary method described in [11,12]. The technique of the earlier work was retained in the present investigation, but instead of having equal concentrations of electrolyte and nonelectrolyte in the capillary and in the beaker, measurement of the coefficient of self-diffusion of the tagged diphosphate ion was made with a definite concentration gradient in this ion between the capillary and the beaker. The concentration of the nonelectrolyte in the beaker was always the same as in the capillary. The same solutions which were used in the earlier work were also studied here; in addition, the system water—sodium diphosphate—glycerin was investigated.

The working principle was that of varying the concentration gradient of untagged phosphate between the capillary and the beaker from one experiment to another so that this gradient approached zero. This not only permitted a determination of the effect of the diffusion current of the untagged phosphate on the current of the tagged phosphate, but also made it possible to extrapolate to zero the values of the diffusion coefficient of the tagged phosphate at the various concentration gradients of untagged phosphate and thus obtain the coefficient of self-diffusion. This idea was borrowed from the paper of I. R. Krichevskii and Yu. V. Tsekhanskaya[12].

All of these experiments were carried out at 25°. The temperature washeld constant to ± 0.05°. The

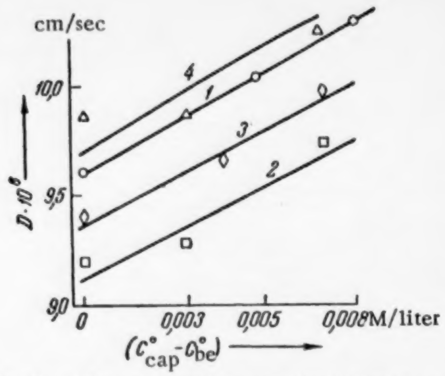

Fig. 1. The relation between the diffusion coefficient and the concentration gradient. C^0_K = 0.025 M phosphate. System content of nonelectrolyte: 1) 0.1 M glucose; 2) 0.1 M glycerin ; 3) 0.1 M lactose; 4) 0.1 M urea .

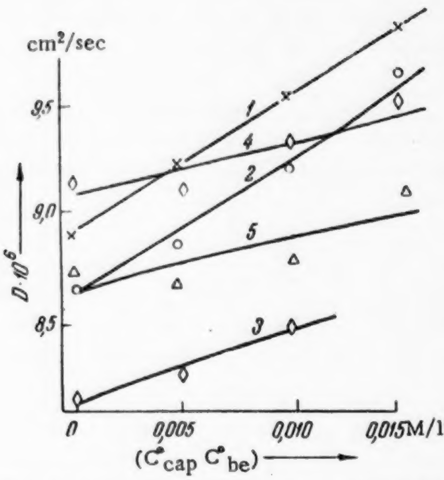

Fig. 2. The relation between the diffusion coefficient and the concentration gradient. C^0_K = =0.05 M phosphate. System content of nonelectrolyte: 1) 0.025 M glucose; 2) 0.1 M glucose; 3) 0.15 M glucose; 4) 0.1 M urea; 5) 0.15 M urea.

experiments were continued for periods ranging from 30 to 48 hours. The radioactivity of the solutions was measured as in [10], using a "B" system and an end-window counting tube with a mica thickness of 15-20 μ. The diffusion coefficient of the tagged electrolyte was calculated from the equation [12]

$$\frac{C^{0'} - C_k}{C_k^{0'}} = 1 - \frac{8}{\pi^2}\sum_{n=0}^{n=\infty}\frac{1}{(2n+1)^2}\exp\left[-\frac{(2n+1)^2 Dt\pi^2}{4L^2}\right], \quad (1)$$

in which D is the diffusion coefficient ($cm^2\ sec^{-1}$), C_K is the activity of the solution in the capillary at the end of diffusion, C^0_K is the activity of the solution in the capillary prior to diffusion, L is the length of the capillary (cm), and t is the duration of the experiment (sec).

The error in the reported values of the diffusion coefficient amounts to as much as ± 2 %.

The diffusion coefficient of the untagged phosphate ion was not measured , but it can be supposed that its value would not differ markedly from that of the coefficient for the tagged phosphate in the diluted solutions with which we worked [13]. Figures 1-4 give the results of all of these experiments in the form of curves showing the diffusion coefficient of the tagged phosphate as a function of the concentration gradient of the untagged phosphate.

The curves of Figures 2 and 3 show the relation between the coefficient of diffusion and the concentration gradient between the capillary and the beaker at a fixed concentration of the nonelectrolyte (same concentration of nonelectrolyte in the capillary and in the beaker), the concentration of the untagged phosphate in the capillary being 0.05 M.

The curves of Figures 1 and 4 are similar, but for phosphate concentrations of 0.025 and 0.1 M in the capillary.

In each case, a relationship falling well within the limits of experimental error is found to exist between the diffusion coefficient of the tagged ion and the concentration gradient of the untagged phosphate. This relation is almost linear, so that extrapolation to zero concentration gradient can readily be carried out. The extrapolated values are in agreement with the values of the coefficient of self-diffusion which were obtained experimentally in the earlier work.

According to Fick's law, the diffusion coefficient is, to a first approximation, proportional to the concentration gradient. Thus, the existence of a linear relationship between the diffusion coefficient of the tagged phosphate ion and the concentration gradient of the untagged phosphate ion is an indication that the diffusion current of the tagged phosphate increases linearly with the diffusion current of the untagged phosphate.

The variation of the diffusion coefficient per unit change in the concentration gradient (mole/liter) is, on the average, about 65-75 %, i.e., the diffusion coefficient increases by a factor of almost 1.5 when there is a concentration gradient of 1 mole/ liter between the capillary and the beaker.

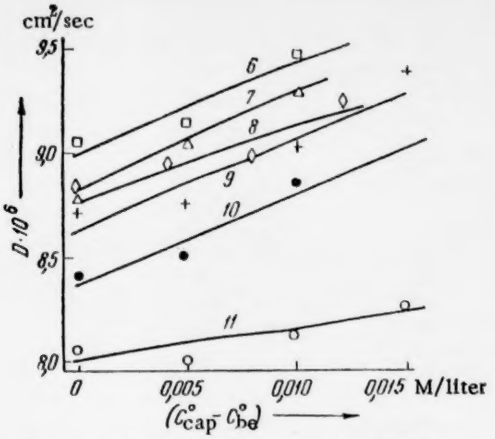

Fig. 3. The relation between the diffusion coefficient and the concentration gradient. C^0_K = 0.05 M phosphate. System content of nonelectrolyte: 6) 0.025 M glycerin, 7) 0.05 M glycerin; 8) 0.1 M glycerin; 9) 0.025 M lactose; 10) 0.50 M lactose; 11) 0.1 M lactose.

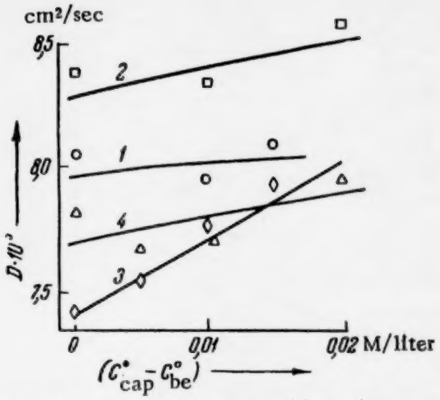

Fig. 4. The relation between the diffusion coefficient and the concentration gradient. C^0_K= 0.1 M phosphate. System content of nonelectrolyte: 1) 0.1 M glucose; 2) 0.1 M glycerin; 3) 0.1 M lactose; 4) 0.1 M urea.

All of these experiments were carried out with similarly directed diffusion currents and the observation was that the current of the tagged ion was increased by the presence of the current of untagged phosphate. The case of diffusion under oppositely directed diffusion currents is one of great interest. The theory of Onsager would indicate that a decrease in the diffusion current of the tagged phosphate is to be expected here.

The author is now engaged in making measurements of this type.

I would like to express my deep appreciation to Professor I. R. Krichevskii for his valuable advice and continued interest in this work.

LITERATURE CITED

[1] F. E. Weir and M. Dole, J. Am. Chem. Soc. 80, No. 2, 302 (1958).

[2] M. Dole, J. Chem. Phys. 25, No. 5, 1082 (1956).

[3] P. J. Dunlop, J. Phys. Chem. 61, No. 12, 1619 (1957).

[4] J. M. Greeth and L. J. Gosting, J. Phys. Chem. 62, No. 1, 58 (1958).

[5] V. A. Marinin, J. Phys. Chem. 32, No. 5, 1068 (1958).

[6] K. Dembig, The Thermodynamics of Stationary Irreversible Processes [In Russian] (Moscow, 1954).

[7] S. R. Groot, Thernodynamics of Irreversible Processes, Amsterdam (1951).

[8] R. L. Baldwin, P. J. Dunlop, and L. J. Gosting, J. Am. Chem. Soc. 77, 5235 (1955).

[9] P. J. Dunlop and L. J. Gosting, J. Am. Chem. Soc. 77, 5238 (1955).

[10] H. Fujita and L. J. Gosting, J. Am. Chem. Soc. 78, 1099 (1956).

[11] H. E. Burkell and J. W. Spinks, Can. J. Chem. 30, 31 (1952).

[12] I. R. Kirchevskii, and Yu. V. Tsekhanskaya, J. Phys. Chem. 30, 2315 (1956).

[13] W. A. Johnson and A. L. Babb, J. Phys. Chem. 60, No. 1, 14 (1956).

Received March 14, 1959

THE REDOX POTENTIAL OF THE Be^+/Be^{++} SYSTEM IN MELTS OF THE ALKALI METAL CHLORIDES

M. V. Smirnov and N. Ya. Chykreev

The Institute of Electrochemistry of the Ural Branch of the Academy
of Sciences of the USSR

(Presented by Academician A. N. Frumkin, April 13, 1959)

It has been shown in our preceding papers [1,2] that chloride melts in contact with metallic beryllium contain not only Be^{++} ions, but Be^+ ions as well. An expression was developed there for the temperature dependence of the equilibrium constant of the reaction $Be^{++}_{(melt)} + Be_{(S)} \rightleftharpoons 2\,Be^+_{(melt)}$ in molten eutectic mixtures of lithium and potassium chlorides containing up to 1.15 Be. This work has been continued with a view to obtaining values for the terms $E^0_{Be/Be^{++}}$, and $E^0_{Be^+/Be^{++}}$ in the respective thermodynamic equations for the reversible potentials of beryllium with respect to the mono-and divalent ions, and for the term $E^0_{Be^+/Be^{++}}$ in the equation for the oxidation-reduction potential of the Be^+/Be^{++} system in salt melts.

This work involved the measurement of the reversible potentials of two types of metallic beryllium over the temperature interval 380-940°. One of these types contained 99.6 % Be; 0.3 % C; 0.05 % Al; 0.03 % Fe; 0.01 % Mn and less than 0.01 % of alkali and alkali-earth metals. The other contained 99.84 % Be; 0.045% Si; 0.02 % Ni; 0.02% Fe and about 0.02 % of alkali , and alkali-earth , metals. Molten eutectic mixtures of lithium and potassium chlorides containing 0.023, 0.169, or 1.13 % Be were used as the electrolyte.

These experiments were carried out in the cell which is sketched in Figure 1. The electrolyte was placed in a beryllium oxide crucible which was, in turn, set into a hermetically sealed quartz tube which was filled with argon. The potential of the beryllium electrode with respect to the chlorine electrode was measured on a high-resistance potentiometer. The cell temperature was measured with a chromel-alumel thermocouple immersed in the salt melt. The cell was heated in a massive metallic block which was set in an electric resistance furnace equipped with an automatic control which held the temperature at any predetermined value with a variation of no more than ± 1.5°. An emf value was considered to be constant if it had changed by less than one millivolt in one hour.

The graphs of Figure 2 show the results of measurements of the temperature variation of the emf of the cell Be $BeCl_2$, LiCl, KCl /Cl_2 , C. The experimental points for the working interval of temperatures fall on straight lines which can be described by the following empirical equations :

for melts with 0.023 % Be $E_1 = 2.637 - 2.36 \cdot 10^{-4} \cdot T \pm 0.006$ v
for melts with 0.169 % Be $E_2 = 2.658 - 3.56 \cdot 10^{-4} \cdot T \pm 0.005$ v
for melts with 1.13 % Be $E_3 = 2.703 - 4.97 \cdot 10^{-4} \cdot T \pm 0.008$ v

Each measured value of the emf involves not only an electrochemical potential difference, but also an oppositely signed thermal emf which arises between the graphite and molybdenum leads to the chlorine and beryllium electrodes of the cell : $E_T = (-0.0076 + 0.174 \cdot 10^{-4} \cdot T) \pm 0.001$ v [3]. The latter emf is substracted to obtain the reversible potential of beryllium with reference to the chlorine electrode :

$$E_1 = -2{,}629 + 2{,}19 \cdot 10^{-4} \cdot T \pm 0{,}007 \text{ v}$$
$$E_2 = -2{,}650 + 3{,}39 \cdot 10^{-4} \cdot T \pm 0{,}006 \text{ v}$$
$$E_3 = -2{,}695 + 4{,}80 \cdot 10^{-4} \cdot T \pm 0{,}009 \text{ v}$$

TABLE 1

T, °K	k	[Be⁺]	[Be⁺⁺]	E	E^0_{Be/Be^+}	$E^0_{Be/Be^{++}}$
Melt with 0,023% Be						
700	$2,26 \cdot 10^{-5}$	$1,14 \cdot 10^{-4}$	$5,77 \cdot 10^{-4}$	−2,476	−1,928	−2,251
800	$1,70 \cdot 10^{-4}$	$2,86 \cdot 10^{-4}$	$4,23 \cdot 10^{-4}$	−2,454	−1,887	−2,186
900	$8,15 \cdot 10^{-4}$	$4,48 \cdot 10^{-4}$	$2,43 \cdot 10^{-4}$	−2,432	−1,834	−2,109
1000	$2,86 \cdot 10^{-3}$	$5,76 \cdot 10^{-4}$	$1,15 \cdot 10^{-4}$	−2,410	−1,767	−2,019
1100	$7,98 \cdot 10^{-3}$	$6,39 \cdot 10^{-4}$	$5,2 \cdot 10^{-5}$	−2,388	−1,691	−1,921
1200	$1,88 \cdot 10^{-2}$	$6,50 \cdot 10^{-4}$	$4,1 \cdot 10^{-5}$	−2,366	−1,607	−1,844
Melt with 0,169% Be						
700	$2,26 \cdot 10^{-5}$	$3,3 \cdot 10^{-4}$	$4,85 \cdot 10^{-3}$	−2,413	−1,930	−2,252
800	$1,70 \cdot 10^{-4}$	$8,55 \cdot 10^{-4}$	$4,32 \cdot 10^{-3}$	−2,379	−1,892	−2,191
900	$8,15 \cdot 10^{-4}$	$1,69 \cdot 10^{-3}$	$4,49 \cdot 10^{-3}$	−2,345	−1,850	−2,126
1000	$2,86 \cdot 10^{-3}$	$2,68 \cdot 10^{-3}$	$2,50 \cdot 10^{-3}$	−2,311	−1,801	−2,052
1100	$7,98 \cdot 10^{-3}$	$3,58 \cdot 10^{-3}$	$1,60 \cdot 10^{-3}$	−2,277	−1,743	−1,972
1200	$1,88 \cdot 10^{-2}$	$4,23 \cdot 10^{-3}$	$9,50 \cdot 10^{-4}$	−2,243	−1,678	−1,883
Melt with 1,13% Be						
700	$2,26 \cdot 10^{-5}$	$8,68 \cdot 10^{-4}$	$3,35 \cdot 10^{-2}$	−2,359	−1,934	−2,257
800	$1,70 \cdot 10^{-4}$	$2,33 \cdot 20^{-3}$	$3,21 \cdot 10^{-2}$	−2,311	−1,893	−2,192
900	$8,15 \cdot 10^{-4}$	$4,88 \cdot 10^{-3}$	$2,95 \cdot 10^{-2}$	−2,263	−1,850	−2,126
1000	$2,86 \cdot 10^{-3}$	$8,56 \cdot 10^{-3}$	$2,58 \cdot 10^{-2}$	−2,215	−1,905	−2,057
1100	$7,98 \cdot 10^{-3}$	$1,30 \cdot 10^{-2}$	$2,14 \cdot 10^{-2}$	−2,167	−1,755	−1,985
1200	$1,88 \cdot 10^{-2}$	$1,76 \cdot 10^{-2}$	$1,68 \cdot 10^{-2}$	−2,119	−1,702	−1,908

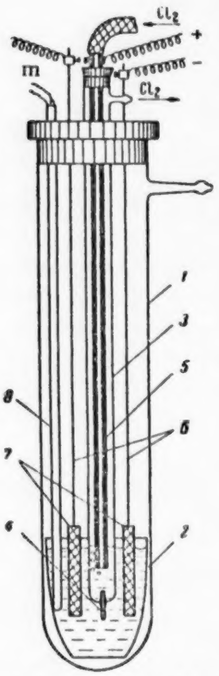

Fig. 1. Cell: 1) quartz tube; 2) BeO crucible; 3) quartz tube; 4) asbestos diaphragm; 5) graphite tube (chlorine electrode); 6) molybdenum lead, 7) beryllium electrode; 8) thermocouple.

Figure 3 gives isotherms of the reversible potential of the beryllium electrode (E vs log [Be]) which were developed from the experimental data. The valence of the beryllium ions contained in a melt which is in contact with the metal can be determined from the slope of the isotherm at the temperature in question. These slopes are :1.96 at 700° K; 1.85 at 800° K; 1.77 at 900°K; 1.70 at 1000° K; 1.67 at 1100°K and 1.61 at 1200°K . This confirms the belief that the melt contains not only Be^{++} ions, but Be^{+} ions as well, the proportion of these latter ions increasing with the temperature.

Knowing the temperature dependence of the equilibrium constant for the reaction $Be^{++}_{(melt)} + Be_{(S)} \rightleftharpoons 2\,Be^{+}_{(melt)}$ to be given by the equation log K = 2.36−(4904/T),the mole fractions of the ions, $[Be^{++}]$ and $[Be^{+}]$, in the melt at any temperature can be calculated through the equation : $[Be^{+}] = \frac{\sqrt{k(k+4[Be])} - k}{2[Be]}$ and $[Be^{++}] = [Be] - [Be^{+}]$, [Be] being the analytically determined mole fraction of beryllium in the melt. At equilibrium, the potential of the beryllium electrode with reference to the univalent ions is equal to the sum of its potential relative to the divalent ions and the redox potential of the Be^{+}/Be^{++} system.

Table 1 gives calculated results on melts containing various amounts of beryllium in the temperature interval 700–1200° K.

The temperature dependence of E^0_{Be/Be^+} and $E^0_{Be/Be^{++}}$ for melts of those concentrations which have been investigated is shown graphically in Figure 4. The results are seen to be quite consistent at temperatures below 900°K. At higher temperatures, the deviations are pronounced. It is clear that this is in part due

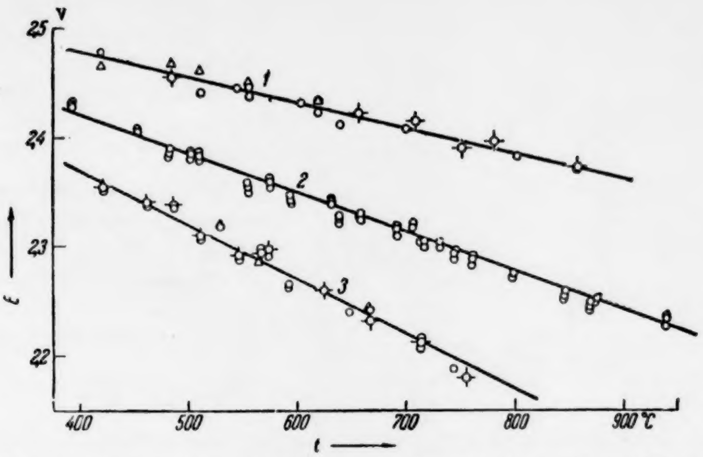

Fig. 2. The temperature dependence of the emf of the cell Be/ $BeCl_2$, LiCl, KCl/ Cl_2, C with an electrolyte containing 0.023 % Be (Curve 1), 0.169 % Be (Curve 2), or 1.13 % Be (Curve 3).

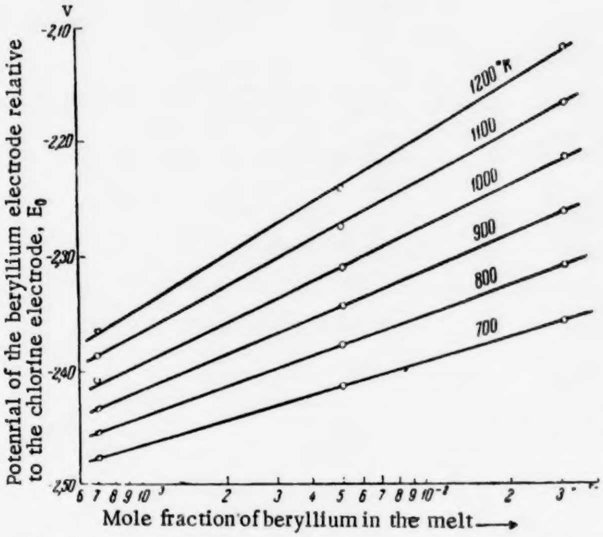

Fig. 3. Isotherms of the beryllium electrode potential.

to the fact that the analytically determined concentration of beryllium in a salt mixture cooled to room temperature is not the same as the concentration in the high temperature melt, the latter concentration being the larger because of the dissolving of the metal in the reaction :

$$Be^{++}_{(melt)} + Be_{(S)} \rightleftharpoons 2Be^{+}_{(melt)}$$

and this difference becomes more significant at the higher temperatures.

The temperature dependence of E^0_{Be/Be^+} and $E^0_{Be/Be^{++}}$ in the interval 700-900° K can be represented by the empirical equations :

$$E^0_{Be/Be^+} = (-\ 2{,}212 + 4{,}0 \cdot 10^{-4} \cdot T)\ v \quad E^0_{Be/Be^{++}} = (-2{,}702 + 6{,}4 \cdot 10^{-4} \cdot T)\ v$$

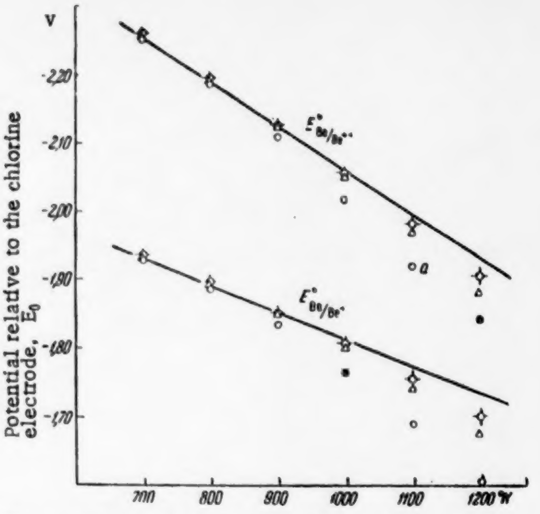

Fig. 4. The temperature dependence of E^0_{Be/Be^+} and $E^0_{Be/Be^{++}}$; melts with: a) 0.023, b) 0.169 and c) 1.13 % Be.

These questions for the temperature dependence can be used to obtain an expression for the constant in the thermodynamic equation for the redox potential of the Be^+/Be^{++} system in melts of the alkali metal chlorides; namely

$$E^0_{Be^+/Be^{++}} = (-3{,}192 + 8{,}8 \cdot 10^{-4} \cdot T)\ \text{v}$$

The decomposition potential of molten beryllium monochloride can be calculated from the value of E^0_{Be/Be^+} if the assumption is made that solutions in the molten chlorides of the alkali metals behave ideally over the entire range of concentrations up to the pure salt:

$$E_{BeCl\,(l)} = (2{,}212 - 3{,}4 \cdot 10^{-4} \cdot T)\ \text{v}$$

From this there follows an expression for the change in free energy in the formation of liquid beryllium monochloride from the elements

$$Be_{(s)} + {}^1/_2\, Cl_{2\,(g)} = BeCl_{(l)}$$
$$\Delta Z = -51\,000 + 7{,}8 \cdot T\ \text{cal/mole}$$

Thus the entropy and the standard heat of formation of liquid beryllium monochloride are

$$\Delta H_{BeCl\,(s)} = -51\,000\ \text{cal/mole and}\ S^0_{BeCl\,(s)} = 21{,}2\ \text{cal/mole} \cdot \text{deg}$$

the former being obtained from the entropy change of the above reaction and the literature data on the entropies of beryllium and chlorine.

LITERATURE CITED

[1] M. V. Smirnov and N. Ya. Chykreev, J. Phys. Chem. 32, 2165 (1958).

[2] M. V. Smirnov and N. Ya. Chykreev, J. Inorg. Chem. 4, No. 11 (1959).

[3] M. V. Smirnov and L. E. Ivanovskii, J. Phys. Chem. 31, 802 (1958).

Received April 13, 1959

AN INVESTIGATION OF THE EFFECT OF ADDED LIQUIDS IN THE FINE DISPERSING OF QUARTZ

G. S. Khodakov and Academician P. A. Rebinder

The All-Union Scientific-Research Institute for Fine Pulverization,
Academy of Building and Architecture, USSR

The Institute of Physical Chemistry of the Academy of Sciences of the USSR

The adsorption of various surface-active substances considerably facilitates the fine dispersing of such solid bodies as quartz, cement, and lime by wet and dry grinding [1-11]. The effectiveness of a surface-active substance is markedly dependent on the nature of this substance, the conditions under which dispersing is being carried out, the properties of the solid body and its state of dispersion. No attention is generally given to the fact that the effectiveness of action of a surface active substance is dependent on the degree of dispersion of the solid body and this results in the marked divergencies which are observed in the evaluation of adsorptional effects. There has, in addition, been no adequate study of the role played by the liquid medium in forming a high dispersion of solid bodies, quartz in particular, and this has been the cause of difficulties in forming dispersions and carrying out dispersional analysis in such systems [12].

We have studied the effect of the addition of acetone, ethyl alcohol, water, benzene, and certain other substances, on the dispersing of quartz sand. A laboratory vibromill [13] was used for the pulverization, and the degree of dispersion was determined from the specific surface as measured through the low temperature adsorption of nitrogen [14] in a specially constructed apparatus [15].

The experimental data of Figures 1 and 2 show that the grinding of quartz sand with 40-80 % water (per weight of quartz) leads to an increase in the specific surface which is many times greater than that which is reached through dry grinding. The effect of the added water increases with an increase in the length of the dispersing process. The presence of the water brings about little change in the rate of dispersing of relatively coarse particles if the grinding lasts for less than 2 minutes. Lengthening the time of dry grinding does not lead to a further increase in the specific surface, whereas even very fine powders with a specific surface of 60-70 m^2/g will disperse with considerable velocity in water.

The specific surface of dry-ground powders reaches a maximum of approximately 10 m^2/g and then remains constant as the grinding period is increased. A brief 10-30 second grinding of these powders with 40 % or more of water results in a marked increase in the specific surface which greatly exceeds the increase that would be expected from a supplementary treatment of such duration. There is no spontaneous increase in the specific surface of the powders from dry grinding, even when these powders are held in water for a long time.

An increase in the specific surface during short-term grinding in water is also observed in the case of powders obtained from the dispersing of quartz sand with small additions of water (up to 4 % by weight of quartz), acetone, alcohol, or benzene. The experimental data of Figures 1 and 2 show that there is little distinction between the kinetics of increase of the specific surface of quartz powders dispersed with these additives (without short-term grinding in water) and the kinetics of dry grinding. On the other hand, short-term grinding of such powders in water leads to an approximate 3-5 fold increase in the specific surface.

The experimental data can be explained by assuming that grinding leads to a curious formation of rather dense, but comparatively unstable, aggregates of particles with still smaller particles filling the pores between

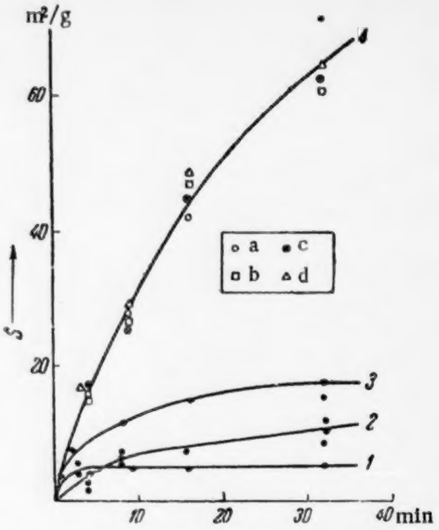

Fig. 1. The dispersing of quartz sand in a gyrational mill at an amplitude of 4 mm : 1) dry, without disaggregation; 2) in acetone, benzene and alcohol, without disaggregation; 3) dry, with disaggregation; 4) in water (a), benzene (b), acetone (c), and alcohol (d) with subsequent disaggregation in water.

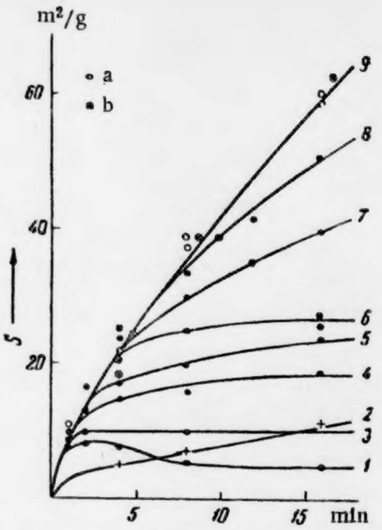

Fig. 2. The dispersing of quartz sand in a gyrational mill at an amplitude of 5 mm: 1) dry, without disaggregation; 2) with 80 % acetone, without disaggregation; 3) with 1.2% water, without disaggregation; 4) dry, with disaggregation in water; 5,6,7, and 8) with 0.04, 0.2, 0.4 and 1.2 % respectively of water with disaggregation; 9) with 80 % water (a) and 80 % acetone (b) with disaggregation.

TABLE 1

The Decrease in the Specific Surface of Highly Dispersed Quartz Powder During Additional "Grinding".

Medium	Duration of additional "grinding", min	Specific surface, m²/g starting material	Specific surface, m²/g after additional "grinding"
Dry	16	58	28
1,2% water	16	58	32
2,5% water	16	58	34
5,0% water	16	58	35
50,0% water	16	60	140
Dry	20	74	22
33% acetone	20	74	40

these particles. This dense packing renders the greater part of the inner surface of these aggregates unavailable for the adsorption of the nitrogen molecules. Most of the methods of dispersional analysis are similar to x-ray analysis in that they mark out these aggregates as coarse individual particles. The primary particles are amorphous and their dimensions are too small [16] for x-ray analysis to give positive results in such a case.

The compact fusion of the powder particles and their disaggregation in water are, to a certain degree, reversible processes. Thus a compact fusion of particles is also observed with a highly dispersed quartz powder which has been first ground in water, dried, and then once more subjected to dry grinding. A considerable diminution of the specific surface is also noted in grinding powders with acetone, and with small amounts of water (Table 1). Aggregates which have been obtained in this way can be readily broken down by grinding in water, the resulting degree of dispersion being equal to or greater than the original.

The very marked influence of the water content of the powder on the effectiveness of dispersing is indicated by the data of Figures 2 and 3 on the grinding of quartz powder to which various amounts of water had been added. Thus, the effectiveness of dispersion with as little as 0.04 % water is much greater than that of dry grinding and this effectiveness sharply increases as the water content of the sand is raised to 1 %. The effectiveness of dispersing precipitately falls as the water content is increased from 2 to 30, but once more rises sharply at 30-40 %, reaching a maximum for wet grinding with 50-80 % water. The diminished effectiveness of grinding at a water content of 2-30 % is related to the development of a structure of quartz sand grains with menisci and fine interlayers of water to impede the grinding.

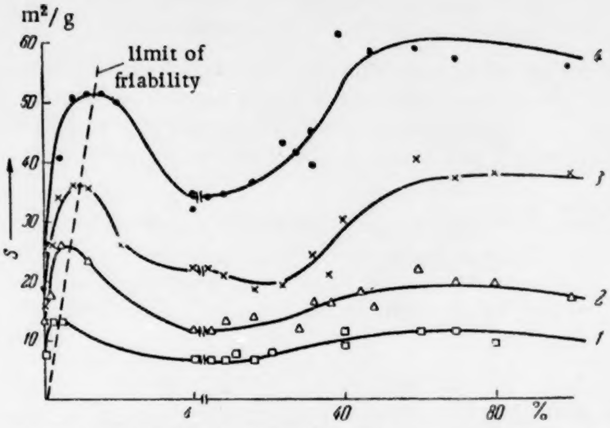

Fig. 3. The relation between the effectiveness of grinding of quartz sand and the percentage of water. Dispersing time : 1) 2 minutes; 2) 4 minutes; 3) 8 minutes; 4) 16 minutes .

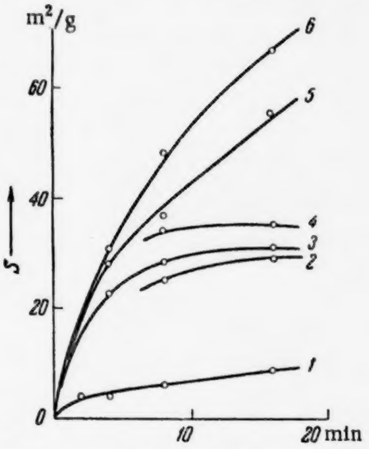

Fig. 4. The dispersing of quartz sand with addition of triethanolamine, oleic acid, or paraffin : 1) with 3% triethanolamine, without disaggregation; 3, 5, 6) with 0.16, 0.32 and 1.2 % triethanolamine, respectively, with disaggregation; 2) with 1 % oleic acid, with disaggregation; 4) with 0.4% paraffin, with disaggregation .

TABLE 2

The Effect of Small Additions of Water, Acetone, Ethyl Alcohol, and Benzene on the Dispersing of Quartz (duration, 16 min ; amplitude, 5 mm)

Liquid content, cm³ per 25 g quartz	Specific surface, m²/g			
	water	acetone	alcohol	benzene
Dry	19	19	19	19
0,05	25	26	21	29
0,1	41	32	28	29
0,3	52	43	41	41
0,6	—	56	62	59
0,9	—	48	59	41
1,2	35	68	60	49

The data of Figures 1 and 2 indicate that the grinding of quartz in acetone, ethyl alcohol, and benzene (with disaggregation, and taking the increase of the specific surface during the time of grinding into account) is just as effective as the grinding in water, the process being unaffected by the presence of aggregates. The effect of even small additions of these substances (not more than enough for a monolayer at the end of dispersing) is quite similar to that of water (Table 2). The data of the table indicate that it is impossible to account for the increase which occurs in the specific surface during grinding with acetone, alcohol, and benzene by supposing these substances to be contaminated with other materials, especially water. If this were so, the benzene used in these experiments would have had to contain as much as 30 % water. In actuality, this benzene was known to contain less than a fraction of one percent of water and other contaminants.

The uniform effectiveness (within the limits of experimental error) of the dispersing of quartz in acetone, alcohol, water, and benzene is in complete agreement with the theory of adsorptional diminution of stability which postulates that the decrease in the interfacial tension is the factor determining the diminution of the stability of solid bodies in liquid media under fixed conditions. The heats of wetting of silica by water, benzene, acetone and ethyl alcohol are, in fact, known [14, 17, 19] to be approximately the same.

The addition of small amounts of triethanolamine to quartz sand leads to a many-fold increase in the effectiveness of dispersing, as is to be seen from Figure 4. On the other hand, there is a relatively small effect from the addition of oleic acid or paraffin, substances in which the heat of wetting of quartz is comparatively low. There is a fusion of particles in each of these cases and this fusion can be broken down by a short-term grinding in water.

The results which have been obtained here are of general applicability since the effects studied in this work are not peculiar to quartz but are , as experiments show, equally characteristic of such solid bodies as corundum and calcite. The action of triethanolamine and oleic acid on the dispersing of calcite is different from that described above in that these substances are much more effective than water, a fact which is related to the much less pronounced hydrophilic nature of calcite .

LITERATURE CITED

[1] P. A. Rebinder, Report, VI Congress of Russian Physicists (Moscow, 1928)[in Russian].

[2] P. A. Rebinder, L. A. Shreiner and K. F. Zhigach, Hardness Reducing Solutions in Boring [in Russian] (Moscow-Leningrad, 1944).

[3] I. L. Éttinger and I. M. Protod'yakonov, Proc. Acad. Sci. USSR 84, 1825 (1952).

[4] I. L. Eichborn, Koll. Zs. 149, 128 (1956) .

[5] A. Gotte and E. Ziegler, VDI-Zs. No. 9, 98 (1956).

[6] L. I. Édel'man and D. S. Sominskii, Proc. Acad. Sci. USSR 114, 844 (1957).*

[7] G. V. Kukolev and L. G. Mel'nichenko, Refractories 13, 447 (1948).

[8] V. I. Klassen and É. I. Popova, Proc. Acad. Sci. USSR 85, No. 1 (1953).

[9] L. I. Chernyi, Proc. State Institute of Mineral Chemical Resources, Vol. 1 (1950).

[10] W. I. Petersen and F. Kreller, Met. und Erz. 38, No. 2 (1941).

[11] E. B. Matskevich and P. Yu. Butyagin, Colloid J. 20, No. 5, 665 (1958).*

[12] L. A. Feigin and V. N. Rozhanskii, Proc. Acad. Sci. USSR 115, 946 (1957).*

[13] M. I. Aronov, Inst. and Exp. Techniques, No. 1, 153 (1958).

[14] S. Brunauer, Adsorption of Gases and Vapors [in Russian] (Moscow, 1948).

[15] D. S. Sominskii and G. S. Khodakov, Scientific Reports, Institute for Building Materials Based on Fine Pulverization No. 29, (Moscow, 1957) .

[16] P. B. Dempster and P. D. Ritchie, J. Appl. Chem. 3, 182 (1953).

[17] R. K. Iller, Colloid Chemistry of Silica and Silicates , N. Y. (1955).

[18] P. A. Rebinder, V. I. Likhtman and L. A. Kochanova, Proc. Acad. Sci. USSR 111, 1278 (1956).

[19] B. S. Shvetsov, Introduction to the Chemistry of Silica [in Russian] (Moscow-Leningrad)

Received May 22, 1959

---

* Original Russian pagination. See C.B. Translation.

STUDY OF THE STRUCTURE OF SOME ETHYLENE AND STYRENE DERIVATIVES BY MEANS OF RAMAN SPECTRA

Ya. S. Bobovich and V. V. Perekalin

(Presented by Academician A. N. Terenin, April 23, 1959)

The structure of unsaturated nitro compounds, being typical compounds with active double bonds, is determined chiefly by conjugation of the nitro group with the double bond. Consequently, the question naturally arose of their position among other compounds with double bonds, activated by electrophilic groups (nitrile, carbonyl, carboxyl, sulfonic, phosphonic). To solve this problem we used the method of measuring the intensities of the lines in the Raman spectra, systematically omitting from the comparative study the states of the double bonds found in conjugation with the indicated substituents. Here many of the ethylene and styrene derivatives were studied by us for the first time. Information as to the method of making the measurements is found in [1].

It is known that the intensity of the Raman spectra lines is a direct characterization of the state of the electron cloud of a chemical bond. Consequently, the intensity of the lines for the vibrations of the double bond and the benzene ring is found in intimate relationship to the nature of the substituting groups, the length of the conjugated chain and the spatial structure of the molecule*, reflecting their participation in the π-electron interaction.

In Tables 1 and 2 we have given the vibration frequencies in cm^{-1}, and (in parentheses), using an arbitrary scale, the intensities of the vibrations of the double bond and the benzene ring.

As can be seen from the data in Table 1, the intensity coefficient $I_{C=C}$ of the vibration line for the isolated double bond has a characteristic value of 0.023 in compound (I). The introduction of a nitro group in the conjugated position exerts substantial influence on the double bond, expressed in a sharp (approximately 8-fold) intensification of the vibration line of this bond in (II). The strong activating influence exerted by the triple bond in (III, IV) also deserves attention. The last fact has also been repeatedly mentioned by other authors.

Conjugation of the bonds C= C and C = O also leads to an increase in the coefficient $I_{C=C}$; to reliably differentiate, within the limits of measurement error, between the role of the H atom and the functional groups CH_3 and OC_2H_5 has not been possible as yet**.

It proved quite unexpected that the intensity coefficients $I_{C=C}$ in vinyl sulfone (IV) and vinyl phosphone (X) were considerably smaller than in the olefin with isolated double bond (I). As far as we know, similar observations are not mentioned in the literature. The low values of the coefficients $I_{C=C}$ in (IV) and (X) also remain incomprehensible from the chemical viewpoint. Actually, the sulfonic group, containing a sulfur atom with a double positive charge, exerts a substantial electrophilic effect on the methylene groups and aromatic rings attached to it in methylene sulfones and aromatic sulfone derivatives [2]; a similar influence of the phosphonic radical is expressed to a lesser degree [3]. In addition, compounds (IX) and (X), like all other compounds with active double bonds, react with compounds having labile hydrogen atoms in the methylene and methyl groups [4,5]. However, it should be kept in mind that the intensity of Raman spectra lines always reflects the static effect of conjugation, whereas in nucleophilic addition reactions it is probably the dynamic effect that appears.

---

* This important problem will not be discussed in the present paper.

** Exact measurements in the spectra of these compounds, dissolved in acetone, are made difficult by the partial superimposition of the vibration lines of the C=O bonds.

TABLE 1

Compound	Vibration of the C=C bond	Compound	Vibration of the C=C bond
I $CH_2 = CH - CH(CH_3)_2$	1660 (0,023)	VIII $CH_2 = CH - Si(C_2H_5)_3$	1590 (0,023)
II $CH_3(CH_2)_2CH = CH - NO_2$	1650 (0,187)	IX 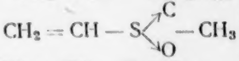 $CH_2 = CH - S(\overset{\nearrow C}{\underset{\searrow O}{}}) - CH_3$	1595 (0,020)
III $CH_2 = CH - C \equiv C - CH_3$*	1590 (0,11)	X 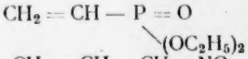 $CH_2 = CH - P(=O)(OC_2H_5)_2$	1595 (0,015)
IV $CH_2 = CH - C \equiv N$ **	1590 (0,044)	XI $CH_2 = CH - CH_2 - NO_2$	1640 (0,023)
V 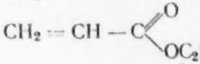 $CH_2 = CH - C(=O)OC_2H_5$	1610 (0,040)	XII $CH_2 = CH - CH_2OH$	1630 (0,022)
VI 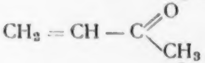 $CH_2 = CH - C(=O)CH_3$	1600 (0,036)	XIII $CH_2 = CH - CH_2Cl$	1620 (0,030)
VII 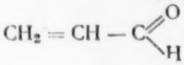 $CH_2 = CH - C(=O)H$	1605 (0,030)	XIV $CH_2 = CH - CH_2Br$	1620 (0,057)

---

* The vibration frequency of the triple bond $C \equiv C$ is equal to 2235 cm^{-1}; $I_{C \equiv C} = 0.15$.

** The vibration frequency of the triple bond $C \equiv N$ is equal to 2225 cm^{-1}; $I_{C \equiv N} = 0.075$. In CH_3CN the analogous values are equal, respectively, to 2250 cm^{-1} and 0.026.

In nitro compounds, in which the double bond and the nitro group are separated by a methylene group, the specific properties of the conjugated nitroolefins, disappear. Thus, in nitroallyl (XI) the intensity coefficient $I_{C=C}$ coincides exactly with the same value in the spectra of (I), (VIII) and (XII). Apparently, in nitroallyl (XI) the methylene group serves as a dependable "barrier", preventing the mutual influence of the nitro group and double bond. It is interesting that the vibration frequencies in the spectra of compounds (I, VIII, XI and XII) show substantial variation here.

The chloro- and bromoallyls (XIII and XIV) stand in a special class. In these compounds, in contrast to nitroallyl (XI) and allyl alcohol (XII), the methylene group between the halogen atoms and the double bond is no longer a "barrier", stabilizing the value of the coefficient $I_{C=C}$.

We can assume that in the haloallyls vibration of the double bond ceases to be sufficiently characteristic, as a result of which a substantial contribution to its intensity is made by the motions of the atoms involving the C-halogen bond. However, this postulation contradicts the fact that the degree of covalency shown by the C-Cl and C-Br bonds differs by a total of only about 4%, while the intensity of the corresponding lines differs by nearly 100%. It would be more valid to associate the effect with the specific nature of the halogen atoms. It will be shown below that the chlorine atom behaves in a similar manner in a number of styrene derivatives.

The fact that the decisive role in intensifying the vibration line of the double bond belongs specifically to the halogen atoms also follows from a comparison of their covalent radii. According to Pauling [6], the covalent radii show substantial increase in going from chlorine to bromine and iodine. If a qualitative description of the mutual influence exerted on each other by the double bond and halogen atoms is approached from the point of view of the quantum mechanical model of a "potential cell", then an over-all lengthening of the "cell" should correspond to increasing the covalent radius of bromine in the allyl bromide molecule, causing an exceedingly sharp enhancement of the Raman spectra lines [7]. At the same time it should be mentioned that the "potential cell" model permits no more than describing the phenomenon. Also remaining unanswered here is the cause for the specific behavior shown by the halogen atoms. Obviously, the logical place to seek the answer to this question is in the structure of the electron clouds of the discussed atoms.

The results of measuring in the spectra of the styrene derivatives (Table 2) are in general, in agreement with the expected order, based on the chemical properties of these compounds. As before, the greatest influence on the C= C double bond was exerted by the directly attached nitro group.

The vibration line of the double bond in the spectrum of the sulfonyl chloride derivative (IV) is also distinguished by a substantial intensity. Comparison of the last compound with the methoxy sulfone derivative (III) and styrene (I) supports our theory as to the specific role of the Cl atom. Conjugation with the C=O bond in the given series of compounds proves to be substantially more effective than in the earlier discussed ethylene derivatives.

TABLE 2

	Compound	Vibration of the C=C bond	Antisymmetric vibration of the benzene ring
I	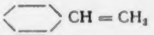 $CH=CH_2$	1640 (0,42)	1610 (0,30)
II	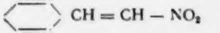 $CH=CH-NO_2$	1630 (4,3)	1600 (2,4)
III	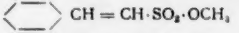 $CH=CH\cdot SO_2\cdot OCH_3$	1610 (1,3) *	
IV	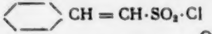 $CH=CH\cdot SO_2\cdot Cl$	1620 (3,3)	1590 (0,8)
V	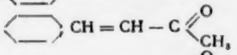 $CH=CH-C(=O)CH_3$	1580 (3,5) *	
VI	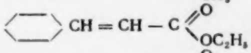 $CH=CH-C(=O)OC_2H_5$	1620 (2,0)	1580 (1,0
VII	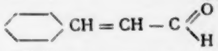 $CH=CH-C(=O)H$	1615 (2,6) *	
VIII	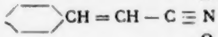 $CH=CH-C\equiv N$	1610 (2,0) *	
IX	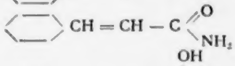 $CH=CH-C(=O)NH_2$	1620 (1,0)	1570 (0,7)
X	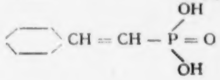 $CH=CH-P(=O)(OH)_2$	1600 (1,0—1,5) *	

---

* The vibration lines of the C= C bond and benzene ring are resolved poorly or not at all. Their total intensity is given.

Here the presence of the amino group weakens the effect somewhat. As before, the compound with a phosphonic group (X) occupies a special place; to be sure, in the given case the presence of this group does not lower the coefficient $I_{C=C}$ when compared to its value in the spectrum of styrene (I) .

LITERATURE CITED

[1] Ya. S. Bobovich and V. V. Perekalin, Proc. Acad. Sci. USSR 121, 1028 (1958).*

[2] V. V. Perekalin, Collected Memoirs of L. E. Porai-Koshits [In Russian] (Leningrad, 1949),p. 159.

[3] A. N. Pudovik and O. N. Grishina, J. Gen. Chem. 23, 267 (1953).*

[4] W. E. Truce and E. Wellisch, J. Am. Chem. Soc. 74, 2881 (1952)

[5] W. Reppe, Lieb. Ann. 601, 115 (1956).

[6] L. Pauling, The Nature of the Chemical Bond [Russian Translation] (Moscow, 1947).

[7] M. V. Vol'kenshtein and S. M. Yazykova, Proc. Acad. Sci. USSR 104,834 (1955).

Received April 2, 1959

---

* Original Russian pagination. See C.B. Translation.

TEMPERATURE DEPENDENCE OF THE RATE OF REVERSE SPONTANEOUS DISSOCIATION PROCESSES

V. I. Gol'danskii

A.N. Lebedev Physical Institute Academy of Sciences of the USSR

(Presented by Academician V. N. Kondrat'ev, April 11, 1959)

In analyzing the possible role of quantum effects in the kinetics of chemical reactions the principal attention is most frequently given to the tunnel transitions through activation barriers (see, for example, [1,2]). At the same time, an examination of the quantum effects in barrierless transitions, associated with the creation of discrete energy, levels, also possesses unconditional interest. An example of such transitions are photochemical spontaneous dissociation processes of the type

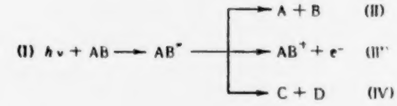

$$\text{(I)}\quad h\nu + AB \longrightarrow AB^{*} \longrightarrow \begin{cases} A + B & \text{(II)} \\ AB^{+} + e^{-} & \text{(III)} \\ C + D & \text{(IV)} \end{cases}$$

illustrated in Fig. 1 (where for clarity we have shown a large E_0 —of the order of D, though the specific nature of the examined case appears quite clearly at fairly small values of E_0 — of the order of kT).

Such processes are quite widespread; for example, the photolysis of aniline, and of many alkyl halides, aldehydes, ketones and alcohols is of the spontaneous dissociation type. Examples are also known in which it is possible for such photolysis to go in several directions ($AB^{*} \begin{smallmatrix} \nearrow A + B \\ \searrow C + D \end{smallmatrix}$ in the given scheme), for example

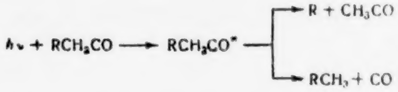

$$h\nu + RCH_2CO \longrightarrow RCH_2CO^{*} \longrightarrow \begin{cases} R + CH_3CO \\ RCH_3 + CO \end{cases}$$

It is clear that all of the mutual transformation processes (I), (II), (III) and (IV) can go through the intermediate excited state AB^{*} , both reverse spontaneous dissociation (process with the emission of light of a definite wavelength) and different variations of the recombination of radicals or ions (in the last case we do not consider coulomb interaction, i.e., we do not discuss purely ionic, but instead ionic-radical or electronic-radical recombination).

It is clear that a definite kinetic energy of the reaction products corresponds to each spontaneous dissociation direction, to the extent that it passes through a definite intermediate excited state. It is also clear that in the collision of the reaction products (for example, A + B), possessing a kinetic energy that corresponds to the given level of excitation AB^{*} , it is possible for any processes of the reverse spontaneous dissociation type to take place, both processes with the emission of light of a definite wavelength and other processes, going through the same intermediate state.

The mutual disturbing influence exerted by the potential curves of attraction and repulsion leads to the situation that instead of a point of intersection of these curves there arises a dissociation gap of effective width G., shown as the striped zone in Fig. 1. The relationship between the probability of spontaneous dissociation (as well as of its reverse processes) and the energy of the system, within the limits of the dissociation gap, is described approximately by the known Landau-Zinner equation. However, as soon as G << kT, it can simply be assumed that this probability is constant within the limits of the entire gap and is equal to zero beyond its limits.

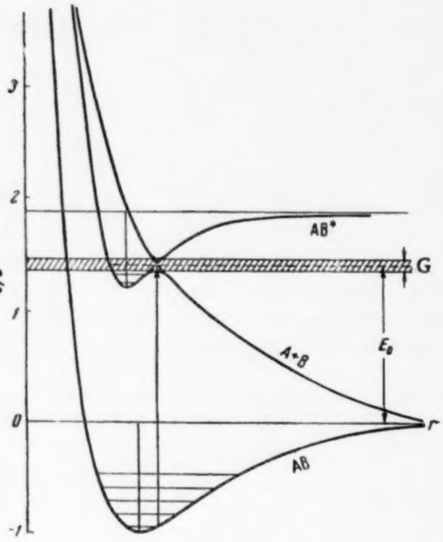

Fig. 1

As is known, the life span of the excited dissociation state lies in the limits between the rotational (10^{-11} sec) and vibrational (10^{-13} sec) periods, which corresponds to $10^{-16} < G < 10^{-14}$ erg. In the intersection of curves, relating to states with different values of the resulting spin, the effective width of the gap G is even smaller and constitutes 10^{-15} to 10^{-17} erg. As a result, the condition $G \ll kT$ not only holds almost always for either room or higher temperature, but frequently is also valid for much lower temperatures.

Thus, we will assume that, within the limits of the dissociation gap, the section of any i-th process, going through the excited state AB*, is constant and equal to $\sigma_i = \sigma_0 \frac{G_i}{G}$, where G_i is the partial width relating to the given process, and σ_0 is the geometric section of interaction.

The temperature dependence of the rate constant of such processes is determined by the shape of the "dissociation resonance" and the distribution character of the reacting particles according to the energies.

With a Maxwellian distribution of the reacting particles according to the rates of their relative movement, the rate constant of the process $A + B \rightarrow AB^* \rightarrow C + D$ is obtained by integrating:

$$Z_{AB}^{CD} = \frac{2\pi}{(\pi kT)^{3/2}} \sqrt{\frac{2}{\mu}} \int_0^\infty \sigma_0 \frac{\Gamma_i}{\Gamma} E e^{-E/kT}\, dE, \tag{1}$$

where E is the energy of the relative movement of A and B, E_0 is the value of E corresponding to the level AB* and μ is the brought mass AB.

To obtain Z_{AB}^{CD} in the general form it is necessary to know the nature of the energy relationship between σ_0 and G_i/G. In two particular cases the problem is greatly simplified. At $\sigma_0 G_i/G = \sigma_i = \text{const.}$ (i.e., in the case of an infinite width of the gap)

$$Z_{AB}^{CD} \sim 2\sqrt{\frac{2kT}{\pi\mu}}\, \sigma_i \ \text{CM}^3/\text{sec}, \tag{2}$$

which is G/G_i times smaller than the usual constant of binary collisions, not requiring an activation energy.

In the more important and singular case of a narrow (when compared to kT) gap, it becomes possible to reduce (1) with good approximation to

$$Z_{AB}^{CD} = \left(\frac{2\pi}{\pi kT^{3/2}}\right) \sqrt{\frac{2}{\mu}}\, \sigma_i \Gamma E_0 e^{-E_0/kT}. \tag{3}$$

It is evident that the presence of a sufficiently narrow dissociation gap leads to a highly specific character for the relationship between the temperature and the rate of a process of the reverse spontaneous dissociation type—the rate proves to be maximum at the temperature $T_m = (2/3)(E_0/k)$, and the normal (positive) temperature coefficient is observed only in the region $T < T_m$ (Fig. 2), in which, as a result, the Arrhenius rule is fulfilled.

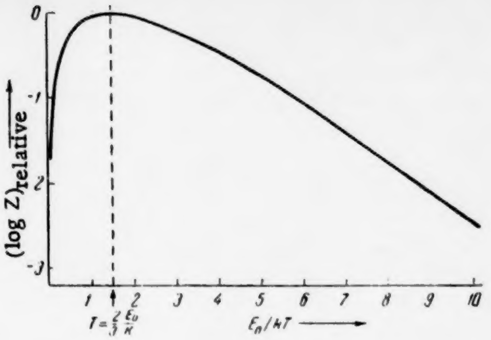

Fig. 2

At higher temperatures ($T > T_m$) the temperature coefficient is negative, and the reaction rate decreases with increase in the temperature, in the limit of higher T as $Z^{CD}_{AB} \sim T^{-\frac{3}{2}}$.

The maximum value of the rate constant of the reaction is

$$(Z^{CD}_{AB})_m = \sqrt{\frac{18}{\pi\mu kT_m}}\,\sigma_i\Gamma e^{-3/2}, \qquad (4)$$

which is $\frac{2}{3}\,\frac{kT_m}{G_i}\,e^{\frac{3}{2}} = \frac{E_0}{G_i}\,e^{\frac{3}{2}}$ times smaller than the usual constant of binary collisions, not requiring an activation energy. It is clear that even with a small activation energy present in the usual processes, they always prove to be less probable at sufficiently low temperatures than the above discussed processes of the reverse dissociation type.

In particular, it is possible to associate the presence of luminescence, accompanying the progress of many chemical reactions (see, for example, [3]), including those at low temperatures, with processes of the reverse spontaneous dissociation type. From this point of view, a study of the spectra of such luminescence in order to determine whether it is only continous (recombination) or whether it contains discrete lines (bands) is of great interest.

In addition, it would be of interest to investigate the relationship between the yield of such luminescence and the energy of the bombarding ions or electrons, beginning with the heat region.

The author wishes to thank N. D. Sokolov and E. E. Nikitin for discussing this work.

LITERATURE CITED

[1] R. P. Bell, Proc. Roy. Soc. (A) 139, 466 (1933); 148, 241 (1935); 158, 128 (1937).

[2] V. I. Gol'danskii, Proc. Acad. Sci. USSR 124, No. 6 (1959).*

[3] R. F. Vasil'ev, O. B. Karpukhin, V. Ya. Shlyapintokh, and N. M. Émanuél', Proc. Acad. Sci. USSR 124, No. 6 (1959).*

Received March 23, 1959

---

* See C. B. Translation.

THE WIDTH OF THE CHEMICAL REACTION ZONE IN A TROTYL DETONATION WAVE

A. N. Dremin and P. F. Pokhil

Institute of Chemical Physics Academy of Sciences of the USSR

(Presented by Academician V. N. Kondrat'ev, April 7, 1959)

In the generally accepted picture of the structure of a stable flat detonation wave (d.w.), which was first proposed by Zel'dovich [1], it is postulated that the wave consists of a shock front, followed by the chemical reaction zone, ending in the Chapman-Zhug plane (Fig. 1). In this paper we give the preliminary results of experimentally measuring the width a of the chemical reaction zone of a trotyl d. w. of variable initial density. The method of measuring used is similar to that described in [2]. The profile of a shock wave in a metal is determined by measuring the initial rate of movement of the free surface W of metal plates of different thickness l. (It is assumed that the shock adiabatic of the metal is known.)

As had been established [3,4], $W=2U_M$ (U_M is the mass rate in the metal). W was measured by means of electric contact transducers, the signals from which were recorded using an OK-15M oscillograph. The results obtained are given in Table 1 and plotted in Fig. 2. In the work we used trotyl that had been ground and sifted through a screen with 20 openings per linear centimeter. Size of the charges: height together with the explosion lens, forming the flat front, 85 mm; diameter 40 mm.

On the average, 5-10 experiments were run for each thickness of the plates. For plates 3 mm and thicker the average relative error of measuring was 1.0-1.5%, and for plates with a thickness of several tenths of a millimeter it was 4.0-5.0%.

Knowing the profile of the shock wave in the metal and the detonation rate D, we calculate a:

$$a = b\frac{D}{D_2}\frac{U_1 + C - D_2}{U_1 + C_1 - \alpha D}(1 - \alpha), \tag{1}$$

where D_2 is the average rate of the shock wave in the metal in the region of the chemical peak influence, U_1 and C_1 are respectively the mass rate and the sound rate in the metal at depth, b, and $\alpha = U_2/D$, where U_2 is the average mass rate of the metal in the region of the chemical peak influence. D_2 and C_1 are determined from known values of W and the shock adiabatic of the metal.

Calculating the total error gives a value of about 20-30%. It must be assumed that the obtained results are accurate to this extent.

Knowing the function W = f(l) permits calculating besides a, also the pressure P and the mass rate U in the chemical reaction zone of the descending d.w. This calculation is made using the acoustic approximation [2]

$$P = \frac{P_M}{2}\left(1 + \frac{\rho_0 D}{\rho_{0M} D_M}\right). \tag{2}$$

Here P is the pressure, ρ_0 is the initial density, and D is the rate of the shock wave (for e.s. this rate is equal to the detonation rate). Subscript M refers to the metal. Starting from the rule of impulse retention and Equation

TABLE 1

ρ_0, g/cm^3	Metal	b, mm	W_b, km/sec	$\overline{W}$, km/sec	Initial rate W of movement of free surface of metal plates with thickness 1											
1,55	Cu	0,62	1,37	1,67	l, mm	5,00	2,74	1,92	1,34	0,74	0,58	0,48	0,30	0,20	0,13	
					W, km/sec	1,31	1,32	1,38	1,36	1,37	1,39	1,47	1,63	1,80	1,91	
1,55	Al	1,26	2,56	2,91	l	8,00	5,97	1,91	1,46	1,00	0,77	0,49	0,28	0,13		
					W	2,28	2,39	2,54	2,54	2,69	2,80	2,99	3,14	3,28		
1,55	Mg	1,50	3,35	3,74	l	5,00	3,00	2,00	1,50	1,20	0,73	0,69	0,49	0,24		
					W	3,30	3,32	3,34	3,35	3,44	3,72	3,72	3,91	4,09		
1,59	Al	1,30	2,60	3,11	l	5,00	3,50	1,46	1,03	1,20	0,80	0,60	0,40	0,20	0,26	
					W	2,48	2,55	2,59	2,72	2,64	2,84	3,06	3,16	3,56	3,28	
1,45	Al	1,80	2,26	2,83	l	8,00	4,97	2,96	1,96	1,43	1,20	1,12	0,60	0,42		
					W	2,03	2,17	2,20	2,27	2,37	2,46	2,51	2,96	3,10		
1,30	Al	2,24	1,92	2,40	l	8,00	6,00	4,98	4,00	2,99	2,00	1,88	1,34	1,10	0,60	0,30
					W	1,67	1,78	1,80	1,86	1,90	1,97	1,99	2,20	2,30	2,67	3,05
1,00	Mg	4,00	1,70	2,15	l	10,00	7,00	5,00	4,00	3,50	3,00	2,06	1,50	0,94	0,42	
					W	1,59	1,62	1,68	1,70	1,77	1,83	2,01	2,19	2,47	2,71	

(2), we obtain the expression for the mass rate U:

$$U = \frac{U_M}{2}\left(1+\frac{\rho_{0M}D_M}{\rho_0 D}\right). \tag{3}$$

The impact adiabatic of magnesium with an initial density ρ_0 Mg = 1.72 g/cm^3 has the form:

$$D_{Mg} = (4,78 + 1,16U_{Mg})\,\text{km/sec} \tag{4}$$

and is valid in the pressure interval from 60 to 400 thousand atm. The impact adiabatic of copper with an initial density ρ_0 Cu = 8.93 g/cm^3 has the form:

$$D_{Cu}=(3,64+1,96U_{Cu})\ \text{km/sec} \tag{5}$$

and is valid in the pressure interval from 170 to 520 thousand atm. The impact adiabatic of aluminum with an initial density ρ_0 Al = 2.70 g/cm^3 is copied in [5] as:

$$D_{Al} = 5,190 + \\ +20,77\lg\left(\frac{2U_{Al}+10,895}{10,895}\right). \tag{6}$$

On the basis of the experimental data, given in Table 1, we calculated the d.w. parameters at the Zhug point (P, U) and a.

The obtained results are given in Table 2.

In calculating a we neglected the reflected shock wave. The influence of this reflected wave was studied using metals with a variable dynamic toughness for determining a. The data for trotyl with an initial density ρ_0 = 1.55 g/cm^3 are given in Table 3.

The dynamic toughness of the e.s. is given in the third column in the Table, and the mean dynamic toughness of the metal in the region of the chemical peak influence is given in the fourth column.

Utilizing the data in Table 3, it becomes possible to construct the function

$$a = f\left(\frac{\rho_{0M}D_M-\rho_0 D}{\rho_0 D}\right).$$

Extrapolating this function to zero, we obtain the value a_0 (0.22 mm) under the conditions of undisturbed detonation. Utilizing the thus obtained value of a_0, we construct the function $\frac{a_0-a}{a_0} = \varphi\left(\frac{\rho_{0M}D_M-\rho_0 D}{\rho_0 D}\right)$, which is shown graphically in Fig. 3.

Assuming that this function remains valid for other trotyl densities, it then becomes possible to determine a_0 for trotyl of all densities.

TABLE 2

ρ_0, g/cm³	D, km/sec	U, km/sec	$P\cdot10^9$ bars	Metal	a, mm	ρ_0, g/cm³	D, km/sec	U, km/sec	$P\cdot10^9$ bars	Metal	a, mm
1,55	6,81	1,77	187	Cu	0,13	1,45	6,48	1,66	156	Al	0,19
1,55	6,81	1,78	186	Al	0,18	1,30	5,99	1,58	123	Al	0,21
1,55	6,81	1,74	183	Mg	0,21	1,00	5,10	1,30	64	Mg	0,32
1,59	6,94	1,76	194	Al	0,17						

TABLE 3

Metal	a mm	$\rho_0 D\cdot10^6$, g/cm²//sec	$\rho_{0M}D_M\cdot10^6$ g/cm²//sec	$\frac{a_0-a_x}{a_0}$, %	$\frac{\rho_{0M}D_M-\rho_0 D}{\rho_0 D}$, %
Mg	0,21	1,06	1,20	4,5	13,2
Al	0,18	1,06	1,92	18,2	81,0
Cu	0,13	1,06	4,72	41,0	345,0

TABLE 4

Metal	ρ_0, g/cm³	a	$\rho_0 D\cdot10^6$, g/cm²//sec	$\rho_{0M}D_M\cdot10^6$, g/cm²/sec	$\frac{\rho_{0M}D_M-\rho_0 D}{\rho_0 D}$, %	$\frac{a_0-a}{a_0}$, %	a_0	$\tau\cdot10^{-6}$, sec
Mg	1,00	0,32	0,51	1,04	104	22	0,41	0,12
Al	1,30	0,21	0,78	1,87	140	26	0,28	0,07
Al	1,45	0,19	0,91	1,93	112	23	0,25	0,06
Al	1,59	0,17	1,10	1,98	80	18,5	0,21	0,05

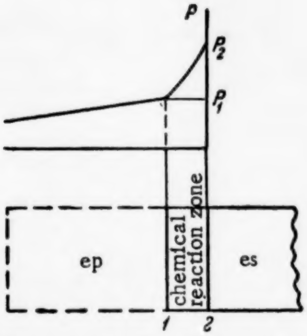

Fig. 1. Profile of the pressure in a flat detonation wave. e.s.) explosive substance; e.p.) explosion products. 1) Chapman-Zhug plane; 2) shock front of d.w.

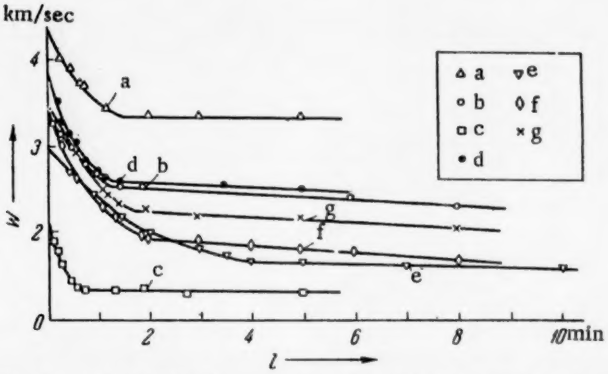

Fig. 2. Relationship between the rate of the free surface W and the thickness of the metal plate for trotyl of variable initial density: a) 1.55 g/cm³ (magnesium plates); b) 1.55 g/cm³ (Al) c) 1.55 g/cm³ (Cu); d) 1.0 g/cm³ (Mg); e) 1.30 g/cm³ (Al); f) 1.45 g/cm³ (Al); g) 1.59 g/cm³ (Al).

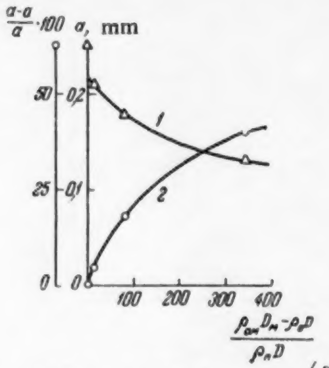

Fig. 3. 1) Function $\underline{a} = f\left(\frac{\rho_{0M}D_M - \rho_0 D}{\rho_0 D}\right)$ and 2) function $\frac{a_0 - a}{a} = \varphi\left(\frac{\rho_{0M}D_M - \rho_0 D}{\rho_0 D}\right)$.

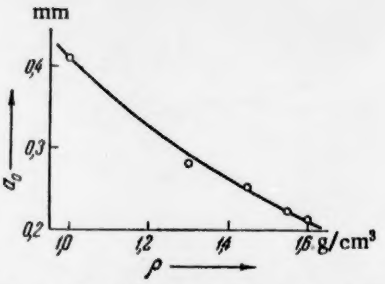

Fig. 4. Relationship between the width of the chemical reaction zone for the trotyl detonation wave and the initial density.

The obtained data are given in Table 4 and plotted in Fig. 4.

The values of the reaction time τ in the d.w. were calculated using the equation:

$$\tau = \frac{a_0}{D - \overline{U}}, \tag{7}$$

where $\overline{U}$ is the mean mass rate in the chemical peak of the d.w., which is calculated using Equation (3).

LITERATURE CITED

[1] Ya. B. Zel'dovich, J. Exptl. and Theoret. Phys. (USSR) No. 10, 542 (1940).

[2] R. E. Duff and E. Houston, J. Chem. Phys. 23, No. 7 (1956).

[3] J. M. Walsh and R. H. Christian, Phys. Rev. 97, No. 6, 1268 (1955).

[4] L. V. Al'tshuler, K. K. Krupnikov, and others, J. Exptl. and Theoret. Phys. (USSR) 34, No. 4 (1958).

[5] J. M. Walsh and M. H. Rice, J. Chem. Phys. 26, No. 4, 815 (1957).

Received March 31, 1959

STUDY OF THE ADSORPTION PROPERTIES OF SPINELS $CoMn_2O_4$ and $MnCo_2O_4$ AND OXIDES Mn_3O_4 AND Co_3O_4

V. R. Linde

Institute of Physical Chemistry Academy of Sciences of the USSR

(Presented by Academician M. M. Dubinin, April 7, 1959)

There exists a large number of binary oxides with the general formula XY_2O_4 (where X and Y are the cations of the metal or metals), belonging to the structure type of spinels, which permits changing within wide limits both the number and valence of the metal cations in the octahedral and tetrahedral sites, i.e., replacing the cations of one metal by the cations of another, or redistributing between the two types of sites the cations of one metal with different charges [1-3].

Despite the large number of investigations that have been devoted to studying the electrical and magnetic properties (which can be varied widely) of spinels and the broad practical application of individual compounds of this type, there is very little information in the literature on the adsorption properties of the spinels and the specific nature of their catalytic action [4-8].

The purpose of the present investigation was to study the adsorption properties of the oxides Mn_3O_4 and Co_3O_4, and also of the normal $CoMn_2O_4$ and inverse $MnCo_2O_4$ cobalt-manganese spinels.

The adsorption measurements were run in a static apparatus at pressures not exceeding 1 mm of Hg. The electrical resistances of the specimens were measured in a quartz cell (Fig. 1) by the method of probes at a constant current in the temperature interval 20-600°. For the electrical and adsorption measurements, and also for determining the specific surface, the powdered adsorbents were pressed into tablets 25•8•8 mm. Probes made of 0.5 mm molybdenum wire were pressed into the tablets 14 mm apart.

The specific surface values of the adsorbents were determined by the B.E.T. method from the equilibrium sorption isotherms of krypton at the temperature of liquid nitrogen [9, 10].

The specimens used in the experiments had the following specific surface values :

Specimen	Mn_3O_4	$CoMn_2O_4$	$MnCo_2O_4$	Co_3O_4
Specific surface, m^2/g	0.40	1.20	23.0	1.5

1) The Mn_3O_4 and Co_3O_4 were prepared by the decomposition of the "chemically pure" nitrates in air at high temperatures [11,12]; 2) the spinels $MnCo_2O_4$ and $CoMn_2O_4$ were synthesized by : a) the decomposition of the nitrates, taken in suitable proportions, at high temperatures, followed by ignition of the obtained oxides for several hours, and b) the ignition of mutually precipitated manganese and cobalt hydroxides [13].

The specific surface of the specimens depends on the ignition temperature of the oxides.

Thus, for the $CoMn_2O_4$ spinels the following dependence of the specific surface on the ignition temperature was observed :

Ignition temperature, °C	800	1000	1200
Specific surface, m^2/g	1.20	0.58	0.26

The formation of the proper structure was checked by the x-ray method. All of the adsorption values θ are related to the B.E.T. unit of surface (1 m^2) .

Sorption of oxygen. The kinetic isotherms for the chemisorption of oxygen on the spinels and oxides at 200° are shown in Fig. 2. The highest values for the degree of filling are obtained for Co_3O_4 (approximately 2 orders of magnitude greater than for the other adsorbents). The weakest sorption properties are possessed by the normal spinel.

The chemisorption of oxygen on the spinels is irreversible. A substantial portion of the oxygen is firmly bound, and is not removed by long evacuation at the sorption temperature (Fig. 3). To determine the kinetic rule for the sorption of oxygen on the spinels we plotted the isotherms at small changes in the pressure ($\Delta p < 0.1 p_{initial}$) ; the time interval of measurement was 3.5 units . As can be seen from Fig. 3, the sorption of oxygen on the inverse spinel obeys the bilogarithmic rule ($\log \theta - \log \tau$), and on the normal spinel it obeys the semilogarithmic rule .

The semilogarithmic rule is best obeyed for the sorption of oxygen on the oxides Co_3O_4 and Mn_3O_4. The presence of the bilogarithmic rule testifies to the exponential distribution of the activation energies of chemisorption for a heterogeneous surface and of a uniform distribution for the case of the semilogarithmic rule[14].The presence of the bilogarithmic rule in the chemisorption of oxygen on other spinels ($MgCr_2O_4$) had also been observed earlier [4].

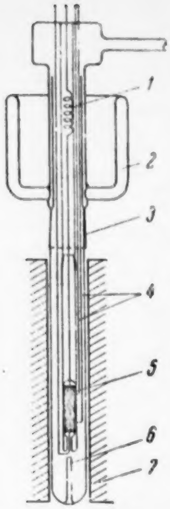

Fig. 1. Cell for measuring the electroconductivity of adsorbent specimens: 1) coil electrode, 2) Dewar vessel, 3) polished section, 4) terminal for connecting the specimen probes , 5) specimen 6) thermocouple well, and 7) heater .

Sorption of propylene. The sorption of propylene was studied on all four adsorbents at temperatures up to 200°. The isotherms for the sorption of propylene on $MnCo_2O_4$ and $CoMn_2O_4$ are shown in Fig. 2. The same as in the case of oxygen , the better adsorbent for propylene is the inverse spinel. Sorption of propylene on the two spinels goes by the semilogarithmic rule, i.e., a heterogeneity of the adsorbent surface is also revealed in the chemisorption of propylene on the spinels. The presence of a substantial amount of firmly bound propylene was observed in the chemisorption on the inverse spinel.

The same as in the oxidation, the chemisorption of propylene on the oxides Mn_3O_4 was not observed clear up to 200°, due to the oxygen in the oxide lattice.

Sorption of CO and CO_2 . Noticeable chemisorption of carbon monoxide or carbon dioxide is absent on the normal spinel $CoMn_2O_4$ up to 200°. On the inverse spinel, both the carbon monoxide chemisorption rate and the degree of filling lie close to the values observed for oxygen . In the chemisorption of CO_2 on the inverse spinel the degrees of filling, for corresponding time intervals, represent about 30% of the values observed in the chemisorption of oxygen.

The relationship between the temperature and the electroconductivity was measured for both spinels in a vacuum and in argon. The specific electroconductivity values of the spinels at 20° are:

$$\sigma \, MnCo_2O_4 = 1.5 \cdot 10^{-4} \text{ ohm}^{-1} \cdot \text{cm}^{-1}$$

$$\sigma \, CoMn_2O_4 = 1 \cdot 10^{-6} \text{ ohm}^{-1} \cdot \text{cm}^{-1}$$

and the electroconductivity activation energies are respectively 0.8 ev and 1.1 ev, which is in agreement with the literature data [13]. The relationship between the electroconductivity and the temperature in the temperature region 20°-600°, in the coordinates $\log \sigma$ vs $1/T$, is a linear function without a break. From the sign of the thermal electromotive force both spinel specimens proved to be semiconductors with hole conductivity. Measuring the dependence of the electroconductivity on the chemisorption of oxygen and of carbon monoxide revealed that at 100° the chemisorption of both oxygen and carbon monoxide caused an increase in the conductivity of the

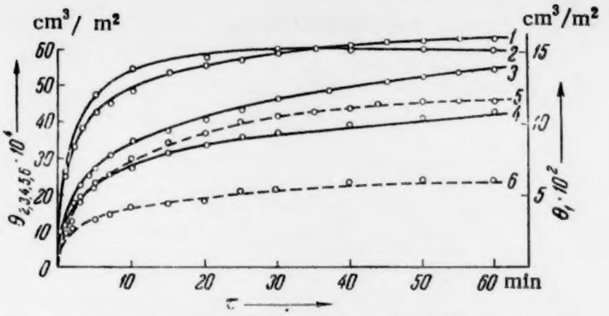

Fig. 2. Kinetic isotherms for the chemisorption of oxygen (1-4) and propylene (5, 6) at 200°. 1) Co_3O_4; 2) Mn_3O_4; 3) $MnCo_2O_4$; 4) $CoMn_2O_4$; 5) $MnCo_2O_4$; 6) $CoMnO_4$.

inverse spinel (Fig.4), which corresponds to a negative surface charge. This unexpected result was confirmed by the measurements of É. Kh. Enikeev, made in our laboratory using the vibrating condenser method. The same influence of the chemisorption of either a donor or an acceptor gas on both the bulk (electroconductivity) and surface (surface charge) electrical properties suggests a complex relationship between the chemisorption process and the electrical properties of spinels. The author considers it his pleasant duty to thank L. Ya. Margolis and Acad. Sci. USSR Corresponding Member S. Z. Roginskii for the valuable advice rendered in the execution of this work, and also M. Ya. Kushner for the x-ray structure measurements.

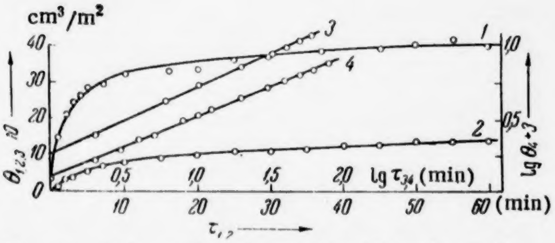

Fig. 3. Primary (1) and secondary (2) isotherms for the chemisorption of oxygen on $MnCo_2O_4$ at 100° and the rule for the chemisorption of oxygen on $CoMn_2O_4$ (3) and on $MnCo_2O_4$ (4).

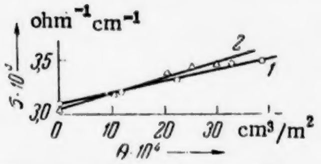

Fig. 4. Change in the electroconductivity of $MnCo_2O_4$ in the chemisorption of oxygen (1) and of carbon monoxide (2) at 100°.

LITERATURE CITED

[1] E. J. Verwey and E. L. Heilmann, J. Chem. Phys. 15, 174 (1947).

[2] J. B. Goodenough and A. Loeb, Phys. Rev. 98, No. 2, 391 (1955).

[3] T. Barth and E. Posnjak, Zs. Kristallogr. 82, 325 (1932).

[4] L. Ya. Margolis, Bull. Acad. Sci. USSR, Div. Chem. Sci. No.3 262 (1951).

[5] L. Ya. Margolis, Dissertation, Inst. Phys. Chem. Acad. Sci. USSR, 1945 [in Russian].

[6] T. Kwan and Y. Fujita, J. Research Inst. Catalysis, Hokkaido Univ. 2, No. 2, 110 (1953).

[7] A. Bielanski, J. Deren and J. Haber, Nature 179, 668 (1957).

[8] G. M. Shwab, E. Roth, C. Grintzos and N. Mavrakis, Monograph "Structure and Properties of Solid Surfaces" p. 465 (1953).

[9] R. A. W. Haul, Angew. Chem. 68, No. 7, 238 (1956).

[10] R. A. Beebe, J. B. Beckwith and J. M. Honig, J. Am. Chem. Soc. 67, 1554 (1945).

[11] E. Ya. Rode, Monograph "Oxygen Compounds of Manganese" [In Russian] (Izd. AN SSSR, 1952).

[12] E. Ya. Rode, J. Inorg. Chem. (USSR) 1, No. 6, 1430 (1956).

[13] B.T. Kolomiets, I. T. Sheftel' and E. V. Kurlina, J. Tech. Phys. (USSR) 27, No. 1, 51 (1957).

[14] S. Z. Roginskii and N. P. Keier, Bull. Acad. Sci. USSR, Div. Chem. Sci. No. 6, 571 (1947).

Received April 3, 1959

DETERMINATION OF THE RELATIVE MOBILITY OF ALKALI METAL IONS IN SILICATE MELTS

V. I. Malkin and V. V. Pokidyshev

Institute of Metallography and Physics of Metals Central Research
Institute of Ferrous Metallurgy

(Presented by Academician G. V. Kurdyumov, April 24, 1959)

It is known [1-6] that in silicate melts containing oxides of the alkali and alkaline-earth metals the electricity is transported only by the ions of these metals. Here the mobility of the cations of the alkali metals exceeds that of the cations of the alkaline-earth metals. To determine the relationship between the radii of the cations and their relative mobility it seemed of interest to compare the mobilities of the cations of different alkali metals in silicate melts.

For this purpose we measured in the present study the transport numbers of the cations in the three-component silicate melts with composition $\overset{\mathrm{I}}{\mathrm{Me}}_2\mathrm{O} \cdot \overset{\mathrm{II}}{\mathrm{Me}}_2\mathrm{O} \cdot 4\mathrm{SiO}_2$, each containing two different alkali metal cations. To measure the transport numbers we used the method based on determining small changes in the concentration of the cation in the anolyte by means of radiactive indicators[1]. We measured the transport numbers of the cations in the melts $Li_2O \cdot K_2O \cdot 4SiO_2$; $Na_2O \cdot Rb_2O \cdot 4SiO_2$; $Na_2O \cdot Cs_2O \cdot 4SiO_2$; $K_2O \cdot Cs_2O \cdot 4SiO_2$; $Li_2O \cdot Cs_2O \cdot 4SiO_2$. The radioactive isotopes Na^{24}, K^{42}, Rb^{86} and Cs^{134} were used. The experiments were run in a corundized cell at 1200°.

The transport numbers were determined using the equation for systems with two cations [4]:

$$x_1 = \frac{\frac{p_1}{E_1}\left[\frac{M}{k}\left(1 - \frac{I_{anol}}{I_{initial}}\right)_1 + E_2 + E_0\right]}{1 - p_1 + \frac{p_1 E_2}{E_1}},$$

where x_1 is the transport number of one of the cations (the cation that is "labeled"), p_1 is the concentration of this ion in the melt before experiment in fractional units, E_1, is the gram-equivalent weight of this cation, E_2 is the gram-equivalent weight of the second cation, E_0 is the gram-equivalent weight of oxygen, I_{init} is the initial radioactivity of the melt, I_{anol} is the radioactivity of the anolyte after experiment, M is the weight of the anolyte in grams after experiment, and k is the quantity of electricity passed, in faradays.

The equation for the transport number of the second cation is symmetrical, and is obtained from Equation (1) by replacing subscript 1 by subscript 2.

The results of measuring the transport numbers in the above-enumerated 5 melts are given in Table 1, as are also the earlier obtained results of measuring in the melts $Na_2O \cdot K_2O \cdot 4SIO_2$ [4] and $Li_2O \cdot Na_2O \cdot 4SiO_2$[8] (the mean values of the transport numbers are given).

In addition, the radii of the cations according to Pauling and their coordination numbers [9] are given in Table 1.

From the data in Table 1 it follows that there is a tendency for the transport number of a cation to increase with increase in its radius. This tendency is due to a decrease in the bond strength of the cation with the anionic network of the melt as the cation radius increases. However, the increase in the relative mobility of the cation with increase in its radius is not monotonic. A large difference in the radii of 2 cations does not always correspond to a large difference in the transport numbers.

Deviation from a monotonic character for the relationship between the relative mobility and the radius of a cation indicates that the relative mobility of cations is not determined only by the difference in the strength of the cation—oxygen bond. The "geometric" factor, linked with the repulsion forces, which must be overcome by the migrating cation, exerts an important influence on the mobility of cations. The presence of repulsion forces retards the migration of larger sized cations more than it does the migration of smaller sized cations.

As a result, with increase in the cation radius the mobility will either increase or decrease, depending on which of the two factors (bond strength or repulsion forces) plays the dominant role. It is possible to link the difference in the role of the repulsion forces in the investigated melts with the ratio of the coordination numbers of the cations in these melts.

In a melt, containing two cations, the structure of the melt becomes denser with increase in the difference in the coordination numbers of the cations, which creates a hindrance to the movement of the cations, and this hindrance, with other conditions constant, is greater the larger the radii of the cations.

Particular proof of this is found in the reduction of the electroconductivity of binary silicate systems, containing one cation, when a third component, giving a second cation, is added [10-12].

TABLE 1

Melt	Cation	Radius according to Pauling in A	Coord. No.	Transport number
$Li_2O \cdot Na_2O \cdot 4SiO_2$	Li^+	0,60	6	—
	Na^+	0,95	6	0,57
$Li_2O \cdot K_2O \cdot 4SiO_2$	Li^+	0,60	6	—
	K^+	1,33	8	0,56
$Li_2O \cdot Cs_2O \cdot 4SiO_2$	Li^+	0,60	6	—
	Cs^+	1,69	12	0,68
$Na_2O \cdot K_2O \cdot 4SiO_2$	Na^+	0,95	6	0,52
	K^+	1,33	8	0,50
$Na_2O \cdot Rb_2O \cdot 4SiO_2$	Na^+	0,95	6	0,49
	Rb^+	1,48	12	0,53
$Na_2O \cdot Cs_2O \cdot 4SiO_2$	Na^+	0,95	6	0,44
	Cs^+	1,69	12	0,54
$K_2O \cdot Cs_2O \cdot 4SiO_2$	K^+	1,33	8	0,42
	Cs^+	1,69	12	0,60

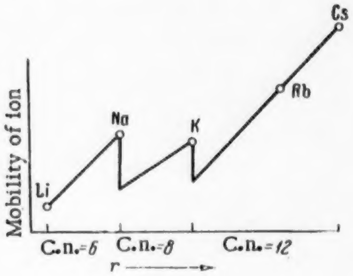

Fig. 1

The obtained results can be schematically depicted by the curve shown in Fig. 1. Each branch of this curve corresponds to a definite coordination number. Within the limits of one branch the relative mobility increases with increase in the radius (melt $Li_2O \cdot Na_2O \cdot 4SiO_2$).

If increasing the radius of the larger of two cations leads to transition into a region with a larger coordination number, then increasing the role of the repulsion forces leads to a relative decrease in the mobility of the larger of the cations (transition from the melt $Li_2O \cdot Na_2O \cdot 4SiO_2$ to the melt $Li_2O \cdot K_2O \cdot 4SiO_2$).

If increasing the radius of the larger of the cations occurs within the limits of one branch of the curve, then due to the predominant role of the bond strength factor there is observed an increase in the difference of the transport number of the 2 cations (transition from the melt $Na_2O \cdot Rb_2O \cdot 4SiO_2$ to the melt $Na_2O \cdot Cs_2O$ $4SiO_2$).

The decisive role of the bond strength factor also appears in the case where the reduction in the size of the smaller of 2 cations takes place within the limits of one branch of the curve. Here the ratio of the mobility of the larger cation to the mobility of the smaller cation decreases (transition from the melt $Na_2O \cdot Cs_2O \cdot 4SiO_2$ to the melt $Li_2O \cdot Cs_2O \cdot 4SiO_2$).

Increasing the size of the smaller of 2 cations with transition into a region with a larger coordination number reduces the role of the repulsion forces, as a result of which the ratio of the mobility of the larger cation to the mobility of the smaller cation increases (transition from the melt $Na_2O \cdot Cs_2O \cdot 4SiO_2$ to the melt $K_2O \cdot Cs_2O \cdot 4SiO_2$).

LITERATURE CITED

[1] J. O'M. Bockris, J. A. Kitchener and A. E. Davies, Trans. Farad. Soc. 48, 536 (1952).

[2] V. I. Malkin and L. A. Shvartsman, Problems of Metallography and Physics of Metals, Coll. Vol. VI (Moscow, 1959).*

[3] O. A. Esin and A. K. Kir'yanov, Bull. Acad. Sci. USSR, Div. Tech. Sci., No. 12, 28 (1955).

[4] V. I. Malkin, S. F. Khokhlov and L. A. Shvartsman, J. Phys. Chem. (USSR) 31, 2485 (1957).

[5] V. I. Malkin, S. F. Khokhlov and L. A. Shvartsman, Proc. Acad. Sci. USSR 106, 491 (1956).

[6] V. I. Malkin, J. Phys. Chem. (USSR) 32, 838 (1958).

[7] V. I. Malkin and L. A. Shvartsman, Proc. Acad. Sci. USSR 102, 961 (1955).

[8] V. I. Malkin and V. V. Pokidyshev, J. Inorg. Chem. (USSR) 3, 2219 (1958).

[9] S. Block and E. Levin, J. Am. Ceram. Soc. 40, 113 (1957).

[10] S. W. Strauss, J. Res. Nat. Bur. Stand. 56, 183 (1956).

[11] B. Lengyel and Z. Boksay, Z. Physik. Chem. 204, 90 (1955).

[12] O. V. Mazurin and E. S. Borisovskii, J. Tech. Phys. (USSR) 27, 275 (1957).

Received April 22, 1959

---

* In Russian.

A CONTRIBUTION TO THE STUDY OF THE MOBILITY OF COPPER IONS IN GERMANIUM

A. Ya. Potemkin, V. N. Potapov and D. A. Petrov

A. A. Baikov Institute of Metallurgy, Academy of Sciences of the USSR

(Presented by Academician I. P. Bardin, April 20, 1959)

The character of the ionization of copper in germanium depends to a large extent on the temperature. It is mentioned in the literature that at room and moderately high temperatures copper exists in germanium as negative ions. According to some data [3], it is electrically neutral in the interval 500-700°, and according to other data [2], it becomes neutral only at 700°. Positive copper ions are observed in the range 800-920° [1,2,4].

However, direct experimental proof that copper at temperatures of 500-700° and lower has a negative charge is lacking. This circumstance is apparently due to the contradictory information that exists as to the state of the copper atom in germanium at temperatures of 500-700° [2,3].

In this communication we give the results of measuring the mobility (electrodiffusion) of copper ions in germanium in the temperature interval 500-680°.

To prepare the specimens, we used germanium crystals of the n-type with a resistivity at room temperature of 10-30 ohm•cm. Specimens measuring $1.8 \cdot 3 \cdot 13$ mm^3 were cut perpendicular to the [111] direction of monocrystal growth in order to obtain a more uniform distribution of the impurities along the length of the specimen. The distribution uniformity of the impurities was checked by taking the distribution of the potential along the length of the specimen. Then a layer of copper about 10 μ thick was electrolytically deposited (from 10 % aqueous $CuSO_4$ solution) on the face surfaces of the specimens. In our experiments this copper layer served as the source for the diffusion of copper into germanium and, in addition, it assured the creation of an ohmic contact when the specimens were placed in an electric circuit. The experiments were run in a special apparatus at a vacuum of 10^{-3}-10^{-4} mm Hg. By means of flat metal contact clamps the specimen was inserted in a series circuit composed of a M-340 ammeter, sliding rheostat and a VSA-6M rectifier, connected to an alternating current source. The specimens were subjected to isothermal annealing in an electric field by the technique of passing through them a constant current of 4-10 amp with a field intensity of 0.5-1 v/cm. The intensity of the electric field in the specimens was determined by the voltage between two attached probes made of pointed tungsten wire, separated by a matter of 3-5 mm. The temperature of the specimens was measured using the method described in [1,2]. After annealing, the specimens were cooled rapidly, which was achieved by turning off the current going through them. Finally, the distribution curve of the potential along the length of the specimen was taken, and from this the mobility of the copper ions and the sign of their charge were determined.

The principle of the method developed by us is depicted schematically in Fig. 1. The specimens, not containing copper, showed a linear distribution of the potential along the length, both prior to isothermal annealing in an electric field, and after it, (Fig. 1,1). In contrast to this, in the specimens having a layer of copper on the faces after isothermal annealing in an electric field, the linear distribution of the potential along the length of the specimen was retained only on the portion ab (Fig. 1, 2), while outside this portion a sharp infraction of the linearity was observed. This infraction was caused by the copper permeating into the depth of the specimens, in which connection the depth of copper penetration from the negative electrode side (x_1) was considerably greater than from the positive electrode side (x_2). The preferential displacement of copper toward the positive electrode ($x_1 > x_2$) is evidence that copper atoms are ionized negatively. From this fact it can be concluded that when a heated specimen is kept in a constant electric field the following two processes take place in it.

TABLE 1

Experimental Data on Studying the Mobility of Copper Ions in Germanium at Various Temperatures

n^*, cm^{-3}	t, °C	E, v/cm	τ, sec	x_e, cm	μ, cm^2/v·sec	D, cm^2/sec
$0{,}8\cdot10^{14}$	540	0,59	5200	0,130	$4{,}2\cdot10^{-5}$	$2{,}9\cdot10^{-6}$
$1{,}6\cdot10^{14}$	550	0,65	5200	0,135	$4{,}1\cdot10^{-5}$	$2{,}9\cdot10^{-6}$
$0{,}6\cdot10^{14}$	575	0,54	4000	0,110	$5{,}1\cdot10^{-5}$	$3{,}7\cdot10^{-6}$
$1{,}0\cdot10^{14}$	600	0,51	5200	0,150	$5{,}7\cdot10^{-5}$	$4{,}3\cdot10^{-6}$
$0{,}6\cdot10^{14}$	650	0,45	5200	0,165	$7{,}0\cdot10^{-5}$	$5{,}5\cdot10^{-6}$

---

* The concentration of the current carriers in the starting specimens was determined by measuring the resistivity.

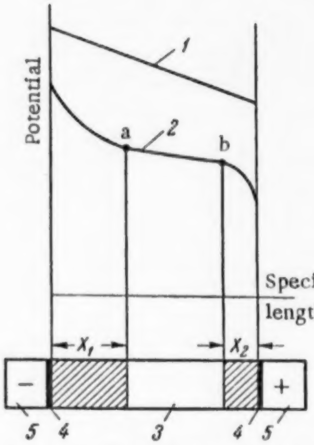

Fig. 1. Distribution of the potential along the specimen length before (1) and after (2) isothermal annealing in an electric field; 3) monocrystalline germanium specimen; 4) layer of electrolytically deposited copper; 5) clamped electrode.

1. From the negatively charged face the negative copper ions move into the interior of the specimen by a distance $x_1 = x_T + x_e$ under the total influence of the heat energy (giving the thermodiffusion displacement x_T) and the electric field (giving the electrodiffusion displacement x_e).

2. From the positively charged face the negative copper ions move into the interior of the specimen by a distance $x_2 = x_T - x_e$ as the result of the thermodiffusion displacement (x_T) predominating over the electrodiffusion displacement (x_e), which in this case is in the direction opposite to the thermodiffusion displacement.

The difference between the total displacements from the negative and positive electrodes, $x_1 - x_2 = (x_T + x_e) - (x_T - x_e) = 2x_e$, is equal to twice the value of the pure drift of the copper ions in germanium under the influence of a constant electric field at the given temperature. As a result, using this method, we were able to separate the electrodiffusion and thermodiffusion effects of the ions of the impurity in the semiconductor.

The value of the copper ion mobility (μ) was determined from the equation:

$$\mu = \frac{x_e}{E\tau} \qquad (\text{cm}^2/\text{v/sec}). \qquad (1)$$

where x_e is the value of the pure drift of the copper ions in cm, E is the intensity of the electric field in the specimen, expressed in v/cm, and τ is the time of keeping the specimens in an electric field, in sec.

The diffusion coefficient of copper in germanium was calculated from the Einstein equation:

$$D = \mu\frac{kT}{q}\ \text{cm}^2/\text{sec} \qquad (2)$$

on the assumption that the copper ion was singly charged. The obtained experimental data are given in Table 1 and plotted in Fig. 2.

As can be seen from Table 1, the mobility of the copper ions in the interval 540-650° reaches $(4.2\text{-}7.0)\cdot10^{-5}$ cm^2/v-sec, which corresponds to a diffusion coefficient of the order of $(2.9\text{-}5.5)\cdot10^{-6}$ cm^2/sec. Under the given experimental conditions, a displacement of copper into the interior of the specimens was not observed at 450° ($E = 0.8$ v/cm, $\tau = 7200$ sec), while in the interval 500-515° ($E = 0.8$ v/cm, $\tau = 7200$ sec) the displacement of copper was slightly too small to permit a valid quantitative estimate.

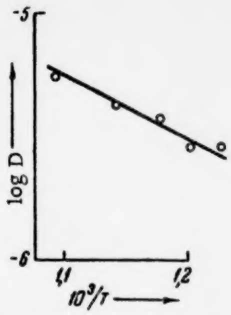

Fig. 2. Relationship between the diffusion coefficient of copper in germanium and the reciprocal of the absolute temperature. Energy of activation $\Delta E = 4900$ cal/mole.

Information is lacking in the literature on the diffusion coefficient of copper in germanium for the temperature interval 540-650°. At 700-900° the diffusion coefficient of copper in germanium reaches $(2.8 \pm 0.3) \cdot 10^{-5}$ cm^2/sec, with an activation energy of 4100 cal/mole [5]. According to our data, obtained from the graph in Fig. 2, the value of the activation energy is 4900 cal/mole, which corresponds to a somewhat smaller diffusion coefficient and a somewhat large activation energy than those given in [5]. This can be explained by a difference in the signs of the charges, and consequently, by a difference in the spread of the copper ions between the temperature interval 540-650° (negative Cu ions) and the temperature interval above 700° (positive copper ions).

In conclusion I wish to sincerely thank both L. S. Milevskii for counsel in carrying out the present work and V. S. Zemskova for supplying the germanium monocrystals.

LITERATURE CITED

[1] J. C. Severiens and C. S. Fuller, Phys. Rev. 92, 1322 (1953).

[2] J. C. Severiens and C. S. Fuller, Phys. Rev. 96, 21 (1954).

[3] B. I. Boltaks, J. Tech. Phys. (USSR) 26, No. 2,457 (1956).

[4] B. I. Boltaks, Semiconductors in Science and Industry [in Russian] (Izd. AN SSSR, 1957), Vol. 1, p. 221.

[5] C. S. Fuller, J. D. Struthers, et al., Phys. Rev. 93, 6, 1182 (1954).

Received April 20, 1959

DECOMPOSITION OF THE CARBIDE PHASE OF WHITE CAST IRON–CEMENTITE UNDER THE ACTION OF NEUTRON RAYS

I. M. Pronman, V. A. Shalashov, A. Kh. Breger
and Yu. A. Zubov

All-Union Scientific Research Institute on Standardization
in Machine Construction

(Presented by Academician V. A. Kargin, April 10, 1959)

A comparatively small number of studies exist on the phase transformations of metals and alloys , arising as the result of neutron irradiation. Thus, the transformation of white tin to the gray form was studied in [1], the transformation of austenite to martensite and ferrite was studied in [2,3], and the phase transformations in alloys of uranium with molybdenum were studied in [4,5]. The completeness of phase transformations under neutron irradiation depends on the mass and charge of the atoms, the stability of the irradiated substance, the energy of the neutrons, and the irradiation dosage, [6, 7, 8].

In this paper we were the first to attempt studying the action of neutron irradiation on cementite, being, as is known, the most important phase in iron-carbon alloys, especially white cast iron [9]. Pure cementite was isolated electrolytically from a commercial white cupola cast iron as the carbide deposit [10]*.

The chemical compositions of the cast iron and isolated carbide are given in Table 1.

Irradiation of the specimens (the pure cementite in aluminum ampuls, and the white cast iron specimens as chips) was done in two aluminum containers, placed in the active zone of the nuclear reactor on ordinary water and enriched with uranium in a total stream of 10^{12} neutrons/cm^2 · sec [11]. A cadmium filter 1 mm thick was fitted in each container to absorb the heat neutrons. The stream of rapid neutrons with an energy of 1 Mev and more was $1\text{-}5 \cdot 10^{10}$ neutrons/cm^2 sec. As a result, the integral irradiation dose with fast neutrons during the entire time of exposure (50 hr) was $0.2\text{-}1 \cdot 10^{16}$ neutrons/cm^2. The temperature of the specimens during irradiation did not exceed 65°. At a distance of 10 cm , the specimens of irradiated cementite generated a dose output of 0.3 μr/sec (ampul from the 1st container) and 0.15 μ r/sec (ampul from the 2nd container). Such a difference in the activity of the specimens indicates that the integral irradiation dose for the specimens found in container 1 was approximately twice that for the specimens irradiated in container 2. Apparently, this is due to the fact that the first container was found in the center of the reactor canal, while the second container was located 10 cm above it. The slight radioactivity of the irradiated specimens made it possible to do further work with them without special protection.

The x-ray study of the original and irradiated cementite was done using a URS-50-I ionization apparatus and Fe-K radiation.

The x-ray patterns of the unirradiated cementite were found to contain all of the lines of cementite [12], and also very weakly the extremely strong graphite line (002), indicating the trace presence of graphite, which, apparently, deposits together with the carbide precipitate during electrolysis. The values found by us for the lattice periods of cementite, a = 4.515 A, b = 5.090 A and c= 6.748 A (determination accuracy ± 0.002 A), are in good agreement with the literature data [13,14].

---

* The preparation of the carbide deposit and its analysis were done by the method and under the direction of N. M. Popova.

TABLE 1

Name	Chemical composition, wt. %								
	C	Si	Mn	Cr	P	S	Fe	Σ_{el}	$100-\Sigma_{el}$ (moisture, etc.)
White cast iron	2,75	1,1	0,75	0,03	0,12	0,16	95,09	100	—
Carbide deposit (cementite)	6,3	0,7	1,71	0,06	—	—	88,2	96,97	3,03

TABLE 2

Phase Composition of Unirradiated and Irradiated Cementite Specimens as a Function of the Annealing Conditions

Expt. No.	Description of specimen	Annealing cond.			Phase composition, wt-%					Remarks
		temperature °C	time at this temperature, hr	rate of cooling, deg/min	Fe_3C	α-Fe	austenite	$C_{graphite}$	Fe_3O_4	
1	Starting cementite, obtained electrolyt. from white cast iron specimens	—	—	—	100	—	—	0,3	—	
2	Cementite, irradiated in the 1st container	—	—	—	95	—	—	0,3	5	
3	Cementite, irrad. in 2nd container	—	—	—	97	—	—	0,3	3	
4	Unirrad. cementite	650	12	2	100	—	—	0,3	—	Cooled in the furnace
5	Unirrad. cementite	850	12	1,5	100	—	—	0,3		Likewise
6	Unirrad. cementite	860	64	1,5	100	—	—	0,3	—	"
7	Unirrad. cementite	950	10	1,2	100	—	—	0,3	—	"
8	Unirrad. cementite	1050**	10	7	83	17	—	0,3	—	"
9	Cementite, irrad. in 1st container	650	12	2	34	66	—	—	—	"
10	Cementite, irrad. in 2nd container	850	12	1,2	22	73	5	—	—	"
11	Mixt. of irrad. cementite from both cont.	650	50	2	20	80	—	—	—	"
12	The same specimen	1050**	10	7	Traces*	97	—	3	—	"

---

* About 0.4 %, apparently, a carbide of the type (Fe, Cr)$_3$C.

** Heated to 1050°, kept at this temperature for 10 hr, cooled in the furnace to 850° at a rate of 7°/min, kept here for 5 hr, then cooled to 500° at a rate of 5°/min and from 500° down at a rate of 0.5°/min.

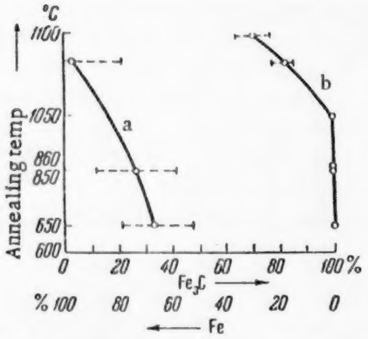

Fig. 1. Change in the Fe_3C and Fe ratios in specimens of irradiated (a) and unirradiated (b) cementite, annealed under the same conditions at different temperatures.

The x-ray patterns of the irradiated Fe_3C specimens contained all of the lines of cementite, and also very weakly the extremely strong Fe_3O_4 line (311). The intensity of this line in the x-ray pattern of the specimen from the first container proved to be approximately twice that of the line in the x-ray pattern of the specimen from the 2nd container, which is found in agreement with the larger integral dose of irradiating container 1. The intensity of the graphite line (002) in the x-ray patterns did not change as the result of irradiation.

The specimens of irradiated and unirradiated cementite were annealed at different temperatures in evacuated quartz ampuls (in a vacuum of 10^{-4} mm Hg). The obtained x-ray patterns of the annealed cementite specimens revealed that whereas in the case of unirradiated cementite annealed at high temperatures and for very long times, no changes took place; in the case of irradiated cementite, annealed at lower temperatures and for much shorter time, there was phase transformation. Here isothermal

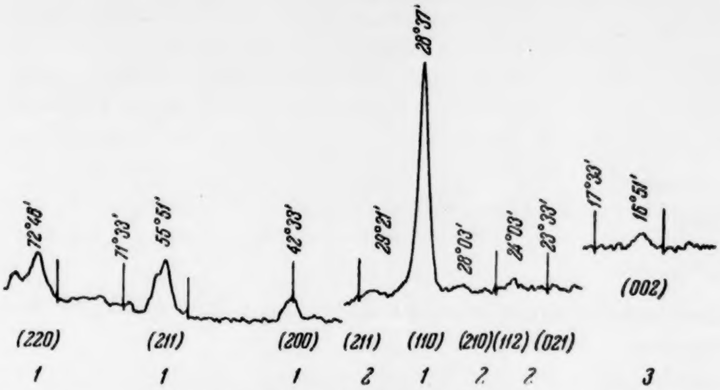

Fig. 2. X-ray pattern of irradiated cementite specimen after annealing at 1050° (see Specimen 12, Table 2) (complete decomposition of the cementite). 1) α-Fe ; 2) Fe_3C ; 3) $C_{graphite}$.

annealing at higher temperatures, corresponding to the austenite region of the Fe-C diagram, leads to more complete phase transformation (Fig. 1).

The data on the change in the phase composition of unirradiated and irradiated Fe_3C specimens as a function of the annealing conditions are given in Table 2. A quantitative estimate of the amount of each phase in wt. % was made on the basis of standard x-ray patterns and the intensities of the lines in the x-ray patterns after each treatment. The accuracy of determining the amount of each phase in wt. % was ± 20% of the measured value.

From the data in Table 2 it can be seen that annealing the irradiated cementite even at 650°, i.e., below the austenite region, leads to a substantial separation of iron (about 2/3 of the entire composition). Such decomposition of the Fe_3C is apparently caused by the presence of a large number of centers for the crystallization of iron in irradiated cementite. The amount of iron, formed due to reduction of the Fe_3O_4 contained in the specimen (5%), is about 14% , i.e., it is approximately 1/5 of the total amount of iron separating in the irradiated specimen. These results were confirmed experimentally by subjecting a prepared mixture of Fe_3C and Fe_3O_4 of the same composition to annealing, followed by x-ray phase analysis.

As a result, the exposure of cementite to neutron rays leads to the formation of iron nuclei in it, which on subsequent annealing at temperatures below the austenite region crystallize into α-Fe, and when annealed at temperatures corresponding to the austenite region into γ-Fe. Here the formation of residual austenite is observed in the latter case (specimen 10).

From the data obtained in Table 2 it can also be seen that, independent of the amount of iron separating in the irradiated specimens, the carbon crystallizes into graphite only at temperatures >1000° (Specimen 12). Here, even with complete decomposition of the cementite, the graphite line (002) (Fig. 2) does not reflect the entire amount of carbon in the specimen (chemical analysis of this specimen revealed 7.2% C, whereas estimating the amount of graphite by the intensity of the (002) line shows about 3%). At the same time, in the case of unirradiated cementite, annealed simultaneously with the irradiated specimen (Specimen 8), there was no crystallization of carbon. As a result, exposing cementite to neutron rays apparently causes the diffusion rate of carbon to increase, and , in addition, graphitization centers are probably born during the irradiation. However, with the given irradiation dose ($2 \cdot 10^{15} - 1 \cdot 10^{16}$ neutrons/cm^2), the centers obviously do not reach critical dimensions, as otherwise the graphite would crystallize at lower temperatures.

As a result, exposing cementite to neutron rays, even with a low dosage (values of the order of 10^{16} neutrons/cm^2), leads to the birth of iron and graphite centers. Larger irradiation doses could probably lead not only to the birth of centers, but also to the crystallization of new phases as a direct result of neutron irradiation. In the elastic collision of fast neutrons with the nuclei of the iron and carbon atoms in the crystal lattice of cementite it is possible for two types of radiation disturbances to arise:

a) the formation and accumulation of embedded atoms and vacancies, leading to "irradiation hardening", and b) more complex disturbances, associated with the formation of "temperature zones" in large atomic volumes of the substance, in which, under the action of high temperatures (above the melting point of the substance) and very rapid cooling (of the order 10^{-10}- 10^{-11} sec), there occurs recrystallization and the birth of energetically more favorable phases [6,7, 14]. The first type of defect is quite unstable and is burned off at low temperatures (around 300°), whereas the second type of radiation disturbances is stable and can lead to phase transformations. The latter, apparently, also exists in the irradiation of cementite, which is the metastable phase in iron-carbon alloys.

Further expansion of this work can prove important, both for understanding the mechanism and kinetics of graphite formation in white cast iron, graphitized steel and other high-carbon alloys, and for practical purposes in obtaining high-strength cast irons.

The authors sincerely thank Acad. V. A. Kargin and Prof. A. A. Zhukhovitskii for their interest in the work and discussion of the results.

LITERATURE CITED

[1] J. Fleeman and G. J. Dienes, J. Applied Phys. 26, No. 6, 652 (1955) (translation in monograph "Action of Nuclear Rays on the Structure and Properties of Metals and Alloys" (Moscow, 1957), p. 117.

[2] A. I. Zakharov and O. P. Maksimova, Proc. Acad. Sci. USSR 114, No. 6, 1195 (1957).*

[3] M. B. Reynolds, J. R. Low and L. O. Sullivan, J. Metals 7, No. 4, 555 (1955) (translation in monograph "Action of Nuclear Rays on the Structure and Properties of Metals and Alloys" (Moscow, 1957), p. 146).

[4] S. T. Konobeevskii, V. I. Kutaitsev and N. F. Pravdyuk, Report of the Soviet Delegation to the International Conference on World Utilization of Atomic Energy, Geneva, 1955 [in Russian] (Izd. AN SSSR, 1955), p. 263).

[5] M. L. Bleiberg, L. J. Jones, and B. Lustman, J. Appl. Phys. 27, No. 11, 1270 (1956).

[6] F. Seitz and J. S. Koehler, Progress in Solid State Physics 2, p. 305 (1956).

[7] S. T. Konobeevskii, Atomic Energy (USSR) 1, No. 2, 63 (1956).

[8] J. A. Brinkman, J. Applied Phys. 25, No. 8, 961 (1954) (translation in monograph " Action of Nuclear Rays on the Structure and Properties of Metals and Alloys". (Moscow, 1957), p. 5).

[9] V. F. Zubarev, Principles of the Graphitization of White Cast Iron and Steel [in Russian] (Moscow, 1957).

[10] N. M. Popova, Carbide Analysis of Steel [in Russian] (Moscow, 1957).

[11] Report of the Soviet Delegation to the International Conference on World Utilization of Atomic Energy, Geneva, 1955 (Izd. AN SSSR, 1955); Yu. G. Nokolaev, Reactor Construction and the Theory of Reactors [in Russian] (Izd. AN SSSR, 1955).

[12] M. P. Arbuzov, J. Tech. Phys. (USSR), 19, No. 10, 1119 (1949).

[13] H. Lipson and N. J. Petch, Minutes of Proceedings of the Iron and Steel Institute, sec. 1, Autumn meeting p. 95 (1940).

[14] G. B. Bokii, Introduction to Crystal Chemistry [in Russian] (Moscow, 1950).

Received April 9, 1959

---

* Original Russian pagination. See C.B. Translation.